

A new phylogenetic hypothesis of Tanystropheidae (Diapsida, Archosauromorpha) and other “protorosaurs”, and its implications for the early evolution of stem archosaurs (#51657)

1

First submission

Guidance from your Editor

Please submit by **17 Sep 2020** for the benefit of the authors (and your \$200 publishing discount) .



Structure and Criteria

Please read the 'Structure and Criteria' page for general guidance.



Raw data check

Review the raw data.



Image check

Check that figures and images have not been inappropriately manipulated.

Privacy reminder: If uploading an annotated PDF, remove identifiable information to remain anonymous.

Files

Download and review all files from the [materials page](#).

35 Figure file(s)

1 Table file(s)

2 Raw data file(s)



Structure and Criteria

Structure your review

The review form is divided into 5 sections. Please consider these when composing your review:

1. BASIC REPORTING
2. EXPERIMENTAL DESIGN
3. VALIDITY OF THE FINDINGS
4. General comments
5. Confidential notes to the editor

 You can also annotate this PDF and upload it as part of your review

When ready [submit online](#).

Editorial Criteria

Use these criteria points to structure your review. The full detailed editorial criteria is on your [guidance page](#).

BASIC REPORTING

-  Clear, unambiguous, professional English language used throughout.
-  Intro & background to show context. Literature well referenced & relevant.
-  Structure conforms to [Peerj standards](#), discipline norm, or improved for clarity.
-  Figures are relevant, high quality, well labelled & described.
-  Raw data supplied (see [Peerj policy](#)).

EXPERIMENTAL DESIGN

-  Original primary research within [Scope of the journal](#).
-  Research question well defined, relevant & meaningful. It is stated how the research fills an identified knowledge gap.
-  Rigorous investigation performed to a high technical & ethical standard.
-  Methods described with sufficient detail & information to replicate.

VALIDITY OF THE FINDINGS

-  Impact and novelty not assessed. Negative/inconclusive results accepted. *Meaningful* replication encouraged where rationale & benefit to literature is clearly stated.
-  All underlying data have been provided; they are robust, statistically sound, & controlled.
-  Speculation is welcome, but should be identified as such.
-  Conclusions are well stated, linked to original research question & limited to supporting results.

Standout reviewing tips

3



The best reviewers use these techniques

Tip

Support criticisms with evidence from the text or from other sources

Example

Smith et al (J of Methodology, 2005, V3, pp 123) have shown that the analysis you use in Lines 241-250 is not the most appropriate for this situation. Please explain why you used this method.

Give specific suggestions on how to improve the manuscript

Your introduction needs more detail. I suggest that you improve the description at lines 57- 86 to provide more justification for your study (specifically, you should expand upon the knowledge gap being filled).

Comment on language and grammar issues

The English language should be improved to ensure that an international audience can clearly understand your text. Some examples where the language could be improved include lines 23, 77, 121, 128 – the current phrasing makes comprehension difficult.

Organize by importance of the issues, and number your points

1. Your most important issue
2. The next most important item
3. ...
4. The least important points

Please provide constructive criticism, and avoid personal opinions

I thank you for providing the raw data, however your supplemental files need more descriptive metadata identifiers to be useful to future readers. Although your results are compelling, the data analysis should be improved in the following ways: AA, BB, CC

Comment on strengths (as well as weaknesses) of the manuscript

I commend the authors for their extensive data set, compiled over many years of detailed fieldwork. In addition, the manuscript is clearly written in professional, unambiguous language. If there is a weakness, it is in the statistical analysis (as I have noted above) which should be improved upon before Acceptance.

A new phylogenetic hypothesis of Tanystropheidae (Diapsida, Archosauromorpha) and other “protorosaurs”, and its implications for the early evolution of stem archosaurs

Stephan N F Spiekman^{Corresp., 1}, Nicholas C Fraser², Torsten M Scheyer¹

¹ Palaeontological Institute and Museum, University of Zurich, Zurich, Switzerland

² National Museums Scotland, Edinburgh, United Kingdom

Corresponding Author: Stephan N F Spiekman
Email address: stephanspiekman@gmail.com

The historical clade “Protorosauria” represents an important group of archosauromorph reptiles that had a wide geographic distribution between the Late Permian and Late Triassic. “Protorosaurs” are characterized by their long necks, which are epitomized in the genus *Tanystropheus* and in *Dinocephalosaurus orientalis*. Recent phylogenetic analyses have indicated that “Protorosauria” is a polyphyletic clade, but the exact relationships of the various “protorosaur” taxa within the archosauromorph lineage is currently uncertain. Several taxa, although represented by relatively complete material, have previously not been assessed phylogenetically. We present a new phylogenetic hypothesis that comprises a wide range of archosauromorphs, including the most exhaustive sample of “protorosaurs” to date and several “protorosaur” taxa from the eastern Tethys margin that have not been included in any previous analysis. The polyphyly of “Protorosauria” is confirmed and therefore we suggest the usage of this term should be abandoned. Tanystropheidae is recovered as a monophyletic group and the Chinese taxa *Dinocephalosaurus orientalis* and *Pectodens zhenyuensis* form a new archosauromorph clade, Dinocephalosauridae, which is closely related to Tanystropheidae. The well-known crocopod and former “protorosaur” *Prolacerta broomi* is considerably less closely related to Archosauriformes than was previously considered.

A new phylogenetic hypothesis of Tanystropheidae (Diapsida, Archosauromorpha) and other “protorosaurs”, and its implications for the early evolution of stem archosaurs

Stephan N. F. Spiekman¹, Nicholas C. Fraser², Torsten M. Scheyer¹

¹University of Zurich, Palaeontological Institute and Museum, Karl-Schmid-Strasse 4, 8006 Zurich, Switzerland

²National Museums Scotland, Chambers St, Edinburgh EH1 1JF, UK

Corresponding author:

Stephan Spiekman

Karl-Schmid-Strasse 4, 8006 Zurich, Switzerland

Email address: stephanspiekman@gmail.com

Abstract

The historical clade “Protorosauria” represents an important group of archosauromorph reptiles that had a wide geographic distribution between the Late Permian and Late Triassic. “Protorosaurs” are characterized by their long necks, which are epitomized in the genus *Tanystropheus* and in *Dinocephalosaurus orientalis*. Recent phylogenetic analyses have indicated that “Protorosauria” is a polyphyletic clade, but the exact relationships of the various “protorosaur” taxa within the archosauromorph lineage is currently uncertain. Several taxa, although represented by relatively complete material, have previously not been assessed phylogenetically. We present a new phylogenetic hypothesis that comprises a wide range of archosauromorphs, including the most exhaustive sample of “protorosaurs” to date and several “protorosaur” taxa from the eastern Tethys margin that have not been included in any previous analysis. The polyphyly of “Protorosauria” is confirmed and therefore we suggest the usage of this term should be abandoned. Tanystropheidae is recovered as a monophyletic group and the Chinese taxa *Dinocephalosaurus orientalis* and *Pectodens zhenyuensis* form a new archosauromorph clade, Dinocephalosauridae, which is closely related to Tanystropheidae. The well-known crocopod and

former “protorosaur” *Prolacerta broomi* is considerably less closely related to Archosauriformes than was previously considered.

Introduction

Non-archosauriform archosauromorphs lived during the Late Permian and Triassic and belong to the archosaurian stem-lineage, the ancestral lineage of crocodylians and birds. Historically, many members of this group were placed within either “Protorosauria” or “Prolacertiformes”. These two groups generally encompassed the same taxa and the usage of one term over the other depended on the inclusion within the clade of either *Protorosaurus speneri* or *Prolacerta broomi*, or both. Since both names generally apply to the same taxa and are often used interchangeably, and because “Protorosauria” Huxley 1871 predates “Prolacertiformes” Camp 1945, we refer to the members of these groups here as “Protorosauria” (sensu Chatterjee 1986). Apart from the two above mentioned taxa, the terrestrial and aquatic long-necked tanystropheids (e.g. *Tanystropheus*, *Macrocnemus*, *Langobardisaurus*, and *Tanytrachelos*) represent the most important and widely included members of “Protorosauria”. Formerly, the enigmatic arboreal drepanosaurids were also referred to the clade, but they have recently been revealed to represent a separate clade of non-saurian diapsids (Pritchard & Nesbitt 2017; Pritchard et al. 2016). As Permo-Triassic non-archosauriform archosauromorphs, “protorosaurs” represent some of the earliest members of the archosaur-lineage and as such are important both for our understanding of early archosauromorph evolution and the acquisition of traits within the archosaur character complex. For instance, the Chinese dinocephalosaurids represent the only known viviparous archosauromorphs (Li et al. 2017b; Liu et al. 2017).

Recent cladistic studies have extensively dealt with early archosauromorph phylogeny (early Archosauria, Nesbitt 2011; early Archosauromorpha with a focus on proterosuchids, Ezcurra 2016; Allokotosauria, Nesbitt et al. 2015; Rhynchosauria, Butler et al. 2015 and Ezcurra et al. 2016; and Tanystropheidae, Pritchard et al. 2015). These, and some earlier analyses, indicate that “Protorosauria” does not form a monophyletic clade as historically considered, but rather represents a paraphyletic or polyphyletic grouping of non-archosauriform archosauromorphs (Fig. 1, but for an exception see Simões et al. 2018, who recovered Protorosauria excluding *Prolacerta* as a monophyletic clade outside Archosauromorpha). However, none of these analyses were constructed to specifically address the interrelationships of “Protorosauria” and many recently described taxa (e.g. the genera *Pectodens*, *Fuyansaurus*, *Dinocephalosaur*, *Raiblianina*, *Elessaurus*, and *Sclerostropheus*) attributed to the group have not been included (Dalla Vecchia 2020; De Oliveira et al. 2020; Fraser et al. 2013; Li et al. 2017a;

Rieppel et al. 2008; Spiekman & Scheyer 2019). Moreover, the two best known tanystropheid genera, *Tanystropheus* and *Macrocnemus*, were recently revised extensively, revealing much additional morphological information, particular with regards to the skull, which has not been incorporated in the abovementioned analyses (Miedema et al. 2020; Spiekman et al. 2020).

Here we present an extensive phylogenetic analysis, focusing on “protorosaur” and other early archosauromorph interrelationships. The new dataset includes 42 operational taxonomic units (OTUs), of which 23 are “protorosaurs”, and employs 307 morphological characters, many of which are new or distinctly revised from previous analyses. Since the definition of “Protorosauria” in the literature is inconsistent, with many taxa having been placed alternately within and outside the group, we first provide a historical overview of “protorosaur” systematics and discuss the taxa that have formerly been included in the group. Several of these are represented by very fragmentary material or have since been identified as belonging to an entirely separate lineage to that of the archosauromorph “protorosaurs”, and they were therefore not included in the phylogenetic analysis.

Historical background of “Protorosauria”

Protorosaurus speneri was one of the earliest known fossil reptiles, first described in Latin by Spener (1710). He considered *Protorosaurus* to be a crocodile, with many similarities specifically to the Nile crocodile, *Crocodylus niloticus* (Gottmann-Quesada & Sander 2009). More than a century later, *Protorosaurus* was recognized as an extinct reptile (Meyer 1830), and subsequently assigned a species definition (Meyer 1832), and covered in an extensive monograph (Meyer 1856). The clade “Protorosauria”, with *Protorosaurus* as the only representative, was erected by Huxley (1871), as part of Sauropsida, then as now considered to be the clade that encompasses all modern birds and reptiles and their direct ancestors. In his classification of the reptiles, Osborn (1903) provided the first definition of “Protorosauria” and assigned *Palaeohatteria*, a synapsid (Fröbisch et al. 2011), and *Kadaliosaurus*, an araeoscelid diapsid (DeBraga & Reisz 1995), to the clade. Therein, the group was closely related to dinosaurs. Williston (1925) placed “protorosaurs” within “Parapsida” alongside squamates, ichthyosaurs, and mesosaurs. Other genera that were included within “Protorosauria” were *Sapheosaurus* and *Pleurosaurus*, now firmly established rhynchocephalians (Hsiou et al. 2019; Rauhut et al. 2012), and *Araeoscelis* and *Aphelosaurus*, now considered to be early non-neodiapsid diapsids (Ezcurra et al. 2014; Reisz et al. 2011b).

After extensive excavations at the Anisian-Ladinian deposits of Monte San Giorgio on the border between Switzerland and Italy, newly discovered specimens allowed for the first comprehensive description of both *Tanystropheus longobardicus* and *Macrocnemus bassanii* (Peyer 1931; Peyer 1937). Initially *Tanystropheus longobardicus* was placed within a newly erected suborder “Tanysitrachelia”, which apart from *Tanystropheus* also included *Trachelosaurus fischeri*, a small, long-necked reptile from the Buntsandstein (Early to Middle Triassic) of Germany (Broili & Fischer 1918). “Tanysitrachelia” was placed within Sauropterygia (Peyer 1931). *Trachelosaurus* is only known from a few disarticulated postcranial elements and therefore its phylogenetic position is uncertain, although it is currently still considered a “protorosaur” (Benton & Allen 1997; Jalil 1997; Rieppel et al. 2003). However, in the later report on *Macrocnemus bassanii*, Peyer (1937) found many comparisons between *Protorosaurus* and both *Macrocnemus* and *Tanystropheus*, and therefore both taxa were reassigned to “Protorosauria”, which was considered closely related to squamates and rhynchocephalians rather than archosaurs therein.

Around the same time *Prolacerta broomi* was described and assigned to the newly erected family “Prolacertidae” (Parrington 1935). “Prolacertidae” was classified as part of “Thecodontia”, a group that was at the time considered either as a “primitive” lineage within Archosauria (Watson 1917), or both ancestral to archosaurs and lepidosaurs (Broom 1914). “Thecodontia” is now unequivocally a paraphyletic grouping and has been abandoned as a clade (Benton 2005). However, based on its incomplete infratemporal bar, *Prolacerta* was considered to be intermediate between “lacertilians” (i.e. squamates) and more “primitive thecodonts” such as *Youngina capensis* (Parrington 1935). The description of a new specimen of *Prolacerta* led to the consideration that it was more closely related to *Protorosaurus* and resulted in the first inclusion of *Prolacerta* into “Protorosauria” (Camp 1945). Camp (1945) favored “Protorosauria” over “Eosuchia” based on seniority, and included taxa placed in “Eosuchia”, “Trachelosauria”, and “Protorosauria” by Williston (1925) within this clade and established it within Lepidosauria. This superorder “Protorosauria” was further subdivided in the orders “Prolacertiformes”, which he synonymized with “Eosuchia” (sensu Broom 1914, meaning it also included Younginiformes), “Trachelosauria” or Tanystropheidae, and, more tentatively, Thalattosauria and “Acrosauria” (the latter containing the rhynchocephalian pleurosaurids).

Kuhn-Schnyder (1954) defined the Middle Triassic *Macrocnemus* and *Tanystropheus* as squamates (German: Eidechsen, which literally translates to lacertids) that were morphologically intermediate between the Jurassic squamates and the supposed “squamate ancestor” *Prolacerta*.

Protorosaurus was not considered, since this interpretation was based mainly on skull anatomy, which was insufficiently understood in *Protorosaurus* at this point. This hypothesis differed from that of Colbert (1945; 1965) and Romer (1956; 1966; 1968), who considered “protorosaurs” as “Euryapsida” (sometimes also called “Synaptosauria”; Cope 1900), a clade which consisted of “protorosaurs” and sauropterygians, thus being similar to Sauropterygia as defined previously by Peyer (1931). This classification, which represented an important systematic paradigm for reptiles, was largely based on the temporal fenestration of the skull. “Euryapsids” were considered as a group that was entirely separate from “anapsids”, synapsids, and diapsids, based on the presence of an upper temporal fenestra, surrounded by the postorbital, squamosal, and parietal, and the absence of a lower temporal fenestra. The inclusion of “protorosaurs” within “euryapsids” was mainly based on *Araeoscelis*, which shows this fenestration type, in contrast to other “protorosaurs” that show the typical diapsid condition. Among others, the “Protorosauria” of Romer (1966) included *Protorosaurus*, *Tanystropheus*, *Trachelosaurus*, and *Trilophosaurus* (currently considered an allokotosaur within non-archosauriform Archosauromorpha; Ezcurra 2016; Nesbitt et al. 2015; Sengupta et al. 2017; Spielmann et al. 2008) within “Protorosauria”. On the other hand, *Prolacerta* and *Macrocnemus* were assigned to “Prolacertiformes” within “Eosuchia”, interpreted as the ‘basalmost’ order of Lepidosauria (“Eosuchia” was maintained contra Camp 1945). “Euryapsida” has generally not been used as a grouping in recent years, and its former members are now distributed within Diapsida (Benton 2005; Merck 1997). Furthermore, an extensive redescription of *Araeoscelis* has shown various differences with taxa such as *Protorosaurus* and *Prolacerta* (Vaughn 1955), and it is now considered an early diapsid that it is not closely related to “protorosaurs” (Ford & Benson 2020). The hypothesis of “Euryapsida” comprised of Sauropterygia and “Protorosauria” was criticized by Kuhn-Schnyder (1963; 1967; 1974). Kuhn-Schnyder (1967) and Wild (1973) argued that because of the ventrally opened lower temporal bar of *Macrocnemus* and *Tanystropheus*, “Protorosauria”, including *Protorosaurus*, belonged to “Prolacertidae” within Lepidosauria.

Based on new material, *Prolacerta* was extensively redescribed by Gow (1975), which included the first detailed description of postcranial remains. This study was the first to conclude that *Prolacerta*, together with *Macrocnemus* and *Tanystropheus*, was clearly not part of the lepidosaurian lineage, but instead was archosaurian in many of its features. These taxa were grouped in the newly erected order “Parathecodontia”, with *Prolacerta* and *Macrocnemus* being further classified together within “Prolacertidae” and *Tanystropheus* within Tanystropheidae. Nevertheless, the need for a detailed phylogenetic re-examination of these taxa was stressed and this revision did not consider *Protorosaurus*.

In the 1970s and the subsequent two decades, a considerable number of taxa were included within “Protorosauria”, further indicating the significance of the group: *Tanytrachelos ahynis* (Olsen 1979), *Langobardisaurus pandolfii* (Bizzarini & Muscio 1995), *Cosesaurus aviceps* (originally considered an avian ancestor; Ellenberger & De Villalta 1974, but later designated as a “protorosaur” by Olsen 1979), *Malerisaurus robinsonae* (Chatterjee 1980), *Kadimakara australiensis* (Bartholomai 1979), *Prolacertoides jimusarensis* (Young 1973), *Malutinisuchus gratus* (Otschev 1986), and *Boreopricea funerea* (Tatarinov 1978). In addition, “Protorosauria” as designated by Evans (1988) included *Megalancosaurus preonensis*, a member of the Drepanosauridae, a family of highly specialized, arboreal diapsids (Calzavara et al. 1980; Pritchard et al. 2016; Renesto et al. 2010). Chatterjee (1980) also included the Carboniferous *Petrolacosaurus kansensis* within “Prolacertiformes”, although this view was swiftly disputed (Evans 1988; Reisz et al. 1984), and *Petrolacosaurus* is now widely considered an araeoscelid diapsid instead (Ezcurra et al. 2014; Ford & Benson 2020; Reisz et al. 2011b).

Cladistics became widespread as a method for establishing phylogenetic relationships between taxa during the 1980s and its implementation on diapsid phylogeny quickly led to a relatively clear-cut division between Lepidosauromorpha and Archosauromorpha, with “Protorosauria” firmly established within the latter group (Bennett 1996; Benton 1984; Benton 1985; Evans 1988; Gauthier 1984; Gauthier 1994; Gauthier et al. 1988b). Chatterjee (1986) pointed out the priority of “Protorosauria” over “Prolacertiformes” based on seniority, but since “Protorosauria” had previously often included *Araeoscelis* and was therefore shown to be polyphyletic, many authors since preferred “Prolacertiformes” (see Evans 1988, pages 226-227 for an overview of the use of both terms within the literature between 1945 and 1988). However, although the place of “protorosaurs” among Archosauromorpha became firmly established, the interrelationships of the various “protorosaurs” was not evaluated cladistically except for Chatterjee (1986) and Evans (1988). Olsen (1979) and Wild (1980a) also provided a hypothesis of “protorosaur” interrelationships on a non-cladistic basis.

This issue would soon be addressed in more detail in several papers. One study included 11 “protorosaurs” (excluding the poorly known *Prolacertoides*) and three outgroups and 48 morphological characters (Benton & Allen 1997). In the same year, the description of a new “protorosaur”, *Jesairosaurus lehmani*, was accompanied by an analysis including ten protorosaurs and eight outgroup taxa, employing 71 characters (Jalil 1997; the initial analysis also included *Trachelosaurus*, *Prolacertoides*, *Malutinisuchus*, and *Kadimakara*, but these poorly known taxa were excluded from the final analysis, as the inclusion of these taxa left “protorosaurs” unresolved). Another study addressing

early archosauromorph phylogeny also included several “protorosaurs” (Dilkes 1998). This analysis included 144 characters and 23 taxa, out of which seven were traditionally considered as “protorosaurs”, including two drepanosaur taxa, which were not included in Benton & Allen (1997) and Jalil (1997). It recovered a monophyletic “Protorosauria” in which *Protorosaurus* formed a sister taxon to two lineages, Drepanosauridae and Tanystropheidae, whereas *Prolacerta* was placed outside the clade as the sister taxon of Archosauriformes. Peters (2000) used the matrices of Evans (1988), Jalil (1997), and Bennett (1996) and reran each of them after adding a number of characters and rescored some characters for certain taxa, for a total taxon sample that included 11 “protorosaurs”, other non-archosauriform archosauromorphs, the pterosaur *Eudimorphodon*, and two enigmatic and possibly gliding diapsids, *Longisquama insignis* (Sharov 1970) and *Sharovipteryx mirabilis* (Cowen 1981; Sharov 1971). *Sharovipteryx* is an enigmatic gliding reptile with a membrane stretched between the hindlimbs, which represents an entirely unique morphology among gliding reptiles. It has very tentatively been ascribed to “protorosaurs” or tanystropheids by some authors (Gans et al. 1987; Pritchard & Sues 2019; Tatarinov 1989; Tatarinov 1994; Unwin et al. 2000), but its phylogenetic position is highly uncertain due to its highly specialized, yet very poorly known morphology. Peters (2000) found that the “protorosaurs”, and *Longisquama* and *Sharovipteryx*, to be very closely associated with *Eudimorphodon*, from which a “protorosaurian” ancestry for pterosaurs was concluded. However, the exact topologies varied strongly between the different analyses, and this hypothesis of pterosaur ancestry has widely been rejected by other pterosaur and archosaur studies (e.g. Hone & Benton 2007; Nesbitt 2011; Padian 1997). The datasets of Benton & Allen (1997), Dilkes (1998), and Jalil (1997) were combined into one larger character list of 239 characters by Rieppel et al. (2003), which was used specifically to address “protorosaur” phylogeny, and in particular the question of “protorosaur” monophyly, which had now been put in doubt (Dilkes 1998). This approach included seven “protorosaur” taxa (*Protorosaurus*, *Drepanosaurus*, *Megalancosaurus*, *Prolacerta*, *Macrocnemus*, *Langobardisaurus*, and *Tanystropheus longobardicus*), and four outgroup taxa (*Petrolacosaurus*, *Youngina*, *Rhynchosaurus*, and *Trilophosaurus*). Additional analyses were performed after subsequently including *Euparkeria* and *Proterosuchus*, and the lesser known “protorosaurs” *Boreoprincea* and *Jesairosaurus*. Although the first analysis found a monophyletic “Protorosauria”, the other two resulted in a paraphyly. Although Rieppel et al. (2003) concluded that the monophyly of “Protorosauria” as previously regarded (e.g. Benton & Allen 1997; Jalil 1997) could not be maintained, they argued the need for an extensive phylogenetic investigation into “protorosaurs”. Senter (2004) investigated the phylogenetic position of drepanosaurs in an analysis that comprised “protorosaurs” (*Prolacerta*, *Macrocnemus*, and *Langobardisaurus*),

Longisquama, non-archosaurian Archosauriformes, birds, a non-avian dinosaur, and a number of early diapsids. This study found drepanosaurs to form a clade with *Longisquama* and *Coelurosauravus*, which was termed “Avicephala”, as the sister group to Neodiapsida, which in his analysis encompassed *Youngina*, the rhynchocephalian *Gephyrosaurus*, and several archosauromorphs. The included “protorosaurs” formed a monophyletic clade within Archosauromorpha. However, an analysis using the same character list by Renesto & Binelli (2006) could not reproduce the same topology. Renesto et al. (2010) reaffirmed the position of drepanosaurs among “protorosaurs”, whereas Pritchard & Nesbitt (2017) recovered Drepanosauromorpha as a separate clade of non-saurian diapsids. Müller (2004) included four different “protorosaur” taxa in his broad-scale analysis of diapsid relationships, which consisted of 184 characters compiled mainly from Rieppel et al. (1999) and DeBraga & Rieppel (1997). This study also inferred a polyphyletic “Protorosauria”, with *Tanystropheus*, *Macrocnemus*, and *Prolacerta* being successive sister taxa to rhynchosaurs and *Trilophosaurus*, whereas drepanosaurs were only quite distantly related to these taxa.

“Protorosaurs” were virtually unknown from China until about 15 years ago, with the exception of the tentative “protorosaur” *Prolacertoides jimusarensis* (Young 1973). However, a number of new finds have been referred to “Protorosauria”, including *Tanystropheus* cf. *longobardicus* (Rieppel et al. 2010; now *Tanystropheus* cf. *hydroides*, see Spiekman et al. 2020), *Tanystropheus* sp. (Li 2007), and *Macrocnemus fuyuanensis* (Jiang et al. 2011; Li et al. 2007), forms very similar to European counterparts, as well as completely new taxa, such as *Dinocephalosaurus orientalis* (Li 2003; Li et al. 2004; Liu et al. 2017; Rieppel et al. 2008), *Fuyansaurus acutirostris* (Fraser et al. 2013), an unnamed taxon closely related to *Dinocephalosaurus* (Li et al. 2017b), and potentially *Pectodens zhenyuensis* (Li et al. 2017a). This has revealed that “protorosaurs” had a Tethys-wide distribution and are considerably more morphologically diverse than previously appreciated. Except for *Dinocephalosaurus orientalis*, which has been included in phylogenetic analyses of Rieppel et al. (2008), Liu et al. (2017), and De Oliveira et al. (2020), none of the Chinese taxa have been phylogenetically assessed so far.

But new “protorosaur” findings have also been reported from outside of China. Fraser & Rieppel (2006) re-examined the “*Tanystropheus antiquus*” material from the Upper Buntsandstein of Baden-Württemberg, Germany, and assigned it to a new taxon, *Amotosaurus rotfeldensis*. Furthermore, Gottmann-Quesada & Sander (2009) provided a monograph on the German *Protorosaurus speneri* material, including the first detailed description and reconstruction of the skull, based on the first discovery of a well-preserved skull in 1972, which previously had only been briefly documented (see

Haubold & Schaumberg 1985 p. 223; Fichter 1995 and references therein). Gottmann-Quesada & Sander (2009) also provided a phylogenetic analysis, which employed the matrix of Dilkes (1998), with several modifications to the character scoring of *Mesosuchus*, *Prolacerta*, and *Protorosaurus*. This resulted in a tree with a polyphyletic “Protorosauria” that recovered *Protorosaurus* as the sister taxon to *Megalancosaurus*. A new species of *Macrocnemus*, *Macrocnemus obristi*, has been described from Alpine Europe (Fraser & Furrer 2013), and a specimen from Monte San Giorgio on the border of Switzerland and Italy was recently assigned to *Macrocnemus fuyuanensis*, the species of *Macrocnemus* which was previously only known from China (Jaquier et al. 2017; Scheyer et al. 2020b). A new species of *Tanystropheus*, *Tanystropheus hydroides*, has also been described from Monte San Giorgio (Spiekman et al. 2020). This new species was previously considered to represent the adult stage of *Tanystropheus longobardicus* (Wild 1973), but long bone histology revealed that the small specimens of *Tanystropheus longobardicus* were skeletally mature, thus representing a separate species from *Tanystropheus hydroides*. Two poorly known new protorosaurs have been reported from Russia based on limited, isolated remains, the large-sized *Vrtramimosaurus dzerzhinskii*, considered to be closely related to *Prolacerta* (Sennikov 2005), and *Augustaburiania vatagini*, a medium-sized tanystropheid (Sennikov 2011). From Poland two new, possibly “protorosaur”, archosauromorphs have been described. *Czatkowiella harae* has been interpreted as being closely related to *Protorosaurus* (Borsuk-Białynicka & Evans 2009b), whereas the highly gracile, and putative glider, *Ozimek volans* is similar to *Sharovipteryx* (Dzik & Sulej 2016). Ezcurra et al. (2014) re-examined material consisting of five vertebrae, three fragmented forelimb elements, and some indeterminable fragments from the Late Permian of Tanzania previously described by Parrington (1956) and assigned it to the new taxon *Aenigmastropheus*. Following an analysis modified from Reisz et al. (2010), used to address both synapsid and diapsid affiliations, it was recovered among “protorosaurs” as the sister taxon to *Protorosaurus*. In addition, they found *Eorasaurus*, previously assigned as a “protorosaur” by Sennikov (1997), to likely be an archosauriform, which would make *Aenigmastropheus* the second known “protorosaur” and non-archosauriform archosauromorph from the Permian. Two more tanystropheid genera, *Sclerostropheus fossai* and *Raibliania calligarisi* were recently identified, based on partial postcranial remains (Dalla Vecchia 2020; Spiekman & Scheyer 2019). Finally, recent findings have shone more light on the occurrence and distribution of tanystropheids in the Americas. Isolated material from the Middle and Late Triassic North America, largely consisting of cervical vertebrae, as well as some other postcranial remains, indicate that tanystropheids were more widespread and also occurred until more recently than previously thought (Formoso et al. 2019; Lessner et al. 2018; Pritchard et al. 2015; Sues & Olsen 2015).

From South America, some likely tanystropheid remains from the Induan to early Olenekian of Brazil have been reported (De Oliveira et al. 2018; De Oliveira et al. 2020), which, if indeed tanystropheids, would represent among the earliest records of the clade, and would indicate a wide, if not nearly cosmopolitan distribution of the clade during the Early Triassic.

The original phylogenetic matrices by Pritchard et al. (2015) and Ezcurra (2016), and their subsequently modified iterations (e.g. Butler et al. 2019; Ezcurra & Butler 2018; Ezcurra et al. 2017; Nesbitt et al. 2017a; Nesbitt et al. 2015; Pritchard et al. 2018; Pritchard & Nesbitt 2017; Pritchard & Sues 2019; Scheyer et al. 2020a; Sengupta et al. 2017; Stocker et al. 2017), represent the two separate datasets that most comprehensively addressed “protorosaur” relationships. The former focused specifically on tanystropheid relationships. It found *Protorosaurus* as the sister taxon to all other archosauromorphs, whereas *Prolacerta* formed the sister taxon to Archosauriformes. Tanystropheidae was recovered as a monophyletic clade and consisted of *Macrocnemus*, *Amotosaurus*, *Tanystropheus*, *Langobardisaurus*, *Tanytrachelos*, and the new Hayden Quarry material that was presented therein. The character list consisted of 200 characters, including novel characters and characters derived from many previous analyses (Benton 1985; Benton & Allen 1997; Conrad 2008; DeBraga & Rieppel 1997; Dilkes 1998; Gauthier 1984; Gauthier et al. 1988a; Gauthier et al. 1988b; Hutchinson et al. 2012; Jalil 1997; Merck 1997; Modesto & Sues 2004; Müller 2004; Nesbitt 2011; Rieppel 1994). Ezcurra (2016) presented a very extensive analysis of early archosauromorph interrelationships that used 600 characters to analyze 96 taxa. Out of these characters, 96 were new. The remaining characters were compiled from the literature (mainly Desojo et al. 2011; Dilkes 1998; Dilkes & Arcucci 2012; Ezcurra et al. 2015; Ezcurra et al. 2010; Ezcurra et al. 2014; Gower & Sennikov 1996; Gower & Sennikov 1997; Jalil 1997; Nesbitt 2011; Nesbitt et al. 2015; Parrish 1992; Pritchard et al. 2015; Senter 2004; Trotteyn & Ezcurra 2014). Like Pritchard et al. (2015), it found *Protorosaurus* to be the sister taxon to all other archosauromorphs and *Prolacerta* to be the sister taxon to Archosauriformes. *Boreopricea* was found as the sister taxon to *Prolacerta* + Archosauriformes and *Jesairosaurus* formed the sister to a monophyletic Tanystropheidae, made up of *Macrocnemus*, *Amotosaurus*, and *Tanystropheus*.

Overview of “protorosaur” taxa

In the following, an overview is provided of taxa which have been attributed to “Protorosauria”, but which have not been included in the present analysis, since they are either represented by insufficient material for inclusion or because it is now widely considered that they are not closely related to *Protorosaurus speneri*, *Prolacerta broomi*, or Tanystropheidae.

Aenigmastropheus parringtoni Ezcurra, Scheyer & Butler 2014. *Aenigmastropheus parringtoni* is known from one specimen, UMZC T836, from the Wuchiapingian (middle Late Permian) of Tanzania. It comprises five cervical and dorsal vertebrae, the distal part of a right humerus, the proximal part of the right ulna, and a number of small fragments. The specimen was first described by Parrington (1956), and was considered to be insufficiently preserved for a confident taxonomic diagnosis. However, it was noted that its morphology contained both primitive diapsid traits as well as archosaurian characteristics. The specimen was recently revised and assigned to a new taxon, which was recovered as the sister taxon to *Protorosaurus speneri* in a cladistic analysis (Ezcurra et al. 2014).

Kadimakara australiensis Bartholomai 1979. *Kadimakara australiensis* is known from two partial skulls first described by Bartholomai (1979). The holotype is represented by the postorbital region, whereas the other specimen comprises a partial snout. Although both specimens do not have any shared preserved regions, they were attributed to the same taxon based on their similar size and shared close similarity to *Prolacerta broomi*. The validity of *Kadimakara australiensis* has been questioned and Borsuk-Białynicka & Evans (2009b) and Evans & Jones (2010) considered the specimens to be congeneric with *Prolacerta broomi*. Ezcurra (2016) corroborated the close affinity of *Kadimakara australiensis* to *Prolacerta broomi*, but only considered the holotype in the revised diagnosis of the taxon therein, since the lack of overlapping morphology precludes the direct comparison between the holotype and referred specimen. Ezcurra (2016) argued in favour of the validity of *Kadimakara australiensis*, pointing out a medial fossa on the posterior half of the parietals as a distinguishing feature between this species and *Prolacerta broomi*. However, other distinguishing features indicated by Bartholomai (1979) were revealed to result from an erroneous interpretation of the morphology of the postorbital bar. *Kadimakara australiensis* originates from the lower beds of the upper part of the Arcadia Formation, central Queensland, Australia, which are of Induan (earliest Triassic) age.

Megacnemus grandis Huene 1954. *Megacnemus grandis* was described based on one isolated long bone exceeding 20 cm in length, which was identified as a femur (Huene 1954). It is likely from the Gogolin Formation of southwest Poland, which is lower Anisian (Middle Triassic) in age (Skawiński et al. 2017). Skawiński et al. (2015) re-examined the specimen and corroborated its “protorosaurian” affinities. However, they also considered the possibility that the specimen represents a humerus rather than a femur, and therefore only identified the bone as a propodial. It has not been included in any phylogenetic analyses due to its extremely poorly known morphology.

Prolacertoides jimusarensis Young 1973. *Prolacertoides jimusarensis* is known from a single, poorly preserved skull (IVPP V3233) and represents the first described *protorosaur* from China, which was considered to be closely related to *Prolacerta broomi* (Young 1973). Ezcurra (2016) provided a more detailed osteological description of the holotype in English, but *Prolacertoides jimusarensis* was omitted from the final analysis therein, due to a lack of preserved morphological characters, which resulted in its inclusion reducing the reliability of the analysis. In analyses 1 and 2 of Ezcurra (2016), which included *Prolacertoides* and other poorly represented taxa, *Prolacertoides jimusarensis* was positioned in a large polytomy including most early archosauromorphs with *Protorosaurus speneri* as the sister taxon. *Prolacertoides jimusarensis* has previously been included phylogenetically in Benton & Allen (1997), Evans (198), Jalil (1997), and Rieppel et al. (2003). Notably, Benton & Allen (1997) retrieved *Prolacertoides jimusarensis* as being the sister taxon to *Trilophosaurus buettneri* and to thus fall outside of the traditional “Protorosauria”. However, its exact phylogenetic affiliations were questioned by all authors due to a lack of morphological information for the taxon.

Rhombopholis scutulata Owen 1842. *Rhombopholis scutulata* was originally described as an amphibian (Owen 1842). It is represented by a single block that contains a number of postcranial bones, including four vertebrae, a number of ribs, and five limb elements that belong to at least two individuals Benton & Walker (1996). In a revision of the reptile material from the Keuper Sandstone Group of England (Anisian, Middle Triassic), this specimen, as well as a number of other specimens, was considered as being closely related to *Macrocnemus bassanii* (Walker 1969). Benton & Walker (1996) provided a redescription of *Rhombopholis scutulata*, and identified it as a “prolacertiform” metataxon, meaning that no autapomorphies could be assigned to it to distinguish it from other “prolacertiforms” and that the different specimens possibly belong to more than one taxon. Thus, the block attributed to *Rhombopholis scutulata* might also include various “prolacertid” remains that only potentially belong to one taxon.

Sharovipteryx mirabilis Sharov 1971. A virtually complete but poorly preserved specimen with long and gracile hindlimbs with an apparent skin membrane present between the legs was initially described as *Podopteryx mirabilis* and interpreted as a gliding reptile (Sharov 1971). However, because the name *Podopteryx* was already occupied by a genus of damselflies, the taxon was renamed *Sharovipteryx mirabilis* by Cowen (1981). *Sharovipteryx mirabilis* was described in detail by Gans et al. (1987). Although the phylogenetic position of *Sharovipteryx mirabilis* is exceedingly hard to assess due to the lack of visible morphological details, it has been incorporated in “Protorosauria” by various authors (e.g. Ivakhnenko & Kurochkin 2008; Peters 2000; Unwin et al. 2000).

Cosesaurus aviceps Ellenberger & De Villalta 1974. *Cosesaurus aviceps* is known from a single specimen, which represents an impression of a complete skeleton. As such, the outline of the specimen is well-preserved, but the detailed morphology of the taxon is very poorly known. The specimen was found at the Montral-Alcover outcrop (Ladinian, Middle Triassic), Sierra de Prades, Tarragona province, Spain. Due to the lack of morphological information, the phylogenetic affinities of *Cosesaurus aviceps* are unclear. It was initially thought to represent an ancestor to birds (Ellenberger 1977; Ellenberger 1978; Ellenberger & De Villalta 1974). However, the now widely accepted view that birds represent a derived clade of theropod dinosaurs refutes this hypothesis. *Cosesaurus aviceps* was redescribed by Sanz & López-Martínez (1984), and considered to bear many similarities to various “protorosaurs”. *Cosesaurus aviceps* has also been found among “protorosaurs” in subsequent phylogenetic analyses (Benton & Allen 1997; Evans 1988; Jalil 1997; Rieppel et al. 2003). In a widely criticized reinterpretation of previous analyses (e.g. Hone & Benton 2007) it was concluded that Pterosauria are a derived lineage with “Prolacertiformes”, which was largely based on several morphological characters observed in *Cosesaurus aviceps*, as well as the poorly known, gracile reptiles *Sharovipteryx mirabilis* and *Longisquama insignis* (Peters 2000). Although *Cosesaurus aviceps* might represent a “protorosaur”, the lack of morphological information does not allow this taxon to be reliably incorporated in phylogenetic analyses, and recent phylogenetic investigations into archosauromorph or “protorosaurian” affinities did not consider this taxon.

Vritramimosaurus dzerzhinskii Sennikov 2005. The holotype of *Vritramimosaurus dzerzhinskii* is a single cervical vertebra, and referred material comprises another cervical vertebra, a caudal vertebra, and two fragmentary vertebrae. They were originally discovered in 1953 and 1954 by B.P. Vjuschkov. *Vritramimosaurus dzerzhinskii* has been described as a “large, specialized prolacertilian” (Sennikov 2005). The material originates from the Rassypnaya locality of the Petropavlovka Formation, Orenburg Region, Russia, which is of uppermost Olenekian (Early Triassic) age. Its estimated overall body size is at least three meters, making *Vritramimosaurus dzerzhinskii* one of the larger early archosauromorphs and considerably larger than *Prolacerta broomi*, to which it is considered to be closely related (Sennikov 2005). However, the limited and fragmentary material allows for only a very ambiguous comparison with other taxa and the taxon has therefore not been included in phylogenetic analyses.

Malerisaurus robinsonae Chatterjee 1980 and *Malerisaurus langstoni* Chatterjee 1986. *Malerisaurus robinsonae* is known from two individuals that are part of the stomach contents of a specimen of the phytosaur *Parasuchus hislopi* from the Maleri Formation (Carnian to Early Norian, early Late Triassic) of central India (Chatterjee 1980). Another specimen from the Tecovas Member, lower Dockum Formation

of western Texas, US, (Carnian, early Late Triassic) was recognized as representing a taxon that was very closely related to *Malerisaurus robinsonae* and assigned to *Malerisaurus langstoni* (Chatterjee 1986). However, this holotype and only known specimen is actually composed of elements belonging to several diapsid taxa, most notably *Trilophosaurus buettneri* (Spielmann et al. 2006). Therefore, *Malerisaurus langstoni* is no longer considered a valid taxon. Furthermore, the validity of the Indian *Malerisaurus robinsonae* was questioned, as this taxon also showed distinct similarities to *Trilophosaurus buettneri* (Spielmann et al. 2006). Following the original interpretation by Chatterjee (1980; 1986) of *Malerisaurus robinsonae* as a “protorosaur” closely related to *Protorosaurus speneri*, it has been incorporated in phylogenetic analyses (Benton 1985; Benton & Allen 1997; Evans 1988; Jalil 1997; Rieppel et al. 2003). *Malerisaurus robinsonae* was removed from the final analyses due to insufficient character preservation in Benton (1985) and Rieppel et al. (2003), whereas it was retrieved as part of a polytomy within Archosauromorpha by Evans (1988). Benton & Allen (1997) included only *Malerisaurus langstoni* in the final analysis and found it as the sister taxon to all included “protorosaurs” except *Protorosaurus speneri*, *Prolacerta broomi*, and *Boreopricea funerea*. Finally, Jalil (1997) included both *Malerisaurus* species as a single OTU and found it to be the sister taxon to *Jesairosaurus lehmani*. *Malerisaurus* spp. have not been included in any of the recently published phylogenetic analyses of early archosauromorphs. Recently, Nesbitt et al. (2017b) identified both *Malerisaurus* species as separate from *Trilophosaurus buettneri*, and considered them to belong to Allokotosauria, more specifically as a member of Azendohsauridae.

Malutinisuchus gratus Otschev 1986. *Malutinisuchus gratus* is a very poorly known taxon that has been considered a prolacertid. It is known from the Belyaevsky I, Bukobay Svita, Ladinian, Orenburg region, Russia (Otschev 1986; Tverdokhlebov et al. 2003). The known material comprises several fragmentary remains, including an elongated cervical vertebra, two partial limb bones, and likely pectoral girdle elements. *Malutinisuchus gratus* was incorporated into phylogenetic analyses by Jalil (1997) and Rieppel et al. (2003), but in both cases omitted from the final analysis due to lack of morphological information. In one of the trees recovered by Jalil (1997) *Malutinisuchus gratus* formed a polytomy with all other taxa forming the clade “Prolacertifomes” therein.

Boreopricea funerea Tatarinov 1978. *Boreopricea funerea* is known from a nearly complete specimen and an anterior end of a snout, collected from a borehole, number 141, at 1112.3 meters deep at Kolguyev Island in the Barents Sea. This borehole is part of the Vetluzhian Series (Induan, earliest Triassic; Benton & Allen 1997). The referred specimen is likely lost (Benton & Allen 1997). *Boreopricea funerea* was originally considered to represent an intermediate form between *Prolacerta broomi* and *Pricea longiceps*

(now considered a junior synonym of *Prolacerta broomi*), and *Macrocnemus bassanii* (Tatarinov 1978). The taxon was later redescribed in more detail by Benton & Allen (1997), who commented on the poor state of the specimen and the absence of certain elements described by Tatarinov (1978) as a consequence of damage that the holotype had sustained after this description, such as the crushing of the skull and the removal and in some cases disappearance of certain postcranial elements. Among these are the interclavicle and ossified sternum, which contained characters that were important in distinguishing *Boreopricea funerea* from other “protorosaurs”. Furthermore, because these elements were removed and later placed back on the card on which the specimen is kept, the identification of the tarsal bones is difficult and ambiguous (Rieppel et al. 2003). *Boreopricea funerea* has been included in several phylogenetic analyses (Benton & Allen 1997; Evans 1988; Ezcurra 2016; Jalil 1997; Rieppel et al. 2003) and an emended diagnosis has been provided by Ezcurra (2016). *Boreopricea funerea* was found as nested between *Prolacerta* and a clade comprising *Macrocnemus*, *Cosesaurus*, *Tanystropheus*, and *Tanytrachelos* (Evans 1988). In the phylogenetic analysis accompanying the redescription of the taxon, *Boreopricea funerea* represented the sister taxon to *Prolacerta* (Benton & Allen 1997). In the final tree of Jalil (1997) *Boreopricea funerea* was positioned between *Langobardisaurus* and a clade comprising *Cosesaurus*, *Tanystropheus*, and *Tanytrachelos*. In the various trees produced by Rieppel et al. (2003) the topology of *Boreopricea funerea* varied. In some cases it was positioned as closely related to *Protorosaurus* and in others as being more closely related to *Prolacerta*. Ezcurra (2016) recovered *Boreopricea funerea* as the sister taxon to the clade composed of *Prolacerta* and all Archosauriformes. Because personal observation was not possible due to the badly damaged skull, no cranial characters were scored in which Tatarinov (1978) and Benton & Allen (1997) were in disagreement by Ezcurra (2016).

Eorasaurus olsoni Sennikov 1997. *Eorasaurus olsoni*, one of the very few known Permian archosauromorphs, is known from several vertebrae. The taxon was originally considered to be most closely related to *Protorosaurus* and was therefore placed within “Protorosauridae” (Sennikov 1997). Ezcurra et al. (2014) provided additional observations and an emended diagnosis for *Eorasaurus olsoni*, and it was retrieved as an archosauriform that formed a trichotomy with *Euparkeria capensis* and *Erythrosuchus africanus* in the included phylogenetic analysis. *Eorasaurus olsoni* was also included by Ezcurra (2016) and formed a massive polytomy and the base Archosauriformes in the analyses 1 and 2 therein, but it was pruned from the final analysis due to insufficient morphology being currently known for the taxon.

Hayden Quarry tanystropheid. Recently a large number of postcranial elements with clearly tanystropheid affinities were described, encompassing vertebrae, femora, and a calcaneum (Pritchard et al. 2015). Because the material is represented by isolated elements, it is unclear whether they all belong to the same taxon, and thus it was thus not referred to any specific taxon. The calcaneum was shown to share apomorphies with that of *Tanytrachelos ahynis*, and was therefore assigned to this species. This material currently represents the only known tanystropheid material from western North America and is of approximately middle Norian age (Late Triassic; Irmis et al. 2011), thus being one of the later representatives of the tanystropheid clade. Although it was not concluded that the Hayden Quarry material represents a single taxon, a hypothetical Hayden Quarry taxon was included in the phylogenetic analysis of Pritchard et al. (2015), which recovered it as the sister taxon to the North American *Tanytrachelos ahynis*. Nevertheless, since the material represents only limited postcranial material, which furthermore cannot unequivocally be assigned to a single taxon, it is not considered for phylogenetic analysis here.

Vallesaurus cenensis Wild 1991. *Vallesaurus cenensis* is known from a single, well-preserved and complete specimen that was discovered in the Cene quarry, upper part of the Zorzino Limestone (Revueltian, early-middle Norian, Late Triassic), in Lombardy, Italy (Renesto & Binelli 2006). Wild (1991) mentioned the specimen and assigned it to the genus *Vallesaurus* but did not formally describe the specimen. The specimen (Renesto 2000) and species (Pinna 1993) were further referred to, and a formal description was provided by Renesto & Binelli (2006). *Vallesaurus cenensis* has additionally been compared to other drepanosaurs by Renesto et al. (2010). Therein, the new species *Vallesaurus zorzinensis* was included in the genus, which differs from *Vallesaurus cenensis* in having an opposable hallux with two phalanges, of which the first one is straight. *Vallesaurus cenensis* has been included in phylogenetic analyses (Pritchard & Nesbitt 2017; Pritchard et al. 2016; Renesto et al. 2010; Senter 2004). Drepanosaurs, such as *Vallesaurus cenensis*, are not included in the present analysis because they likely represent a separate lineage of reptiles outside of Archosauromorpha, and are therefore only distantly related to other “protorosaurs” (Pritchard & Nesbitt 2017).

Drepanosaurus unguicaudatus Pinna 1980. *Drepanosaurus unguicaudatus* was first described based on the holotype, which consists of a largely complete, articulated skeleton, missing the skull and anterior cervical vertebrae, and several juvenile specimens (Pinna 1980). This was followed by a more extensive description (Pinna 1984), and these findings were later summarized in English (Pinna 1986). Renesto (1994c) revised the morphology of *Drepanosaurus unguicaudatus*, especially regarding the highly

specialized forelimbs, and it was suggested that the juvenile specimens belong to *Megalancosaurus preonensis*. This suggestion was reinforced by Renesto (2000), who considered the holotype as the only known specimen of *Drepanosaurus unguicaudatus*, whilst a juvenile specimen (MCSNB 4783), previously described by Renesto & Paganoni (1995), was attributed to *Drepanosaurus* sp. A revised diagnosis and overview of the provenance of the species was provided in Renesto et al. (2010). Pritchard et al. (2016) described new remains from North America, which were assigned to *Drepanosaurus* sp., which provided new insight into the unique configuration of the grasping forelimb of the taxon. *Drepanosaurus unguicaudatus* has been included in several phylogenetic analyses (Dilkes 1998; Evans 1988; Pritchard & Nesbitt 2017; Pritchard et al. 2016; Renesto et al. 2010; Senter 2004).

Megalancosaurus preonensis Calzavara, Muscio & Wild 1980. *Megalancosaurus preonensis* is known from middle Norian Forni Dolostone of Friuli and Zorzino Limestone of Lombardy, Italy (Renesto et al. 2010). The holotype of *Megalancosaurus preonensis*, which comprises of a complete skull and cervical series, the expanded neural spines of the anterior dorsal vertebrae, several fragments of dorsal ribs, and a right forelimb, was described by Calzavara et al. (1980) and interpreted as an arboreal archosaur. Feduccia & Wild (1993) and Feduccia (1996) suggested that *Megalancosaurus preonensis* was possibly a glider and considered it to be closely related to birds, thus arguing that Triassic archosaurs, rather than theropod dinosaurs, are the sister group to birds. An additional specimen of *Megalancosaurus preonensis* was described, which provided new information on the postcranium of the taxon (Renesto 1994a). Additionally, three specimens that were previously identified as juvenile specimens of *Drepanosaurus unguicaudatus* (Pinna 1980), were re-assigned to the taxon as well (Renesto 1994a). The arboreal lifestyle suggested for *Megalancosaurus preonensis* was questioned by Padian & Chiappe (1998), which considered an aquatic lifestyle for the taxon. The hypothesis that drepanosaurs are the sister group to birds was refuted in a study that also assigned two additional specimens to the species (Renesto 2000). The skull of *Megalancosaurus preonensis* was redescribed in detail by Renesto & Dalla Vecchia (2005). A second species, *Megalancosaurus endennae*, was erected and two specimens that were previously identified as *Megalancosaurus preonensis* were re-assigned to this species (Renesto et al. 2010). *Megalancosaurus endennae* mainly differs from *Megalancosaurus preonensis* in the presence of an opposable hallux in the pes. Another specimen lacking the hindlimb, **MFSN 18443a**, was reassigned to *Megalancosaurus* sp. A functional interpretation of the forelimbs of *Megalancosaurus* spp. was provided by Castiello et al. (2016). *Megalancosaurus preonensis* has been included in several phylogenetic analyses (Benton & Allen 1997; Dilkes 1998; Evans 1988; Pritchard & Nesbitt 2017; Pritchard et al. 2016; Renesto et al. 2010; Senter 2004).

The following taxa are included as operational taxonomic units (OTUs) for the phylogenetic analysis:

Petrolacosaurus kansensis Lane 1945

Age. Late Missourian, late Pennsylvanian, Late Carboniferous.

Occurrence. Garnett Quarry, Rock Lake Member of the Stanton Formation, Kansas, USA (Reisz 1981; Reisz et al. 1982)..

Holotype. **KUVP 1424**, largely complete right hindlimb.

Hypodigm. The referred specimens are listed in (Reisz 1981, p. 4-5).

Diagnosis. The emended diagnosis is provided by Reisz (1981).

Remarks. *Petrolacosaurus kansensis* was first described based on a largely complete hindlimb (the holotype **KUVP 1424**) and pelvis, and identified as a pelycosaur (Lane 1945). Additional postcranial elements from the same locality were assigned to *Podargosaurus hibbardi* in the same study. Additional specimens, including skull material, revealed that *Podargosaurus* was indistinguishable from *Petrolacosaurus kansensis* and therefore its material was reassigned to the latter (Peabody 1952). The systematic position of *Petrolacosaurus kansensis* was disputed, but an additional specimen preserving the skull in more detail revealed it as an early diapsid reptile (Reisz 1977) and it has been described in detail by Reisz (1981). *Petrolacosaurus kansensis* represents one of the best-known Carboniferous diapsids and as such has been widely used as an outgroup in studies on diapsid phylogeny (e.g. Dilkes 1998; Evans 1988; Ezcurra 2016; Ezcurra et al. 2014; Jalil 1997; Pritchard et al. 2015; Simões et al. 2018). A recent phylogenetic hypothesis of early amniotes suggests that the diapsid temporal configuration of *Petrolacosaurus kansensis* was likely independently acquired from that of neodiapsids, including saurians (Ford & Benson 2020).

Orovenator mayorum Reisz, Modesto & Scott 2011

Age. Earliest Artinskian, Early Permian (Cohen et al. 2013; Woodhead et al. 2010).

Occurrence. Claystone fissure fills in the Ordovician Arbuckle Limestone, Dolese Brothers Limestone Quarry, Richards Spur, Comanche County, Oklahoma, USA.

Holotype. **OMNH 74606**, a crushed partial skull missing several elements, including large parts of the skull roof and occipital region.

Hypodigm. **OMNH 74607**, a crushed partial skull preserving most of the skull roof, as well as an axial, postaxial, and caudal vertebra.

Diagnosis. The most recent diagnosis was provided by Ford & Benson (2018).

Remarks. *Orovenator mayorum* is an Early Permian reptilian, known from the Richards Spur locality, which represents a unique upland fissure fill deposit (Ford & Benson 2020; MacDougall et al. 2017; Sullivan et al. 2000). Therefore, it was hypothesized that early reptilians from this locality were adapted to an upland environment, and that this in turn would explain their rare occurrence in the fossil record in the Early and Middle Permian (Reisz et al. 2011a). Following the initial description and phylogenetic analysis including *Orovenator mayorum* by Reisz et al. (2011a), in which it was recovered as the sister-taxon to all other known neodiapsids, the taxon was redescribed by Ford & Benson (2018) based on μ CT scans. An extensive recent phylogenetic analysis recovered *Orovenator mayorum* as a member of Varanopidae, a clade historically considered to belong to Synapsida, but which was here found on the reptilian lineage outside Neodiapsida (Ford & Benson 2020). The cranial morphology suggests nocturnality and burrowing behavior in *Orovenator mayorum* (Ford & Benson 2018).

Acerosodontosaurus piveteaui Currie 1980

Age. Lopingian (roughly equivalent to the *Dicynodon* AZ of the Karoo Basin), Late Permian (Smith et al. 2012).

Occurrence. Sakamena River Valley, Lower Sakamena Formation, southern Madagascar (Currie 1980).

Holotype. **MNHN 1908-32-57**, a skeleton preserved partially as imprints in two slabs. The posterior half of the skull and mandibles are preserved. Of the postcranium, most of the dorsal vertebral series is preserved, as well as part of the forelimbs, the pelvis and sacral region, and hindlimbs.

Diagnosis. The most recent emended diagnosis is provided by Ezcurra (2016).

Remarks. *Acerosodontosaurus piveteaui* was first described by Currie (1980) and indicated to be closely related to *Youngina capensis*. A redescription of the only specimen of *Acerosodontosaurus piveteaui* revealed that the infratemporal bar is incomplete, in contrast to *Youngina capensis* (Bickelmann et al.

2009). An aquatic lifestyle has been suggested for *Acerosodontosaurus piveteaui*, which is supported by observed skeletal paedomorphosis of the carpal bones. In a phylogenetic analysis addressing the relationships of stem-turtles, *Acerosodontosaurus piveteaui* was recovered in a clade with *Claudiosaurus germaini* within Pantestudines as the sister group to all other members of this clade (Li et al. 2018).

Claudiosaurus germaini Carroll 1981

Age. Lopingian (roughly equivalent to the *Dicynodon* AZ of the Karoo Basin), Late Permian (Smith et al. 2012).

Occurrence. Lower Sakamena Formation near the village of Leoposa, southern Madagascar (Caldwell 1995; Carroll 1981).

Holotype. **MNHN 1978-6-1**, a largely complete skeleton and poorly preserved skull missing the posterior tail section.

Hypodigm. A list of referred specimens can be found in (Carroll 1981, p. 337-338). Several specimens are located in private specimens. Additional undescribed specimens are housed in the SAM (Simões et al. 2018).

Diagnosis. The diagnosis was provided by Carroll (1981).

Remarks. *Claudiosaurus germaini* is a non-saurian diapsid known from various specimens from the Late Permian of southern Madagascar. Its depositional environment, as well as its morphology, as indicated by the enlarged hindlimbs and pedes, and skeletal paedomorphosis, suggest it had an aquatic lifestyle (Caldwell 1995; Carroll 1981).

Youngina capensis Broom 1914

Age. Capitanian to Changhsingian (Rubidge et al. 2013; Smith & Evans 1996)

Occurrence. *Tropidostema*, *Cistecephalus*, and *Dicynodon* AZs (Assemblage Zones), Balfour and Middleton Formations of the Beaufort Group, part of the Karoo Supergroup, South Africa (Broom 1914; Smith & Evans 1996).

Holotype. AMNH 5561, a complete skull and mandibles and a partial articulated vertebral column.

Hypodigm. The most inclusive hypodigm has been provided by Ezcurra (2016), who supplemented a previous hypodigm of Gow (1975) with specimens found since then.

Diagnosis. The most recent emended diagnosis of *Youngina capensis* was provided by Ezcurra (2016).

Remarks. *Youngina capensis* is a Late Permian non-saurian neodiapsid with a generalized morphology known from a large array of well-preserved specimens. Its morphology has thus been investigated frequently (e.g. Broom 1914; Broom 1922; Currie 1981; Evans 1987; Gardner et al. 2010; Goodrich 1942; Gow 1975; Smith & Evans 1996; Watson 1957). *Youngina capensis* represents an important taxon for phylogenetic analyses that investigate early diapsid and saurian relationships (e.g. Ezcurra 2016; Ezcurra et al. 2014; Ford & Benson 2020; Simões et al. 2018). Specimens that were previously assigned to separate taxa, *Youngoides romeri* (Olson & Broom 1937), *Youngoides minor* (Broom & Robinson 1948), *Youngopsis kitchingi* (Broom 1937), *Youngopsis rubidgei* (Broom & Robinson 1948), and *Acanthotoposaurus bremneri* (Evans & Van Den Heever 1987), have all been shown to be conspecific with *Youngina capensis* (Evans 1987; Gow 1975; Reisz et al. 2000).

Gephyrosaurus bridensis Evans 1980

Age. Hettangian, and possibly Sinemurian, Early Jurassic (Whiteside et al. 2016).

Occurrence. Pontalun and Pant quarries of the St. Bride's fauna, southern Wales (Evans & Kermack 1994; Whiteside et al. 2016).

Holotype. **UCL T.1503**, a right dentary.

Hypodigm. The material of *Gephyrosaurus bridensis* comprises an extensive amount of isolated remains (over 1,000 specimens following Evans 1980). No complete list of referred specimens is available.

Diagnosis. The diagnosis was provided by Evans (1980, p. 204-205)

Remarks. *Gephyrosaurus bridensis* is exclusively known from extensive isolated remains that have been assigned to a single taxon based on the complementary articulation surfaces between the various elements, as well as their morphology and relative size. *Gephyrosaurus bridensis* has been described in detail in one study addressing the skull (Evans 1980), and another addressing the postcranium (Evans 1981). Although known from younger, Early Jurassic, deposits, *Gephyrosaurus bridensis* is considered the sister taxon to the clade encompassing the Triassic rhynchocephalians *Planocephalosaurus robinsonae*

and *Clevosaurus* spp. and more crownward rhynchocephalians (e.g. Hsiou et al. 2015; Scheyer et al. 2020a; Simões et al. 2018). An additional species, *Gephyrosaurus evansae*, was recently described from the Rhaetian (Late Triassic) 'Microlestes' quarry at Holwell near Bristol, UK (Whiteside & Duffin 2017).

Planocephalosaurus robinsonae Fraser 1982

Age. Early Rhaetian, Late Triassic (Whiteside et al. 2016).

Occurrence. Late Triassic fissure fills of Cromhall and Tytherington quarries, Bristol and Gloucestershire, UK (Fraser 1982; Whiteside & Marshall 2008).

Holotype. **AUP No. 11061**, an isolated left maxilla.

Hypodigm. As for *Gephyrosaurus bridensis*, *Planocephalosaurus robinsonae* is represented by a large amount of isolated elements (at least 750 specimens from Cromhall quarry according to Fraser 1982), and no complete list of referred specimens is available.

Diagnosis. The diagnosis of *Planocephalosaurus robinsonae* is provided by Fraser (1982, p. 710).

Remarks. Like *Gephyrosaurus bridensis*, *Planocephalosaurus robinsonae* is known from the Late Triassic to Early Jurassic fissure fills of southwestern England and southern Wales. Consequently, its material is also comprised of a large amount of three-dimensionally preserved, isolated remains that can be assigned to a single taxon based on their relative connectivity, morphological similarity, and size (although Simões et al. 2018 considered the assignment of postcranial elements to this taxon only tentative). The skull was described by Fraser (1982), and the postcranium has subsequently been described by Fraser & Walkden (1984). *Planocephalosaurus robinsonae* represents one of the best-known early rhynchocephalians and bears several primitive features compared to more derived rhynchocephalians such as *Clevosaurus* spp. Specimens of *Planocephalosaurus* have also been identified from the Ruthin quarry, southern Wales, but were not assigned to the species level (Whiteside et al. 2016). Small tooth bearing fragments from the Lower Tecovas Formation, Chinle Group (late Carnian) in Texas, USA, were assigned to a new species, *Planocephalosaurus lucasi* (Heckert 2004).

Protorosaurus speneri Meyer 1832

Age. Traditionally Tatarian, although conodont data points towards a more specific Wuchiapingian age, Late Permian (Ezcurra et al. 2014; Legler & Schneider 2008).

Occurrence. The Middridge and Quarrington quarries near Durham, Marl Slate, England (Evans & King 1993) and various localities of the Kupferschiefer Formation of Middle Germany (all localities are listed in Table 1 of Gottmann-Quesada & Sander 2009).

Holotype. Since no formal holotype had previously been assigned, **NHMW 1943I4**, known as the Swedenborg specimen, was assigned the lectotype by Gottmann-Quesada & Sander (2009).

Hypodigm. Table 1 of Gottmann-Quesada & Sander (2009) listed 28 specimens that were included in that study. More specimens that can tentatively be assigned to the species are known, which are distributed among various institutions and private collections across Europe, and a complete hypodigm is missing. Most specimens comprise of postcranial material, whereas skull material is comparatively rare and only known from five different specimens: **RCSHC/Fossil Reptiles 308**, **WMsN P 47361**, **TWCMS S1348(.1 and .2)**, **IGWuG 463016**, and **NMK S 180**. Only **NMK S 180** represents a complete and well-preserved skull.

Diagnosis. Ezcurra (2016) provided the most recent diagnosis for the species.

Remarks. *Protorosaurus speneri* represents the best-known Permian archosauromorph. The first specimen, **RCSHC/Fossil Reptiles 308** or the Spener specimen was described by Spener (1710), and interpreted as a fossil of a Nile crocodile (*Crocodylus niloticus*). *Protorosaurus speneri* was erected and described in detail based on additional material (Meyer 1830; Meyer 1832; Meyer 1856). Additional specimens were described (e.g. Evans & King 1993; Fichter 1995; Haubold & Schaumberg 1985), and recently the taxon was extensively revised (Gottmann-Quesada & Sander 2009). Most of the approximately 40 known specimens are from the Kupferschiefer Formation of Germany, whereas two come from the contemporary Marl Slate of England (Evans & King 1993). Most recent phylogenetic analyses recovered *Protorosaurus speneri* as the sister taxon to all other archosauromorphs (e.g. Ezcurra 2016; Pritchard et al. 2015; for an alternative placement of *Protorosaurus speneri* and tanystropheids outside Archosauromorpha, see Simões et al. 2018).

Czatkowiella harae Borsuk-Białynicka & Evans 2009

Age. earliest Late Olenekian (Shishkin & Sulej 2009).

Occurrence. Czatkowice 1, a fissure or cave infill of the Czatkowice quarry near Kraków, Poland.

Holotype. **ZPAL R.V/100**, an isolated, nearly complete right maxilla bearing teeth.

Hypodigm. A large number of isolated cranial and postcranial elements that could confidently be distinguished from other tetrapod remains of the Czatkowice 1 locality. A large number of these bones are presented and described by Borsuk-Białynicka & Evans (2009b).

Diagnosis. The diagnosis was provided by Borsuk-Białynicka & Evans (2009b).

Remarks. The material now referred to *Czatkowiella harae* was originally discovered in 1978 at Czatkowice 1. It is represented by many isolated and fragmented remains, which were found among similar remains belonging to other small diapsids, such as the euparkeriid *Osmolskina czatkowicensis* (Borsuk-Białynicka & Evans 2003; Borsuk-Białynicka & Evans 2009a; Borsuk-Białynicka & Sennikov 2009), the lepidosauromorph *Sophineta cracoviensis* (Evans & Borsuk-Białynicka 2009), the kuehneosaurid *Pamelina polonica* (Evans 2009), and three distinct procolophonids (Borsuk-Białynicka & Lubka 2009). Apart from the most diagnostic elements, bones were assigned to *Czatkowiella harae* largely based on size and fitting individual elements together. The morphology of *Czatkowiella harae* corresponds to that of many early archosauromorphs. Its most distinguishing feature is the presence of three-headed anterior dorsal ribs. It has only been considered phylogenetically by Borsuk-Białynicka & Evans (2009b), who recovered *Czatkowiella harae* as the sister taxon to *Protorosaurus speneri*. The taxon is somewhat problematic for inclusion in phylogenetic analyses, since it cannot be fully demonstrated that the isolated and fragmented remains all represent a single taxon. Here, we follow the identification by Borsuk-Białynicka & Evans (2009b) in all but the most tentatively assigned bones (e.g. the squamosal) and as for all other taxa scored, the reference specimen(s) for each scoring are provided in the Supplementary Material. This allows subsequent workers to critically evaluate scorings, as well as exclude certain specimens that further investigation might find belong to a different taxon. Because the inclusion of potentially composite taxa can negatively influence the accuracy of phylogenetic analyses, *Czatkowiella harae* is omitted from the analyses 3 and 4 here.

Tanystropheus longobardicus Bassani 1886

Age. latest Anisian-Ladinian (Spiekman et al. 2020; Spiekman & Scheyer 2019; Stockar 2010).

Occurrence. Besano Formation and the Cassina beds, Meride Limestone, of Monte San Giorgio, Switzerland and Italy.

Neotype. The holotype specimen was destroyed during WWII in Milan (Nosotti 2007; Spiekman & Scheyer 2019; Wild 1973). Neotype established by Wild (1973): **PIMUZ T 2791** – Almost complete and largely articulated, bituminous specimen, lacking the distal half of the tail.

Hypodigm. **PIMUZ T 2779, PIMUZ T 2781, PIMUZ T 2795, PIMUZ T 2485, PIMUZ T 2482, PIMUZ T 2484, PIMUZ T 3901, PIMUZ T 1277, MSNM BES SC 265, and MSNM BES SC 1018.**

Diagnosis. The most recent diagnosis for the taxon was provided by Spiekman et al. (2020, Methods S1).

Remarks. *Tanystropheus longobardicus* was first described based on a single, partially articulated specimen from the Besano Formation of Monte San Giorgio. It was interpreted as a pterosaur and assigned to *Tribelesodon longobardicus*, with the generic name referring to the tricuspid teeth that were present in the jaws (Arthaber 1922; Bassani 1886; Nopsca 1923). This specimen has unfortunately been lost, but it has been figured in Arthaber (1922). The discovery of additional specimens from the Besano Formation revealed that the elements which were interpreted as elongated phalanges represented elongate cervical vertebrae that were similar to those that were known from the Upper Muschelkalk of the Germanic Basin, which had been assigned to *Tanystropheus conspicuus* (Peyer 1930; Peyer 1931). Therefore, the species was re-assigned to *Tanystropheus longobardicus*. Wild (1973) described the species in detail, and assigned **PIMUZ T 2791** as the neotype. Additional specimens were described in Wild (1980a), including a specimen from the slightly younger Meride Limestone, which was assigned to the separate species *Tanystropheus meridensis*. However, this specimen, as well as an additional specimen that was found from the Meride Limestone (Renesto 2005), were shown to be morphologically indistinguishable from the specimens from the Besano Formation, and therefore *Tanystropheus meridensis* was considered a junior synonym of *Tanystropheus longobardicus* (Nosotti 2007; Spiekman & Scheyer 2019). The functional morphology and configuration of the neck of *Tanystropheus longobardicus* was treated extensively by Tschanz (1986). A small-sized *Tanystropheus* skeleton lacking the skull from the Falang Formation of China was identified as *Tanystropheus* sp., and might represent the only known occurrence of *Tanystropheus longobardicus* from China, indicating a Tethys-wide distribution of the species (Li 2007). Nosotti (2007) described in detail specimens from the Italian side of the Besano Formation and revised the species. Recently, a combined morphological and palaeohistological study revealed that the small sized specimens of *Tanystropheus* from Monte San Giorgio, which bear distinct

tricuspid marginal teeth, are skeletally mature (Spiekman et al. 2020). This indicates that the small-sized specimens represent a separate species from the large-sized specimens, and the former were re-assigned to the new species *Tanystropheus hydroides*. *Tanystropheus longobardicus* was therefore a relatively small-sized *Tanystropheus* species, likely not exceeding 2 metres in total length, which fed on small prey, including soft-shelled invertebrates.

Tanystropheus hydroides Spiekman, Neenan, Fraser, Fernandez, Rieppel, Nosotti & Scheyer 2020

Age. Latest Anisian-earliest Ladinian (Spiekman et al. 2020; Stockar 2010).

Occurrence. Besano Formation of Monte San Giorgio, Switzerland and Italy.

Holotype. **PIMUZ T 2790**, a compressed skull and anterior eight cervical vertebrae in semi-articulation.

Hypodigm. **PIMUZ T 2787, PIMUZ T 2793, PIMUZ T 2818, PIMUZ T 2819, PIMUZ T 183, SNSB-BSPG 1953 XV 2, and MSNM V 3663.**

Diagnosis. The diagnosis for *Tanystropheus hydroides* has been provided in Spiekman et al. (2020, p. 2).

Remarks. Specimens of *Tanystropheus hydroides* were previously considered as the adult morphotype of *Tanystropheus longobardicus*, but they were recently shown to represent a separate, large-sized species (Spiekman et al. 2020). Specimens of *Tanystropheus hydroides* were described as *Tanystropheus longobardicus* in Peyer (1931), Kuhn-Schnyder (1947; 1959), and Wild (1973). A *Tanystropheus* specimen has been described from China that attained a size similar to *Tanystropheus hydroides* (Rieppel et al. 2010). Although the postcranial skeleton of this specimen cannot be distinguished from *Tanystropheus hydroides*, the absence of a skull has not allowed the specimen to be assigned to this species with certainty. However, it is clear that the genus, and possibly the species *Tanystropheus hydroides*, had a Tethys-wide distribution (Spiekman & Scheyer 2019). *Tanystropheus hydroides* was an aquatic ambush predator that employed its long-neck and a laterally directed snapping bite to catch its prey, which consisted of fish and cephalopods (Spiekman et al. 2020).

GMPKU P 1527

Age. Earliest Carnian (Rieppel et al. 2010).

774 Occurrence. The upper part of the Zhuganpo Member of the Falang Formation of Nimaigu near Xingyi
775 City, Wusha District, Guizhou Province, southwestern China.

776 Remarks. A large-sized *Tanystropheus* skeleton from China that is largely complete, but lacking the skull,
777 anterior segment of the neck, the distal end of the tail, and most of the pedes, was identified as
778 *Tanystropheus* cf. *longobardicus* (Rieppel et al. 2010). Recently, it was shown that the large-sized
779 specimens of *Tanystropheus* from Monte San Giorgio represent a separate species from the small-sized
780 specimens, and have been assigned to *Tanystropheus hydroides* (Spiekman et al. 2020). Therefore, the
781 assignment of **GMPKU P 1527** has consequently been altered to *Tanystropheus* cf. *hydroides*. However,
782 because this specimen is known from the eastern side of the Tethys Ocean, whereas the referred
783 specimens of *Tanystropheus hydroides* derive its western margin, this specimen cannot be unequivocally
784 assigned to the species, particularly because cranial morphology appears to be more variable than that of
785 the postcranium within the genus. Because of the biogeographical importance of this specimen as the
786 best-known *Tanystropheus* remains from the eastern Tethys it was incorporated as a separate OTU here.

787

788 *Tanystropheus “conspicuus”* Meyer 1855

789 Age. Late Anisian to Ladinian (Menning & Hendrich 2016; Spiekman & Scheyer 2019).

790 Occurrence. Various localities of the Upper Muschelkalk and Lettenkeuper of Central Europe. An overview
791 of all known localities can be found in Supplementary Table 1 of Spiekman & Scheyer (2019).

792 Lectotype. U-MO BT 740, an isolated, three-dimensionally preserved cervical vertebra.

793 Hypodigm. The referred specimens of *Tanystropheus “conspicuus”* are listed in Supplementary Table 1 of
794 Spiekman & Scheyer (2019).

795 Remarks. A number of elongate bones from the Upper Muschelkalk of Bayreuth, Germany, were identified
796 as reptilian vertebrae and assigned to *Tanystropheus “conspicuus”* by Meyer (1855). These bones had
797 previously also been described by Count Georg zu Münster, who had interpreted these bones as limb
798 bones of a saurian reptile, which he had named “*Macroscelosaurus*”. However, since this work has been
799 lost and this generic name has fallen into disuse (*nomen oblitum*), the generic name *Tanystropheus* has
800 received precedence (Wild 1973, p. 148). Following the description of the semi-articulated specimens of
801 *Tanystropheus longobardicus* (Peyer 1930; Peyer 1931), Huene (1931) considered material previously
802 identified as “*Thecodontosaurus latespinatus*”, “*Thecodontosaurus primus*”, and “*Procerosaurus cruralis*”

from the Upper Muschelkalk of Europe to very likely belong to *Tanystropheus* “*conspicuus*”. Wild (1973) provided a systematic palaeontology section in which these taxa were synonymized with *Tanystropheus conspicuus*. Fragmentary and isolated remains of *Tanystropheus* “*conspicuus*” are known from the Upper Muschelkalk and Lettenkeuper throughout Central Europe (late Anisian to Ladinian; Menning & Hendrich 2016). This material comprises isolated cervical, dorsal, sacral, and caudal vertebrae, two femora, and an ischium. Peyer (1931) refrained from providing a detailed comparison of *Tanystropheus longobardicus* with *Tanystropheus* “*conspicuus*” and “*Tanystropheus antiquus*” from the Germanic Basin. Wild (1973) distinguished *Tanystropheus* “*conspicuus*” from *Tanystropheus longobardicus* on the basis of comparatively wider rib attachment sites and a concavity on the anterior end of the neural spine of the cervical vertebrae. Although he considered these minor differences to be insufficient for a species definition, the distinction between the two taxa was maintained in expectation of additional specimens that would allow for a more complete comparison. A recent revision of *Tanystropheus* spp. revealed that no distinct morphological differences could be identified between *Tanystropheus* “*conspicuus*”, *Tanystropheus hydroides* (therein the large morphotype of *Tanystropheus longobardicus*), and *Tanystropheus haasi* (Spiekman & Scheyer 2019). However, since the referred material of both *Tanystropheus* “*conspicuus*” and *Tanystropheus haasi* is insufficient for a detailed comparison and both are only known from fragmentary and isolated postcranial elements, these taxa were considered as nomina dubia.

“*Tanystropheus antiquus*” Huene 1905

Age. Latest Olenekian to middle Anisian (Menning & Hendrich 2016; Spiekman & Scheyer 2019).

Occurrence. Lower Muschelkalk of Silesia, Poland (Gogolin Formation), Germany (Schaumkalk Formation), and the Netherlands (Vossenveld Formation) (see also Supplementary Table 1 of Spiekman & Scheyer 2019).

Syntype. **SMNS 16687**, **SMNS 10110**, **MGUWr 3872s**, **MGUWr 3888s**, **MGUWr 3895s**, **MGUWr 3902s** and some uncatalogued **MGUWr** specimens, all consisting of single cervical vertebrae. Wild (1973) had assigned **SMNS 10110** as the lectotype, but considered the **MGUWr** specimens to have been lost.

Hypodigm. All specimens assigned to “*Tanystropheus* (c.f.) *antiquus*” are listed in Supplementary Table 1 of Spiekman & Scheyer (2019).

Diagnosis. Recent diagnoses were provided for this taxon by Sennikov (2011) for "*Protanystropheus antiquus*" and Fraser & Rieppel (2006) for "*Tanystropheus antiquus*".

Remarks. Following the description of the syntype of "*Tanystropheus antiquus*" from the Lower Muschelkalk of Gogolin and Krapkowice, Silesia, Poland (Huene 1905), other isolated *Tanystropheus*-like remains from the Lower Muschelkalk were attributed to the species (e.g. Huene 1931; Kuhn 1971; Schmidt 1928; Schmidt 1938; Spiekman et al. 2019). Ortlam (1966) referred material of the uppermost Buntsandstein (Anisian) to *Tanystropheus longobardicus* and *Macrocnemus bassanii*, but this material was later assigned to "*Tanystropheus antiquus*" by Wild (1980b). The Buntsandstein precedes the Muschelkalk and in contrast to the latter represents largely fluvial sediments (Feist-Burkhardt et al. 2008), and Wild (1980b) concluded that the discovery of "*Tanystropheus antiquus*" from the Buntsandstein, indicated that at least the juvenile individuals had a terrestrial lifestyle. Both Wild (1987) and Evans (1988) later suggested that "*Tanystropheus antiquus*" might belong to a separate genus, based on the large morphological discrepancy between this taxon and other *Tanystropheus* species. Fraser & Rieppel (2006) revised the Buntsandstein specimens and concluded that it represented a separate taxon from "*Tanystropheus antiquus*" and assigned it to the new taxon *Amotosaurus rotfeldensis*. Despite a lack of diagnostic characters in the material, Fraser & Rieppel (2006) tentatively maintained the assignment of the Lower Muschelkalk specimens to "*Tanystropheus antiquus*". Sennikov (2011) compared "*Tanystropheus antiquus*" to *Augustaburiania vatagini*, and also concluded that the former was generically distinct from *Tanystropheus* spp. and renamed the taxon "*Protanystropheus antiquus*".

The relative length of the cervical vertebrae might indeed indicate that "*Tanystropheus antiquus*" is more closely related to *Augustaburiania vatagini* or *Amotosaurus rotfeldensis* than to other *Tanystropheus* species. However, the taxonomic status of "*Tanystropheus antiquus*" is currently unclear, since many specimens of the syntype material (Huene 1902; Huene 1905) were long considered to have been lost (Fraser & Rieppel 2006; Sennikov 2011; Wild 1973; Wild 1980b). However, these specimens have recently resurfaced and were briefly discussed by Skawiński et al. (2017). Any taxonomic evaluation of this taxon would first require a detailed revision of this type material to assess whether subsequently referred specimens of "*Tanystropheus antiquus*" from other localities represent the same species (Spiekman et al. 2019; Spiekman & Scheyer 2019; Wild & Oosterink 1984). Such a revision is currently underway (Szczygielski, personal commun. 2019), and therefore the taxonomic status of "*Tanystropheus antiquus*" is not addressed here. However, we include a preliminary "*Tanystropheus antiquus*" OTU in our analyses based on the strong morphological similarity of the tanystropheid cervical vertebrae from the Lower

Muschelkalk of Central Europe. Our scoring of this OTU is based on two complete cervical vertebrae, **SMNS 16687** and **Coll. Oosterink A638**. The former specimen comes from the Lower Muschelkalk of Krapkowice, Poland, and constitutes part of the syntype of “*Tanystropheus antiquus*”, and the latter derives from the Lower Muschelkalk of Winterswijk, the Netherlands (Spiekman et al. 2019; Wild & Oosterink 1984).

Sclerostropheus fossai Wild 1980

Age. Late Norian (Rigo et al. 2009; Tackett & Tintori 2019).

Occurrence. N-slope of Canto Alto, near Poscante in Val Brembana, Bergamo Province, Italy (Wild 1980a).

Holotype. **MCSNB 4035**, a partial, articulated cervical column.

Diagnosis. The diagnosis was recently provided by Spiekman & Scheyer (2019).

Remarks. *Sclerostropheus fossai* is known from a single specimen, which constitutes a partial, semi-articulated cervical column, and was previously considered within the genus *Tanystropheus* (Wild 1980a). However, the morphology of the cervical vertebrae and ribs differs distinctly from that of other *Tanystropheus* species, which was briefly indicated by Renesto (2005), and it was recently assigned to the new genus *Sclerostropheus* (Spiekman & Scheyer 2019). Together with *Langobardisaurus pandolfii*, *Sclerostropheus fossai* represents a second tanystropheid taxon known from the Norian of northern Italy.

Macrocnemus bassanii Nopsca 1930

Age. latest Anisian-Ladinian.

Occurrence. Besano Formation and Meride Limestone of Monte San Giorgio, Switzerland and Italy (Jaquier et al. 2017; Peyer 1937; Renesto & Avanzini 2002; Rieppel 1989; Stockar 2010).

Holotype. **MSNM 14624**, A cast of MSNM specimen Besano I, a poorly preserved specimen which was destroyed in Milan during WWII (Fraser & Furrer 2013).

Hypodigm. Rieppel (1989, p. 374) provided the hypodigm for the *Macrocnemus bassanii* material housed at PIMUZ. The specimen listed there as A 111/208 is now catalogued as **PIMUZ T 4822**. Additionally, two specimens of *M. bassanii* are housed in the MSNM: **MSNM BES SC 111**; a complete and fully articulated

juvenile including skin remains; **MSNM V 457**, a disarticulated adult specimen, in which a number of skull and jaw bones are preserved, as well as several cervical, dorsal, and caudal vertebrae, gastralia, ribs, and both pelvic girdles and both hindlimbs, excluding the feet.

Diagnosis. The most recent diagnosis was provided by Jaquier et al. (2017).

Remarks. *Macrocnemus bassanii* is the type species of the genus and is known from the Middle Triassic of Switzerland and Italy. It was first described by Nopsca (1930), based on the poorly preserved, and now lost holotype, of which a cast has been preserved. The taxon was described in more detail following the discovery of multiple well-preserved specimens (Peyer 1937). Further details of the skull were provided by Kuhn-Schnyder (1962) and Rieppel & Gronowski (1981). The postcranium and its functional considerations were discussed by Rieppel (1989), which indicated that *Macrocnemus bassanii* was facultatively bipedal. An excellently preserved juvenile specimen, preserving soft tissue was described by Premru (1991) and Renesto & Avanzini (2002). The skull of *Macrocnemus bassanii* was recently redescribed in detail aided by synchrotron tomography, which revealed many similarities in the cranial configuration of the skull with *Prolacerta broomi* (Miedema et al. 2020). *Macrocnemus bassanii* is currently firmly established as a tanystropheid (e.g. Ezcurra 2016; Pritchard et al. 2015).

Macrocnemus fuyuanensis Li, Zhao & Wang 2007

Age. Late Anisian-Ladinian.

Occurrence. Besano Formation of Monte San Giorgio, Switzerland and Zhuganpo Member of the Falang Formation, Yun-nan Province, China (Jaquier et al. 2017; Jiang et al. 2011; Li et al. 2007; Scheyer et al. 2020b).

Holotype. **IVPP V15001** - Mostly complete and largely articulated skeleton missing most of the skull.

Hypodigm. **GMPKU-P-3001**, almost complete and fully articulated specimen, missing almost the complete tail; **PIMUZ T 1559**, virtually complete and disarticulated specimen, missing parts of the skull, almost the complete tail, and missing the hindlimbs.

Diagnosis. The most recent diagnosis for the species was provided by Scheyer et al. (2020b).

Remarks. *Macrocnemus fuyuanensis* was first described based on the holotype specimen by Li et al. (2007), and distinguished from *Macrocnemus bassanii* based on the limb ratios as well as the number of

dorsal vertebrae. Jiang et al. (2011) described another specimen of *Macrocnemus fuyuanensis* with a completely preserved skull, **GMPKU-P-3001**, and concluded that it differed from *Macrocnemus bassanii* in a number of characters. A specimen from the upper Besano Formation was described by Jaquier et al. (2017). This specimen was more similar in limb proportions to *Macrocnemus fuyuanensis* than to *Macrocnemus bassanii*, and also differed from the latter in the morphology of the interclavicle, and identified as *Macrocnemus* aff. *fuyuanensis*. Furthermore, these authors revised the cranial morphology of *Macrocnemus fuyuanensis* specimen **GMPKU-P-3001**, indicating that it did not substantially differ from that of *Macrocnemus bassanii*. The holotype **IVPP V15001** was redescribed and revealed new anatomical details for the taxon, particularly with regards to the palate and pectoral girdle (Scheyer et al. 2020b). The morphology of the interclavicle of the holotype was in correspondence with that of the Swiss specimen **PIMUZ T 1559**, and distinctly differed from that of specimens assigned to *Macrocnemus bassanii*. Therefore, **PIMUZ T 1559** was re-assigned to *Macrocnemus fuyuanensis* and the species thus occurred on both the eastern and western margins of the Tethys Ocean. *Tanystropheus* sp., another well-known tanystropheid, also had a Tethys-wide distribution. However, it is currently uncertain whether the Chinese specimens of this genus represent the same species as the European forms (Spiekman et al. 2020; Spiekman & Scheyer 2019).

Macrocnemus obristi Fraser & Furrer 2013

Age. Early Ladinian.

Occurrence. Prosanto Formation of Ducanfurugga near Davos, canton Graubünden, Switzerland (Fraser & Furrer 2013).

Holotype. **PIMUZ A/III 1467** (housed in the Bündner Naturmuseum, Chur, Switzerland), an articulated partial skeleton, which consists of the posterior dorsal vertebrae, pelvic girdle and hindlimbs, and most of the tail.

Hypodigm. **PIMUZ A/III 722**, a right pes preserved in dorsal view.

Diagnosis. The diagnosis was provided by Fraser & Furrer (2013, p. 200)

Remarks. *Macrocnemus obristi* is known from two specimens from the Prosanto Formation (Fraser & Furrer 2013). It differs from *Macrocnemus bassanii* and *Macrocnemus fuyuanensis* based on the ratio of the femur and tibia (Fraser & Furrer 2013; Jaquier et al. 2017). Due to its recent description and only

partially known morphology, *Macrocnemus oibrsti* has previously not been included in any phylogenetic analysis.

Tanytrachelos ahynis Olsen 1979

Age. Late Carnian

Occurrence. Virginia Solite Quarry B, Upper member of the Cow Branch Formation, part of the Dan River Group (Newark Supergroup), USA (Casey et al. 2007; Liutkus-Pierce et al. 2014; Olsen 1979).

Holotype. **YPM 7496**, a largely complete, articulated specimen.

Hypodigm. Hypodigm listed by Olsen (1979, p. 4-5, and note on p. 13), most specimens currently housed in the VMNH.

Diagnosis. The diagnosis for *Tanytrachelos ahynis* was provided by Olsen (1979)

Remarks. *Tanytrachelos ahynis* was described by Olsen (1979) and is known from hundreds of specimens from Solite Quarry B in Virginia (Casey et al. 2007). However, many detailed morphological features are unknown for *Tanytrachelos ahynis*, due to the poor preservation of the specimens. Recently, the authors subjected a relatively well-preserved specimen (**NMS G.2017.11.1**) to synchrotron radiation micro-computed tomography. This revealed the inner anatomy of the cervical vertebrae in some detail, highlighting that as in *Tanystropheus* spp. and *Macrocnemus bassanii* the neural canal passes through the vertebral centrum in *Tanytrachelos ahynis*. However, morphological details could not be observed due to the poor preservation of the specimen, which is likely attributable to diagenetic factors (Liutkus-Pierce et al. 2014). The Solite Quarry B is represented by lacustrine deposits (Fraser et al. 1996), and *Tanytrachelos ahynis* had an aquatic lifestyle (Casey et al. 2007; Olsen 1979). As in *Tanystropheus longobardicus* and *Tanystropheus hydroides*, the presence of paired heterotopic bones parallel to the anterior caudal vertebrae in approximately half of the articulated specimens preserving this region indicates sexual dimorphism.

AMNH FARB 7206

Age. Carnian, Late Triassic (Colbert & Olsen 2001)

Occurrence. Lockatong or Stockton Formation of Hudson County, New Jersey

Remarks. Small reptilian specimens from the approximately contemporaneous Lockatong Formation of New Jersey have been compared to *Tanytrachelos ahynis*, and although it could not be excluded that some of these specimens might represent *Tanytrachelos ahynis*, not enough diagnostic features were preserved to positively identify any of these specimens to this taxon (Olsen 1979). However, one of these specimens, **AMNH FARB 7206**, was recently referred to *Tanytrachelos ahynis* by Pritchard et al. (2015). This specimen was here scored separately from the specimens from the Solite Quarry B to test this hypothesis and shown to differ in the shape of the cervical vertebrae and the curvature of the femur, raising doubts as to whether this specimen can be referred to *Tanytrachelos ahynis*. Additionally, Pritchard et al. (2015) referred a single calcaneum from the middle Norian Hayden Quarry locality of New Mexico to this species based on the striking similarities in morphology between this element, and the calcaneum of **AMNH FARB 7206**. Since it is currently uncertain whether the latter can be referred to *Tanytrachelos ahynis*, we also consider the assignment of the Hayden Quarry calcaneum to *Tanytrachelos ahynis* as equivocal. Therefore, only specimens from the Solite Quarry B can currently be confidently assigned to *Tanytrachelos ahynis*.

Amotosaurus rotfeldensis Fraser & Rieppel 2006

Age. Early Anisian.

Occurrence. Quarry Kossig (Upper Buntsandstein) of Baden-Württemberg, Germany (Fraser & Rieppel 2006; Ortlam 1966).

Holotype. **SMNS 50830**, a largely disarticulated skeleton, including an articulated cervical series, maxilla, parabasisphenoid, scapulacoracoids and pelvic girdles, and scattered dorsal vertebrae.

Hypodigm. Many specimens housed in the SMNS, some of which are unprepared or unaccessioned, including: **SMNS 54783 a and b**, a slab and counterslab preserving two largely disarticulated skeletons, including a poorly preserved skull roof, cervical vertebrae, an articulated dorsal vertebral series, three articulated hindlimbs including pedes, and a partial forelimb including manus; **SMNS 50691**, three slabs, preserving a partial pes, a coracoid and maxilla, and a partial skull in ventral view, ilium, and dorsal vertebrae, respectively; **SMNS 54784a and b**, a slab and counterslab preserving the palatal region of a skull and a partial cervical series; **SMNS 54810**, disarticulated skeletons, including both cranial and

extensive postcranial remains; **SMNS 90600**, posterior part of the vertebral column, including sacral and anterior caudal vertebrae; **SMNS 90601**, articulated maxilla and jugal; **SMNS 90540**, two skulls in palatal view; **SMNS unnumbered (1)**, partial mandible and cervical vertebrae and ribs; **SMNS unnumbered (2)**, disarticulated cranial elements and a partial cervical series; **SMNS unnumbered (3)**, skull in palatal view three anterior cervical vertebrae; **SMNS unnumbered (4)**, sacral region.

Diagnosis. The diagnosis of *Amotosaurus rotfeldensis* was provided by Fraser & Rieppel (2006, p. 867).

Remarks. Several specimens of associated skeletons from the Buntsandstein of Baden-Württemberg were assigned to *Macrocnemus bassanii* and *Tanystropheus longobardicus* by Ortlam (1966). However, Wild (1980b) considered this material to represent juvenile specimens of “*Tanystropheus antiquus*”, which is known from several isolated remains, mostly cervical vertebrae, from the Lower Muschelkalk of the Germanic Basin (Spiekman & Scheyer 2019). Fraser & Rieppel (2006) re-examined the specimens from the Buntsandstein and assigned it to the new taxon *Amotosaurus rotfeldensis*. The genus was named in honour of R. Wild (amoto = wild in Latin). Ezcurra (2016) and Pritchard et al. (2015) incorporated *Amotosaurus rotfeldensis* in their phylogenetic analyses and provided several new morphological observations for the taxon.

Augustaburiania vatagini Sennikov 2011

Age. Latest Olenekian.

Occurrence. Donskaya Luka locality, right slope of the Don River valley, Lipovskaya Formation, Ilovlyanskii District, Volgograd Region, Russia (Sennikov 2011).

Holotype. **PIN 1043/587**, an isolated middle cervical vertebra.

Hypodigm. The referred specimens are listed in Sennikov (2011, p. 98).

Diagnosis. The diagnosis was provided by Sennikov (2011).

Remarks. *Augustaburiania vatagini* is known from the latest Olenekian (Early Triassic) of Donskaya Luka of the Don River valley, Russia, and thus represents one of the earliest known tanystropheids together with likely tanystropheid material from the Sanga do Cabral Formation (Induan–early Olenekian) of Brazil (De Oliveira et al. 2018; De Oliveira et al. 2020). Like other tanystropheids, such as “*Tanystropheus antiquus*” and *Tanystropheus “conspicuus”*, *Augustaburiania vatagini* is solely known from isolated

postcranial remains, largely represented by cervical vertebrae. The relative length of the mid-cervical vertebrae of *Augustaburiania vatagini* is longer than that of “*Tanystropheus antiquus*” and *Amotosaurus rotfeldensis*, but shorter than that of other *Tanystropheus* species. Furthermore, the cervical vertebrae of *Augustaburiania vatagini* can be distinguished by a distinct concave margin of the centrum of the cervical vertebrae, although the expression of this character in the referred material is subject to much intraspecific variation. Furthermore, the number of cervical vertebrae of *Augustaburiania vatagini*, which was considered to be eight or nine, cannot be established, since no articulated cervical vertebrae have been preserved. Species differentiation based on isolated remains, particularly when relying on cervical vertebrae, is problematic, as their morphology is subject to intraspecific variation and their relative position in the cervical column (Spiekman & Scheyer 2019). As such, although *Augustaburiania vatagini* is known from older deposits than any other European tanystropheids, and the morphology of the cervical vertebrae shows minor differences from those of other taxa, the taxonomic status of *Augustaburiania vatagini* remains hard to assess.

Raibliania calligarisi Dalla Vecchia 2020

Age. Early Carnian (Julian).

Occurrence. Predil Limestone near Prasnig Brook, Tarvisio, Udine Province, Italy (Dalla Vecchia 2020).

Holotype. **MFSN 27532**, a partial skeleton comprising the thoracic part of the vertebral column, a single partial cervical vertebra, sacral vertebrae, part of the pelvic girdle and left femur, and a purported tooth.

Diagnosis. The diagnosis was provided by Dalla Vecchia (2020).

Remarks. *Raibliania calligarisi* was recently described from a single specimen from the early Carnian of northern Italy. It is closely related to *Tanystropheus longobardicus* and is slightly younger than the known occurrence of this species (Spiekman et al. 2020). *Raibliania calligarisi* can be distinguished from other tanystropheids based on the morphology of neural spines of the dorsal vertebrae, the pleurapophyses of the posterior dorsal vertebrae, the iliac blade, the anterior portion of the pubis, and a single, disarticulated tooth (Dalla Vecchia 2020). The identification of the single, isolated tooth is somewhat equivocal, as it is located far from where the head would have been preserved. *Raibliania calligarisi* is here considered in a phylogenetic context for the first time. Another specimen discovered in the vicinity of the holotype of *Raibliania calligarisi*, **MFSN 13228**, consisting of three articulated caudal vertebrae, represents the only

other described tetrapod remains from the locality. This specimen has not been referred to *Raibliania calligaris* due to the lack of overlapping morphology between it and the holotype (Dalla Vecchia 2020). Although the relative size of the vertebrae corresponds to that of the holotype of *Raibliania calligaris*, the morphology of the neural spine differs distinctly from that of *Tanystropheus longobardicus*, to which *Raibliania calligaris* is closely related.

Prolacerta broomi Parrington 1935

Age. Induan.

Occurrence. Middle Beaufort beds, *Lystrosaurus* AZ, Katberg Formation, South Africa; Transantartic Mountains, Fremouw Formation, Antarctica (Groenewald & Kitching 1995; Peacock et al. 2019).

Holotype. **UMZC 2003.40** - A partial skull and mandible.

Hypodigm. The referred specimens are listed in Spiekman (2018, p. 4-5).

Diagnosis. The latest diagnosis of *Prolacerta broomi* was provided by Spiekman (2018).

Remarks. *Prolacerta broomi* was first described by Parrington (1935) based on a crushed partial skull found in the Katberg Formation, *Lystrosaurus* Zone, near Harrismith, South Africa. *Prolacerta broomi* has played an important role in discussions on the evolutionary origin of modern reptile groups, and has been considered both as an ancestral lepidosaur (e.g. Camp 1945; Parrington 1935) and archosaur (e.g. Romer 1956). *Prolacerta broomi* was first identified as a “protorosaur” by Camp (1945). Following the discovery of more specimens, the complete morphology of *Prolacerta broomi*, including the postcranium was described (Gow 1975). This revealed that *Pricea longiceps* Broom & Robinson 1948 represented a junior synonym of *Prolacerta broomi*. The braincase of *Prolacerta broomi* was described by Evans (1986). Based on new specimens as well as a reappraisal of previously described South African material, Modesto & Sues (2004) provided a redescription of the skull of *Prolacerta broomi*. Specimens of *Prolacerta broomi* have also been described from Antarctica, consisting of several smaller, likely juvenile specimens, and a single, large-sized specimen, which is slightly larger than the specimens known from South Africa (Colbert 1987; Spiekman 2018). Although previously considered a member of the “protorosaurs”, recent phylogenetic analysis indicate that *Prolacerta broomi* is more closely related to Archosauriformes than *Protorosaurus speneri* and tanystropheids are (e.g. Dilkes 1998; Ezcurra 2016; Modesto & Sues 2004; Pritchard et al. 2015; Rieppel et al. 2003). *Prolacerta broomi* has been used widely as an outgroup in phylogenetic

analyses on Archosauriformes and early crown-archosaurs (e.g. Butler et al. 2015; Desojo et al. 2011; Dilkes & Sues 2009; Nesbitt 2011; Sookias 2016).

1091

1092 *Ozimek volans* Dzik & Sulej 2016

1093 Age. Late Carnian or early Norian (Dzik & Sulej 2016; Szulc et al. 2017).

1094 Occurrence. Grabowa Formation (Silesian Keuper) of Krasiejów, Upper Silesia, Poland.

1095 Holotype. **ZPAL AbIII/2512**, partial skeleton missing the skull.

1096 Hypodigm. A complete hypodigm can be found in Dzik & Sulej (2016).

1097 Diagnosis. The diagnosis was provided in Dzik & Sulej (2016).

1098 Remarks. *Ozimek volans* was recently described based on several partial and disarticulated skeletons (Dzik
1099 & Sulej 2016). An elongate vertebra now referred to this taxon was previously linked to either pterosaurs
1100 or *Tanystropheus* due to its extreme elongation (Dzik & Sulej 2007). It is considered a close relative of the
1101 gliding reptile *Sharovipteryx mirabilis* and was possibly also a glider, although a comparison is limited due
1102 to the poorly known morphology of *Sharovipteryx mirabilis*. The morphology of *Ozimek volans* is highly
1103 derived and differs distinctly from other “protorosaurs” in the relative length and gracile construction of
1104 the limb bones and the configuration of the pectoral girdle, which includes an enlarged coracoid and
1105 possibly ossified sternum. Although formally assigned to the family Sharovipterygidae, *Ozimek volans* was
1106 considered a “protorosaur” based on the presence of elongate cervical vertebrae, the posterior curvature
1107 of the scapula, and the procoelous articulation surfaces of the cervical vertebrae (which occur in
1108 *Tanytrachelos ahynis* and *Langobardisaurus pandolfii* among tanystropheids, but which is widespread in
1109 diapsids, e.g. drepanosaurs; Dzik & Sulej 2016). Unfortunately, the skull morphology of *Ozimek volans* is
1110 only partially known and identification of many cranial bones is uncertain due to their disassociation and
1111 peculiar morphology. *Ozimek volans* has been included in the phylogenetic analysis of Pritchard & Sues
1112 (2019), in which it was recovered within Tanystropheidae as the sister taxon to a clade comprising
1113 *Langobardisaurus pandolfii* and *Tanytrachelos ahynis*.

1114

1115 *Ellessaurus gondwanoccidens* De Oliveira, Pinheiro, Da Rosa, Dias da Silva & Kerber 2020

1116 Age. Induan-Olenekian (De Oliveira et al. 2020; Dias-da-Silva et al. 2017).

1117 Occurrence. Bica São Tomé, Sanga do Cabral Formation, São Francisco de Assis, Rio Grande do Sul,
1118 southern Brazil.

1119 Holotype. **UFSM 11471**, a left hindlimb, partial pelvis, a single sacral vertebra and three caudal vertebrae.

1120 Diagnosis. The diagnosis was provided by De Oliveira et al. (2020).

1121 Remarks. *Ellessaurus gondwanoccidens* is known from a single hind limb, partial pelvis, and a few sacral
1122 and caudal vertebrae, and has been identified as a tanystropheid (De Oliveira et al. 2020). Several isolated
1123 cervical vertebrae with a typical tanystropheid morphology have also been described from the Sanga do
1124 Cabral Formation, from which *Ellessaurus gondwanoccidens* is known (De Oliveira et al. 2018). However,
1125 due to the limited morphological information currently available for *Ellessaurus gondwanoccidens*, its
1126 identification as a tanystropheid is somewhat uncertain. The phylogenetic analysis presented by De
1127 Oliveira et al. (2020) that excludes *Jesairosaurus lehmani* and *Dinocephalosaurus orientalis* recovered
1128 *Ellessaurus gondwanoccidens* as the sister taxon to all other tanystropheids. However, the analysis that
1129 includes both *Jesairosaurus lehmani* and *Dinocephalosaurus orientalis* did not recover *Ellessaurus*
1130 *gondwanoccidens* within Tanystropheidae (Supplementary Material of De Oliveira et al. 2020). Instead,
1131 *Ellessaurus gondwanoccidens* formed a large polytomy with most of the included archosauromorphs. The
1132 lack of overlapping morphology between the described material of *Ellessaurus gondwanoccidens* and the
1133 non-archosauriform archosauromorph *Teyujagua paradoxa*, which are both known from the same
1134 locality, implies that it cannot be ruled out that these taxa are synonymous.



1135

1136 *Jesairosaurus lehmani* Jalil 1997

1137 Age. Late Olenekian-early Anisian (Jalil 1999).

1138 Occurrence. Site 5003 of Busson, at the base of the Zarzaitine Formation, Algeria.

1139 Holotype. **ZAR 06**, a nearly complete skull and mandibles, the neural arches of the five distalmost cervical
1140 vertebrae, the complete left and partial right pectoral girdle, and the proximal end of the left humerus.

1141 Hypodigm. The hypodigm was provided by Jalil (1997) and Ezcurra (2016).

1142 Diagnosis. The most recent diagnosis was provided by Ezcurra (2016).

1143 Remarks. The material now assigned to *Jesairosaurus lehmani* was originally considered as procolophonid
1144 remains (Lehman 1971). However, detailed observation was hampered by the specimens being covered

by a hard hematite layer. Additional preparation revealed the diapsid affinity of the material (Jalil 1990), and the material was later described in detail and assigned to *Jesairosaurus lehmani* (Jalil 1997). Ezcurra (2016) provided a morphological redescription of *Jesairosaurus lehmani*. Jalil (1997) identified *Jesairosaurus lehmani* as a “protorosaur” and in a phylogenetic analysis, found it to be the sister taxon to *Malerisaurus langstoni*, whereas the clade they formed, plotted as the sister group to a tanystropheid clade which included *Boreopricea funerea* and *Cosesaurus aviceps*. In a re-analysis of this matrix by Rieppel et al. (2003) *Jesairosaurus lehmani* formed a polytomy with other “protorosaurs”, including drepanosaurs, and archosauriforms. In the recent analysis by Ezcurra (2016), *Jesairosaurus lehmani* was recovered as the sister taxon to Tanystropheidae. The unstable position of *Jesairosaurus lehmani* might be related to the poorly resolved relationships of former “protorosaurs” and the difficulty of confident character assessment for this taxon because the specimens are encrusted in hematite, severely hampering their preparation (Jalil 1997).

Langobardisaurus pandolfii Renesto 1994

Age. Middle Norian (Alaunian/Revueltian)

Occurrence. The uppermost section of the Zorzino Limestone Cene quarry, Lombardy, Italy (Renesto 1994b), lower member of the Forni Dolostone of Friuli, Italy (Renesto & Dalla Vecchia 2000), and the Seefeld Formation, near Innsbruck, Austria (Saller et al. 2013).

Holotype. **MCSNB 2883** – An articulated partial skeleton, missing both forelimbs completely, as well as parts of the skull, feet, and tail.

Hypodigm. **MCSNB 4860**, complete and articulated juvenile preserved in ventral view, with the skull covered by the neck and trunk in external view; **MFSN 1921**, a virtually complete and articulated adult specimen, including a well-preserved skull. Only the posterior part of the tail and part of the left forelimb are missing; **MFSN 26829**, a partial articulated adult specimen, preserving a nearly complete right hindlimb, a partial left hindlimbs, and some poorly visible parts of the vertebral column and potentially of the pelvic girdle; **P 10121**, a nearly complete impression of an articulated adult, only missing part of the tail, with some fragments of the limb bones and teeth preserved.

Diagnosis. The latest emended diagnosis for *Langobardisaurus pandolfii* was provided by (Saller et al. 2013).

Remarks. Renesto (1994b) was the first to describe the genus *Langobardisaurus* based on two specimens originally found in 1974, which were assigned to *Langobardisaurus pandolfii* and considered to be closely related to known tanystropheids, specifically *Macrocnemus bassanii*. It was interpreted as a terrestrial insectivore based on the presence of three cusped teeth, which are quite distinct to the teeth of other archosauromorphs. Bizzarini & Muscio (1995) proposed a new species, *Langobardisaurus rossii*, based on a new but poorly preserved specimen from the Forni Dolostone of Friuli, Italy. This specimen was later considered as a probably rhynchocephalian lepidosauromorph, mainly inferred from its body proportions, particularly the relative size of the head, cervical region, and trunk region (Renesto & Dalla Vecchia 2007). However, the poor preservation of this specimen prevents an unequivocal taxonomic determination. Another species, *Langobardisaurus? tonelloi*, was tentatively ascribed to the genus based on a complete specimen (**MFSN 1921**) by Muscio (1996). The species was considered to differ from *Langobardisaurus pandolfii* in its phalangeal formula and dentition. However, Renesto & Dalla Vecchia (2000) could not find any differences between the phalangeal formula in these two taxa and considered the minor differences in dentition to be attributable to ontogenetic variation, and thus considered *Langobardisaurus tonelloi* to likely represent a junior synonym of *Langobardisaurus pandolfii*, which was later corroborated by Saller et al. (2013). **MFSN 1921** allowed for the first detailed description of the skull of *Langobardisaurus pandolfii* and revealed a unique dentition among archosauromorphs, consisting of an edentulous premaxilla and anterior margin of the maxilla, followed by tricuspid teeth more posteriorly on the maxilla and dentary, and terminating in a very large, molar-like crushing posteriormost tooth on both the maxilla and dentary. Renesto & Dalla Vecchia (2000) hypothesized that *Langobardisaurus pandolfii* used this highly specialized dentition to feed on large insects, crustaceans, and small scaly fishes. Renesto et al. (2002) described another specimen, **MFSN 26829**, and considered facultative bipedal locomotion for *Langobardisaurus pandolfii*, which has also been proposed for *Macrocnemus bassanii* (Rieppel 1989). **P 10121**, a poorly preserved specimen of *Langobardisaurus pandolfii* consisting of the impression, as well as bone fragments, of a nearly complete skeleton, was described from the Seefeld Formation of Austria, thus extending the biogeographic range of the taxon outside Italy (Saller et al. 2013).

Dinocephalosaurus orientalis Li 2003

Age. Anisian.

1203 Occurrence. Xinmin, Panxian, and Luoping, Guanling Formation, Guizhou Province, China. (Li 2003; Liu et
1204 al. 2017; Rieppel et al. 2008).

1205 Holotype. **IVPP V13767**, an almost complete skull and the three anteriormost cervical vertebrae and
1206 associated ribs.

1207 Hypodigm. **ZMNH M8752**, an undescribed specimen of which the pelvic morphology was briefly
1208 mentioned in comparison to that of *Fuyuanosaurus* by Fraser et al. (2013); **LPV 30280**, a partial, articulated
1209 skeleton including some disarticulated skull bones, most of the cervical column, parts of the thorax,
1210 hindlimbs, and proximal tail. Within the thorax some elements belonging to an embryo are preserved,
1211 which indicates that this specimen was pregnant when it died (Liu et al. 2017), **IVPP V13898**, a relatively
1212 complete skeleton including a skull preserved in ventral view, a complete cervical series, and parts of the
1213 thorax including an articulated fore and hindlimb (Rieppel et al. 2008).

1214 Diagnosis. The most recent diagnosis of *Dinocephalosaurus orientalis* was provided by Rieppel et al.
1215 (2008).

1216 Remarks. *Dinocephalosaurus orientalis* was first described based on the holotype which only preserves
1217 the skull and three anteriormost cervical vertebrae (Li 2003). The discovery of a specimen preserving much
1218 of the postcranial skeleton subsequently revealed a striking convergence between *Dinocephalosaurus*
1219 *orientalis* and *Tanystropheus* spp. (Li et al. 2004). *Dinocephalosaurus orientalis* shares the extreme
1220 elongation of the neck with *Tanystropheus* spp., but achieved this elongation through different means,
1221 since its neck is made up of comparatively much shorter cervical vertebrae and the neck consists of at
1222 least 33 vertebrae, whereas that of *Tanystropheus hydroides* and *Tanystropheus longobardicus* was made
1223 up of 13 (Li et al. 2017b; Rieppel et al. 2010; Rieppel et al. 2008). Additionally, the postcranial morphology
1224 of *Dinocephalosaurus orientalis* shows clear adaptations to a fully aquatic lifestyle, most notably the
1225 paddle-like front and hindlimbs. As for *Tanystropheus* spp., the unique morphology of *Dinocephalosaurus*
1226 *orientalis* has led to various hypotheses regarding its lifestyle and feeding method. Li et al. (2004)
1227 tentatively suggested suction feeding for *Dinocephalosaurus orientalis*, which was refuted by Peters
1228 (2005) and Demes & Krause (2005). The former argued that *Dinocephalosaurus orientalis* was a benthic
1229 ambush predator and a very poor swimmer. This suggestion was in return repudiated by LaBarbera &
1230 Rieppel (2005). A general anatomical description of *Dinocephalosaurus orientalis* was provided by Rieppel
1231 et al. (2008). This study included a phylogenetic analysis in which *Dinocephalosaurus orientalis* was
1232 incorporated into the combined dataset provided by Rieppel et al. (2003), which found a polytomy formed

by *Jesairosaurus lehmani*, *Dinocephalosaurus orientalis*, drepanosaurs, and tanystropheids. Liu et al. (2017) described a new *Dinocephalosaurus* specimen, which preserves articulated remains of a juvenile *Dinocephalosaurus* within the thorax of the adult, indicating the first example of vivipary in an archosauromorph reptile. This study also provided an updated version of the phylogenetic analysis of Rieppel et al. (2008), in which they recovered *Dinocephalosaurus orientalis* as the sister taxon to Tanystropheidae. Another embryo bearing close similarities to *Dinocephalosaurus orientalis* was described by Li et al. (2017b). It represents a separate taxon, since it differs distinctly from *Dinocephalosaurus orientalis* in its relative limb proportions and in having 24 rather than at least 33 cervical vertebrae. However, it has not been assigned to a separate species due to the very early ontogenetic stage of the specimen and it was instead referred to as a “dinocephalosaur”, indicating the presence of multiple closely related *Dinocephalosaurus*-like taxa.

Fuyuansaurus acutirostris Fraser, Rieppel & Li 2013

Age. Ladinian (Dong et al. 1997; although the conodont *Paragondolella polygnathiformis* indicates an earliest Carnian age; Jiang et al. 2009).

Occurrence. Zhunganpo Member of the Falang Formation, Guizhou Province, China (Fraser et al. 2013).

Holotype. **IVPP V17983**, a partial skeleton preserving a skull, cervical vertebral column, a few dorsal vertebrae, and a pectoral and pelvic girdle.

Diagnosis. The only diagnosis of *Fuyuansaurus acutirostris* so far was provided by Fraser et al. (2013).

Remarks. *Fuyuansaurus acutirostris* is a small archosauromorph with a long neck and an elongate rostrum, known from a single, possibly juvenile, specimen. It has been interpreted as an aquatic taxon and bears clearly tanystropheid features in the presence of a long neck, made up of elongated cervical vertebrae and corresponding ribs, and the shape of the scapula (Fraser et al. 2013). It can be distinguished from other tanystropheids by its elongate and tapered snout and a pelvic girdle that lacks a thyroid fenestra between the pubis and ischium. *Fuyuansaurus acutirostris* has previously not previously been included in a phylogenetic analysis.

Pectodens zhenyuensis Li, Fraser, Rieppel, Zhao & Wang 2017

1261 Age. Anisian.

1262 Occurrence. Member II of the Guanling Formation, Luoping, Yunnan Province, China (Li et al. 2017a).

1263 Holotype. **IVPP V18578**, a nearly complete and articulated skeleton including skeleton.

1264 Diagnosis. The diagnosis was provided by (Li et al. 2017a).


1265 Remarks. *Pectodens zhenyuensis* is a small, highly gracile archosauromorph with an elongate neck, tail,
1266 and limbs. It bears certain characteristics typical of “protorosaurs”, most notably in having a long neck
1267 with elongate cervical vertebrae and ribs. Li et al. (2017a) addressed the similarities of *Pectodens*
1268 *zhenyuensis* to “Protorosauria”, but considered its inclusion in this group only tentative, since it lacks
1269 several diagnostic features, such as the presence of a hooked fifth metatarsal and a thyroid fenestra
1270 between the pubis and ischium, and because it differed from other “protorosaurs” in the shape of its skull
1271 and marginal dentition. Most carpal bones are missing in the only known specimen, even though the
1272 manus is fully articulated, possibly because these bones had not yet ossified due to the early ontogenetic
1273 stage of the specimen. The phylogenetic position of *Pectodens zhenyuensis* has previously not been
1274 tested.

1275

1276 *Mesosuchus browni* Watson 1912

1277 Age. Early Anisian.

1278 Occurrence. Burgersdorp Formation of the Beaufort Group near Aliwal North, Subzone B of the
1279 Cynognathus AZ, Eastern Cape Province, South Africa (Dilkes 1998; Hancox 2000).

1280 Holotype. **SAM-PK-5882**, a partial skull consisting of the snout, braincase, and palatal regions,  mandibles,
1281 a partial vertebral column, an incomplete scapula and pelvic girdle, and partial fore and hindlimbs.

1282 Hypodigm. The hypodigm of *Mesosuchus browni* was provided by Dilkes (1998) and also listed by Ezcurra
1283 (2016).

1284 Diagnosis. The most recent diagnosis was provided by Dilkes (1998).

1285 Remarks. *Mesosuchus browni* is considered the best known non-rhynchosaurid rhynchosaur (Butler et al.
1286 2015; Hone & Benton 2008). Like the other early rhynchosaurs *Howesia browni* and *Eohyosaurus*
1287 *wolvaardti*, as well as the archosauriforms *Euparkeria capensis* and *Erythrosuchus africanus*, it is known

from the Burgersdorp Formation near Aliwal North in the Eastern Cape, South Africa (Butler et al. 2015; Ezcurra et al. 2016; Rubidge 2005). *Mesosuchus browni* has been studied several times (Broom 1913a; Broom 1913b; Broom 1925; Haughton 1922; Haughton 1924a; Watson 1912), and has been most comprehensively described by Dilkes (1998). In many ways *Mesosuchus browni* shows a morphology which is intermediate between that of rhynchosaurids and other early archosauromorphs. **SAM-PK-6536** represents a particularly informative specimen, as it includes a complete, virtually undistorted skull. The braincase of this specimen was recently described in detail by Sobral & Müller (2019), and revealed a pneumatic sinus between the basal tubera. Pneumatization of the braincase was previously considered a derived archosaur trait, but its presence in *Mesosuchus browni* indicates it had evolved much earlier in the archosauromorph lineage.

Howesia browni Broom 1905

Age. Early Anisian.

Occurrence. Burgersdorp Formation of the Beaufort Group near Aliwal North, Subzone B of the Cynognathus AZ, Eastern Cape Province, South Africa (Dilkes 1995; Hancox 2000).

Holotype. **SAM-PK-5884**, a flattened partial skull missing the snout and occipital regions, and lower jaws.

Hypodigm. **SAM-PK-5885**, a flattened partial skull missing the snout, and lower jaws, and an atlas-axis complex; **SAM-PK-5886**, a postcranial skeleton consisting of a partial vertebral column, an incomplete pelvic girdle and left hindlimb, and a complete right tarsus.

Diagnosis. The most recent diagnosis was provided by Dilkes (1995).

Remarks. *Howesia browni* is a non-rhynchosaurid rhynchosaur closely related to *Mesosuchus browni* that was first described by Broom (1905a). Following additional preparation of the three known specimens, *Howesia browni* was extensively described by Dilkes (1995).

Eohyosaurus wolvaardti Butler, Ezcurra, Montefeltro, Samanthi & Sobral 2015

Age. Early Anisian

1314 Occurrence. Burgersdorp Formation of the Beaufort Group near Aliwal North, Cynognathus AZ, Subzone
1315 B (Butler et al. 2015).

1316 Holotype. **SAM-PK-K10159**, skull and mandibles missing the anterior part of the snout.

1317 Diagnosis. The diagnosis was provided by Butler et al. (2015).

1318 Remarks. Butler et al. (2015) described *Eohyosaurus wolvaardti* and included it in a phylogenetic analysis.
1319 It was recovered as the sister taxon to rhynchosaurids and was thus found to be more closely related to
1320 this clade than *Mesosuchus browni* and *Howesia browni*. In another phylogenetic analysis focusing on
1321 rhynchosaurs, it was found in a polytomy with rhynchosaurids, *Mesosuchus browni*, *Howesia browni*, and
1322 *Noteosuchus colletti*, the last being a poorly known early rhynchosaur from the Induan of South Africa
1323 (Ezcurra et al. 2016).

1324

1325 *Pamelaria dolichotrachela* Sen 2003

1326 Age. Anisian (Lucas 2010).

1327 Occurrence. Yerrapalli Formation, Gondwana Supergroup, Pranhita–Godavari Basin, southern India.

1328 Holotype. **ISIR 316**, a partial skeleton including a largely complete skull.

1329 Hypodigm. The referred specimens are listed in Sen (2003) and Ezcurra (2016).

1330 Remarks. *Pamelaria dolichotrachela* is known from three specimens originating from the Yerrapalli
1331 Formation (Middle Triassic) of India and was originally identified as a “protorosaur” (Sen 2003). However,
1332 recent phylogenetic analyses have revealed that *Pamelaria dolichotrachela* is an allokotosaur, closely
1333 related to *Azendohsaurus* spp. and *Shringasaurus indicus* (Ezcurra 2016; Nesbitt et al. 2015; Sengupta et
1334 al. 2017; and subsequent modifications of these matrices).

1335

1336 *Azendohsaurus madagaskarensis* Flynn, Nesbitt, Parrish, Ranivoharimanana & Wyss 2010)

1337 Age. Late Ladinian to early Carnian.

1338 Occurrence. Locality M-28 close to the eastern bank of the Malio River, west of Isalo National Park,
1339 southern Madagascar, Isalo II of the Makay Formation (Nesbitt et al. 2015).

1340 Holotype. **UA 7-20-99-653**, partial skull and five anterior cervical vertebrae.

1341 Hypodigm. A list of referred specimens can be found in appendix 1 of Nesbitt et al. (2015).

1342 Diagnosis. The most recent diagnosis was provided in Nesbitt et al. (2015).

1343 Remarks. *Azendohsaurus madagaskarensis* is the best-known species of the genus, but the first described
 1344 species is *Azendohsaurus laaroussii*. The latter taxon was originally described from a few teeth and dental
 1345 fragments and interpreted as an ornithischian dinosaur (Dutuit 1972), and later a sauropodomorph
 1346 dinosaur (e.g. Gauffre 1993). Postcranial remains from the type locality of *Azendohsaurus laaroussii* can
 1347 likely also be referred to this species, and indicate that the taxon did not belong to Dinosauria (Cubo &
 1348 Jalil 2019; Jalil & Knoll 2002). Comprehensive three-dimensionally preserved remains of various
 1349 individuals from the late Middle Triassic to early Late Triassic of southern Madagascar, which closely
 1350 resembled the known material of *Azendohsaurus laaroussii*, were assigned to *Azendohsaurus*
 1351 *madagaskarensis*. The skull and mandibles were initially described by Flynn et al. (2010). A description of
 1352 the postcranium and a phylogenetic hypothesis for *Azendohsaurus madagaskarensis* was provided by
 1353 Nesbitt et al. (2015). This revealed a new clade of non-archosauriform archosauromorphs, Allokotosauria,
 1354 that includes *Azendohsaurus* spp., *Trilophosaurus* spp., *Pamelaria dolichotrachela*, *Spinosuchus caseanus*,
 1355 *Shringasaurus indicus*, and *Teraterpeton hrynewichorum*. This clade has subsequently been recovered in
 1356 other analyses (e.g. Ezcurra 2016; Sengupta et al. 2017), confirming it as one of the three major lineages
 1357 of non-archosauriform archosauromorphs, together with Rhynchosauria and Tanystropheidae.
 1358 *Azendohsaurus madagaskarensis* represents one of the best-known non-archosauriform
 1359 archosauromorphs. It was herbivorous and has a relatively large body size among early
 1360 archosauromorphs, being approximately 2 to 3 metres in length.

1361

1362 *Trilophosaurus buettneri* Case 1928

1363 Age. Carnian (Parker & Martz 2010; Spielmann et al. 2008).

1364 Occurrence. *Trilophosaurus* site 1 and *Trilophosaurus* quarries 1-3, Colorado City Formation; Walker's
 1365 Tank and lower Kalgary site, Tecovas Formation, western Texas, USA (Spielmann et al. 2008).

1366 Holotype. **UMMP 2338**, an incomplete right dentary bearing teeth.

1367 Hypodigm. A list of referred specimens can be found in appendix 1 of Spielmann et al. (2008).

1368 Diagnosis. The most recent diagnosis is provided by Spielmann et al. (2008, p. 11)


1369 Remarks. *Trilophosaurus buettneri* was first described based on a dentary fragment bearing teeth (Case
1370 1928) and interpreted to be closely related to procolophonids. Additional specimens that gave a much
1371 more complete account of the taxon were described by Gregory (1945). Gregory (1945) referred
1372 *Trilophosaurus buettneri* to “Protorosauria”. The skull of *Trilophosaurus buettneri* was later redescribed
1373 by Parks (1969). Another species referred to the genus, “*Trilophosaurus jacobsi*”, was proposed to
1374 represent a junior synonym of *Spinosuchus caseanus* by Nesbitt et al. (2015). *Trilophosaurus buettneri* was
1375 redescribed and reinterpreted as a non-archosauriform archosauromorph outside “Protorosauria” by
1376 Spielmann et al. (2008). *Trilophosaurus buettneri* was later found within the newly erected clade
1377 Allokotosauria (e.g. Ezcurra 2016; Nesbitt et al. 2015). The manus of *Trilophosaurus buettneri* was
1378 redescribed by Nesbitt et al. (2015). *Trilophosaurus buettneri* was herbivorous and has a remarkable
1379 dentition, characterized by an edentulous, beak-like snout and transversely or labiolingually very wide
1380 tricuspid teeth further posterior in the jaws. An arboreal lifestyle has been suggested for *Trilophosaurus*
1381 *buettneri* by Spielmann et al. (2005), based on the relative proportions of the appendicular skeleton and
1382 the presence of large curved claws. Although similar claws occur in other allokotosaurs (e.g.
1383 *Azendohsaurus madagaskarensis*), a similar interpretation has not been made for these taxa Nesbitt et al.
1384 (2015).

1385

1386 *Teyujagua paradoxa* Pinheiro, França, Lacerda, Butler & Schultz 2016

1387 Age. Induan-Olenekian (Dias-da-Silva et al. 2017; Pinheiro et al. 2019).

1388 Occurrence. Bica São Tomé, Sanga do Cabral Formation, São Francisco de Assis, Rio Grande do Sul,
1389 southern Brazil.

1390 Holotype. **UNIPAMPA 653**, a nearly complete skull and mandibles, as well as parts of the first five cervical
1391 vertebrae.

1392 Diagnosis. The most recent diagnosis was provided by Pinheiro et al. (2019).

1393 Remarks. *Teyujagua paradoxa* was first described by Pinheiro et al. (2016) and subsequently described in
1394 more detail with the aid of μ CT data by Pinheiro et al. (2019). The skull and mandibles of *Teyujagua*
1395 *paradoxa* exhibit a remarkable combination of plesiomorphic features, typical of non-archosauriform
1396 archosauromorphs (e.g. absence of the antorbital fenestra), and derived features which represent

1397 synapomorphies for Archosauriformes (e.g. the presence of an external mandibular fenestra). This is also
1398 reflected in the position of *Teyujagua paradoxa* in previous phylogenetic analyses including this species,
1399 in which it was recovered as the sister taxon to Archosauriformes (Pinheiro et al. 2016; Pinheiro et al.
1400 2019).

1401

1402 *Euparkeria capensis* Broom 1913

1403 Age. Early Anisian

1404 Occurrence. Burgersdorp Formation of the Beaufort Group near Aliwal North, Subzone B of the
1405 Cynognathus AZ, Eastern Cape Province, South Africa (Ewer 1965; Hancox 2000; Sookias 2016).

1406 Holotype. **SAM-PK-5867**, a complete skull and mandibles and a largely complete and articulated
1407 postcranial skeleton, only missing most of the hands and feet and the majority of the tail.

1408 Hypodigm. A complete hypodigm is listed in Sookias (2016)

1409 Diagnosis. An emended diagnosis was recently provided in Sookias (2016).

1410 Remarks. *Euparkeria capensis* is a small, carnivorous archosauriform that has received a lot of interest due
1411 to its morphology and phylogenetic position, as it represents a well-known early archosauriform that is
1412 closely related to Archosauria. The most extensive morphological description of *Euparkeria capensis* was
1413 provided by Ewer (1965). Recently, a detailed revision of the Euparkeriidae, a monophyletic clade
1414 comprising *Euparkeria capensis* and its closest relatives, included a morphological reevaluation of this
1415 taxon (Sookias 2016; Sookias & Butler 2013; Sookias et al. 2014). The braincase has recently been
1416 described in detail by Sobral et al. (2016).

1417

1418 *Erythrosuchus africanus* Broom 1905

1419 Age. Early Anisian (Abdala et al. 2005).

1420 Occurrence. Various localities in South Africa, most notably near Aliwal North and Burgersdorp, Eastern
1421 Cape Province, and Rouxville, Free State Province, Burgersdorp Formation of the Beaufort Group,
1422 *Cynognathus* AZ subzone B, Karoo Supergroup (Abdala et al. 2005; Gower 2003).

1423 Holotype. **SAM-PK-905**, an incomplete postcranial skeleton, mainly consisting of the pectoral and pelvic
1424 girdles, partial forelimb, and vertebrae.

1425 Hypodigm. A list of the referred specimens is provided in Appendix 1 of Gower (2003).

1426 Diagnosis. The most recent diagnosis for *Erythrosuchus africanus* is provided by Ezcurra (2016).

1427 Remarks. *Erythrosuchus africanus* is a large-sized carnivorous archosauriform with a skull that is
1428 particularly large compared to the postcranium. It was first described based on a partial postcranial
1429 skeleton by Broom (1905b). A new and more completely preserved specimen, including a partial skull,
1430 was described by Huene (1911). *Erythrosuchus africanus* was more recently described extensively by
1431 Gower (2003), and separate studies addressed the morphology of the pes (Gower 1996), and braincase
1432 (Gower 1997).

1433

1434 **Material and Methods**

1435 To resolve the phylogenetic relationships of tanystropheids and other “protorosaurs”, a new
1436 comprehensive character matrix was constructed consisting of 307 characters. These include 42 new
1437 characters, with the remaining characters having been compiled and modified from the literature
1438 (mainly from Ezcurra 2016 and Pritchard et al. 2015, but also sourced from Benton & Allen 1997; Dilkes
1439 1998; Jalil 1997; Pritchard et al. 2018; Senter 2004; Simões et al. 2018; and Sookias 2016). The matrix
1440 contains 23 ratio characters, and 48 multistate characters are ordered as they are considered to form a
1441 transformational series in which at least one state represents a clear intermediate between two other
1442 states. Currently there is ongoing debate whether discrete characters should be ordered and whether to
1443 discretize continuous data by using ratios (Grand et al. 2013; Simões et al. 2016), but their application
1444 has been considered phylogenetically informative in previous studies of archosauromorph relationships
1445 (Ezcurra 2016; Nesbitt 2011). To test for the influence of ordered and ratio characters for our dataset,
1446 one round of analyses was performed including the ratio characters and with characters indicated as
1447 ordered treated as such, and another round without ratio characters and with all remaining characters
1448 unordered. A total of 42 OTUs are included, the large majority of which were scored based on personal
1449 observations of relevant specimens. *Petrolacosaurus kansensis* was assigned as the outgroup. Poorly
1450 represented or problematic taxa were pruned for the final analyses (these are taxa with less than 25% of
1451 characters scored, in addition to *Czatkowiella harae*, which was pruned because this taxon could
1452 possibly represent a chimera, see Table 1), resulting in final trees consisting of 32 OTUs. A full list of all

character scorings and the specimens and literature that have been employed are provided in the Supplementary Information. The specimens that were scored are specified for each character individually for future assessment and comparison. The analyses were performed in TNT 1.5 (maximum parsimony criterion; Goloboff & Catalano 2016), using several rounds of equally weighted 'New Technology Search' algorithms to adequately explore tree space and maximize the likelihood of finding the global optimum. Initial trees were calculated with 'Sectorial Search', 'Ratchet', 'Drift' and 'Tree Fusing' algorithms using 100 iterations each and 1000 random addition sequences (RAS). Relative fit difference was set at 0.1 and up to 10 suboptimal trees were retained. The saved trees were subsequently put through two separate analyses of three rounds each. One analysis applying 'Sectorial search', 'Ratchet', and 'Ratchet', in that order; and the other 'Ratchet', 'Sectorial search', and 'Ratchet'. All rounds ran 1000 iterations and additionally included 1000 iterations of 'Tree fusing'. At this stage suboptimal trees were discarded, and the strict consensus tree was calculated from the remaining trees. Bremer and Bootstrap support values were calculated, the latter using 'Traditional search' at 1000 iterations.

Character sampling and formulation

Following detailed investigations of early archosaur phylogenetic relationships (e.g. Nesbitt 2011), the phylogeny of non-archosaurian archosauromorphs has received much attention in recent years and several detailed character lists for this group exist, with one analysis focusing on tanystropheids (Pritchard et al. 2015) and another on allokotosaurs (Nesbitt et al. 2015). However, the most comprehensive analysis, consisting of 600 characters, was provided by Ezcurra (2016), in which characters of these previous analyses were included, as well as those of many other studies. Furthermore, for many of the characters included at least one of the character states was figured, limiting subjective interpretation of the characters by the reader. Several subsequent studies have used and slightly modified the matrix provided by Ezcurra (2016) depending on the clade that was focused on in each respective study (e.g. Butler et al. 2019; Ezcurra et al. 2019; Sengupta et al. 2017; Stocker et al. 2017).

Due to its comprehensiveness and well-explained characters, the character list of Ezcurra (2016) was used as the main source for our characters. However, only those characters that were relevant to the sampled taxa were included, as many characters in the original list were used to differentiate between taxa not included herein, such as proterochampsids, archosaurs, and choristoderes. Additional characters were incorporated mainly from the character list of Pritchard et al. (2015), and supplemented by characters from Pritchard et al. (2018), Nesbitt et al. (2015), Nesbitt (2011), Sookias (2016), Simões et al.

(2018), Dilkes (1998), Jalil (1997), Benton & Allen (1997), and Senter (2004). Certain characters taken from the literature were modified to fit more precisely with the specific morphologies observed in the sampled taxa. Finally, new characters were constructed based on detailed morphological comparisons of the included taxa. Autapomorphies of a single species were also incorporated into characters as they represent important morphological information and since these characters might prove phylogenetically relevant after future findings. New characters and characters that have been distinctly modified from previous analyses are discussed and figured.

All characters were critically assessed on their logical construction and whether character states represent valid tests of similarity or primary homology. Issues regarding character construction, specifically how to optimize the construction of characters as to represent similarity tests, are a continuing source of debate (e.g. Brazeau 2011; Kearney & Rieppel 2006; Rieppel & Kearney 2007). Criteria for character construction to minimize “non-meaningful” character scorings have been suggested by Simões et al. (2016) and examples of problematic characters have also been pointed out by Nesbitt (2011). We assessed all our characters in light of these suggestions, as these criteria provide important considerations for character construction. However, we find that the application of each criterion is dependent on various factors. The taxa included in our analysis all represent Permo-Triassic non-archosaur members of the archosauromorph lineage, as well as early lepidosauromorphs and non-saurian diapsids. This phylogenetically relatively narrow sample is expected to exhibit less morphological variation and cases of homoplasy than larger scale analyses (e.g. both extant and extinct Lepidosauromorpha and closely related taxa as in Simões et al. 2018). Therefore, in certain cases, characters that might otherwise not follow the criteria proposed in Simões et al. (2016) (e.g. the shape of the orbit, Type I A.7, or the use of continuous characters, Type II of Simões et al. 2016) are maintained when, based on detailed comparisons and careful consideration, the character states therein were deemed to likely represent valid similarity tests to the taxa involved. We pose that although these criteria as formulated represent useful tools, the complexity of morphological variation entails that careful observation and logical assessments of similarity by experts on the taxonomic sample at hand should be leading in character construction (Kearney & Rieppel 2006; Rieppel & Kearney 2007). Therefore, a character which might be problematic as a test of homology when applied to one set of taxa, might still be valid when looking at a different taxonomic sample. Following Brazeau (2011) the presence or absence of a feature was formulated as a separate character from its morphology for unordered characters. In these cases, the character describing the morphology of this feature was scored as inapplicable in taxa in which the character is absent.

1515 *Character list*

1516 1) Ezcurra (2016) ch. 20. *Snout, antorbital length (anterior tip of the skull to anterior margin of*
1517 *the orbit) versus total length of the skull: 0.29-0.40 (0); 0.43-0.62 (1); 0.70-0.76 (2), ORDERED RATIO*
1518 *(Ezcurra 2016: Figs. 17 and 18).*

1519 This character was considered to be interdependent with character 76 of Ezcurra (2016). Since this
1520 character 20 could be applied to more taxa than character 76, the former was preferred and the latter
1521 excluded.

1522 2) Modified from Ezcurra (2016) ch. 21. *Snout, dorsoventral height at the level of the anterior tip*
1523 *of the maxilla versus dorsoventral height at the level of the anterior border of the orbit: 0.15-0.27 (0);*
1524 *0.32-0.51 (1); 0.56-0.80 (2), ORDERED RATIO (Ezcurra 2016: Figs. 17 and 19).*

1525 Character states were defined after comparison of all the different measured ratios.

1526 3) Ezcurra (2016) ch. 22. *Snout, proportions at the level of the anterior border of the orbit:*
1527 *transversely broader than dorsoventrally tall or subequal (0); dorsoventrally taller than transversely*
1528 *broad (1) (Ezcurra 2016: Fig. 16).*

1529 4) Modified from Ezcurra (2016) ch. 27. *Premaxilla, main body size: length of the tooth bearing*
1530 *margin in lateral view (in edentulous taxa the ventral margin of the premaxilla contributing to the*
1531 *ventral margin of the upper jaw; =main body) versus the length of the snout (anterior tip of the skull to*
1532 *the anterior border of the orbit): 0.08-0.18 (0); 0.20-0.38 (1); 0.44-0.60 (2), ORDERED RATIO (Ezcurra*
1533 *2016: Fig. 17).*

1534 The original distinction between the character states was not considered to be phylogenetically
1535 relevant, and therefore it was decided here to distinguish the states based on ratios that were
1536 discretized a posteriori.

1537 5) Ezcurra (2016) ch. 29. *Premaxilla, downturned main body: absent, alveolar margin sub-parallel*
1538 *to the main axis of the maxilla (0); slightly, in which the alveolar margin is angled at approximately 20*
1539 *degrees to the alveolar margin of the maxilla (1); strongly, prenasal process obscured by the postnasal*
1540 *process in lateral view (if the postnasal process is long enough) and postnasal process parallel or*
1541 *posteroventrally orientated with respect to the main axis of the premaxillary body (2), ORDERED (Ezcurra*
1542 *2016: Figs. 16-19).*

1543 6) Ezcurra (2016) ch. 30. *Premaxilla, angle formed between the alveolar margin and the anterior*
 1544 *margin of the premaxillary body in lateral view: acute or right-angled (0); obtuse (1) (Ezcurra 2016: Figs.*
 1545 *20 and 21). This character is inapplicable in taxa with a hooked premaxilla.*

1546 7) Modified from Ezcurra (2016) ch. 34. *Premaxilla, prenarial process: absent or incipient (0); present and*
 1547 *less than the anteroposterior length of the main body of the premaxilla (1); present and longer than the*
 1548 *anteroposterior length of the main body of the premaxilla (2), ORDERED (Ezcurra 2016: Figs. 17 and 21).*
 1549 *This character is scored as inapplicable in taxa with confluent external nares.*

1550 An absent or incipient state was added and the character was ordered, since the character is considered
 1551 a transformational series and state 1 represents a clear intermediate between states 0 and 2.
 1552 Furthermore, the inapplicability criterion was included, since confluent external nares preclude the
 1553 presence of a prenarial process.

1554 8) Modified from Ezcurra (2016) ch. 35. *Premaxilla, base of the prenarial process:*
 1555 *anteroposteriorly shallow, being not much wider at its base than further distally on the process (0);*
 1556 *anteroposteriorly deep, being much wider at its base than further distally on the process (1). (Ezcurra*
 1557 *2016: Figs. 12, 17, 20 and 21). This character is inapplicable in taxa that lack a prenarial process.*

1558 This character was further clarified in its description and an inapplicability criterion was included.

1559 9) Modified from Ezcurra (2016) ch. 36 and 40. *Premaxilla, postnarial process (= posterodorsal process, =*
 1560 *maxillary process, = subnarial process): absent (0); short, ends well anterior to the posterior margin of*
 1561 *the external naris (1); well-developed, forms most of the ventral border of the external naris or excludes*
 1562 *the maxilla from participation in the external naris but process does not contact prefrontal (2); well-*
 1563 *developed, forms most of the ventral border of the external naris and postnarial process of premaxilla*
 1564 *contacts prefrontal (3), ORDERED (Ezcurra 2016: Figs. 17 and 19).*

1565 Characters 36 and 40 of Ezcurra (2016) were combined here because a contact between the premaxilla
 1566 and the prefrontal always requires the premaxilla to exclude the maxilla from the external nares. Thus,
 1567 these conditions can be considered as part of the same transformational series.

1568 10) Ezcurra (2016) ch. 37. *Premaxilla, postnarial process (= posterodorsal process, = maxillary*
 1569 *process, = subnarial process): wide, plate-like (0); thin (1). This character is not applicable to taxa that*
 1570 *lack a postnarial process (Ezcurra 2016: Fig. 20).*

11) Modified from Ezcurra (2016) ch. 41, and Nesbitt et al. (2015): ch. 247. *Premaxilla, plate-like palatal shelf or process on the medial surface (contribution to secondary palate by premaxillae): absent (0); present (1) (Ezcurra 2016: Figs. 12, 20 and 21)*

The character was redescribed to indicate that the “process” referred to represents a rather wide shelf-like structure. For further explanation, see character 247 of (Nesbitt et al. 2015).

12) Modified from Pritchard et al. (2015) ch. 1. *Premaxilla, distinct posterodorsally to anteroventrally directed grooves terminating at the ventral margin of the bone: absent (0); present (1).*

This character describes the presence of posterodorsally to anteroventrally directed grooves present in *Langobardisaurus pandolfii* MFSN 1921 that were previously mistakenly identified as premaxillary teeth (Saller et al. 2013). This character was reformulated here to describe this feature more specifically.

13) Modified from Ezcurra (2016) ch. 42. *Premaxilla, number of tooth positions: 8 or more (0); 5 or 6 (1); 4 (2); 3 (3); 2 (4); 1 or edentulous (5) ORDERED (Ezcurra 2016: Figs. 16 and 17).*

The states of this character were modified since the original distinction did not cover all observed variation and because state 1 partially covered the same number of teeth as state 0 in the original description. Characters 69 and 278 of Ezcurra (2016) were omitted here, because they were considered to be strongly interdependent with this character.

14) Modified from Ezcurra (2016) ch. 43. *Premaxilla, orientation of the tooth series or the occlusal surface of premaxilla in ventral view: approximately parasagittal (0); strongly transverse and (in case of tooth-bearing premaxillae) anterior teeth covering each other in lateral view (1). This character is inapplicable in taxa with a hooked and beak-like premaxilla (Ezcurra 2016: Fig. 21).*

The inapplicability criterion of this character was modified. It was previously scored as inapplicable in taxa with an edentulous premaxilla. However, we consider that the differentiating morphology addressed by this character can also occur in taxa that lack premaxillary teeth. However, a hooked or beak-like shape morphology does not allow for a transverse occlusal surface.

15) Ezcurra (2016) ch. 24. *Premaxilla-maxilla, suture: simple continuous contact (0); notched along the ventral margin (1) (Ezcurra 2016: Figs. 17 and 19).*

This character was also illustrated and discussed in Supplementary Figure 10 of Pritchard et al. (2018). However, we prefer this character formulation over that of Pritchard et al. (2018).

16) Modified from Ezcurra (2016) ch. 25. *Premaxilla-maxilla, subnarial foramen between the elements: absent (0); present (1) (Nesbitt 2011: Figs. 14, 17 and 19). Not applicable to taxa that have a ventral notch on the suture of the premaxilla and maxilla.*

The inapplicability criterion was included because the presence of a ventral notch on the border between the premaxilla and maxilla precludes the possibility of a subnarial foramen. Character states 1 and 2 of the previous iteration of this character were fused because the distinction between these two states is hard to establish confidently. Furthermore, this distinction is most likely irrelevant to the taxon sample included in this analysis.

17) New, similar to ch. 33 of Ezcurra (2016), ch. 6 of Pritchard et al. (2015), ch. 17 of Dilkes (1998), and ch. 6 of Pritchard et al. 2018. *Premaxilla-maxilla, contact between the premaxilla and maxilla: simple abutting contact (0); overlapping contact in which the premaxilla overlaps the maxilla laterally (1); overlapping contact in which the maxilla overlaps the premaxilla laterally (2); contact in which the premaxilla has a posteriorly directed peg on its posterolateral margin articulating with the maxilla, often accompanied by a groove (3); complicated connection in which the premaxilla has posteriorly projected peg on its medial surface which locks the maxilla against the premaxilla medially (4) (Fig. 2).*

The connection between the premaxilla and maxilla in early archosauromorphs has been discussed in depth and is considered phylogenetically informative. We have reformulated this character based on recent new findings with regards to the articulation between these elements in *Tanystropheus hydroides* (state 1) and *Macrocnemus bassanii* (state 4; Miedema et al. 2020; Spiekman et al. 2020). Among the taxa sampled here, most taxa have a simple abutting contact between premaxilla and maxilla, with neither bone distinctly overlapping the other (state 0; the sampled non-archosauromorph diapsids, *Czatkowiella harae*, *Prolacerta broomi*, *Trilophosaurus buettneri*, *Euparkeria capensis*, and *Proterosuchus fergusi*). In the sampled rhynchosaurs, the maxilla overlaps the premaxilla laterally (state 2; *Mesosuchus browni*). Certain taxa bear a small peg, meaning a short pin or bolt, on the posterolateral end of their premaxilla, which connects to the lateral surface of the maxilla (state 3; *Azendohsaurus madagaskarensis* and *Erythrosuchus africanus*). The configuration of *Macrocnemus bassanii*, in which a peg is present on the medial side of the premaxilla that interlocks with an anteriorly facing peg on the medial side of the maxilla (Miedema et al. 2020), is considered to be non-homologous with the pegs on the posterolateral end of the premaxilla described for state 3, and is therefore scored as a separate state here.

1629 18) Ezcurra (2016) ch. 45. *Septomaxilla: present (0); absent (1) (Ezcurra 2016: Fig. 16).*

1630 The presence of this small element in the anterior snout region is hard to establish, and therefore we
 1631 were not able to confidently consider it as absent for any taxon. Therefore, this character is not
 1632 phylogenetically informative for the present analysis, but it is nevertheless maintained as it presents an
 1633 overview of the presence of the septomaxilla among early archosauromorphs. Contrary to previous
 1634 interpretations, we were able to identify a septomaxilla in the rhynchosaur *Mesosuchus browni* (SAM-
 1635 PK-6536).

1636 19) Ezcurra (2016) ch. 52, and Nesbitt et al. (2015): ch. 203. *Maxilla, anterior maxillary foramen:*
 1637 *absent (0); present (1) (Ezcurra 2016: Fig. 17).*

1638 20) Modified from Nesbitt et al. (2015): ch. 202. *Maxilla, dorsal portion, shape: obtuse angle*
 1639 *between the dorsal and posterior margin of the maxilla, which is straight or slightly convex (0); the*
 1640 *dorsal apex of the maxilla ends abruptly and its posterior margin is concave (1) (Fig. 3).*

1641 The description of state 0 was modified to more precisely describe the condition observed in *Prolacerta*
 1642 *broomi* and *Protorosaurus speneri*. The character as described by Nesbitt et al. (2015) was preferred
 1643 over character 58 of Ezcurra (2016), since state 2 of the latter implies the presence of an antorbital
 1644 fenestra, which is scored here already in a separate character (22). In the description of character 202 of
 1645 Nesbitt et al. (2015) it was pointed out that in *Azendohsaurus madagaskarensis* and *Azendohsaurus*
 1646 *laaroussii* the posterodorsal margin of the maxilla is concave, similar to that of Archosauriformes, in
 1647 which this forms the anterior margin of the antorbital fenestra. A curved posterodorsal margin of the
 1648 maxilla occurred in many non-archosauriform archosauromorphs (see also character 58 of Ezcurra 2016
 1649 and its scoring). The presence of a distinct ascending process of the maxilla, considered to be a saurian
 1650 trait, (sensu the scoring of character 57 in Ezcurra 2016) is considered to be too ambiguous as a
 1651 phylogenetic character in the sampled taxa. For instance, the maxillae of *Youngina capensis* (AMNH
 1652 FARB 5561), *Protorosaurus speneri* (NMK S 180), and *Prolacerta broomi* (BP/1/5880) do not bear a
 1653 clearly defined process and the maxillae are approximately equally tall relative to their respective snouts
 1654 in all three taxa. Nevertheless, the former two taxa were previously considered to bear an ascending
 1655 process, in contrast to *Youngina capensis*. Furthermore the presence of a process-like dorsal portion of
 1656 the maxilla is strongly dependent on the relative height of the anterior portion of the snout at the level
 1657 of the anterior margin of the orbit, and this morphology is already covered by character 10 here.

21) Modified from Ezurra (2016) ch. 59. *Maxilla, anterior part of the dorsal margin: convex (0); straight (1); concave (2)* (Ezurra 2016: Fig. 22).

The anterior part of the dorsal margin is convex in *Prolacerta* (BP/1/5880; Spiekman 2018), *Trilophosaurus* (TMM 31025-207), *Protorosaurus speneri* (NMK S 180), *Mesosuchus browni* (SAM-PK-6536), *Youngina capensis* (SAM-PK-K7578), *Orovenator mayorum* (OMNH 74606), *Petrolacosaurus kansensis* (KUVV 9951), and *Gephyrosaurus bridensis* (Evans 1980). It is completely straight in *Macrocnemus bassanii* (PIMUZ T 4822) and *Proterosuchus fergusi* (RC 846; Ezurra & Butler 2015b), which is here considered as a separate state, as it is homologous to neither the concave nor convex state, but instead represents an intermediate state.

22) Ezurra (2016) ch. 13, and Pritchard et al. (2015): ch. 13. *Antorbital fenestra: absent (0); present (1)*.

23) New *Maxilla, antorbital fossa: absent (0); or present (1)* (Fig. 4). *This character is inapplicable in taxa that have an antorbital fenestra.*

A large circular concavity is present on the lateral margin of the maxilla of *Dinocephalosaurus orientalis* (IVPP V13767) as described by Rieppel et al. (2008). This character is clearly different from the antorbital fossa as described for *Erythrosuchus* (Gower 2003), which refers to a depression within which the large antorbital fenestra is located. Because of the clear affinities with the antorbital fenestra, this fossa is considered to represent a separate structure and the fossa described here, which does not occur in congruence with an antorbital fenestra, is currently only known to be present in *Dinocephalosaurus orientalis*.

24) Ezurra (2016) ch. 64 *Maxilla, posterior end of the horizontal process distinctly ventrally deflected from the main axis of the alveolar margin: absent (0); present (1)* (Ezurra 2016: Figs. 17 and 22).

25) Modified from Ezurra (2016) ch. 68 *Maxilla, alveolar margin in lateral view: straight (0); concave (1); convex (2); sigmoid, anteriorly concave and posteriorly convex (3); sigmoid, anteriorly convex, starting close to mid-length, and posteriorly concave (4)* (Ezurra 2016: Figs. 16 and 19) (Fig. 5).

This character was modified to distinguish between a concave, straight, or convex margin, since it was considered that these distinctions might be phylogenetically informative for this sample of taxa.

1686 26) Modified from Ezcurra (2016) ch. 75. *Maxilla, number of tooth positions: 11-17 (0); 19-40 (1).*
 1687 *This character is inapplicable in taxa with multiple tooth rows in the maxilla.*

1688 Character states were defined after determining the tooth count in all included taxa.

1689 27) Ezcurra (2016) ch.47. *Maxilla-jugal, anguli oris crest: absent (0); present (1) (Ezcurra 2016: Fig.*
 1690 *16).*

1691 28) New, combination of ch. 47 of Ezcurra (2016) and part of ch. 8 of Pritchard et al. (2015). *Maxilla-*
 1692 *jugal, anguli oris crest: both the jugal and the maxilla are distinctly laterally offset (0); only the jugal is*
 1693 *distinctly laterally offset (1) (Ezcurra 2016: Fig. 16). This character is scored as inapplicable in taxa that*
 1694 *lack an anguli oris crest.*

1695 The term anguli oris crest is typically used to describe the very conspicuous lateral offset of the jugal
 1696 seen in rhynchosaurid rhynchosaurs (e.g. Butler et al. 2015; Langer & Schultz 2000; Montefeltro et al.
 1697 2010). This crest might have facilitated a muscular cheek (Benton 1983). A much less conspicuous anguli
 1698 oris crest, which is partially formed by the posterolateral end of the maxilla, was recently described for
 1699 the non-rhynchosaurid rhynchosaur *Eohyosaurus wolvaardti* (Butler et al. 2015). A similar lateral offset
 1700 of the maxilla as seen in this taxon, which creates a substantial space between the lateral margin of the
 1701 crest and the posterior portion of the maxillary tooth row, was considered for the trilophosaurid
 1702 allokotosaurs *Trilophosaurus buettneri* and *Teraterpeton hrynewichorum* in Pritchard et al. (2015)
 1703 character 8. We consider the description of this character to address the same morphological structure
 1704 as seen in *Eohyosaurus wolvaardti* and therefore fused the characters. Although state 1 could possibly
 1705 represent an intermediate morphology between states 0 and 2, this cannot be ascertained, and
 1706 therefore this character is not ordered here. A similar lateral offset might also be present in
 1707 *Langobardisaurus pandolfii*. However, scoring this character for *Langobardisaurus pandolfii* is currently
 1708 ambiguous, since the preservation of this region is poor in the only specimen in which it is visible (MFSN
 1709 1921).

1710 29) Ezcurra (2016) ch. 9. *External nares, confluent: absent (0); present (1) (Ezcurra 2016: Fig. 16,*
 1711 *17 and 20).*

1712 30) Modified from Ezcurra (2016) ch. 12. *External naris, shape: sub-circular (0); oval (1) (Ezcurra*
 1713 *2016: Fig. 19). This character is inapplicable in taxa with confluent external nares.*

1714 An inapplicability criterion was added to this character.

1715 31) New *External naris: located close to the anterior end of the skull (0); a thick anterior margin of*
1716 *the premaxilla results in the external nares being posteriorly displaced (1) (Fig. 6).*

1717 In most taxa scored, the anterior margin of the external naris is closely positioned towards the anterior
1718 end of the snout. However, in the tanystropheids *Tanystropheus hydroides* (PIMUZ T 2790),
1719 *Tanystropheus longobardicus* (MSNM BES SC 1018), *Macrocnemus bassanii* (PIMUZ T 2477), *Pectodens*
1720 *zhenyuensis* (IVPP V18578), *Dinocephalosaurus orientalis* (IVPP V13767) and the archosauriform
1721 *Erythrosuchus africanus* (BP/1/5207), the anterior margin of the external naris is separated considerably
1722 from the anterior end of the snout by the main body of the premaxilla.

1723 32) Modified from Ezcurra (2016) ch. 78 *Nasal, shape of anterior margin at midline: strongly*
1724 *convex with anterior process and nasal forming an internarial bar (0); transverse with little convexity (1)*
1725 *(Ezcurra 2016: Fig. 16). This character is inapplicable in taxa in which the external nares are completely*
1726 *separated by an internarial bar.*

1727 This character is scored as inapplicable in taxa with a complete internarial bar, since this is always
1728 formed, at least in part, by an anterior process of the nasal. Thus, scoring taxa with a complete
1729 internarial bar for this character would result in overscoring this trait, as it is already addressed in
1730 character 5. Among the taxa with confluent external nares, only the nasals of *Azendohsaurus*
1731 *madagaskarensis* bear anterior processes on the anteromedial margin of the nasal.

1732 33) New *Nasal, antorbital recess: absent (0); or present (1) (Fig. 7).*

1733 The antorbital recess is described for *Dinocephalosaurus orientalis* by Rieppel et al. (2008). It is a large
1734 gully posterior to the external naris that is largely formed in the nasal bone, but the maxilla and possibly
1735 the prefrontal also contribute to it. This recess is non-homologous to the depression of the nasal
1736 described by character 80 of Ezcurra (2016). This recess has recently also been identified in
1737 *Tanystropheus hydroides* (Jiang et al. 2011; Spiekman et al. 2020).

1738 34) Modified from Pritchard et al. (2018) ch. 311. *Nasal, lateral surface: meets dorsoventrally short*
1739 *length of medial surface of dorsal process/portion of the maxilla (0); meets entire dorsoventral height of*
1740 *medial surface of supra-alveolar portion of maxilla (1). This character is inapplicable in taxa with an*
1741 *antorbital fenestra.*

See character description of character 311 of Pritchard et al. (2018). The inapplicability criterion was added because it was considered that the presence of an antorbital fenestra implies that the nasal cannot have a wide articulation facet with the maxilla.

35) Modified from Dilkes (1998) ch. 15. *Lacrima*, contacts nasal and reaches external naris (0); contacts nasal but does not reach naris (1); or does not contact nasal or reach naris (2), ORDERED. This character is inapplicable in taxa in which the premaxilla contacts the prefrontal.

This character was ordered because it is considered to represent a transformational series and state 1 represents an intermediate between states 0 and 2. Furthermore, the inapplicability criterion was included, because a contact between the premaxilla and prefrontal precludes a contact between the lacrimal and nasal.

36) Ezcurra (2016) ch. 90. *Lacrimal*, naso-lacrimal duct position: opens on the posterolateral edge of the lacrimal (0); opens on the posterior surface of the lacrimal (1). This character is inapplicable if the prefrontal encloses part of the naso-lacrimal duct (Ezcurra 2016: Fig. 19).

37) Ezcurra (2016) ch. 95. *Jugal*, anterior extension of the anterior process: anterior to the level of mid-length of the orbit (0); up to or posterior to the level of mid-length of the orbit (1).

38) New, similar to Ezcurra (2016) ch. 92. *Jugal*, anterior process is dorsoventrally expanded anteriorly: absent, the anterior process tapers anteriorly and articulates with the dorsal surface of the posterior process of the maxilla (0); present, the anterior process of the jugal is expanded and partially covers the lateral surface of the posterior process of the maxilla (1) (Fig. 8).

In the majority of the taxa sampled here, the anterior process of the jugal fits into a groove or slot on the dorsal surface of the posterior process of the maxilla and is in some cases partially covered by the maxilla in lateral view. In the archosauriforms *Euparkeria capensis* (SAM-PK-5867) and *Erythrosuchus africanus* (BP/1/5207) the jugal is distinctly dorsoventrally taller and partially overlaps the maxilla in lateral view.

39) Modified from Sookias (2016) ch. 81. *Jugal*, bulges ventrolaterally at the point where its three processes meet: absent (0); present (1). This character is scored as inapplicable in taxa that lack a posterior process of the jugal (Fig. 8).

This character describes the condition in the archosauriforms *Proterosuchus fergusi* (SAM-PK-11208), *Erythrosuchus africanus* (BP/1/5207), and *Teyujagua paradoxa* (Pinheiro et al. 2019). In these taxa the

posterior process of the jugal is located further laterally than their anterior processes. This is caused by a lateral bulging of the jugal at the point where the anterior, posterior, and ascending/dorsal processes of the bone meet. This morphology is clearly distinct from the anteromedially to posterolaterally directed crest described as the anguli oris crest and therefore coded as a separate character.

40) Ezcurra (2016) ch. 98. *Jugal, multiple pits on the lateral surface of the main body: absent (0); present (1) (Ezcurra 2016: Fig. 17).*

41) Ezcurra (2016) ch. 99 *Jugal, ascending process forming the entire anterior border of the infratemporal fenestra: absent (0); present, postorbital excluded from the anterior border of the infratemporal fenestra (1). This character is inapplicable in taxa in which the anterior process of the squamosal possesses an extensive contact with the postorbital and contacts the jugal, or lacks an infratemporal fenestra or an ascending process on the jugal. (Ezcurra 2016: Fig. 17).*

42) New *Jugal, posterior process: present (0); absent (1) (Fig. 9).*

A posterior process, typically present in archosauromorphs, is completely absent in *Claudiosaurus germani* (Carroll 1981), *Pectodens zhenyuensis* (IVPP V18578), *Dinocephalosaurus orientalis* (IVPP V13767), and *Trilophosaurus buettneri* (Spielmann et al. 2008).

43) Modified from Ezcurra (2016) ch. 100. *Jugal, length of the posterior process versus the height of its base: 0.49-1.27 (0); 1.59-3.77 (1); 4.07-5.90 (2), ORDERED RATIO. This character is inapplicable in taxa that lack a posterior process of the jugal (Ezcurra 2016: Figs. 17 and 19).*

The upper margin of state 2 was increased, but otherwise the ratios distribution of Ezcurra (2016) was maintained because these states formed clear demarcations between distinct morphologies as measured in the sampled taxa. The presence of a posterior process and the relative length of the posterior process were considered here as separate characters, since in multiple taxa the presence of the process could be established, but its relative length could not, due to the process not being fully preserved.

44) Modified from Ezcurra (2016) ch. 5. *Skull, dermal sculpturing on the dorsal surface of the frontals, parietals, and nasals: absent (0); shallow or deep pits scattered across surface and/or low ridges (1) (Ezcurra 2016: Fig. 16).*

State 2 of character 5 in Ezcurra (2016) was not included here, because it was not applicable to the taxa sampled here.

1800 45) Ezcurra (2016) ch. 109. *Prefrontal, subtriangular medial process: absent, nasal-frontal suture*
 1801 *transversely broad (0); present, nasal-frontal suture strongly transversely reduced (1) (Ezcurra 2016: Fig.*
 1802 *7).*

1803 46) Ezcurra (2016) ch. 111 and Nesbitt et al. (2015) ch. 237. *Prefrontal, lateral surface of the orbital*
 1804 *margin: smooth or slight grooves present (0); rugose sculpturing present (1) (Ezcurra 2016: Fig. 17).*

1805 47) Modified from Ezcurra (2016) ch. 16. *Orbit, shape: subcircular (0); distinctly dorsoventrally*
 1806 *taller than long (1).*

1807 States 0 and 1 of character 16 in Ezcurra (2016) represent a relatively minor morphological difference of
 1808 which the accurate observation is easily hampered by compression of specimens. Therefore this
 1809 character was modified to distinguish between the roughly subcircular orbits present in most of the
 1810 sampled taxa, and the very dorsoventrally tall orbits of *Proterosuchus fergusi* (SAM-PK-11208),
 1811 *Proterosuchus alexanderi* (NM QR 1484), and *Erythrosuchus africanus* (BP/1/5207).

1812 48) Modified from Ezcurra (2016) ch. 17. *Orbit, elevated rim: absent or incipient (0); present,*
 1813 *orbital margin of the jugal and/or postorbital slightly elevated to form a rim (1) (Ezcurra 2016: Figs. 16*
 1814 *and 17).*

1815 State 2 of character 17 in Ezcurra (2016) was excluded because it was not applicable to the sampled
 1816 taxa.

1817 49) Modified from Ezcurra (2016) ch. 113. *Frontal, suture with the nasal: transverse (0); oblique,*
 1818 *forming an angle of at least 60 degrees with long axis of the skull and frontals entering between both*
 1819 *nasals (1); oblique and nasals entering considerably between frontals in a non-interdigitate suture (2);*
 1820 *frontals enter nasals medially and nasals enter frontals laterally creating a W-shaped suture (3); frontals*
 1821 *possesses a three-pronged anterior process that articulates with the nasals (4). This character is*
 1822 *inapplicable if the nasal is received by a slot in the frontal or the nasal does not contact the frontal*
 1823 *(Ezcurra 2016: Fig. 23 and Nesbitt 2011: Fig. 18).*

1824 Character states 3 and 4 are new. State 3 is exhibited by *Youngina capensis* (BP/1/3859) and
 1825 *Tanystropheus hydroides* (PIMUZ T 2790) and state 4 by *Tanystropheus longobardicus* (PIMUZ T 2484).

1826 50) Ezcurra (2016) ch. 114. (character formulation slightly modified) *Frontal, orbital border in*
 1827 *skeletally mature individuals: absent or anteroposteriorly short and forms less than half of the dorsal*

1828 *edge of the orbit (0); anteroposteriorly long and forms at least more than half of the dorsal edge of the*
1829 *orbit (1) (Ezcurra 2016: Fig. 23).*

1830 51) Ezcurra (2016) ch. 118. *Frontal, dorsal surface adjacent to sutures with the postfrontal (if*
1831 *present) and parietal: flat to slightly concave (0); possesses a longitudinal and deep depression (1)*
1832 *(Ezcurra 2016: Fig. 16).*

1833 52) Ezcurra (2016) ch. 119. (inapplicability criterion slightly modified) *Frontal, longitudinal groove:*
1834 *longitudinally extended along most of the surface of the frontal (0); anterolaterally-to-posteromedially*
1835 *extended along the posterior half of the frontal (1). This character is inapplicable in taxa that lack a*
1836 *longitudinal depression on the frontal (Ezcurra 2016: Fig. 16).*

1837 53) Ezcurra (2016) ch. 121. *Frontal, olfactory tract on the ventral surface of the frontal: maximum*
1838 *transverse constriction point well posterior to the moulds of the olfactory bulbs and posterolateral*
1839 *margin of the bulbs delimited by a low ridge (0); maximum transverse constriction of the olfactory tract*
1840 *immediately posterior to the moulds of the olfactory bulbs and posterolateral margin of the bulbs well-*
1841 *delimited by a thick, tall ridge (1). This character is inapplicable in taxa that lack olfactory bulb moulds*
1842 *and constriction of the olfactory tract canal (Ezcurra 2016: Fig. 23).*

1843 54) Ezcurra (2016) 112 and Pritchard et al. (2015) ch. 14. *Frontal, frontals fused to one another:*
1844 *absent (0); present (1) (Ezcurra 2016: Fig. 23).*

1845 This character should only be scored in adult specimens, with the exception of juvenile specimens in
1846 which the frontals have already fused.

1847 55) New *Frontal, elongate (0); very wide and plate-like, a single frontal (or half of a fused frontal)*
1848 *being almost as wide as long (1) (Fig. 10).*

1849 This character describes the very wide frontals seen in *Tanystropheus hydroides* (PIMUZ T 2790) and
1850 *Tanystropheus longobardicus* (MSNM BES SC 1018).

1851 56) Pritchard et al. (2015) ch. 16. *Frontal, shape of contact with parietal in dorsal view: roughly*
1852 *transverse in orientation (0); frontal exhibits posterolateral processes, forming anteriorly curved U-*
1853 *shaped contact (1) (Ezcurra 2016: Figs. 8 and 23).*

1854 This character is similar to character 116 in Ezcurra (2016). However, the version of this character in
1855 Pritchard et al. (2015) is preferred because it is more specific to the taxon sample studied here.

57) New, combining information from ch. 122 in Ezcurra (2016), ch. 15 in Pritchard et al. (2015), and ch. 313 in Pritchard et al. (2018). *Postfrontal, suture with the frontal: anteroposteriorly or sagittally orientated (0); distinctly posteromedially inclined by a medial process of the postfrontal, resulting in posteriorly strongly narrowed frontal (1); distinctly posterolaterally inclined, resulting in a posteriorly expanded frontal and reduced postfrontal (2) (Fig. 11).*

This character, describing the contact between the frontal and postfrontal, combines the description of several characters of previous analyses. In all non-archosauromorph diapsids included here, as well as in most non-archosauriform archosauromorphs (tanystropheids, *Prolacerta broomi*, *Czatkowiella harae*, and *Protorosaurus speneri*), the articulation between the postfrontal and frontal is sagittally orientated. However, in the rhynchosaurs *Howesia browni* and *Mesosuchus browni*, as well as the allokotosaurs *Trilophosaurus buettneri* and *Azendohsaurus madagaskarensis*, the postfrontal bears a distinct medial process, resulting in a posteriorly narrow frontal and a posteromedially orientated suture between the postfrontal and frontal. This morphology was described by character 313 of Pritchard et al. (2018). However, in the archosauriforms, a posteriorly wider frontal reduces the size of the postfrontal, as seen in the archosauriforms *Proterosuchus fergusi*, *Proterosuchus alexanderi*, and *Erythrosuchus africanus* included here. This morphology was described by character 122 of Ezcurra (2016) as well as character 15 of Pritchard et al. (2015). In most archosaur groups, as well as Proterochampsia, the postfrontal has been lost completely (see character 44 of Nesbitt 2011). However, since no taxa belonging to these clades are included here, a separate character state referring to this has not been included.

58) New, combination of ch. 18 of Pritchard et al. (2015) and ch. 123 of Ezcurra (2016) (=ch. 27 of Pritchard et al. 2015). *Postfrontal, lacks a posterior process and does not participate in the border of the supratemporal fenestra (0); has a posterior process and participates in the border of the supratemporal fenestra (1) (Ezcurra 2016: Fig. 16).*

In all scored taxa, the presence of a posterior process of the postfrontal, or a roughly T-shaped postfrontal, implies that the postfrontal contributes to the margin of the supratemporal fenestra, and thereby prevents a contact between the postorbital and parietal (*Youngina capensis*, *Gephyrosaurus bridensis*, and *Planocephalosaurus robinsonae*). Therefore we consider the contribution of the postfrontal to the supratemporal fenestra dependent on the presence of a T-shape of the postfrontal, and therefore combined the characters describing this morphology.

1885 59) Ezcurra (2016) ch. 124. *Postfrontal, shape of dorsal surface: flat or slightly concave towards*
 1886 *raised orbital rim (0); depression with deep pits (1). Scored as inapplicable in taxa that lack a postfrontal*
 1887 *(Ezcurra 2016: Fig. 16).*

1888 60) Ezcurra (2016) ch. 130. *Postorbital, posterior process extends close to or beyond the level of the*
 1889 *posterior margin of the supratemporal fenestrae: absent (0); present (1) (Ezcurra 2016: Fig. 17).*

1890 Character 137 of Ezcurra (2016), the contribution of the squamosal to the intertemporal bar, is
 1891 considered to be interdependent with the posterior extension of the posterior process of the
 1892 postorbital. Therefore, this character was not included here.

1893 61) Ezcurra (2016) ch. 131. *Postorbital, extension of the ventral process: ends much higher than the*
 1894 *ventral border of the orbit (0); ends close to or at the ventral border of the orbit (1) (Ezcurra 2016: Fig.*
 1895 *17).*

1896 62) Modified from Dilkes (1998) ch. 23. *Postorbital, length of the ventral process versus the length of the*
 1897 *posterior process of the postorbital: 0.40-1.20 (0); 1.30-2.50 (1) RATIO.*

1898 The ratios were modified and the identification of the processes was slightly modified in order for them
 1899 to be congruent with other character descriptions here.

1900 63) Modified from Ezcurra (2016) ch. 126. *Postorbital-squamosal, upper temporal bar: located*
 1901 *approximately at level of mid-height of the orbit (0); located approximately aligned to the dorsal border*
 1902 *of the orbit (1) (Ezcurra 2016: Figs. 17 and 19). Scored as inapplicable in taxa without an infratemporal*
 1903 *fenestra and in taxa in which the upper temporal bar is very tall, reaching from the dorsal margin of the*
 1904 *orbit to or beyond mid-height of the orbit.*

1905 An inapplicability criterion was added to this character, because in *Trilophosaurus buettneri* (Spielmann
 1906 et al. 2008) the infratemporal fenestra is absent, and therefore an upper temporal bar is not present,
 1907 and because in *Tanystropheus hydroides* (PIMUZ T 2790) the upper temporal bar is dorsoventrally tall
 1908 and therefore covers the lateral side of the skull from the dorsal border of the orbit to about mid-height
 1909 of the orbit.

1910 64) Modified from Ezcurra (2016) ch. 127. *Postorbital-squamosal, contact: restricted to the dorsal*
 1911 *margin of the elements (0); the anterior process of the squamosal continues along the posterior margin*
 1912 *of the ventral process of the postorbital and contacts the jugal (1) (Nesbitt 2011: Figs. 17 and 19). This*
 1913 *character is scored as inapplicable in taxa that lack an infratemporal fenestra.*

1914 State 1 of character 127 in Ezcurra (2016) was not included here, because it is not applicable to any of
 1915 the included taxa. An inapplicability criterion was included because it was considered that the
 1916 morphology of *Trilophosaurus buettneri* (Spielmann et al. 2008), in which an infratemporal fenestra is
 1917 absent, represents a non-homologous morphology from state 0, even though the squamosal and jugal
 1918 likely did not meet in this taxon.

1919 65) Ezcurra (2016) ch. 18. *Infratemporal fenestra: present (0); absent (1).*

1920 66) Ezcurra (2016) ch. 137. *Squamosal, anterior process forms more than half of the lateral border*
 1921 *of the supratemporal fenestra: absent (0); present (1) (Ezcurra 2016: Fig. 16). This character is*
 1922 *inapplicable in taxa lacking a supratemporal fenestra.*

1923 67) Modified from Ezcurra (2016) ch. 143 and Pritchard et al. (2015) ch. 33. *Squamosal, ventral*
 1924 *process: present (0); absent or completely confluent with anterior process (1) (Fig. 12).*

1925 This character was modified based on the observed morphologies in the sampled taxa. In *Tanystropheus*
 1926 *hydroides* (PIMUZ T 2790) no clear ventral process can be distinguished, but instead the anterior process
 1927 of the squamosal is dorsoventrally tall and plate-like. It is unclear whether this is the result of a
 1928 confluence of the anterior and ventral processes. In *Trilophosaurus buettneri* (Spielmann et al. 2008) the
 1929 ventral process is also absent.

1930 68) Ezcurra (2016) ch. 139 (slightly reformulated). *Squamosal, ventral process: angle between the*
 1931 *ventral and anterior processes of the squamosal 90 degrees or less, forming a roughly square outline (0);*
 1932 *angle between the ventral and anterior processes of the squamosal more than 90 degrees, forming a*
 1933 *gentle, widely rounded posterodorsal border of the infratemporal fenestra (1) (Ezcurra 2016: Figs. 8, 17,*
 1934 *18 and 24). This character is scored as inapplicable in taxa that lack a ventral process of the squamosal.*

1935 69) Modified from Pritchard et al. (2015) ch. 34. *Squamosal, ventral process: forming a massive*
 1936 *flange that covers the quadrate entirely in lateral view (0); anteroposteriorly slender (1). This character is*
 1937 *scored as inapplicable in taxa that lack a ventral process on the squamosal.*

1938 See character description of character 135 of Ezcurra (2016), which covers the same distinction. The
 1939 character description of Pritchard et al. (2015) was preferred here, because it is more informative. The
 1940 inapplicability criterion is added to prevent overscoring for the absence of a ventral process of the
 1941 squamosal.

1942 70) Modified from Ezcurra (2016) ch. 140. *Squamosal medial process: short, forming up to half or*
 1943 *less of the posterior border of the supratemporal fenestra (0); long, forming entirely or almost entirely*
 1944 *the posterior border of the supratemporal fenestra (1) (Ezcurra 2016: Fig. 16). This character is scored as*
 1945 *inapplicable in taxa that lack a medial process of the squamosal.*

1946 The inapplicability criterion was added.

1947 71) New, similar to Ezcurra (2016) ch. 149. *Squamosal medial process, dorsoventrally short (0);*
 1948 *dorsoventrally tall and plate-like, forming a tall surface of the posterior margin of the supratemporal*
 1949 *fenestra (1). This character is scored as inapplicable in taxa that lack a medial process of the squamosal*
 1950 *(Fig. 12).*

1951 72) Modified from Ezcurra (2016) ch. 141. *Squamosal, posterior process is distinct and extends*
 1952 *posterior to the dorsal head of the quadrate absent (0); present (1) (Ezcurra 2016: Fig. 18, 19, and 24).*
 1953 *This character is inapplicable in taxa where the quadrate is completely covered by the squamosal in*
 1954 *lateral view.*

1955 The description of this character was modified to more clearly describe the morphology observed in the
 1956 taxon sample studied here.

1957 73) Ezcurra (2016) ch. 157. *Supratemporal: broad element (0); slender, in parietal and squamosal*
 1958 *trough (1); absent (2) ORDERED (Ezcurra 2016: Fig. 17).*

1959 The definitive absence of the supratemporal is hard to establish because it is often a small element that
 1960 is easily obscured by specimen disarticulation or compression. Therefore, this bone is only scored as
 1961 absent when it can be confidently established as such from well-preserved specimens.

1962 74) Ezcurra (2016) ch. 159 and Pritchard et al. (2015) ch. 19. *Parietal, median contact between both*
 1963 *parietals: suture present (0); fused with loss of suture (1) (Ezcurra 2016: Fig. 16).*

1964 State 0 can only be scored based on skeletally mature specimens.

1965 75) Ezcurra (2016) ch. 160. *Parietal, extension over interorbital region: absent or slight (0); present*
 1966 *(1) (Ezcurra 2016: Figs. 6 and 23).*

1967 76) Ezcurra (2016) ch. 162. *Parietal, pineal fossa on the median line of the dorsal surface: absent (0);*
 1968 *present (1). This character should not be scored for early juveniles (Ezcurra 2016: Fig. 8) (Fig. 13).*

1969 This character was considered to be present in *Kadimakara australiensis* and several archosauriforms
 1970 (see scorings of Ezcurra 2016, character 162). However, we consider a similar fossa, as present in these
 1971 taxa, can also be identified in *Azendohsaurus madagaskarensis* (Flynn et al. 2010), *Trilophosaurus*
 1972 *buettneri* (Spielmann et al. 2008), and *Dinocephalosaurus orientalis* (IVPP V13767).

1973 77) Modified from Ezcurra (2016) ch. 164. *Parietal, pineal foramen in dorsal view: large (0);*
 1974 *reduced to a small, circular pit or concavity (1); absent (2) (Ezcurra 2016: Figs. 6 and 8), ORDERED.*

1975 The character was ordered, since it is considered a transformational series in which state 1 represents a
 1976 clear intermediate between states 0 and 2. Furthermore the concavity statement was added to state 1,
 1977 because in some taxa this depression is not pit-like.

1978 78) Modified from Ezcurra (2016) ch. 165. *Parietal, position of the pineal foramen in dorsal view:*
 1979 *enclosed by parietals and clearly on the posterior part of the bones (0); enclosed by parietals at roughly*
 1980 *mid-length of the bones (1); enclosed by parietals on the anterior part of the bones close to the frontals*
 1981 *(2); enclosed by both frontals and parietals (3), ORDERED (Ezcurra 2016: Figs. 6 and 8). This character is*
 1982 *scored as inapplicable in taxa that lack a pineal foramen.*

1983 The pineal foramen is displaced distinctly posteriorly on the parietals in the non-saurian diapsids
 1984 *Planocephalosaurus robinsonae* (Fraser 1982), *Orovenator mayorum* (Ford & Benson 2018), and
 1985 *Youngina capensis* (AMNH FARB 5561), and this was therefore considered as a separate character state.
 1986 This morphology was extensively discussed in Ford and Benson (2018).

1987 79) Modified from Pritchard et al. (2015) ch. 21. *Parietal, orientation of posterolateral process:*
 1988 *roughly transverse (0); strongly angled posterolaterally (1) (Fig. 13).*

1989 In the majority of the sampled taxa, the posterolateral processes have a posterolateral orientation.
 1990 However, in *Tanystropheus hydroides* (PIMUZ T 2819), *Tanystropheus longobardicus* (PIMUZ T 2484),
 1991 *Dinocephalosaurus orientalis* (IVPP V13767), *Protorosaurus speneri* (NMK S 180), and *Azendohsaurus*
 1992 *madagaskarensis* (Flynn et al. 2011), the posterolateral process is a completely transverse or lateral
 1993 orientation. In *Jesairosaurus lehmani*, this character varies somewhat depending on the specimen.

1994 80) Ezcurra (2016) ch 168. *Parietal, posterolateral process height: dorsoventrally low, usually*
 1995 *considerably lower than the supraoccipital (0); dorsoventrally deep, being plate-like in occipital view and*
 1996 *subequal to the height of the supraoccipital (1) (Ezcurra 2016: Fig. 27).*

1997 81) New *Parietal, supratemporal fossa medial to the supratemporal fenestra: absent (0); present*
1998 *(1) (Fig. 13).*

1999 82) Ezcurra (2016) ch. 161. (inapplicability criterion slightly reformulated). *Parietal, supratemporal*
2000 *fossa medial to the supratemporal fenestra: well-exposed in dorsal view and mainly dorsally or*
2001 *dorsolaterally facing (0); poorly exposed in dorsal view and mainly laterally facing (1) (Ezcurra 2016: Fig.*
2002 *16). This character is scored as inapplicable in taxa that lack a supratemporal fossa on the parietal.*

2003 83) Modified from Pritchard et al. (2015) ch. 20 and Ezcurra (2016) ch. 8. *Parietal, medial extent of*
2004 *the supratemporal fossa: restricted to the lateral edge of the parietal, resulting in a broad flat parietal*
2005 *table (0); expanded distinctly medially, resulting in a mediolaterally narrow parietal table (1);*
2006 *supratemporal fossae strongly expanded medially and only separated by a ridge running along the*
2007 *midline of the parietal, the sagittal crest (2), ORDERED. This character is scored as inapplicable in taxa*
2008 *that lack a supratemporal fossa on the parietal (Fig. 13).*

2009 This character was modified to clarify the distinction between the different states. The supratemporal
2010 fossa can either be restricted to the lateral portion of the parietal, expressed more widely on the
2011 parietal, or cover most of the dorsal surface of the parietal between the supratemporal fenestrae, only
2012 leaving a thin sagittal crest between the two fossae. This character is very variable in *Prolacerta broomi*
2013 with all three states observed in different specimens (state 0: BP/1/471, state 1: BP/1/5375 and UCMP
2014 37151, state 2: BP/1/5066 and BP/1/5880).

2015 84) Ezcurra (2016) ch. 171. *Postparietal, size (pair of postparietals if they are not fused to*
2016 *each other): sheet-like, not much narrower than the supraoccipital (0); small, splint-like (1); absent as a*
2017 *separate ossification (2) ORDERED (Ezcurra 2016: Fig. 23).*

2018 85) Ezcurra (2016) ch. 172 and Pritchard et al. (2015) ch. 25. *Postparietal, fusion between*
2019 *counterparts: absent (0); present, forming an interparietal (1). This character is inapplicable in taxa that*
2020 *lack postparietals.*

2021 86) Ezcurra (2016) ch. 173 and Pritchard et al. (2015) ch. 37. *Tabular: present (0); absent (1).*

2022 87) Ezcurra (2016) ch. 150 and Pritchard et al. (2015) ch. 38. *Quadratojugal: absent or fused to the*
2023 *quadrate (0); present (1) (Ezcurra 2016: Fig. 24).*

2024 88) Modified from Ezcurra (2016) ch. 153. *Quadratojugal, anterior process: absent, anteroventral*
2025 *margin of the bone rounded and the quadratojugal and jugal do not connect and therefore the lower*

temporal bar is incomplete (0); incipient, short anterior prong on the anteroventral margin of the bone and the quadratojugal and jugal connect and therefore the lower temporal bar is complete (1); distinctly present, in which the lower temporal bar is complete, but process terminates well posterior to the base of the posterior process of the jugal (2); distinctly present, in which the lower temporal bar is complete and participates in the posteroventral border of the infratemporal fenestra, and process terminates close to the base of the posterior process of the jugal (3), ORDERED. This character is inapplicable in taxa that lack an infratemporal fenestra or quadratojugal (Ezcurra 2016: Figs. 17 and 19).

The description of this character was modified to more clearly describe the morphology observed in the taxon sample studied here.

89) Ezcurra (2016) ch. 156. *Quadratojugal, posterior extension of the ventral end: absent, without a posteriorly arched quadratojugal (0); limited, ventral condyles of the quadrate broadly visible in lateral view (1); strongly developed, overlapping completely or almost completely the ventral condyles of the quadrate in lateral view (2), ORDERED (Ezcurra 2016: Fig. 18). This character is inapplicable in taxa lacking a quadratojugal.*

90) New, combination of ch. 176 and ch. 182 in Ezcurra (2016). *Quadrate, posterior margin in lateral view: straight along entire shaft (0); continuously concave (1); sigmoidal, with a concave dorsal portion and convex ventral portion (2) (Ezcurra 2016: Fig. 24).*

These characters were combined because they both relate to the shape of the quadrate shaft. The presence of a quadrate conch is omitted because its presence is likely closely related to a fusion of the quadratojugal to the quadrate in lepidosauromorphs. This fusion is already coded for by character 87 and its inclusion here would result in the overscoring of this morphology.

91) Ezcurra (2016) ch. 180 and Nesbitt et al. (2015) ch. 207. *Quadrate, dorsal end hooked posteriorly in lateral view: absent (0); present (1) (Ezcurra 2016: Figs. 17 and 24).*

92) New *Quadrate, ventral condyles: lateral and medial condyles not distinctly separated and therefore the ventral surface of the quadrate is rounded, flat, or slightly concave (0); condyles separated by a deep concavity on the ventral surface of the quadrate (1) (Fig. 14).*

93) Ezcurra (2016) ch. 183. *Quadrate, ventral condyles: subequally distally extended (0); medial condyle distinctly more distally projected than the lateral one (1) (Fig. 14).*

2054 94) New *Quadrate, pterygoid flange: anteriormost extension at about mid-height of the midshaft*
 2055 *(0); dorsally located, the anteriormost extension of the flange is at close to the dorsoventral level of the*
 2056 *dorsal head of the quadrate (1) (Fig. 14).*

2057 This character describes the difference seen in the morphology of the pterygoid flange, as can be clearly
 2058 observed between for instance *Tanystropheus hydroides* (PIMUZ T 2790) and *Macrocnemus bassanii*
 2059 (PIMUZ T 2477).

2060 95) Pritchard et al. (2015) ch. 45. *Vomer, teeth: absent (0); present (1).*

2061 96) Modified from Ezcurra (2016) ch. 187. *Vomer, teeth distribution: shagreen tooth distribution*
 2062 *with no clear rows distinguishable (0); teeth distributed in multiple clearly defined rows (1); teeth*
 2063 *distributed mainly in a single row, but multiple teeth present immediately anterior to the contact with*
 2064 *the pterygoid (2); teeth distributed in a single row along entire extension (3). This character is*
 2065 *inapplicable in taxa that lack vomerine teeth.*

2066 The presence of vomerine teeth and their distribution were considered in one ordered character in
 2067 character 187 in Ezcurra (2016). However, we do not consider any of the various tooth distributions to
 2068 represent an intermediate stage between any of the others. Therefore, we considered the presence of
 2069 vomerine teeth as a separate character, and the distribution of these teeth, if they are present, as a
 2070 separate, unordered character.

2071 97) New, related to ch. 189 of Ezcurra (2016). *Palatal dentition, size (height and diameter) of teeth on*
 2072 *the vomer: small, considerably smaller than those of the marginal dentition (0); relatively large, similar*
 2073 *to those of the marginal dentition (1). This character is inapplicable in taxa lacking vomerine teeth (Fig.*
 2074 *15).*

2075 Character 189 in Ezcurra (2016) describes the relative size of the teeth on the palatine and pterygoid.
 2076 However, in our sampled taxa, a distinct difference in the size of the dentition could also be observed in
 2077 the vomer, and this was therefore formulated into a separate character, since the size of the vomerine
 2078 teeth does not appear to be dependent on the size of the palatine or pterygoid teeth in the sampled
 2079 taxa.

2080 98) Ezcurra (2016) ch. 190 (description of state 1 slightly reformulated). *Palatine, transverse*
 2081 *extension: narrow, subequal contribution of the palatine and pterygoid to or pterygoid main component*

2082 of the palate posteriorly to the choanae (0); broad, the palatine is the main component of the palate
2083 posteriorly to the choanae (1) (Ezcurra 2016: Fig. 26).

2084 99) Modified from Ezcurra (2016) ch. 191. Palatine, anterior processes forming the posterior border
2085 of the choana: subequal in anterior extension or anterolateral process longer (0); anteromedial process
2086 longer (1) (Ezcurra 2016: Fig. 26).

2087 Character state 2 of character 191 in Ezcurra (2016) was not included here, because it is not applicable
2088 to any of the sampled taxa.

2089 100) Ezcurra (2016) ch. 188. Palatine-pterygoid, teeth on the palatine and ventral surface of
2090 the anterior ramus of the pterygoid: present (0); absent (1) (Ezcurra 2016: Figs. 13, 24 and 26).

2091 101) Part of Ezcurra (2016) ch. 189. Palatal dentition, size (height and diameter) of teeth on the
2092 palatine: small, considerably smaller than those of the marginal dentition (0); relatively large, similar to
2093 those of the marginal dentition (1). This character is inapplicable in taxa lacking palatine teeth (Ezcurra
2094 2016: Figs. 25 and 26) (Fig. 15).

2095 Character 189 in Ezcurra (2016) treats the size of the dentition on the palatine and pterygoid as a single
2096 character. Because the relative size of the teeth on the palatine and pterygoid differs in *Tanystropheus*
2097 *longobardicus* (PIMUZ T 2484) it was decided here to treat the size of the teeth on both elements as
2098 separate characters.

2099 102) Ezcurra (2016) ch. 195. Pterygoid, teeth on the ventral surface of the anterior ramus (=palatal
2100 process), excluding tiny palatal teeth if present: present in two distinct fields (=T2 and T3 of Welman
2101 1998) (0); present in three distinct fields (=T2, T3a and T3b) (1); present in three distinct fields (=T2a, T2b
2102 and T3) (2); present in one field that occupies most of the transverse width of the ramus (=T2 + T3) (3);
2103 present in only one posteromedially-to-anterolaterally orientated field (=T2) (4); present in only one field
2104 adjacent to the medial margin of the ramus (=T3) (5); present in no definable fields but the entire
2105 pterygoid is covered by a shagreen of teeth (6). This character is inapplicable in taxa that lack teeth in
2106 the palatine and the ventral surface of the anterior ramus of the pterygoid (Ezcurra 2016: Figs. 25 and
2107 26).

2108 103) Ezcurra (2016) ch. 196. Pterygoid, number of rows on palatal tooth field T2: more than two or do
2109 not dispose on distinct rows (0); two rows parallel to each other (1); single row (2). This character is
2110 inapplicable if the tooth field T2 is subdivided in T2a and T2b or is absent (Ezcurra 2016: Figs. 25 and 26).

2111 104) Ezcurra (2016) ch. 197. *Pterygoid, number of rows on palatal tooth field T3: more than two or*
 2112 *not disposed in distinct rows (0); two parallel rows (1); single row (2). This character is inapplicable if the*
 2113 *tooth field T3 is subdivided into T3a and T3b or is absent (Ezcurra 2016: Figs. 25 and 26).*

2114 Character 199 in Ezcurra (2016) treats a row of teeth sticking out on the medial side of the anterior
 2115 ramus of the pterygoid (=T4 of Welman 1998) as a separate character. It is found here, based on
 2116 observations on *Macrocnemus bassanii* (PIMUZ T 1559) and *Prolacerta broomi* (CT-scan of BP/1/5066)
 2117 that tooth field T3 in these taxa bears more than two distinct rows. Furthermore, the medial margin of
 2118 the anterior ramus of the pterygoid is curved, resulting in a number of these teeth facing lateroventrally,
 2119 whilst others face mediolaterally. Therefore, we conclude that tooth field T4 actually represents the
 2120 mediolaterally facing teeth of tooth field T3. Therefore character 199 in Ezcurra (2016) has not been
 2121 included here.

2122 105) Part of Ezcurra (2016) ch. 189. *Palatal dentition, size (height and diameter) of teeth on the*
 2123 *ventral surface of the anterior ramus of the pterygoid: small, considerably smaller than those of the*
 2124 *marginal dentition (0); relatively large, similar to those of the marginal dentition (1). This character is*
 2125 *inapplicable in taxa lacking teeth on the anterior ramus of the pterygoid (Ezcurra 2016: Figs. 25 and 26)*
 2126 *(Fig. 15).*

2127 See description of character 101.

2128 106) Part of Ezcurra (2016) ch. 202. *Pterygoid, teeth on the lateral ramus (=transverse flange):*
 2129 *absent (0); present (1) (Ezcurra 2016: Figs. 13, 25 and 26). This character is inapplicable in taxa that bear*
 2130 *shagreen teeth on the pterygoid.*

2131 The inapplicability criterion was added because this tooth row cannot be distinguished from other
 2132 pterygoid teeth when the pterygoid is covered by shagreen teeth. We separated this character from
 2133 character 107 because we consider the presence of teeth on the lateral ramus of the pterygoid to
 2134 represent a separate criterion from the number of tooth rows if such teeth are present. Therefore, we
 2135 do not consider the presence of a single row of teeth to represent an intermediate step in a
 2136 transformational series between no teeth present and two rows present.

2137 107) Part of Ezcurra (2016) ch. 202. *Pterygoid, distribution of teeth on the lateral ramus (=transverse*
 2138 *flange): teeth distributed in a single row on the posterior edge (=T1 of Welman 1998) (0); teeth*
 2139 *distributed in multiple rows (1) (Ezcurra 2016: Figs. 13, 25 and 26). This character is inapplicable in taxa*
 2140 *that lack teeth on the lateral ramus of the pterygoid or have shagreen teeth covering the pterygoid.*

2141 See description of character 107.

2142 108) New *Pterygoid, anterior end of the anterior ramus: tapers to an end (0); rounded (1) (Fig. 15).*

2143 In most of the sampled taxa, the anterior ramus of the pterygoid gradually tapers anteriorly and thus
2144 has an anteriorly pointed end. In contrast, in *Tanystropheus hydroides* (PIMUZ T 2787) and
2145 *Dincephalosaurus orientalis* (Rieppel et al. 2008) the anterior ramus of the pterygoid is much wider
2146 anteriorly and has a rounded anterior margin.

2147 109) New *Pterygoid, lateral/distal end of the posterior margin of the lateral ramus*
2148 *(=transverse flange) curved posteriorly: absent (0); present (1). This character is scored as inapplicable in*
2149 *taxa with a strongly posterolaterally orientated lateral ramus of the pterygoid (Fig. 16).*

2150 This character is closely related to character 201 in Ezcurra (2016). However, because this new character
2151 distinguishes within Tanystropheidae, it is considered to be more informative and therefore preferred.
2152 Character 201 of Ezcurra (2016) was not included in order to prevent overscoring of this morphology.

2153 110) Modified from Ezcurra (2016) ch. 207. *Ectopterygoid, lateral process is not curved posteriorly*
2154 *(0); is curved posteriorly but not expanded (1); is both curved and expanded posteriorly, giving the*
2155 *ectopterygoid a hook-shape in dorsal or ventral view (2) (Ezcurra 2016: Figs. 7 and 26) (Fig. 15),*
2156 *ORDERED.*

2157 The lateral portion of the ectopterygoid can be separated into three different morphologies. In some
2158 taxa, it is not curved, nor expanded. In other taxa, the lateral end curves posteriorly but it is not
2159 expanded anteroposteriorly. Finally, in certain taxa, the lateral portion of the ectopterygoid is curved
2160 posteriorly and is expanded anteroposteriorly. Since state 1 is considered to represent an intermediate
2161 state between 0 and 2 in a transformational series, this character was ordered.

2162 111) Ezcurra (2016) ch. 204 (state 0 reformulated). *Ectopterygoid, articulation with pterygoid:*
2163 *ectopterygoid overlaps the pterygoid ventrally (0); interlaced articulation, complex articulation between*
2164 *ectopterygoid and pterygoid (1) (Ezcurra 2016: Fig. 26).*

2165 112) Modified from Ezcurra (2016) ch. 205. *Ectopterygoid, connection with pterygoid: does not reach*
2166 *the posterolateral corner of the lateral ramus (=transverse flange) (0); reaches the posterolateral corner*
2167 *of the lateral ramus (1) (Ezcurra 2016: Fig. 26). This character is scored as inapplicable in taxa in which*
2168 *the ectopterygoid simply overlaps the pterygoid.*

2169 An inapplicability criterion is added because the ectopterygoid only reaches the posterolateral corner of
2170 the lateral ramus of the pterygoid when the ectopterygoid forms an interlacing suture with the
2171 pterygoid. In taxa with this type of articulation, the ectopterygoid wraps around the posterolateral
2172 corner of the transverse flange in some cases.

2173 113) Ezcurra (2016) ch. 244 and Pritchard et al. (2015) ch. 65. *Parasphenoid/parabasisphenoid,*
2174 *dentition on cultriform process: present (0); absent (1).*

2175 114) New *Parasphenoid/parabasisphenoid, length of the cultriform process versus its height at its*
2176 *anteroposterior midpoint: 4.00-7.00 (0); 9.00-18.00 (1) RATIO.*

2177 This character treats the large discrepancy in the relative length of the cultriform process. In most taxa it
2178 is a thin elongate element, whereas in allokotosaurs and rhynchosaurs it is much shorter and
2179 dorsoventrally taller.

2180 115) New *Parasphenoid/parabasisphenoid, anterior projections of the cristae trabeculares, present*
2181 *(0); absent (1).*

2182 The cristae trabeculares are small bony projections on the anterolateral surface of the cultriform process
2183 of the parabasisphenoid, which occur in certain non-saurian diapsids and lepidosaurs. These structures
2184 and their occurrence among diapsids were discussed in detail by Ford and Benson (2018, page 18).

2185 116) Ezcurra (2016) ch. 236. *Parasphenoid/parabasisphenoid, posterodorsal portion: incompletely*
2186 *ossified (0); completely ossified (1).*

2187 117) Modified from Ezcurra (2016) ch. 237. *Parasphenoid/parabasisphenoid, intertuberal plate:*
2188 *present (0); absent (1) (Ezcurra 2016: Figs. 10 and 28).*

2189 Character states 1 and 2 of character 237 in Ezcurra (2016) were fused here, because there was no clear
2190 distinction between a rounded and a straight posterior edge of the intertuberal plate in the sampled
2191 taxa, and this distinction is likely only relevant in more derived archosauriforms.

2192 118) Modified from Ezcurra (2016) ch. 239. *Parasphenoid/parabasisphenoid, recess (=median*
2193 *pharyngeal recess, =hemispherical sulcus, =hemispherical fontanelle): absent, the ventral floor of the*
2194 *parabasisphenoid posterior to the basiptyergoid processes (and posterior to a potentially present*
2195 *intertuberal plate) is flat (0); present, the ventral floor forms a shallow depression (1); the ventral floor is*
2196 *deeply excavated (2) (Ezcurra 2016: Fig. 27), ORDERED.*

2197 The pharyngeal recess originally identified in archosauriforms, but has subsequently also been described
 2198 for certain non-archosauriform archosauromorphs (e.g. *Azendohsaurus madagaskarensis*; Flynn et al.
 2199 2010, and *Mesosuchus browni*; Sobral & Müller 2019). Observation of this character in the sampled taxa
 2200 indicates that this character occurs in two states. The pharyngeal recess was first described as a very
 2201 deep ventral cavity (e.g. the basisphenoid recess of Witmer 1997). This occurs in *Tanystropheus*
 2202 *hydroides* (PIMUZ T 2790) and *Erythrosuchus africanus* (BP/1/3893) among the sampled taxa. However,
 2203 a much shallower excavation of the ventral surface of the parabasisphenoid posterior to the
 2204 basiptyergoid processes occurs in the majority of non-archosauriform archosauromorphs, as well as
 2205 *Youngina capensis* (Gardner et al. 2010). This shallow excavation was also identified as the pharyngeal
 2206 recess by Sobral et al. (2016) and Sobral & Müller (2019). We here distinguish the shallow excavation
 2207 from the deeper excavation as separate character states for the first time, and consider the former to
 2208 possibly represent an intermediate morphology between the absence of a pharyngeal recess and the
 2209 deeply excavated pharyngeal recess.

2210 119) Ezcurra (2016) ch. 238. *Parasphenoid/parabasisphenoid, semilunar depression on the*
 2211 *posterolateral surface of the bone: absent (0); present (1). This character is inapplicable in taxa that the*
 2212 *posterodorsal portion of the parasphenoid/parabasisphenoid is not ossified, resulting in an unossified*
 2213 *gap between this element and the prootic (Ezcurra 2016: Fig. 28).*

2214 120) Ezcurra (2016) ch. 235 and Nesbitt et al. (2015) ch. 208 (description of state 1 slightly
 2215 reformulated). *Basisphenoid/parabasisphenoid, orientation of the body between the posterior end of*
 2216 *the bone and the basiptyergoid processes: horizontal (0); oblique, main axis posterodorsally-to-*
 2217 *anteroventrally orientated (1) (Ezcurra 2016: Figs. 27 and 28).*

2218 121) Ezcurra (2016) ch. 225. *Basioccipital-parasphenoid/parabasisphenoid, contact with each other in*
 2219 *skeletally mature individuals: loose, overlapping suture (0); tightly sutured, sometimes by an*
 2220 *interdigitated suture, or both bones fused to each other (1) (Ezcurra 2016: Fig. 28).*

2221 122) New *Basioccipital-parasphenoid/parabasisphenoid, two pneumatic foramina in between the*
 2222 *basioccipital and parabasisphenoid: absent (0); present (1).*

2223 Pneumatic foramina were described as present in a number of early archosauromorphs by Sobral &
 2224 Müller (2019). This character is now implemented in a quantitative phylogenetic analysis for non-
 2225 archosauriform archosauromorphs for the first time. See Figs. 3 and 13 in Sobral & Müller (2019).

2226 123) Ezcurra (2016) ch. 226. *Basioccipital-parasphenoid/parabasisphenoid, basal tubera: absent (0);*
2227 *present (1) (Ezcurra 2016: Fig. 27).*

2228 124) Modified from Ezcurra (2016) ch. 227. *Basioccipital-parasphenoid/parabasisphenoid, low ridge*
2229 *between basal tubera: absent or very strongly reduced (0); present (1). This character is scored as*
2230 *inapplicable in taxa that lack basal tubera (Ezcurra 2016: Fig. 27) (Fig. 16).*

2231 Character 227 in Ezcurra (2016) is applicable to a wide range of archosauromorphs. This character was
2232 modified to more specifically address the variation observed in the taxa sampled here. A clear but low,
2233 transversely orientated ridge is present between the basal tubera of the basioccipital of *Tanystropheus*
2234 *hydroides* (PIMUZ T 2790) and *Tanystropheus longobardicus* (PIMUZ T 2484). Such a ridge cannot be
2235 observed in any of the other sampled taxa.

2236 125) Modified from Pritchard et al. (2018) ch. 318. *Basioccipital, ventral margin: prominent*
2237 *embayment or ridge between basal tubera at least as transversely broad as occipital condyle (0);*
2238 *transversely narrow embayment or ridge between basal tubera, narrower than occipital condyle (1). This*
2239 *character is scored as inapplicable in taxa that lack basal tubera.*

2240 The inapplicability criterion was added. See the description of character 318 in Pritchard et al. (2018).

2241 126) Ezcurra (2016) ch. 229. *Basioccipital, articular surface of the occipital condyle: concave (0);*
2242 *hemispherical (1) (Ezcurra 2016: Fig. 28).*

2243 127) Ezcurra (2016) ch. 211 and Pritchard et al. (2015) ch 62. *Otoccipital, fusion between opisthotic*
2244 *and exoccipital: absent or partial (0); present (1) (Ezcurra 2016: Fig. 27).*

2245 128) New, combination of character 209 of Ezcurra (2016) (= character 60 of Pritchard et al. 2015) and
2246 character 219 of Ezcurra (2016) (= character 59 of Pritchard et al. 2015). *Exoccipital, morphology*
2247 *of the dorsal end: exoccipital columnar through dorsoventral height, forming transversely narrow dorsal*
2248 *contact with more dorsal occipital elements (0); dorsal portion of exoccipital exhibits dorsomedially*
2249 *inclined process that forms transversely broad contact with more dorsal occipital elements but*
2250 *exoccipitals do not meet on the dorsal margin of the foramen magnum (1); dorsal portion of exoccipital*
2251 *exhibits dorsomedially inclined process that meets the process of the opposite exoccipital on the dorsal*
2252 *margin of the foramen magnum, thus excluding the supraoccipital from contributing to the margin of the*
2253 *foramen magnum (2), ORDERED (Fig. 16). This character is inapplicable in taxa without a discernable*
2254 *suture between the supraoccipital and the exoccipital or fused opisthotic-exoccipital.*

2255 These two characters were fused because the exclusion of the supraoccipital from the margin of the
2256 foramen magnum implies that the exoccipitals connect to each other dorsally, which is caused by an
2257 extensive dorsomedial inclination of the dorsal portions of the exoccipitals.

2258 129) Modified from Ezcurra (2016) ch. 221. *Exoccipital, medial margin of their distal ends: no contact*
2259 *with its counterpart (0); contact with its counterpart to partially or fully exclude basioccipital from the*
2260 *floor of the endocranial cavity (1) (Ezcurra 2016: Fig. 27).*

2261 States 1 and 2 of character 221 in Ezcurra (2016) were fused here, because it is very difficult to
2262 distinguish between them in the sampled taxa.

2263 130) Ezcurra (2016) ch. 213 (both states slightly reformulated). *Opisthotic, paroccipital processes*
2264 *orientation: extend laterally or slightly posterolaterally (0); deflected strongly posterolaterally at an*
2265 *angle of more than 20 degrees from the transverse plane of the skull (1) (Ezcurra 2016: Fig. 16).*

2266 131) Pritchard et al. (2015) ch. 58. *Opisthotic, paroccipital process: ends freely (0); contacts the*
2267 *suspensorium (1).*

2268 132) Ezcurra (2016) ch. 216. *Opisthotic, fossa immediately lateral to the foramen magnum: absent*
2269 *(0); present (1).*

2270 133) Modified from Ezcurra (2016) ch. 217. *Opisthotic, ventral ramus shape: pyramidal, with a*
2271 *tapering distal end (0); club-shaped with a large bulbous distal head (1); columnar-like shaft of the ramus*
2272 *and an anteroposteriorly expanded but not a bulbous distal head (2); anteroposteriorly flattened shaft of*
2273 *the ramus, forming a blade-like ramus in lateral view and an anteroposteriorly expanded but not a*
2274 *bulbous distal head (3) (Ezcurra 2016: Fig. 28) (Fig. 17).*

2275 This character was modified to more precisely fit the morphology of the ventral ramus of the opisthotic
2276 as we observed it for the sampled taxa.

2277 134) Ezcurra (2016) ch. 218 (state 1 slightly reformulated). *Opisthotic, ventral ramus: extends*
2278 *further laterally than the lateralmost edge of the exoccipital in posterior view (0); ventral ramus*
2279 *completely or almost completely covered by the lateralmost edge of the exoccipital in posterior view (1)*
2280 *(Ezcurra 2016: Fig. 27).*

2281 135) Ezcurra (2016) ch. 223. *Pseudolagenar recess, opening externally between the ventral surface of*
2282 *the ventral ramus of the opisthotic and the basal tubera: present (0); absent (1) (Ezcurra 2016: Fig. 27).*

2283 136) Modified from Ezcurra (2016) ch. 19. *Posttemporal fenestra, size: large, roughly similar in size*
 2284 *to the supraoccipital (0); strongly reduced in size and much smaller than the supraoccipital (1); absent or*
 2285 *developed as a foramen or very narrow slit (2) ORDERED (Ezcurra 2016: Fig. 27).*

2286 This character has been modified according to observations on the sampled taxa. In most taxa, the
 2287 posttemporal fenestra is large with little variation in its construction. However, in *Azendohsaurus*
 2288 *madagkarensis* (Flynn et al. 2010), the parietal encloses the fenestra laterally, distinctly reducing it in
 2289 size. In *Erythrosuchus africanus* (BP/1/4680), *Proterosuchus fergusi* (SAM-PK-K10603), and
 2290 *Proterosuchus alexanderi* (NM QR 1484), the fenestra is only represented by a very narrow slit or
 2291 foramen.

2292 137) Ezcurra (2016) ch. 254 (reformulated). *Prootic, a clear crest on the lateral surface that is roughly*
 2293 *orientated posterodorsally to anteroventrally (crista prootica sensu Sobral & Müller 2019) is absent (0);*
 2294 *crista prootica present (1) (Ezcurra 2016: Fig. 28) (Fig. 17).*

2295 138) New *Prootic, a clear crest along the lateral surface that curves dorsally at the anterior margin*
 2296 *of the prootic is absent (crista alaris sensu Sobral & Müller 2019) (0); crista alaris is present (1) (Fig. 17).*

2297 Although character 254 in Ezcurra (2016) addressed the presence of crista prootica in a phylogenetic
 2298 context, the presence of another crest on the lateral surface of the prootic, the crista alaris, is also
 2299 variable for the sampled taxa, which is addressed with this character.

2300 139) Pritchard et al. (2015) ch. 75 (reformulated). *Prootic, paroccipital contribution: does not*
 2301 *contribute to anterior surface of paroccipital process (0); contributes laterally tapering lamina to the*
 2302 *anterior surface of the paroccipital process (1) (Fig. 17).*

2303 140) Modified from Ezcurra (2016) ch. 258 and Pritchard et al. (2015) ch. 72. *Laterosphenoid,*
 2304 *ossification: absent (0); present, laterosphenoid is a narrow dorsoventrally orientated bone and lacks an*
 2305 *anterior portion (1); present, laterosphenoid with an anterior portion located along the ventral surface of*
 2306 *the parietal and frontals (2) (Ezcurra: Fig. 28) (Fig. 17), ORDERED.*

2307 The presence of a laterosphenoid was until recently not known for non-archosauriform
 2308 archosauromorphs. However, a laterosphenoid has now also been identified in *Azendohsaurus*
 2309 *madagkarensis* (Flynn et al. 2010) and *Tanystropheus hydroides* (PIMUZ T 2790). In these taxa, the
 2310 laterosphenoid is small and does not extend far anteriorly as in archosauriforms. This information is
 2311 added to the character. The small, unexpanded laterosphenoid, is considered to represent an

2312 intermediate step between the absence of a laterosphenoid and the larger, further anterior reaching
2313 laterosphenoid of archosauriforms.

2314 141) Ezcurra (2016) ch. 296. *Stapes, shape: robust, with thick shaft (0); slender, rod-like shaft (1).*

2315 142) Ezcurra (2016) ch. 297 and Pritchard et al. (2015) ch. 77. *Stapes, stapedia foramen piercing the*
2316 *columellar process: present (0); absent (1).*

2317 143) Simões et al. (2018) ch. 176. *Splenia: present (0); absent (1).*

2318 144) Modified from Ezcurra (2016) ch. 266. *Dentary, height at the third alveolus of the bone (or*
2319 *directly posterior to the tapering anterior end of the dentary in taxa with an anteriorly edentulous*
2320 *dentary) versus length of the alveolar margin (including edentulous anterior end if present): 0.02-0.11*
2321 *(0); 0.15-0.19 (1); 0.21-0.29 (2); 0.34-0.36 (3) ORDERED RATIO (Ezcurra 2016: Figs. 17 and 18).*

2322 Instead of comparing the length of the alveolar margin of the dentary to the minimum height of the
2323 dentary, it was here considered to compare it to the height of the dentary at the third alveolus, as this
2324 represents a more consistent measurement across the sampled taxa.

2325 145) Ezcurra (2016) ch. 267 (reformulated). *Dentary, shape of the tooth bearing portion (including*
2326 *edentulous anterior end if present): roughly straight (0); dorsally curved for all or most of its*
2327 *anteroposterior length (1); ventrally curved or deflected at its anterior end (2) (Ezcurra 2016: Figs. 17 and*
2328 *29).*

2329 146) New *Dentary, distinct dorsoventral expansion forming a keel at the anterior end of the*
2330 *dentary: absent (0); present (1). This character is inapplicable in taxa with an edentulous anterior end of*
2331 *the dentary (Fig. 18).*



2332 State 1 represents an autapomorphy for *Tanystropheus hydroides* (PIMUZ T 2790) among the sampled
2333 taxa.

2334 147) Ezcurra (2016) ch. 270. *Dentary, position of the Meckelian groove on the anterior half of the*
2335 *bone: dorsoventral centre of the dentary (0); restricted to the ventral border (1) (Nesbitt 2011: Fig. 27).*

2336 148) Ezcurra (2016) ch. 272. *Dentary, posterodorsal process, in which its dorsal margin is confluent with*
2337 *the dorsal margin of the lower jaw: absent (0); present (1) (Ezcurra 2016: Figs. 17 and 29).*

2338 149) Ezcurra (2016) ch. 273. *Dentary, posteroventral process, in which its margins are not confluent*
 2339 *with the dorsal or ventral margin of the lower jaw: absent (0); present (1) (Ezcurra 2016: Figs. 17 and*
 2340 *29).*

2341 150) Modified from Ezcurra (2016) ch. 275. *Dentary, posteroventral process, in which its ventral*
 2342 *margin is confluent with the ventral margin of the lower jaw: absent (0); present (1) (Ezcurra 2016: Figs.*
 2343 *17 and 29).*

2344 Character state 2 of character 275 in Ezcurra (2016) was omitted here because the majority of the
 2345 included taxa here do not bear an external mandibular fenestra.

2346 151) Ezcurra (2016) ch. 276. *Dentary, posteroventral process length: extended posteriorly to the level*
 2347 *of the posterodorsal and/or posteroventral processes (0); extended posteriorly beyond the level of the*
 2348 *posterodorsal and/or posteroventral processes (1). This character is inapplicable in taxa that lack a*
 2349 *posteroventral process in the dentary (Ezcurra 2016: Fig. 29).*

2350 152) Ezcurra (2016) ch. 262 and Pritchard et al. (2015) ch. 84. *Lower jaw, external mandibular fenestra:*
 2351 *absent (0); present (1) (Ezcurra 2016: Figs. 17 and 29).*

2352 153) New, combination of ch. 261 (partially) of Ezcurra (2016) and character 319 of Pritchard et al.
 2353 (2018) *Lower jaw, distinct dorsal process behind the alveolar margin: absent, with a slightly convex*
 2354 *dorsal margin behind the alveolar portion (0); present but low, not protruding dorsally behind the*
 2355 *anterior process of the jugal (1); present and tall, protruding dorsally behind the anterior process of the*
 2356 *jugal (2) (Ezcurra 2016: Fig. 29), ORDERED.*

2357 Both characters from the literature were considered to be informative and strongly related and they
 2358 were therefore combined here. The identification of which bone forms the coronoid process is not
 2359 considered because this often is hard to establish confidently in the sampled taxa. Furthermore, this
 2360 information is strongly interdependent with the subsequent character (154).

2361 154) New. *Separate coronoid bone: present (0); absent (1).*

2362 Although it has been previously established that several archosauromorphs lack a separate coronoid
 2363 bone, this has not been coded as a character in phylogenetic analyses until now.

2364 155) Modified from Ezcurra (2016) ch. 286. *Surangular, lateral shelf: absent (0); present, low ridge*
 2365 *near dorsal margin (1); present, laterally or ventrolaterally projecting shelf with a lateral edge (2)*
 2366 *(Ezcurra 2016: Figs. 18 and 29).*

2367 States 2 and 3 of character 286 in Ezcurra (2016) were combined here because this distinction was
 2368 considered to be somewhat subjective and not of relevance for the sampled taxa.

2369 156) Ezcurra (2016) ch. 288 and Pritchard et al. (2015) ch. 80. *Surangular, anterior surangular foramen*
 2370 *on the lateral surface of the bone, near surangular-dentary contact: absent (0); present (1) (Ezcurra*
 2371 *2016: Fig. 29).*

2372 157) Ezcurra (2016) ch. 289 and Pritchard et al. (2015) ch. 81. *Surangular, posterior surangular*
 2373 *foramen on the lateral surface of the bone, positioned directly anterolateral to the glenoid fossa: absent*
 2374 *(0); present (1) (Ezcurra 2016: Fig. 29).*

2375 158) Modified from Ezcurra (2016) ch. 282. *Surangular-angular, suture along the anterior half of the*
 2376 *bones in lateral view: anteroposteriorly convex ventrally (0); roughly straight (1); anteroposteriorly*
 2377 *concave ventrally (2) (Ezcurra 2016: Fig. 29) (Fig. 18) ORDERED.*

2378 In *Tanystropheus hydroides* (PIMUZ T 2790), *Trilophosaurus buettneri* (Spielmann et al. 2008), and
 2379 *Orovenator mayorum* (Ford and Benson 2018) the surangular-angular suture is neither convex nor
 2380 concave but straight, which was therefore included as a separate character state here. A straight suture
 2381 is considered an intermediate step in a transformational series from concave to convex and the
 2382 character has therefore been ordered.

2383 159) Modified from Ezcurra (2016) ch. 290 and Pritchard et al. (2015) ch. 82. *Angular, dorsoventral*
 2384 *exposure on the lateral surface of the lower jaw: wide (0); forming about half of the dorsoventral height*
 2385 *of the mandible at its greatest width (1); narrow (2) (Ezcurra 2016: Fig. 29) (Fig. 18) ORDERED.*

2386 In *Tanystropheus hydroides* (PIMUZ T 2790), *Tanystropheus longobardicus* (PIMUZ T 2484),
 2387 *Azendohsaurus madagaskarensis* (Flynn et al. 2011), *Proterosuchus fergusi* (SAM-PK-11208), and
 2388 *Proterosuchus alexanderi* (NM QR 1484) covers approximately half of the lateral surface of the mandible
 2389 posteriorly, which was therefore included as separate character state here. This exposure is considered
 2390 an intermediate step in a transformational series from a very wide to a very narrow exposure and the
 2391 character has therefore been ordered.

2392 160) Pritchard et al. (2015) ch. 83 (state 0 reformulated). *Angular, exposure on lateral mandibular*
 2393 *surface: terminates significantly anterior to the glenoid (0); extends to the glenoid (1).*

2394 161) Modified from Senter (2004) ch. 16. *Location of glenoid fossa compared to tooth row of the*
 2395 *dentary: roughly at the same dorsoventral level as the tooth row (0); considerably ventrally displaced*
 2396 *compared to the tooth row (1) (Fig. 18).*

2397 In several tanystropheids (*Tanystropheus hydroides*, PIMUZ T 2790; *Tanystropheus longobardicus*,
 2398 PIMUZ T 2482; *Tanytrachelos ahynis*, YPM 7496a; *Pectodens zhenyuensis*, IVPP V18578; and
 2399 *Dinocephalosaurus orientalis*, IVPP V13767), and in *Azendohsaurus madagaskarensis* (Flynn et al. 2011)
 2400 and *Gephyrosaurus bridensis* (Evans 1980), the glenoid fossa is located distinctly ventrally compared to
 2401 the dentary tooth row. This character was first employed by Senter (2004).

2402 162) Ezcurra (2016) ch. 283. *Articular, retroarticular process: absent (0); anteroposteriorly short,*
 2403 *being poorly developed posteriorly to the glenoid fossa (1); anteroposteriorly long, extending*
 2404 *considerably posterior to the glenoid fossa (2) ORDERED (Ezcurra 2016: Figs. 17 and 29).*

2405 163) Ezcurra (2016) ch. 284. *Articular, retroarticular process: not upturned (0); upturned (1). This*
 2406 *character is scored as inapplicable in taxa that lack a retroarticular process (Ezcurra 2016: Figs. 17 and*
 2407 *29).*

2408 164) Pritchard et al. (2015) ch. 92. *Marginal dentition, arrangement: single row of marginal teeth*
 2409 *(0); multiple zahnreihen in maxilla and dentary (1).*

2410 Characters 73 and 279 in Ezcurra (2016) treat the number of tooth rows on the upper and lower jaws
 2411 separately. We consider these characters to be strongly interdependent for the sampled taxa and
 2412 therefore prefer to treat both jaws in one character here.

2413 165) New *Marginal dentition, anterior teeth are interlocking fangs forming a fish-trap sensu*
 2414 *(Rieppel 2002): absent (0); present (1). This character is inapplicable in taxa with an edentulous*
 2415 *premaxilla (Fig. 18).*

2416 In *Tanystropheus hydroides* (PIMUZ T 2790), *Tanystropheus longobardicus* (MSNM BES SC 1018), and
 2417 *Dinocephalosaurus orientalis* (IVPP V13767), the anterior marginal dentition is fang-like and elongate.
 2418 These teeth interlock to form a ‘fish-trap’ type dentition.

2419 166) Modified from Ezcurra (2016) ch. 280. *Marginal dentition, occlusion of marginal teeth: single-*
 2420 *sided overlap (excluding potentially present interlocking fish-trap dentition anteriorly) (0); flat occlusion*
 2421 *(1); teeth interlocking tightly (2). This character is inapplicable in taxa in which multiple tooth rows are*
 2422 *present on the marginal dentition (Ezcurra 2016: Fig. 14).*

2423 The character states were modified to more specifically address the morphologies observed in the
 2424 sampled taxa.

2425 167) Ezcurra (2016) ch. 298. *Marginal dentition, posterior extent of mandibular and maxillary tooth*
 2426 *rows: subequal (0); maxillary teeth extending further posteriorly (1).*

2427 168) Ezcurra (2016) ch. 277. *Marginal dentition, posteriormost dentary teeth: on the anterior half of*
 2428 *lower jaw (0); on the posterior half of lower jaw (1) (Ezcurra 2016: Fig. 17).*

2429 169) Ezcurra (2016) ch 299. *Marginal dentition, tooth implantation: subthecodont (=protothecodont)*
 2430 *(0); ankylothecodont (teeth fused to the bone at the base of the crown by bony ridges and the root can*
 2431 *be discerned; there is continuous tooth replacement) (1); pleurodont (2); acrodon (teeth fused to the*
 2432 *bone in adults so that no root can be discerned) (3); thecodont (4) (Ezcurra 2016: Figs. 12, 14 and 22).*

2433 170) Ezcurra (2016) ch. 308. *Marginal dentition, multiple maxillary and dentary tooth crowns*
 2434 *distinctly mesiodistally expanded above the root: absent (0); present (1) (Ezcurra 2016: Fig. 14).*

2435 171) Modified from Ezcurra (2016) ch. 303. *Marginal dentition, maxillary teeth: straight or very*
 2436 *slightly recurved (0); distinctly recurved (1) (Ezcurra 2016: Fig. 14). This character is not applicable in taxa*
 2437 *with maxillary teeth that expand above the root or that possess multiple tooth rows in the maxilla.*

2438 Certain taxa have very slightly recurved teeth (e.g. *Petrolacosaurus kansensis*, *Czatkowiella harae*, and
 2439 *Orovenator mayorum*). However, we choose not to maintain a separate character state for this
 2440 morphology as in these taxa not all teeth are recurved and many are straight, therefore forming a very
 2441 minimal distinction from the straight morphology. Only taxa in which the curvature of the teeth is
 2442 distinct are scored as 1.

2443 172) Ezcurra (2016) ch. 304. *Marginal dentition, serrations on the maxillary/dentary crowns: absent*
 2444 *(0); distinctly present on the distal margin and usually apically restricted, low or absent on the mesial*
 2445 *margin (1); present and distinct on both margins (2) (Ezcurra 2016: Fig. 14).*

2446 173) Ezcurra (2016) ch. 306. *Marginal dentition, multiple maxillary or dentary tooth crowns with*
2447 *longitudinal labial or lingual striations or grooves: absent (0); present (1) (Ezcurra 2016: Fig. 14).*

2448 174) Modified from Pritchard et al. (2015) ch. 98. *Marginal dentition, tooth shape at crown base:*
2449 *circular or labiolingually compressed (0); labiolingually wider than mesiodistally long (1).*

2450 States 0 and 1 of character 98 of Pritchard et al. (2015) were fused here, because the distinction
2451 between labiolingually compressed and circular teeth is very difficult to assess in the sampled taxa, as it
2452 represents an often minor distinction and many of the sampled specimens are compressed.

2453 175) Modified from Pritchard et al. (2015) ch. 93. *Marginal dentition, morphology of crown base:*
2454 *all tooth crowns form a single, pointed or rounded crown (0); at least some tooth crowns form a*
2455 *flattened platform with pointed cusps (1); at least some tooth crowns have three, mesiodistally arranged*
2456 *cusps (2).*

2457 The character states were modified to more specifically address the morphologies observed in the
2458 sampled taxa.

2459 176) Ezcurra (2016) ch. 310. *Cervical, dorsal, sacral and caudal vertebrae, notochordal canal piercing*
2460 *the centrum: present throughout ontogeny (0); absent in adults (1) (Ezcurra 2016: Fig. 31).*

2461 177) Ezcurra (2016) ch. 313. *Presacral vertebrae, at least one or more cervical or anterior dorsal with*
2462 *parallelogram-shaped centra in lateral view, in which the anterior articular surface is situated higher*
2463 *than the posterior one: absent (0); present (1) (Ezcurra 2016: Figs. 11 and 33).*

2464 178) New. *Cervical vertebrae, maximum height of postaxial anterior or middle cervical neural*
2465 *spines: considerably taller than the posterior articular surface of the centrum (0); approximately equally*
2466 *tall as the posterior articular surface of the centrum (1); considerably shorter than the posterior articular*
2467 *surface of the centrum (2); low neural spines are only present at the anterior and posterior ends of the*
2468 *vertebrae but are completely or virtually lost at their anteroposterior midpoints (3); neural spine is*
2469 *completely reduced or lost (4) (Ezcurra 2016: Fig. 11) (Fig. 19), ORDERED.*

2470 Characters 342 and 344 in Ezcurra (2016) addressed the height of the neural spine in the postaxial
2471 cervical vertebrae, which is a variable and phylogenetically important trait among tanystropheids. We
2472 have combined the information of these two characters, because we considered them to be
2473 interdependent, and modified the states distinctly to address the specific morphologies observed in the
2474 sampled taxa.

2475 179) New. *Cervical vertebrae, shape of distal margin of anterior and middle cervical postaxial*
 2476 *neural spines in lateral view: slightly convex (0); completely straight along anteroposterior length (1);*
 2477 *concave (2) (Fig. 20). This character is inapplicable in taxa that have reduced the neural spine of their*
 2478 *anterior and mid cervicals completely or at their anteroposterior midpoint.*

2479 We find that in a number of taxa the distal margin of the neural spine of the anterior to mid cervical
 2480 vertebrae is completely straight along its entire anteroposterior length (e.g. *Macrocnemus bassanii*,
 2481 PIMUZ T 4822; and *Pamelaria dolichotrachela*, ISIR 316/1). This straight margin often, but not always,
 2482 occurs together with a distally expanded neural spine (= spine table). However, due to both structures
 2483 also occurring without the presence of the other, they were scored here as separate characters.
 2484 Furthermore, the distal margin of the neural spines of certain taxa are conspicuously concave
 2485 (particularly in *Dinocephalosaurus orientalis*, Rieppel et al. 2008).

2486 180) New, combination of Ezcurra (2016) ch. 320 and 321. *Cervical vertebrae, distal expansion of*
 2487 *the anterior to middle postaxial cervical neural spines (not mammillary process): absent (0); present,*
 2488 *gradual transverse expansion of the distal half of the neural spine (1); present, but transverse expansion*
 2489 *is restricted to the distal end of the neural spine (= spine table) (2) (Fig. 20). This character is inapplicable*
 2490 *in taxa that have reduced the neural spine of their anterior and mid cervicals completely.*

2491 A distal expansion of the postaxial neural spines was previously addressed by character 117 in Pritchard
 2492 et al. (2015) and characters 320 and 321 in Ezcurra (2016). Here, we combined information of these
 2493 characters to form a new character that addresses the variation seen in this trait in the sampled taxa.
 2494 We consider the gradual transverse expansion to represent a separate state from the presence of a
 2495 spine table, following Ezcurra (2016). However, since a gradual expansion and a distinct spine table both
 2496 address a widening of the neural spine, which is separate from the presence of mammillary processes,
 2497 we consider them part of the same morphological character. This character should only be scored in
 2498 skeletally mature specimens, since a transverse expansion of the neural spine is generally absent in early
 2499 ontogenetic stages.

2500 181) Modified from Simões et al. (2018) ch. 228. *Presacral vertebrae, type of articular surface:*
 2501 *opistocoelous (0); procoelous (1); amphicoelous (2); acoelous (3). This character is inapplicable in taxa*
 2502 *that have a notochordal canal running through their centra.*

2503 The articulation surfaces of the centra of presacral vertebrae was previously considered by characters
2504 101 and 102 in Pritchard et al. (2015), which considered the anterior and posterior surfaces separately.
2505 We follow Simões et al. (2018) and treat the articulation surfaces of the centra as a single character.

2506 182) Nesbitt (2011) ch. 177. *Presacral vertebrae, postaxial intercentra: present (0); absent (1).*

2507 The presence of intercentra was scored separately for postaxial cervical vertebrae and dorsal vertebra in
2508 characters 346 and 366 in Ezcurra (2016). However, we score only the presence or absence of postaxial
2509 intercentra since in most cases for the sampled taxa, the presence of intercentra often occurs in both
2510 segments of the vertebral column. Thus, separating these segments results in overscoring of the
2511 presence of postaxial intercentra.

2512 183) Ezcurra (2016) ch. 326 and Nesbitt et al. (2015) ch. 243. *Cervical vertebrae, centrum of atlas in*
2513 *skeletally mature individuals: separate from axial intercentrum (0); fused to axial intercentrum (1)*
2514 *(Ezcurra 2016: Fig. 30).*

2515 184) New. *Cervical vertebrae, proatlas elements dorsal to atlantal neural arches: present (0);*
2516 *absent or fused with atlantal neural arch (1) (Fig. 21).*

2517 No proatlases are present in *Tanystropheus hydroides* (PIMUZ T 2790), in contrast to all other sampled
2518 taxa for which this character could be scored.

2519 185) Modified from Ezcurra (2016) ch. 328. *Cervical vertebrae, height of neural spine of the axis:*
2520 *ratio between the maximum height of the neural spine and the posterior articular surface height of the*
2521 *centrum of the axis: 0.40-0.60 (0); 0.75-1.25 (1); 1.45-2.25 (2), ORDERED RATIO (Ezcurra 2016: Fig. 30).*

2522 The distinction between the states of character 328 of Ezcurra (2016) is considered to be ambiguous.
2523 Therefore, the states were modified into ratios to make a more discrete distinction between the states.

2524 186) Ezcurra (2016) ch. 329. *Cervical vertebrae, shape of the neural spine of the axis: expanded*
2525 *posterodorsally or the height of the anterior portion is equivalent to the posterior height (0); expanded*
2526 *anterodorsally (1) (Ezcurra 2016: Fig. 30).*

2527 187) Ezcurra (2016) ch. 331. *Cervical vertebrae, lengths of the fourth or fifth cervical centra versus the*
2528 *heights of their anterior articular surfaces: 0.60-2.45 (0); 2.70-5.15 (1); 6.30-8.00 (2); 8.30-11.10 (3);*
2529 *15.00-21.00 (4) ORDERED RATIO (E: Fig. 15).*

2530 Character states were defined after comparison of all the different measured ratios.

2531 188) Ezcurra (2016) ch. 332 *Cervical vertebrae, diapophysis and parapophysis of anterior to middle*
 2532 *cervical postaxial vertebrae: single facet or both situated on the same process (0); situated on different*
 2533 *processes and well-separated (1); situated on different processes and nearly touching (2) (Ezcurra 2016:*
 2534 *Fig. 30).*

2535 189) New, combination of ch. 334 and 340 of Ezcurra (2016) *Cervical vertebrae, laminae extending*
 2536 *posteriorly from the base of the dia –and/or parapophysis in anterior and middle postaxial cervical*
 2537 *vertebrae: absent (0); present (1) (Ezcurra 2016: Fig. 30).*

2538 Laminae project from the base of the dia –and/or parapophysis in most of the sampled taxa, except for
 2539 *Youngina capensis* (BP/1/3859), *Erythrosuchus africanus* (BP/1/5207), *Mesosuchus browni* (SAM-PK-
 2540 5882), and *Planocephalosaurus robinsonae* (Fraser & Walkden 1984). The laminae as described in
 2541 character 340 in Ezcurra (2016) are considered to represent the same structure as that of character 334
 2542 and therefore these characters were fused.

2543 190) Ezcurra (2016) ch. 336. *Cervical vertebrae, epipophysis in postaxial cervicals: absent (0); present*
 2544 *in at least the third to fifth cervical vertebrae (1) (Ezcurra 2016: Figs. 30 and 33).*

2545 191) Modified from Pritchard et al. (2018) ch. 271. *Cervical vertebrae, posterior extension of*
 2546 *epipophysis: not extended posterior to the postzygapophysis (0); overhanging the postzygapophysis*
 2547 *posteriorly (1). This character is inapplicable in taxa that lack epipophyses on their cervical vertebrae*
 2548 *(Fig. 22).*

2549 In all tanystropheids, with the exception of certain specimens of *Tanystropheus “conspicuus”* (U-MO BT
 2550 740), *Sclerostropheus fossai* (MCSNB 4035), *Macrocnemus fuyuanensis* (IVPP V15001), *Langobardisaurus*
 2551 *pandolfii* (MCSNB 2883), the epipophyses are well-developed and extend posteriorly beyond the level of
 2552 the postzygapophyses. In all other sampled taxa that bear epipophyses, they are not extended as far
 2553 posteriorly. The character was modified from character 271 of Pritchard et al. (2018) because the
 2554 distinction between states 1 and 2 therein was considered to be difficult to distinguish confidently in the
 2555 sampled taxa.

2556 192) Modified from Ezcurra (2016) ch. 338 and Nesbitt et al. (2015) ch. 213. *Cervical vertebrae,*
 2557 *anterior cervical vertebrae (presacral vertebrae 3-5) postzygapophyses: postzygapophyseal trough*
 2558 *(sensu Rieppel 2001) formed by a well-developed posteriorly extending shelf (= transpostzygapophyseal*
 2559 *lamina) which in some cases bears a notch on its posterior end: absent (0); present (1) (Fig. 23).*

2560 This character was modified based on detailed observations of the vertebrae of *Tanystropheus* spp.

2561 193) Modified from Pritchard et al. (2015) ch. 113. *Cervical vertebrae, neural spine base of anterior*
 2562 *postaxial cervical vertebrae: elongate, subequal in length to the neural arch (0); shortened, spine*
 2563 *restricted to posterior half of neural arch (1). This character is inapplicable in taxa that have completely*
 2564 *reduced the neural spine of their anterior and mid cervicals.*

2565 The inapplicability criterion was added.

2566 194) New, combination of Ezcurra (2016) ch. 343 and Pritchard et al. (2015) ch. 116. *Cervical*
 2567 *vertebrae, orientation of the anterior margin of the neural spine of anterior and middle postaxial cervical*
 2568 *vertebrae: straight or posterodorsally inclined (0); anterodorsally inclined at an angle of more than 60*
 2569 *degrees from the horizontal plane (1); anterodorsally inclined at an angle of less than 60 degrees from*
 2570 *the horizontal plane (2) (Ezcurra 2016: Figs. 30 and 33), ORDERED. This character is inapplicable in taxa*
 2571 *that have completely reduced the neural spine of their anterior and mid cervicals.*

2572 The notch referred to by character 115 in Pritchard et al. (2015) was reinterpreted as an anterior
 2573 overhang or inclination by character 343 in Ezcurra (2016). Here, this inclination is considered to
 2574 represent a similar morphology as the inclination described by character 116 of Pritchard et al. (2015),
 2575 and therefore these characters were fused here. The degree of an anterodorsal inclination of the
 2576 anterior margin of the neural spine in the anterior to middle postaxial cervical vertebrae is strongly
 2577 variable among the sampled taxa, and therefore we distinguish between two clearly demarcated states.
 2578 State 1 represents an intermediate morphology between states 0 and 2, and the character was
 2579 therefore ordered. This character is scored as ? for *Tanystropheus hydroides*, *Tanystropheus*
 2580 *longobardicus*, and *Tanystropheus "conspicuus"*. In these taxa the anterior margin of the neural spine is
 2581 complex as it is bifurcated and therefore does not allow for a confident scoring of this character (see fig.
 2582 57 of Nosotti 2007).

2583 195) Modified from Ezcurra (2016) ch. 324. *Cervical vertebrae, total number: six or fewer (0);*
 2584 *between seven and 10 (1); between 11 and 13 (2); more than 13 (3), ORDERED.*

2585 The states were modified based on the distribution of the number of cervical vertebrae in the sampled
 2586 taxa.

2587 196) New. *Cervical vertebrae, presence of a foramen on the ventral surface of the centrum around*
 2588 *the anteroposterior midpoint: absent (0); present (1) (Fig. 24).*

2589 A conspicuous nutrient foramen (foramina venae vertebralis sensu Wild 1973) is present on the ventral
2590 surface of several cervical vertebrae of *Tanystropheus "conspicuus"* (e.g. U-MO BT 740) and
2591 *Gephyrosaurus bridensis* (Evans 1981). This foramen is absent in other taxa for which this character
2592 could be assessed.

2593 197) Pritchard et al. (2015) ch. 109 (reformulated). *Cervical vertebrae, anterior to mid postaxial*
2594 *cervical vertebrae, shape of ventral surface in the coronal plane excluding keel: rounded or curved (0);*
2595 *ventral face flattened (1).*

2596 198) New. *Cervical vertebrae, neural canal of anterior to mid cervical vertebrae separated from*
2597 *vertebral centrum (0); neural canal enters into a cavity of the vertebral centrum (1) (Spiekman et al.*
2598 *subm.: Fig. 29).*

2599 In the tanystropheids *Macrocnemus bassanii*, *Tanytrachelos ahynis*, and *Tanystropheus* spp. the neural
2600 canal of the anterior to mid cervical vertebrae enters the vertebral centrum. This morphology was first
2601 described for *Tanystropheus "conspicuus"* by Edinger (1924) and has recently been identified for several
2602 other tanystropheids through micro computed tomography. Although this character has so far not be
2603 examined for most taxa, it might represent a widespread feature among tanystropheids.

2604 199) Ezcurra (2016) ch. 349 (state 2 reformulated). *Cervical ribs, shape: short, being less than two*
2605 *times the length of its respective vertebra, and tapering at a high angle to the neck (0); short, being less*
2606 *than two times the length of its respective vertebra, and shaft parallel to the neck (1); very long, at least*
2607 *some ribs being more than two times the length of its respective vertebra, and parallel to the neck (2)*
2608 *(Nesbitt 2011: Figs. 28 and 30) (Fig. 25).*

2609 200) Modified from Ezcurra (2016) ch. 350 and Pritchard et al. (2015) ch. 105. *Cervical ribs, anterior*
2610 *free-ending process (=accessory process) on anterior surface of anterior cervical ribs: absent (0); present*
2611 *and short, not reaching anterior to the prezygapophyses of the corresponding vertebra when in*
2612 *articulation (1); present and long, extending anterior to the prezygapophyses of the corresponding*
2613 *vertebra when in articulation (2) (Ezcurra 2016: Fig. 30) (Fig. 25), ORDERED.*

2614 The anterior free-ending process of the cervical ribs in certain tanystropheids (*Sclerostropheus fossai*,
2615 MCSNB 4035; *Tanytrachelos ahynis*, VMNH 120346a; *Pectodens zhenyuensis*, IVPP V18578;
2616 *Dinocephalosaurus orientalis*, Rieppel et al. 2008) and *Czatkowiella harae* (ZPAL RV/937) is particularly
2617 elongate and extends distinctly anterior to the corresponding vertebra. This represents a clearly
2618 separate morphology from the shorter processes seen in most archosauromorphs, and therefore

treated as a new, separate character state. The short processes are considered an intermediate morphology in a transformational series between the absence of the process and the elongate processes, and therefore the character is ordered.

201) Modified from Ezcurra (2016) ch. 320. *Presacral vertebrae, mammillary processes (sensu Ezcurra & Butler 2015b) occurring in the posterior cervical to mid-dorsal vertebrae: absent (0); present (1) (Ezcurra 2016: Figs. 31, 32 and 34).*

We follow the description of Ezcurra & Butler (2015b) for our identification of mammillary processes. Therefore we differentiate mammillary processes from a transverse expansion of the neural spine (=spine table) by the presence of a longitudinal cleft between the process and the spine in the former, which results in a neural spine with three separate projections on its distal end rather than a single flattened surface, as in the latter. The presence of mammillary processes are considered to preclude the possibility of a distally expanded neural spine in the anterior to mid-dorsal vertebrae, since an expansion is already formed by the mammillary processes. This character should only be scored in skeletally mature specimens, since mammillary processes are generally not yet developed in early ontogenetic stages.

202) New. *Dorsal vertebrae, shape of distal margin of anterior to middle dorsal neural spines in lateral view: slightly convex in lateral view (0); completely straight along anteroposterior length in lateral view (1). This character is inapplicable in taxa that possess mammillary processes (Fig. 26).*

As in the cervical vertebrae, the anterior to mid dorsal vertebrae of certain taxa bears a straight dorsal margin of the neural spine. This character is scored separately from character 179 because several of the sampled taxa exhibit clear variation in the presence of the dorsal expansion of the neural spine between the dorsal and cervical vertebrae.

203) New, combining Ezcurra (2016) ch. 320 and 321, and Pritchard et al. (2015) ch. 125. *Dorsal vertebrae, distal expansion of the dorsal neural spines (not mammillary process) of the anterior to mid dorsal vertebrae: absent (0); present, gradual transverse expansion of the distal half of the neural spine (1); present, but transverse expansion is restricted to the distal end of the neural spine (= spine table) (2) (Fig. 26). This character is inapplicable in taxa that bear mammillary processes on their dorsal vertebrae.*

This character describes the same morphology as is described for the cervical vertebrae in character 180. The occurrence of the expansion in the cervical and dorsal vertebrae is split into two different characters for the same arguments as character 202. This character should only be scored in skeletally

2649 mature specimens, since a transverse expansion of the neural spine is generally absent in early
2650 ontogenetic stages.

2651 204) Modified from Senter (2004), ch. 42. *Dorsal vertebrae, total number of dorsal vertebrae: ≤ 24*
2652 *(0); ≥ 25 (1).*

2653 The states of this character were modified to distinguish between the very high number of dorsal
2654 vertebrae seen in *Dinocephalosaurus orientalis* (Rieppel et al. 2008) and the 13 to 20 dorsal vertebrae
2655 seen in other taxa. No other states are incorporated because the exact number of dorsal vertebrae is
2656 hard to establish in many of the sampled taxa.

2657 205) Modified from Ezcurra (2016) ch. 352. *Dorsal vertebrae, length versus height of the centrum*
2658 *(excluding neural arch and spine) at mid-length in posterior dorsals: 0.66-1.39 (0); 1.48-1.86 (1); 1.95-*
2659 *2.17 (2); 2.35-3.30 (3), ORDERED RATIO.*

2660 The formulation of the character and the ratios were slightly modified.

2661 206) Modified from Ezcurra (2016), ch. 354. *Dorsal vertebrae, lateral fossa on the centrum below the*
2662 *neurocentral suture: absent (0); present (1) (Ezcurra 2016: Figs. 31 and 34).*

2663 States 1 and 2 of character 254 in Ezcurra (2016) were combined because this distinction was somewhat
2664 ambiguous and uninformative for the sampled taxa.

2665 207) Modified from Nesbitt (2011) ch. 199. *Dorsal vertebrae, development of the transverse process*
2666 *in middle dorsals: short, projecting only slightly beyond the lateral surface of the neural arch (0); long (1)*
2667 *(Ezcurra 2016: Fig. 32).*

2668 This character was modified based on the observed morphologies in the sampled taxa.

2669 208) Ezcurra (2016), ch. 359. *Dorsal vertebrae, hyposphene-hypantrum accessory intervertebral*
2670 *articulation in middle-posterior dorsals: absent (0); present (1) (Ezcurra 2016: Figs. 31 and 32).*

2671 209) Ezcurra (2016) ch. 361. *Dorsal vertebrae, dorsally opening pit lateral to the base of the neural*
2672 *spine: absent (0); shallow (fossa) (1); developed as a deep pit (2) ORDERED (Ezcurra 2016: Fig. 34).*

2673 210) Ezcurra (2016) ch. 363. *Dorsal vertebrae, fan-shaped neural spine in lateral view: absent (0);*
2674 *present (1).*

2675 211) Modified from Pritchard et al. (2015) ch. 129. *Dorsal vertebrae, height of neural spines in mid-*
 2676 *dorsals: tall, greater in dorsoventral height than anteroposterior length (0); long and low, approximately*
 2677 *similar in dorsoventral height and anteroposterior length or less in height than in length (1).*

2678 We modified the character so that it only applies to mid-dorsal vertebrae, because anterior dorsal
 2679 vertebrae often have a different morphology from more posterior vertebrae, and their inclusion
 2680 therefore might result in inconsistent character scoring.

2681 212) Pritchard et al. (2015) ch. 121. *Dorsal vertebrae, position of parapophysis (or ventral margin of*
 2682 *dorsal synapophysis) in posterior dorsals: positioned partially on lateral margin of centrum (0);*
 2683 *positioned entirely on neural arch (1).*

2684 213) Pritchard et al. (2015) ch. 122 (reformulated). *Dorsal ribs, proximal end of anterior dorsal ribs:*
 2685 *holocephalous (one facet) (0); dichocephalous (two facets) (1); tricephalous (three facets) (2).*

2686 214) Modified from Ezcurra (2016) ch. 368. *Dorsal ribs, proximal end of middle dorsal ribs:*
 2687 *dichocephalous (0); holocephalous (1). This character is inapplicable in taxa that have holocephalous*
 2688 *anterior dorsal ribs, since these imply the presence of holocephalous middle dorsal ribs.*

2689 The inapplicability criterion has been added.

2690 215) Ezcurra (2016) ch. 372 and Nesbitt et al. (2015) ch. 216. *Sacral ribs, anteroposterior length of the*
 2691 *first primordial sacral rib versus the second primordial sacral rib in dorsal view: primordial sacral rib one*
 2692 *is longer anteroposteriorly than primordial sacral rib two (0); primordial sacral rib two is about the same*
 2693 *length or longer anteroposteriorly than primordial sacral rib one (1).*

2694 216) Ezcurra (2016) ch. 373 and Pritchard et al. (2015) ch. 131. *Sacral ribs, second rib shape: single unit*
 2695 *(0); bifurcates distally into anterior and posterior processes (1) (Ezcurra 2016: Fig. 35).*

2696 217) Ezcurra (2016) ch. 374 and Pritchard et al. (2015) ch. 132. *Sacral ribs, morphology of posterior*
 2697 *process: pointed bluntly (0); pointed sharply (1). This character is inapplicable in taxa without a*
 2698 *bifurcated second sacral rib (Ezcurra 2016: Fig. 35). This character is inapplicable in taxa without*
 2699 *bifurcating sacral ribs.*

2700 218) Ezcurra (2016) ch. 375 (reformulated). *Sacral and caudal vertebrae, transverse processes/ribs of*
 2701 *sacral and anterior caudal vertebrae in skeletally mature individuals: rib/transverse process and vertebra*
 2702 *unfused (0); rib/transverse process and vertebra fused to each other (1) (Ezcurra 2016: Fig. 35).*

2703 219) Modified from Ezcurra (2016) ch. 377. *Caudal vertebrae, length of the transverse process + rib*
 2704 *versus length across zygapophyses in anterior caudal vertebrae (third to fifth caudal): 0.62-1.30 (0); 1.60-*
 2705 *2.00 (1); 2.20-2.72 (2) ORDERED RATIO (Ezcurra 2016: Fig. 35).*

2706 We specified on which caudal vertebrae this character should be scored and modified the ratios based
 2707 on the findings in the sampled taxa.

2708 220) Modified from Dilkes (1998) ch. 88. *Caudal vertebrae, height versus maximum*
 2709 *anteroposterior length of proximal caudal neural spine (measured in one of the first five caudals): 0.50-*
 2710 *0.83 (0); 0.90-1.05 (1); 1.12-1.70 (2); 2.00-2.50 (3), ORDERED RATIO.*

2711 Character states were defined after comparison of all the different measured ratios.

2712 221) Modified from Pritchard et al. (2015) ch. 134. *Caudal vertebrae, orientation of transverse*
 2713 *processes: base of process perpendicular to the long axis of the vertebra or slightly posterolaterally*
 2714 *angled (0); processes distinctly angled posterolaterally from base (1).*

2715 The states were modified to represent a clearer morphological distinction between them based on the
 2716 sampled taxa.

2717 222) Modified from Dilkes (1998) ch. 141. *Chevrons, curvature of haemal spines in mid-caudal*
 2718 *vertebrae. No curvature or posterior curvature (0); anterior curvature present (1).*

2719 The states were modified to represent a clearer morphological distinction between them based on the
 2720 sampled taxa.

2721 223) Modified from Pritchard et al. (2015) ch. 136. *Chevrons, shape of haemal spine: tapers along*
 2722 *its anteroposterior length (0); maintains breadth along its length (1); gradually broadens distally (2);*
 2723 *broadens abruptly distally, forming an inverted T shape (3).*

2724 This character was modified based on the observed morphologies in the sampled taxa.

2725 224) New. *Chevrons, anteroposterior length of vertebral centrum versus proximodistal length of*
 2726 *corresponding haemal spine in anterior caudals (third to fifth caudal): 0.30-0.55 (0); 0.65-1.10 (1) (Fig.*
 2727 *27).*

2728 The relative length of the chevrons in the anterior caudal vertebrae differs among the sampled taxa and
 2729 is possibly phylogenetically informative and it was therefore included as a character here.

2730 225) Pritchard et al. (2015) ch. 200. *Heterotopic ossifications: absent in a minimum of 5 individuals*
2731 *(0); present (1) (Fig. 28).*

2732 See the character description of character 200 in Pritchard et al. (2015).

2733 226) Ezcurra (2016) ch. 384. *Scapulocoracoid, both bones fuse with each other in skeletally mature*
2734 *individuals: present (0); absent (1) (Ezcurra 2016: Fig. 36).*

2735 227) New, combination of ch. 385 and 388 of Ezcurra (2016) *Scapulocoracoid, the anterior margin at*
2736 *the level of the suture between both bones: roughly continuous margin (0); distinct notch present (1);*
2737 *large fenestra between scapula and coracoid (scapulocoracoidal fenestra) present (2) (Ezcurra 2016: Fig.*
2738 *36) (Fig. 29).*

2739 Characters 385 and 388 in Ezcurra (2016) are fused because both refer to the anterior margin of the
2740 scapulocoracoid and the presence of state 1 precludes the possibility of state 2, and vice versa.
2741 However, because it is not clear whether the notch and the fenestra represent transitional
2742 morphologies of the same structure, the character is not ordered.

2743 228) Modified from Pritchard et al. (2015) ch. 145 and Ezcurra (2016) ch. 389. *Scapula, scapular blade,*
2744 *dorsally or posterodorsally orientated blade with a rectangular outline (0); blade is largely posteriorly*
2745 *directed and semi-circular in outline with a continuously curved anterior/dorsal margin (1) (Fig. 29).*

2746 The semi-circular or semi-lunar shape of the scapula in tanystropheids represents a unique morphology
2747 among archosauromorphs and has been previously incorporated in phylogenetic analyses. We have
2748 redescribed this character to more specifically address this morphology as it is observed in a wide
2749 sample of tanystropheids.

2750 229) Modified from Ezcurra (2016) ch. 390 and Nesbitt et al. (2015) ch. 219. *Scapula, anterior margin*
2751 *of the scapular blade in lateral view, excluding the margin of a potentially present scapulocoracoidal*
2752 *fenestra: straight or convex along entire length (0); distinctly concave (1) (Ezcurra 2016: Fig. 36). This*
2753 *character is inapplicable in taxa that have a semicircular scapular blade.*

2754 This character was modified to prevent it from being interdependent with characters 227 and 228.

2755 230) Modified from Ezcurra (2016) ch. 391 and Nesbitt et al. (2015) ch. 220 *Scapula, constriction*
2756 *distal to the glenoid: minimum anteroposterior length greater than half the proximodistal length of the*
2757 *scapula (0); minimum anteroposterior length less than half but more than a quarter of the proximodistal*

length of the scapula (1); minimum anteroposterior length less than a quarter of the proximodistal length of the scapula (2) (Ezcurra 2016: Figs. 36 and 37), ORDERED. This character is inapplicable in taxa that have a semi-circular scapular blade.

This character was modified based on the observed morphologies in the sampled taxa. The inapplicability criterion was added because a semi-circular shape of the scapular blade implies that it is comparatively much wider than the other morphologies. Thus, scoring those scapulae for this character would always result in state 0, thus representing an overscoring of the semi-circular shaped scapular blade.

231) Ezcurra (2016) ch. 392. *Scapula, supraglenoid foramen: absent (0); present (1).*

232) Ezcurra (2016) ch. 398 (state 2 reformulated). *Coracoid, posterior border in lateral view: unexpanded posteriorly (0); moderately expanded posteriorly (1); strongly expanded posteriorly - the entire border, not only the posteroventral region as is the case in the postglenoid process - and, as a result, the articulated scapula and coracoid are L-shaped in lateral view (in taxa in which the scapular blade is not semi-circular in shape) (2) ORDERED (Ezcurra 2016: Fig. 37).*

233) Ezcurra (2016) ch. 404 and Pritchard et al. (2015) ch. 140. *Cleithrum: present (0); absent (1).*

234) Ezcurra (2016) ch. 405. *Interclavicle: present (0); absent (1) (Ezcurra 2016: Fig. 15).*

235) Modified from Ezcurra (2016) ch. 406. *Interclavicle, long anterior process, resulting in a cross-shaped interclavicle in ventral or dorsal view: present (0); absent (1) (Ezcurra 2016: Fig. 38). This character is inapplicable in taxa that lack an ossified interclavicle.*

An inapplicability criterion was added.

236) Modified from Ezcurra (2016) ch. 407 and Pritchard et al. (2015) ch. 143. *Interclavicle, anterior margin with a median notch: absent (0); present (1) (Ezcurra 2016: Fig. 38). This character is inapplicable in taxa that lack an ossified interclavicle.*

An inapplicability criterion was added.

237) Modified from Ezcurra (2016) ch. 409 *Interclavicle, webbed between lateral and posterior processes: present, proximal half of the bone subtriangular or diamond-shaped (0); absent, sharp angles between processes (1) (Ezcurra 2016: Fig. 38). This character is inapplicable in taxa that lack an ossified interclavicle.*

2786 An inapplicability criterion was added.

2787 238) Modified from Ezcurra (2016) ch. 411 and Pritchard et al. (2015) ch. 144. *Interclavicle, posterior*
 2788 *ramus: little change in width along entire length (0); gradual transverse expansion present (1)* (Ezcurra
 2789 2016: Fig. 38). *This character is inapplicable in taxa that lack an ossified interclavicle.*

2790 An inapplicability criterion was added.

2791 239) New. *Limbs, flipper-like, indicated by the presence of a rod-like shape of the stylopodial and*
 2792 *zygapodial elements, a simple disc-like shape of the tarsal and carpal bones, and hyperphalangy: absent*
 2793 *(0); present (1).*

2794 In *Dinocephalosaurus orientalis* (Rieppel et al. 2008) the limbs have been modified to function as flippers
 2795 for aquatic propulsion. The presence of at least one more *Dinocephalosaurus*-like taxon indicates that
 2796 more non-archosauriform archosauromorphs might have had flippers (Li et al. 2017b).

2797 240) New. *Long bone histology, fibrolamellar bone tissue in the cortex: absent (0); present (1).*

2798 Early archosauromorphs exhibit considerable variation in their bone tissue (e.g. Botha-Brink & Smith
 2799 2011; Cubo & Jalil 2019; Jaquier & Scheyer 2017; Werning & Irmis 2010). The presence of fibrolamellar
 2800 bone tissue can contain a strong phylogenetic signal, as it has important implications for growth rates
 2801 and metabolism. Therefore, this character has been included in a phylogenetic context here for the first
 2802 time.

2803 241) Ezcurra (2016) ch. 415. *Humerus, torsion between proximal and distal ends: approximately 45*
 2804 *degrees or more (0); 35 degrees or less (1)* (Ezcurra 2016: Fig. 39).

2805 242) Modified from Ezcurra (2016) ch. 416. *Humerus, transverse width of the proximal end versus*
 2806 *total length of the bone in skeletally mature individuals: 0.10-0.41 (0); 0.44-0.70 (1)* (Ezcurra 2016: Fig.
 2807 39).

2808 State 0 was slightly modified to fit the observed morphologies in the sampled taxa.

2809 243) Ezcurra (2016) ch. 420. *Humerus, conical process on the proximal surface, placed immediately*
 2810 *adjacent to the base of the deltopectoral crest: absent (0); present (1)* (Ezcurra 2016: Fig. 39).

2811 244) Ezcurra (2016) ch. 423. *Humerus, ventral margin of the deltopectoral crest developed as a thick*
 2812 *subcylindrical tuberosity that is well-differentiated from the thinner dorsal margin: present (0); absent (1)*
 2813 *(Ezcurra 2016: Fig. 39).*

- 2814 245) Ezcurra (2016) ch. 425. *Humerus, entepicondyle size in skeletally mature individuals: moderately*
 2815 *large (0); strongly developed (1) (Ezcurra 2016: Fig. 39).*
- 2816 246) Ezcurra (2016) ch. 426 and Pritchard et al. (2015) ch. 153. *Humerus, entepicondylar foramen:*
 2817 *present (0); absent (1) (Ezcurra 2016: Fig. 39).*
- 2818 247) Ezcurra (2016) ch. 427. *Humerus, ectepicondylar region: foramen present (0); foramen absent,*
 2819 *supinator process and groove present (1); supinator process, groove or foramen absent (2) (Ezcurra*
 2820 *2016: Fig. 39).*
- 2821 248) Modified from Ezcurra (2016) ch. 414. *Humerus, total length of the humerus versus the total*
 2822 *length of the femur: 0.65-0.85 (0); 0.90-1.05 (1), RATIO.*
- 2823 This character is modified to compare the total length of the humerus to the femur rather than the
 2824 entire forelimb to the entire hindlimb.
- 2825 249) Pritchard et al. (2015) ch. 157 and Ezcurra (2016) ch. 430 (reformulated). *Ulna, olecranon process:*
 2826 *absent, not ossified or very low in skeletally mature individuals (0); present (1) (Ezcurra 2016: Fig. 40).*
- 2827 250) Ezcurra (2016) ch. 433. *Ulna, lateral tuber (=radius tuber) on the proximal portion: absent in*
 2828 *skeletally mature individuals (0); present (1) (Nesbitt 2011: Figs. 40 and 31).*
- 2829 251) Modified from Ezcurra (2016) ch. 435. *Radius, total length versus total length of the humerus:*
 2830 *0.50-0.72 (0); 0.81-0.92 (1); 1.00-1.10 (2), ORDERED RATIO (Ezcurra 2016: Fig. 15).*
- 2831 Character states were defined after comparison of all the different measured ratios.
- 2832 252) Ezcurra (2016) ch. 440 and Pritchard et al. (2015) ch. 161. *Carpals, perforating foramen between*
 2833 *intermedium and ulnare: present (0); absent in skeletally mature individuals (1). This character is*
 2834 *inapplicable in taxa that lack an intermedium.*
- 2835 253) New, combination of ch. 441 and 442 of Ezcurra (2016). *Centrale of the manus of skeletally*
 2836 *mature individuals: both the lateral and medial centrale are present (0); only the lateral centrale is*
 2837 *present (1); only the medial centrale is present (2); both are absent (3).*
- 2838 254) Ezcurra (2016) ch. 443. *Carpals, pisiform: present (0); absent in skeletally mature individuals (1)*
 2839 *(Ezcurra 2016: Fig. 40).*

- 2840 255) Benton & Allen (1997) ch. 31 and Jalil (1997) ch. 46 *First distal carpal: present (0); absent in*
 2841 *skeletally mature individuals (1).*
- 2842 256) Ezcurra (2016) ch. 444 and Pritchard et al. (2015) ch 159. *Carpals, distal carpal five: absent in*
 2843 *skeletally mature individuals (0); present (1) (Ezcurra 2016: Fig. 40).*
- 2844 257) Ezcurra (2016) ch 445. *Manus, longest metacarpal + digit: longer than humeral length (0);*
 2845 *subequal to shorter than humeral length (1).*
- 2846 258) Modified from Ezcurra (2016) ch. 446 *Metacarpus, length of the longest metacarpal versus*
 2847 *length of the longest metatarsal: 0.30-0.41 (0); 0.46-0.65 (1), RATIO.*
- 2848 Character states were defined after comparison of all the different measured ratios.
- 2849 259) Modified from Ezcurra (2016) ch. 448. *Metacarpus, width of the distal end of the metacarpal I*
 2850 *versus its total length: 0.25-0.33 (0); 0.38-0.50 (1); 0.56-0.67 (2), ORDERED RATIO (Ezcurra 2016: Fig. 40).*
- 2851 Character states were defined after comparison of all the different measured ratios.
- 2852 260) Ezcurra (2016) ch. 450. *Metacarpus, metacarpal IV: longer than metacarpal III (0); equal or*
 2853 *shorter than metacarpal III (1) (Ezcurra 2016: Fig. 40).*
- 2854 261) Ezcurra (2016) ch. 453 *Manual digits, second phalanx of manual digit II: shorter than the first*
 2855 *phalanx of manual digit II (0); longer than the first phalanx of manual digit II (1) (Nesbitt 2011: Fig. 32).*
- 2856 262) Modified from Ezcurra (2016) ch. 451 and Nesbitt et al. (2015) ch. 222. *Manual digits, unguals*
 2857 *length: about the same length or shorter than the last non-ungual phalanx of the same digit (0);*
 2858 *distinctly longer than the last non-ungual phalanx of the same digit (1). This character is inapplicable in*
 2859 *taxa in which the terminal phalanx of each digit does not form an ungual.*
- 2860 An inapplicability criterion was added because in the aquatic *Dinocephalosaurus orientalis* no ungual is
 2861 formed by the terminal phalanges.
- 2862 263) Modified from Ezcurra (2016) ch. 454. *Manual digits, number of phalanges in digit IV: five (0);*
 2863 *four (1) (Nesbitt 2011: Fig. 32).*
- 2864 State 2 of character 454 in Ezcurra (2016) was removed because it was irrelevant for the sampled taxa.

264) Modified from Ezcurra (2016) ch 460. *Ilium, preacetabular process: absent or incipient (0); present, being considerably anteroposteriorly shorter than its dorsoventral height (1); present, being longer than two thirds of its height (2), ORDERED.*

States 2 and 3 of character 460 in Ezcurra (2016) were fused and redescribed to address the specific morphology observed in the sampled taxa.

265) Modified from Sookias (2016) ch. 268. *Ilium, shape of preacetabular process: rounded (0); approximately straight-sided with a distinct angle between the anterior and dorsal margins (1). This character is inapplicable in taxa that lack a preacetabular process on the ilium.*

States 1 and 2 were fused and state 3 was removed of the original character of Sookias (2016) to specifically address the observed morphologies in the sampled taxa.

266) Modified from Pritchard et al. (2015) ch. 170 and Ezcurra (2016) ch. 461. *Ilium, anterior process/tuber on the anterior margin of the ilium: anterior process/tuber absent or incipient (0); clearly defined anteriorly projecting tuber on the anterior margin of the preacetabular process (1). This character is inapplicable in taxa that lack a preacetabular process on the ilium (Fig. 30).*

Pritchard et al. (2015) indicated the presence of a small tuber on the anterior margin of the iliac blade in certain tanystropheids to represent the same structure as the preacetabular process, which was incorporated into their character 170. This character interpreted the presence of an anteriorly expanded preacetabular process to represent a more strongly exhibited version of this tuber. However, we consider this tuber to represent a separate structure on the preacetabular process, since this tuber occurs in certain taxa that also have a smooth, anterodorsally curved preacetabular process. The presence of a small finger-like tuber on the anterior margin of the preacetabular process is subject to intraspecific variation and occurs in *Tanystropheus longobardicus* (PIMUZ T 1277), a juvenile specimen of *Macrocnemus bassanii* (MSNM BES SC 111), and *Fuyuansaurus acutirostris* (IVPP V17983) among the sampled taxa and it is considered to represent an informative character independent of the size of the preacetabular process. This tuber is very similar to that seen in "*Exilisuchus tubercularis*" (Ochev 1979; Fig. 9 of Ezcurra 2016).

267) Modified from Ezcurra (2016) ch. 463. *Ilium, length of the postacetabular process measured from the most proximal point on the posterior/ventral margin of the process versus anteroposterior length of the acetabulum: 0.40-0.71 (0); 0.88-1.32 (1); 1.43-1.80 (2), ORDERED RATIO (Ezcurra 2016: Fig. 41).*

2895 The measurement of the length of the postacetabular process was specified and character states were
 2896 defined after comparison of all the different measured ratios.

2897 268) Ezcurra (2016) ch. 464 and Pritchard et al. (2015) ch. 164. *Ilium, main axis of the postacetabular*
 2898 *process in lateral or medial view: posterodorsally orientated (0); mainly posteriorly orientated (1)*
 2899 *(Ezcurra 2016: Figs. 9 and 41).*

2900 269) Modified from Ezcurra (2016) ch. 465. *Ilium, caudifemoralis brevis muscle origin on the*
 2901 *lateroventral surface of the postacetabular process: not dorsally or laterally rimed by a brevis shelf (0);*
 2902 *dorsally rimed by a low brevis shelf (1) (Ezcurra 2016: Fig. 9).*

2903 State 0 of character 465 in Ezcurra (2016) has been removed because it is irrelevant to the sampled taxa.

2904 270) Pritchard et al. (2015) ch. 166. *Ilium, supra-acetabular crest: crest absent, anterodorsal margin*
 2905 *of acetabulum similar in development to posterodorsal margin (0); prominent anterodorsal lamina*
 2906 *frames the anterodorsal margin of the acetabulum (1).*

2907 271) Pritchard et al. (2015) ch. 167 *Ilium, shape of supra-acetabular margin: dorsalmost margin of*
 2908 *acetabulum is unsculptured (0); prominent, bulbous rugosity superior to acetabulum (1). This character is*
 2909 *inapplicable in taxa that lack a distinct supra-acetabular crest.*

2910 272) Pritchard et al. (2015) ch. 165 *Ilium, anteroventral process extending from anterior margin of*
 2911 *pubic peduncle: absent (0); present, process draping across anterior surface of pubis (1).*

2912 273) Ezcurra (2016) ch. 471 and Pritchard et al. (2015) ch. 163. *Pubis-ischium, thyroid fenestra: absent*
 2913 *(0); present (1) (Ezcurra 2016: Fig. 41).*

2914 274) Pritchard et al. (2015) ch. 175 *Pubis, lateral surface, development of a lateral tubercle (sensu*
 2915 *Vaughn 1955): present (0); absent (1).*

2916 275) Ezcurra (2016) ch. 477. *Pubis, pubic apron: absent, symphysis extended along the ventral margin*
 2917 *of the pelvic girdle and visible in lateral view (0); present, symphysis restricted anteriorly and obscured by*
 2918 *the pubic shaft in lateral view (1) (Ezcurra 2016: Fig. 41).*

2919 This character is discussed on page 61 and figured in Fig. 58 of Nesbitt et al. (2015).

2920 276) Modified from Ezcurra (2016) ch. 482 and Nesbitt et al. (2015) ch. 225. *Ischium, maximal length*
 2921 *versus anteroposterior length of the acetabulum: 1.47-2.23 (0); 2.51-2.90 (1). RATIO*

2922 Character states were defined after comparison of all the different measured ratios.

2923 277) Ezcurra (2016) ch. 486. *Ischium, symphysis raised on a distinct low peduncle: absent (0); present*
2924 *(1) (Ezcurra 2016: Fig. 41).*

2925 This character is discussed on page 62 Nesbitt et al. (2015).

2926 278) Modified from Pritchard et al. (2015) ch. 176 and Ezcurra (2016) ch. 488. *Ischium, distinct*
2927 *concavity or constriction on the posterior half of the ventral margin of the ischium, thus separating a*
2928 *distinct posterior process from the rest of the ischium: absent (0); present (1) (Ezcurra 2016: Fig. 41) (Fig.*
2929 *30).*

2930 This character was discussed by Pritchard et al. (2015), in which this character was considered
2931 homologous to the spina ischia described by El-Toubi (1949). We reformulate the character based on
2932 our observations of the ischia in the sampled taxa. A posterior process of the ischium is formed by a
2933 distinct concavity or constriction of the ventral margin of the ischium in *Planocephalosaurus robinsonae*,
2934 *Pectodens zhenyuensis*, and *Langobardisaurus pandolfii*. Furthermore, this trait is also present in some,
2935 but not all, specimens of *Macrocnemus bassani*, *Macrocnemus fuyuanensis*, *Tanystropheus*
2936 *longobardicus*, and *Amotosaurus rotfeldensis*. Therefore, this character clearly shows a large amount of
2937 intraspecific variability.

2938 279) Ezcurra (2016) ch. 491. *Femur, proximal articular surface in skeletally mature individuals: well-*
2939 *ossified, being flat or convex (0); partially ossified, being concave and sometimes with a circular pit (1)*
2940 *(Ezcurra 2016: Fig. 42).*

2941 280) Modified from Ezcurra (2016) ch. 504. *Femur, attachment of the caudifemoralis musculature on*
2942 *the posterior surface of the bone: crest-like and with intertrochanteric fossa (=internal trochanter), and*
2943 *convergent with proximal end (0); crest-like and with intertrochanteric fossa (=internal trochanter), and*
2944 *not convergent with proximal end (1); crest-like and without intertrochanteric fossa (=fourth trochanter),*
2945 *and not convergent with proximal end (2) (Ezcurra 2016: Figs. 42 and 43). This character is inapplicable*
2946 *to taxa without a distinct process for the attachment of the caudifemoralis musculature on the femur.*

2947 Character 504 in Ezcurra (2016) is ordered. We decided not to order this character here because we do
2948 not consider it clear that the states represent intermediate steps in a transformational series.

2949 281) Ezcurra (2016) ch. 511. *Femur, distal condyles: prominent, strong dorsoventral expansion (in*
 2950 *sprawling orientation) restricted to the distal end (0); not projecting markedly beyond shaft and expand*
 2951 *gradually if there is any expansion (1) (Ezcurra 2016: Fig. 43).*

2952 See description of character 318 in Nesbitt (2011).

2953 282) Ezcurra (2016) ch. 512. *Femur, distal articular surface: uneven, lateral (=fibular) condyle*
 2954 *projecting distally distinctly beyond medial (=tibial) condyle (0); both condyles prominent distally and*
 2955 *approximately at same level (1); both condyles do not project distally (distal articular surface concave or*
 2956 *almost flat) (2) (Ezcurra 2016: Figs. 42 and 43).*

2957 283) Ezcurra (2016) ch. 513. *Femur, anterior extensor groove: absent, anterior margin of the bone*
 2958 *straight or convex in distal view (0); present, anterior margin of the bone concave in distal view (1)*
 2959 *(Ezcurra 2016: Fig. 42).*

2960 284) Ezcurra (2016) ch. 515. *Femur, shape of lateral (=fibular) condyle in distal view: lateral surface is*
 2961 *rounded and mound-like (0); lateral surface is triangular and sharply pointed (1) (Ezcurra 2016: Fig. 42).*

2962 285) Benton & Allen (1997) ch. 39. *Femur, length of tibia relative to length of femur: tibia shorter*
 2963 *than, or subequal to, femur in length (0); tibia longer than femur (1).*

2964 286) Pritchard et al. (2015) ch. 177. *Femur, shape in lateral view: femoral shaft exhibits sigmoidal*
 2965 *curvature (0); femoral shaft linear with slight ventrodorsal curvature (1).*

2966 287) Ezcurra (2016) ch. 528 *Fibula, transverse width at mid-length: subequal to transverse width of*
 2967 *the tibia (0); distinctly narrower than transverse width of the tibia (1) (Ezcurra 2016: Fig. 15).*

2968 288) Ezcurra (2016) ch. 531 *Fibula, distal end in lateral view: angled anterodorsally (asymmetrical)*
 2969 *(0); rounded or flat (symmetrical) (1) (Ezcurra 2016: Fig. 44, Nesbitt 2011: Fig. 41).*

2970 289) Modified from Ezcurra (2016) ch. 532. *Proximal tarsals, articulation between astragalus and*
 2971 *calcaneum: roughly flat (0); concavoconvex with concavity on the astragalus (1); fused (2) (Ezcurra 2016:*
 2972 *Fig. 45).*

2973 State 1 of character 532 of Ezcurra (2016) is excluded because it does not apply to the sampled taxa.
 2974 This character can best be observed in plantar view. For a detailed description of the articulation
 2975 between the astragalus and calcaneum, see the extensive discussion in Sereno (1991), in particular Figs.
 2976 3-4, 8 therein, and Cruickshank (1979).

2977 290) Ezcurra (2016) ch. 539. *Astragalus, posterior groove: present (0); absent (1) (Nesbitt 2011: Fig.*
2978 *46).*

2979 This character is extensively discussed in page. 353 of Gower (1996). Due to the three-dimensional
2980 structure of the astragalus and the variation observed in its morphology in the sampled taxa, it is hard to
2981 distinguish the groove from other curves and concavities in the bone in certain taxa, since this character
2982 was originally formed to describe the astragalus of archosauriforms. Taxa are scored as 0 when a clear
2983 concavity is present on the ventral/plantar surface of the astragalus, often connecting to the perforating
2984 foramen between the astragalus and calcaneum.

2985 291) Pritchard et al. (2015) ch. 184 (reformulated) and part of Ezcurra (2016) ch. 557. *Distal tarsals,*
2986 *pedal centrale: present (0); absent as a separate ossification, being either unossified or fused to the*
2987 *astragalus in skeletally mature individuals (1) (Ezcurra 2016: Figs. 45 and 46).*

2988 292) New, combination of Ezcurra (2016) ch. 558, same as Pritchard et al. (2015) ch. 193, and Ezcurra
2989 (2016) ch. 559, same as Pritchard et al. (2015) ch. 194. *Distal tarsals of skeletally mature individuals,*
2990 *distal tarsal 1 and 2: both present (0); only one of the two elements is present (1); both absent (2),*

2991 **ORDERED.** 

2992 Characters 558 and 559 in Ezcurra (2016) were fused here, because in certain taxa (*Macrocnemus*
2993 *bassanii*, PIMUZ T 4822; *Macrocnemus fuyuanensis*, IVPP V15001; and *Amotosaurus rotfeldensis*, SMNS
2994 54783a/b) one of the distal tarsals is present, but it cannot be established confidently whether this
2995 represents distal tarsal 1 or 2. We consider this of secondary importance, as this character treats the
2996 degree of ossification in the tarsus, and both distal tarsals ossify at roughly the same developmental
2997 stage (Rieppel 1989).

2998 293) Ezcurra (2016) ch. 563 and Pritchard et al. (2015) ch. 195. *Distal tarsals, distal tarsal 5: present (0);*
2999 *absent in skeletally mature individuals (1).*

3000 294) Modified from Ezcurra (2016) ch. 564. *Pes, foot length (articulated fourth metatarsal and digit)*
3001 *versus tibia-fibula length: 0.60-1.00 (0); 1.02-1.60 (1); 2.00-2.50 (2) (Ezcurra 2016: Fig. 15), ORDERED*
3002 *RATIO.*

3003 Character states were defined after comparison of all the different measured ratios.

3004 295) Ezcurra (2016) ch. 533 and Pritchard et al. (2015) ch. 186. *Proximal tarsals, foramen for the*
3005 *passage of the perforating artery between the astragalus and calcaneum (=perforating foramen):*
3006 *present (0); absent in skeletally mature individuals (1) (Ezcurra 2016: Fig. 45).*

3007 296) Ezcurra (2016) ch. 565. *Metatarsus, configuration: metatarsals diverging from ankle (0);*
3008 *compact, metatarsals I-IV tightly bunched (1) (Ezcurra 2016: Fig. 46).*

3009 297) Modified from Ezcurra (2016) ch. 569. *Metatarsus, length of metatarsal I versus metatarsal III:*
3010 *0.30-0.36 (0); 0.42-0.51 (1); 0.54-0.83 (2), ORDERED RATIO (Ezcurra 2016: Fig. 46).*

3011 Character states were defined after comparison of all the different measured ratios.

3012 298) Modified from Ezcurra (2016) ch. 571. *Metatarsus, length of the metatarsal II versus length of*
3013 *the metatarsal IV: 0.52-0.67 (0); 0.70-0.91 (1); 0.94-1.07 (2), ORDERED RATIO (Ezcurra 2016: Fig. 46).*

3014 Character states were defined after comparison of all the different measured ratios.

3015 299) Modified from Ezcurra (2016) ch. 574. *Metatarsus, length of metatarsal IV versus length of*
3016 *metatarsal III: 0.85-1.00 (0); 1.04-1.08 (1); 1.11-1.28 (2) ORDERED RATIO (Ezcurra 2016: Fig. 46).*

3017 Character 581 in Ezcurra (2016) is not included in our analysis, because the length of the entire digit is
3018 strongly dependent on the length of the metatarsal, and these characters are therefore interdependent.
3019 It was preferred to compare the relative lengths of the metatarsals over the lengths of the entire digits
3020 because this can be scored in a wider range of the sampled taxa. Character states were defined after
3021 comparison of all the different measured ratios.

3022 300) Modified from Ezcurra (2016) ch. 577 (reformulated). *Metatarsus, metatarsal V with a hook-*
3023 *shaped proximal end: absent (0); present, with a gradually medially curved proximal process (1); present,*
3024 *with an abruptly medially flexed proximal process and, as a result, the metatarsal acquires a L-shape in*
3025 *dorsal or ventral view (2) (Ezcurra 2016: Fig. 46).*

3026 301) Ezcurra (2016) ch. 576 (reformulated). *Metatarsus, dorsal prominence separated from the*
3027 *proximo-medial surface by a concave gap in metatarsal V: absent (0); present (1) (Ezcurra 2016: Fig. 46,*
3028 *Nesbitt 2011: Fig. 47). This character is inapplicable in taxa that lack a hook-shaped metatarsal V.*

3029 302) Ezcurra (2016) ch. 578 and Pritchard et al. (2015) ch. 196 *Metatarsus, metatarsal V outer process*
3030 *on the proximal lateral margin: absent, smooth curved margin (0); present, prominent pointed process*
3031 *(1).*

303) Ezcurra (2016) ch. 579. *Metatarsus, metatarsal V lateral plantar tubercle: absent (0); present (1)*
(Ezcurra 2016: Fig. 46).

304) Ezcurra (2016) ch. 580. *Metatarsus, metatarsal V medial plantar tubercle: absent (0); present (1)*
(Ezcurra 2016: Fig. 46).

305) Modified from Benton & Allen (1997) ch. 45. *Metatarsus, length of metatarsal IV versus the*
proximodistal length of metatarsal V: 1.25-1.65 (0); 1.90-2.85 (1); 3.16-3.65 (2); 4.00-5.15 (3), ORDERED
RATIO.

Character states were defined after comparison of all the different measured ratios.

306) Ezcurra (2016) ch. 584 and Pritchard et al. (2015) ch. 199. *Pedal digits, phalanx V-1: subequal to or*
shorter than other non-ungual phalanges (0); metatarsal-like, considerably longer than other non-ungual
phalanges (1).

307) Ezcurra (2016) ch 587 and Nesbitt et al. (2015) ch. 233 *Pedal digits, ventral tubercle in unguals:*
absent or small (0); well-developed and extended ventral to the articular portion of the ungual (1).

Results

As mentioned above, the taxonomic status of “*Tanystropheus antiquus*” is currently uncertain and under revision (Spiekman et al. 2019; Spiekman & Scheyer 2019; Szczygielski, personal commun. 2019). Due to the taxonomic uncertainty regarding this OTU, analyses 1 and 2 were performed once with the complete sample of taxa (iteration A) and once with the complete sample of taxa except for “*Tanystropheus antiquus*” (iteration B). In analysis 1 the characters indicated as ordered were treated as such (Fig. 31), whereas analysis 2 treated all characters as unordered, and excluded all 23 ratio characters (Fig. 32). Analysis 1A found 1132 most parsimonious trees (MPTs) of 1177 steps with a consistency index (CI) of 0.352 and a retention index (RI) of 0.575 (Fig. 31a), and analysis 1B found 587 MPTs of 1173 steps with a CI of 0.352 and RI of 0.575 (Fig. 31b). The second analysis found 1646 MPTs of 974 steps with a CI of 0.375 and RI of 0.581 for analysis 2A (Fig. 32a), and 1996 MPTs of 971 steps with a CI of 0.376 and RI of 0.583 for analysis 2B (Fig. 32b). Analyses 3 and 4 are the pruned analyses, with analysis 3 including ordered characters and analysis 4 excluding ratio characters and treating all remaining characters as unordered. Analysis 3 found 11 MPTs of 1130 steps with a CI of 0.366 and RI of 0.604 (Fig. 33). Analysis 4 found a single MPT of 934 steps with a CI of 0.391 and RI of 0.611 (Fig. 34). Support values for the trees can be found in the figure captions.

3061 Comparison of analyses 1 and 2

3062 The base of the tree of analysis 1 is poorly resolved with a large polytomy that is formed by the
 3063 non-saurian diapsids, excluding the outgroup *Petrolacosaurus kansensis*, and the monophyletic
 3064 Archosauromorpha and Lepidosauromorpha clades (Fig. 31). Analysis 2 shows a slightly higher resolution
 3065 and a polytomy is formed at the base of the tree by *Claudiosaurus germaini*, *Acerosodontosaurus*
 3066 *piveteaui*, *Youngina capensis*, and Sauria (Fig. 32). *Orovenator mayorum* is the sister taxon to this
 3067 polytomy. Although it is generally considered that *Orovenator mayorum* is most distantly related to Sauria
 3068 of all the taxa included here except for the outgroup *Petrolacosaurus kansensis* (Ford & Benson 2020;
 3069 Reisz et al. 2011a), there is no clear consensus in the relationships between *Youngina capensis*,
 3070 *Claudiosaurus germaini*, and *Acerosodontosaurus piveteaui* (Bickelmann et al. 2009). Since the focus of
 3071 this study is not to resolve early diapsid phylogeny, only these taxa, which are among the morphologically
 3072 best-known early diapsids, were included, and the lack of resolution can possibly be attributed to the low
 3073 taxonomic sample for this part of the tree. Both analyses recover a monophyletic Archosauromorpha and
 3074 Lepidosauromorpha, and the monophyletic clades Rhynchosauria, Allokotosauria, and Archosauriformes
 3075 within Archosauromorpha. In both analyses 1A and 2A a huge polytomy is formed by most non-
 3076 archosauriform archosauromorphs (Figs. 31a and 32a). In analysis 1, *Czatkowiella harae* is recovered as
 3077 the sister taxon to all other archosauromorphs and *Protorosaurus speneri* as the sister taxon to all
 3078 archosauromorphs except for *Czatkowiella harae* (Fig. 31). Both taxa are part of the large polytomy in
 3079 analysis 2A (Fig. 32a). In analysis 1A, two clades are recovered among the OTUs generally considered to
 3080 be tanystropheid. One clade comprising all three *Macrocnemus* species, which together form a polytomy,
 3081 and the second clade is made up of **AMNH FARB 7206**, *Tanytrachelos ahynis*, and *Langobardisaurus*
 3082 *pandolfii* as successive sister taxa. These OTUs are part of the large unresolved polytomy in analysis 2A.
 3083 When “*Tanystropheus antiquus*” is excluded, the tree resolution improves distinctly, particularly in
 3084 analysis 1B (Fig. 31b). This analysis recovers a monophyletic Tanystropheidae. The unresolved clade of the
 3085 three *Macrocnemus* species forms the sister group to all other tanystropheids and the clade containing
 3086 **AMNH FARB 7206**, *Tanytrachelos ahynis*, and *Langobardisaurus pandolfii* forms the sister group to a large,
 3087 unresolved clade that includes the remaining tanystropheids. Analysis 2B does not recover a monophyletic
 3088 Tanystropheidae, but the exclusion of “*Tanystropheus antiquus*” does result in the recovery of several
 3089 additional clades (Fig. 32b). As in both iterations of analysis 1 **AMNH FARB 7206**, *Tanytrachelos ahynis*,
 3090 and *Langobardisaurus pandolfii* form a clade, with *Langobardisaurus pandolfii* and *Tanytrachelos ahynis*
 3091 as direct sister taxa. *Macrocnemus bassanii* and *Macrocnemus fuyuanensis* form a clade and an
 3092 unresolved clade is formed by the four *Tanystropheus* OTUs and *Raiblikania calligaris*. In both iterations

of analysis 2 and in iteration B of analysis 1, *Prolacerta broomi* is found as the sister taxon to all other crocopods within a monophyletic Crocopoda (Figs. 31b and 32), but in iteration A of analysis 1 *Prolacerta broomi* is found outside this clade within the larger polytomy that also includes most tanystropheids (Fig. 31a). This differs from other recent analyses in which *Prolacerta broomi* was found to be more closely related to Archosauriformes than both rhynchosaur and allokotosaur (e.g. Ezcurra 2016; Nesbitt et al. 2015; Pinheiro et al. 2019; Pritchard et al. 2018; Pritchard & Sues 2019; Pritchard et al. 2015; Spiekman 2018). Both in analyses 1 and 2, the interrelationships between the monophyletic clades Allokotosauria, Rhynchosauria, and *Teyujagua paradoxa* + Archosauriformes are unresolved. In iteration A of analysis 2 Rhynchosauria is unresolved, whereas in analysis 1 and iteration B of analysis 2 *Eohyosaurus wolvaardti* and *Howesia browni* are more closely related to each other than to *Mesosuchus browni*.

Comparison of analyses 3 and 4

The strict consensus tree of analysis 3 is largely resolved, whereas that of analysis 4 is completely resolved. Both trees are largely in agreement with each other, and recover a monophyletic Sauria, Lepidosauromorpha, Archosauromorpha, Rhynchosauria, Allokotosauria, and Archosauriformes. Nevertheless, the trees differ in several important aspects. In analysis 3 *Claudiosaurus germaini* is found as sister taxon to all other included taxa apart from *Petrolacosaurus kansensis*, and the other non-saurian diapsids form a polytomic sister clade to Sauria (Fig. 33). In analysis 4 *Orovenator mayorum*, *Claudiosaurus germaini*, and a clade of *Acerosodontosaurus piveteaui* and *Youngina capensis* form successive sister groups to Sauria (Fig. 34). In this regard, analysis 4 is in congruence with other analyses on early amniote relationships, whereas analysis 3 differs with the regards to the position of *Orovenator mayorum* (Bickelmann et al. 2009; Ford & Benson 2018; Reisz et al. 2011a). Both analyses find *Protorosaurus speneri* to be the sister taxon to all other archosauromorphs. Analysis 4 finds a monophyletic Tanystropheidae. In contrast, Analysis 3 finds two separate clades comprised of taxa that have previously been considered as tanystropheids or putative tanystropheids. One clade consists of *Jesairosaurus lehmani*, *Dinocephalosaurus orientalis*, and *Pectodens zhenyuensis* as successive sister taxa. All these taxa have previously been considered as putative tanystropheids or closely allied to the tanystropheid clade as “protorosaurs” (Ezcurra 2016; Jalil 1997; Li et al. 2017a; Rieppel et al. 2008). The second clade comprises taxa that have broadly been interpreted as tanystropheids, and additionally includes the putative tanystropheids *Fuyansaurus acutirostris* and *Ozimek volans*. The clade comprising *Macrocnemus bassanii* and *Macrocnemus fuyuanensis* forms the sister group to the other members of this tanystropheid clade, which together form a polytomy consisting of *Fuyansaurus acutirostris*, *Tanytrachelos ahynis*,

3124 *Langobardisaurus pandolfii*, a clade consisting of *Ozimek volans* and *Amotosaurus rotfeldensis*, and a clade
 3125 consisting of *Tanystropheus longobardicus* and *Tanystropheus hydroides*. In analysis 4 the tanystropheid
 3126 clade is completely resolved and formed by the following successive sister groups: *Jesairosaurus lehmani*,
 3127 a clade comprising of *Dinocephalosaurus orientalis* and *Pectodens zhenyuensis*, *Fuyuansaurus acutirostris*,
 3128 a clade consisting of *Macrocnemus bassanii* and *Macrocnemus fuyuanensis*, a clade consisting of
 3129 *Tanytrachelos ahynis* and *Langobardisaurus rotfeldensis*, and two clades, one consisting of *Ozimek volans*
 3130 and *Amotosaurus rotfeldensis*, and the other of *Tanystropheus longobardicus* and *Tanystropheus*
 3131 *hydroides*. The topology of Crocopoda, the clade consisting of *Prolacerta broomi*, *Teyujagua paradoxa*,
 3132 Allokotosauria, Rhynchosauria, and Archosauriformes is largely congruent between the two analyses. The
 3133 topology of Allokotosauria, Rhynchosauria, and Archosauriformes is the same between the two analyses
 3134 and in both cases *Prolacerta broomi* represents the sister taxon to all other crocopods and *Teyujagua*
 3135 *paradoxa* is the sister taxon to Archosauriformes. The only difference is in the relative positions of
 3136 Rhynchosauria and Allokotosauria. In analysis 3 Rhynchosauria is the sister group to *Teyujagua paradoxa*
 3137 and Archosauriformes, whereas in analysis 4 Allokotosauria occupies this position.

3138 *Clade definitions and synapomorphies*

3139 Based on the results of analysis 4 (Fig. 34), which represents the most stable analysis and makes
 3140 the least assumptions about character transformations (i.e. it does not order characters and excludes
 3141 artificially defined ratios), the included clades can be defined as followed.

3142 **Unnamed clade (*Orovenator mayorum* + *Claudiosaurus germaini* + *Acerosodontosaurus piveteaui* +**
 3143 ***Youngina capensis* + Sauria)**

3144 Unambiguous synapomorphies. There are no synapomorphies for this clade in the present analysis.

3145 **Unnamed clade (*Claudiosaurus germaini* + *Acerosodontosaurus piveteaui* + *Youngina capensis* + Sauria)**

3146 Unambiguous synapomorphies. Lacrimal contacts nasal but does not reach external naris (35-1);
 3147 postfrontal with a posterior process and participates in the border of the supratemporal fenestra (58-1);
 3148 parietal with a supratemporal fossa medial to the supratemporal fenestra (81-1); palatine with the
 3149 anteromedial process being longer than the anterolateral process (99-1); parabasisphenoid recess with
 3150 the ventral floor forming a shallow depression (118-1).

3151 **Unnamed clade (*Acerosodontosaurus piveteaui* + *Youngina capensis* + Sauria)**

Unambiguous synapomorphies. Scapula with a distinctly concave anterior margin of the scapular blade in lateral view (229-1); minimum anteroposterior length of the scapula less than half but more than a quarter of the proximodistal length of the scapula (230-1); femur with distal condyles not projecting markedly beyond shaft (281-1); metatarsus compact, metatarsals I-IV tightly bunched (296-1).

Unnamed clade (*Acerosodontosaurus piveteaui* + *Youngina capensis*)

Unambiguous synapomorphies. Postorbital with a posterior process extending close to or beyond the level of the posterior margin of the supratemporal fenestrae (60-1); dorsal vertebrae with parapophyses positioned entirely on neural arch (212-1).

Sauria Gauthier 1984

Unambiguous synapomorphies. Postparietal absent as a separate ossification (84-2); tabular absent (86-1); quadrate, posterior margin in lateral view continuously concave (90-1); pterygoid without teeth on the lateral ramus (106-0); parabasisphenoid without an intertuberal plate (117-1); anterior surangular foramen on the lateral surface of the surangular, near surangular-dentary contact (156-1); chevrons gradually broaden distally (223-2); hook-shaped metatarsal V with a gradually medially curved proximal process (300-1).

Lepidosauromorpha Gauthier 1984

Unambiguous synapomorphies. Jugal, anterior extension of the anterior process up to or posterior to the level of mid-length of the orbit (37-1); frontals fused to one another (54-1); postorbital-squamosal contact, the anterior process of the squamosal continues along the posterior margin of the ventral process of the postorbital and contacts the jugal (64-1); supratemporal absent (73-2); quadratojugal absent or fused to the quadrate (87-0); broad palatine is the main component of the palate posteriorly to the choanae (98-1); palatine dentition relatively large, similar to those of the marginal dentition (101-1); pterygoid, teeth on the ventral surface of the anterior ramus present in three distinct fields (=T2, T3a and T3b) (102-1); parabasisphenoid recess absent (118-0); splenial absent (143-1); dentary without posterodorsal process (148-0); dentary with posterocentral process (149-1); cervical vertebrae, centrum of atlas fused to axial intercentrum (183-1); height of neural spines in mid-dorsals long and low, approximately similar in dorsoventral height and anteroposterior length or less in height than in length (211-1); primordial sacral rib two is about the same length or longer anteroposteriorly than primordial sacral rib one (215-1); caudal vertebrae, transverse processes distinctly angled posterolaterally from base (221-1); anterior curvature of haemal spines in mid-caudal vertebrae (222-1); humerus, ectepicondylar

3182 region with foramen (247-0); ilium with anteroventral process extending from anterior margin (272-1);
 3183 pubis-ischium, thyroid fenestra present (273-1); proximal tarsals, astragalus and calcaneum fused (289-
 3184 2); metatarsal V with a medial plantar tubercle (304-1).

3185 **Archosauromorpha Huene 1946**

3186 Unambiguous synapomorphies. Maxilla, alveolar margin in lateral view concave (25-1); postfrontal
 3187 without a posterior process and postfrontal does not participate in the border of the supratemporal
 3188 fenestra (58-0); parietal, supratemporal fossae strongly expanded medially and only separated by a ridge
 3189 running along the midline of the parietal, the sagittal crest (83-2); suture between the surangular and
 3190 angular anteroposteriorly convex ventrally along the anterior half of the bones in lateral view (158-0);
 3191 articular, retroarticular process upturned (163-1); diapophysis and parapophysis of anterior to middle
 3192 cervical postaxial vertebrae situated on different processes and nearly touching (188-2); long transverse
 3193 processes in middle dorsals (207-1); coracoid, posterior border in lateral view moderately expanded
 3194 posteriorly (232-1); interclavicle webbed between lateral and posterior processes (237-0); humerus,
 3195 torsion between proximal and distal ends 35 degrees or less (241-1); humerus with entepicondylar
 3196 foramen (246-0).

3197 **Unnamed clade (*Jesairosaurus* + *Dinocephalosauridae* + *Tanystropheidae* + *Crocopoda*)**

3198 Unambiguous synapomorphies. Premaxilla, acute or right angle between the alveolar margin and the
 3199 anterior margin of the premaxillary body in lateral view (6-0); postnarial process of premaxilla well-
 3200 developed and forms most of the ventral border of the external naris but process does not contact
 3201 prefrontal (9-2); subnarial foramen present between premaxilla and maxilla (16-1); the dorsal apex of the
 3202 maxilla ends abruptly and its posterior margin is concave (20-1); ribs of second sacral vertebra bifurcate
 3203 distally into anterior and posterior processes (216-1); scapula without supraglenoid foramen (231-0);
 3204 anterior margin of interclavicle with a median notch (236-1); metatarsal V without outer process on the
 3205 proximal lateral margin (302-0).

3206 **Unnamed clade (*Jesairosaurus lehmani* + *Dinocephalosauridae* + *Tanystropheidae*)**

3207 **Definition...** All taxa more closely related to *Tanystropheus longobardicus* Bassani 1886 and
 3208 *Dinocephalosaurus orientalis* Li 2003 than to *Protorosaurus speneri* Meyer 1832, *Mesosuchus browni*
 3209 Watson 1912, or *Pamelaria dolichotrachela* Sen 2003.

Temporal range. Early Triassic (latest Olenekian, *Augustaburiania vatagini*, but likely Induan to early Olenekian; De Oliveira et al. 2018) to late Late Triassic (late Norian, *Sclerostropheus fossai*).

Unambiguous synapomorphies. Pterygoid, lateral/distal end of the posterior margin of the lateral ramus curved posteriorly (109-1); height of neural spines in mid-dorsals tall, greater in dorsoventral height than anteroposterior length (211-1); parapophysis (or ventral margin of dorsal synapophysis) in posterior dorsals positioned entirely on neural arch (212-1); primordial sacral rib two is about the same length or longer anteroposteriorly than primordial sacral rib one (215-1); ilium, preacetabular process approximately straight-sided with a distinct angle between the anterior and dorsal margins (268-1).

Unnamed clade (Dinocephalosauridae + Tanystropheidae)

Unambiguous synapomorphies. Premaxilla without plate-like palatal shelf or process on the medial surface (11-0); maximum height of postaxial anterior or middle cervical neural spines considerably shorter than the posterior articular surface of the centrum (178-2); postaxial cervicals with epipophyses (190-1); between 11 and 13 cervical vertebrae (195-2); scapular blade is largely posteriorly directed and semi-circular in outline with a continuously curved anterior/dorsal margin (228-1); distinct concavity or constriction on the posterior half of the ventral margin of the ischium, thus separating a distinct posterior process from the rest of the ischium (278-1).

Dinocephalosauridae new clade

Definition. All taxa more closely related to *Dinocephalosaurus orientalis* Li 2003 and *Pectodens zhenyuensis* Li, Fraser, Rieppel, Zhao & Wang 2017 than to *Macrocnemus bassanii* Nopsca 1930 or *Tanystropheus longobardicus* Bassani 1886.

Temporal range. Anisian (Middle Triassic)

Unambiguous synapomorphies. Jugal without a posterior process (42-1); glenoid fossa of the articular considerably ventrally displaced compared to the tooth row (161-1); anterior free-ending process on anterior surface of anterior cervical ribs long, extending anterior to the prezygapophyses of the corresponding vertebra when in articulation (200-2); metatarsal V without a hook-shaped proximal end (300-0).

Tanystropheidae Camp 1945

3237 Definition. All taxa more closely related to *Macrocnemus bassanii* Nopsca 1930 and *Tanystropheus*
3238 *longobardicus* Bassani 1886 than to *Dinocephalosaurus orientalis* Li 2003 or *Pectodens zhenyuensis* Li,
3239 Fraser, Rieppel, Zhao & Wang 2017.

3240 Temporal range. Early Triassic (latest Olenekian, *Augustaburiania vatagini*, but possibly Induan to early
3241 Olenekian; De Oliveira et al. 2018) to late Late Triassic (late Norian, *Sclerostropheus fossai*).

3242 Unambiguous synapomorphies. distal margin of anterior and middle cervical postaxial neural spines
3243 completely straight along anteroposterior length in lateral view (179-1); dichoccephalous anterior dorsal
3244 ribs (213-1); ilium dorsally rimed by a low brevis shelf (269-1).

3245 **Unnamed clade (*Macrocnemus* spp. + *Tanytrachelos ahynis* + *Langobardisaurus pandolfii* + *Ozimek***
3246 ***volans* + *Amotosaurus rotfeldensis* + *Tanystropheus* spp.)**

3247 Unambiguous synapomorphies. Squamosal medial process long, forming entirely or almost entirely the
3248 posterior border of the supratemporal fenestra (70-1); supra-acetabular margin of ilium with a prominent,
3249 bulbous rugosity superior to acetabulum (271-1); pubis-ischium, thyroid fenestra present (273-1).

3250 ***Macrocnemus* spp.**

3251 Unambiguous synapomorphies. Parietal without a pineal foramen (77-2); pterygoid with teeth on the
3252 lateral ramus (106-1), pterygoid, lateral/distal end of the posterior margin of the lateral ramus not curved
3253 posteriorly (109-0); thecodont marginal teeth implantation (169-4); maxillary teeth distinctly recurved
3254 (171-1); maximum height of postaxial anterior or middle cervical neural spines approximately equally tall
3255 as the posterior articular surface of the centrum (178-1); between seven and 10 cervical vertebrae (195-
3256 1); only one of the two elements distal tarsals 1 and 2 is present (292-1); metatarsal V with medial plantar
3257 tubercle (304-1).

3258 **Unnamed clade (*Tanytrachelos ahynis* + *Langobardisaurus pandolfii* + *Ozimek volans* + *Amotosaurus***
3259 ***rotfeldensis* + *Tanystropheus* spp.)**

3260 Unambiguous synapomorphies. Frontal contribution to the orbital border anteroposteriorly long and
3261 forms at least more than half of the dorsal edge of the orbit (50-1); tooth bearing portion of the dentary
3262 ventrally curved or deflected at its anterior end (145-2); anterior to mid postaxial cervical vertebrae with
3263 ventral face flattened (197-1); presence of heterotopic ossifications (225-1); pedal phalanx V-1
3264 metatarsal-like, considerably longer than other non-ungual phalanges (306-1).

3265 **Unnamed clade (*Tanytrachelos ahynis* + *Langobardisaurus pandolfii*)**

3266 Unambiguous synapomorphies. Procoelous presacral vertebrae (181-1); short cervical ribs, being less than
3267 two times the length of its respective vertebra, and shaft parallel to the neck (199-1); preacetabular
3268 process of the ilium longer than two thirds of its height (264-2); femoral shaft linear with slight
3269 ventrodistal curvature in lateral view (286-1).

3270 **Unnamed clade (*Ozimek volans* + *Amotosaurus rotfeldensis* + *Tanystropheus* spp.)**

3271 Unambiguous synapomorphies. Postorbital, posterior process extends close to or beyond the level of the
3272 posterior margin of the supratemporal fenestrae (60-1); retroarticular process not upturned (163-0);
3273 epipophyses of cervical vertebrae overhanging the postzygapophyses posteriorly (191-1); interclavicle
3274 absent (234-1).

3275 **Unnamed clade (*Ozimek volans* + *Amotosaurus rotfeldensis*)**

3276 Unambiguous synapomorphies. Tibia longer than femur (285-1).

3277 ***Tanystropheus* spp.**

3278 Unambiguous synapomorphies. Eleven to 17 maxillary tooth positions (26-0); frontals very wide and plate-
3279 like, a single frontal (or half of a fused frontal) being almost as wide as long (55-1); posterolateral processes
3280 of the parietal orientated roughly transverse (79-0); dorsal end of the quadrate hooked posteriorly in
3281 lateral view (91-1); glenoid fossa of the articular considerably ventrally displaced compared to the tooth
3282 row (161-1); anterior marginal dentition are interlocking fangs forming a fish-trap (165-1); second sacral
3283 rib is a single unit, i.e. not bifurcated (216-0); transverse width of the fibula subequal to that of the tibia
3284 (287-0).

3285 **Crocopoda Ezcurra 2016**

3286 Unambiguous synapomorphies. Premaxilla slightly downturned, in which the alveolar margin is angled at
3287 approximately 20 degrees to the alveolar margin of the maxilla (5-1); premaxilla-maxilla suture notched
3288 along the ventral margin (15-1); prootic with crista prootica (137-1); surangular shelf with low ridge near
3289 dorsal margin (155-1); posteriormost dentary teeth on the anterior half of lower jaw (168-0);
3290 ankylotheodont marginal teeth implantation (169-1); cervical ribs short, being less than two times the
3291 length of its respective vertebra, and shaft parallel to the neck (199-1); dichoccephalous anterior dorsal
3292 ribs (213-1); fibrolamellar bone tissue in the cortex of long bones (240-1); supra-acetabular margin of ilium

3293 with a prominent, bulbous rugosity superior to acetabulum (271-1); distal condyles of the femur with a
3294 prominent, strong dorsoventral expansion restricted to the distal end (281-0); articulation between
3295 astragalus and calcaneum concavoconvex with concavity on the astragalus (289-1).

3296 **Unnamed clade (Allokotosauria + Rhynchosauria + *Teyujagua paradoxa* + Archosauriformes)**

3297 Unambiguous synapomorphies. postnarial process of premaxilla wide and plate-like (10-0); maxilla,
3298 alveolar margin in lateral view straight or convex (25-0/2); external nares confluent (29-1); orbit with an
3299 elevated rim (48-1); frontal-parietal contact roughly transverse in dorsal view (56-0); posterolateral
3300 processes of parietal dorsoventrally deep, being plate-like in occipital view and subequal to the height of
3301 the supraoccipital (80-1); posterodorsal portion of the parabasisphenoid completely ossified (116-1);
3302 orientation of the parabasisphenoid oblique, main axis posterodorsally-to-anteroventrally oriented (120-
3303 1); basioccipital-parabasisphenoid tightly sutured, sometimes by an interdigitated suture, or both bones
3304 fused to each other (121-1); basioccipital-parabasisphenoid with two pneumatic foramina between them
3305 (122-1); prootic contributes laterally tapering lamina to the anterior surface of the paroccipital process
3306 (139-1).

3307 **Rhynchosauria Osborn 1903**

3308 Unambiguous synapomorphies. Lateral surface of the nasal meets entire dorsoventral height of medial
3309 surface of supra-alveolar portion of maxilla (34-1); shallow or deep pits scattered across surface of the
3310 skull and/or low ridges (44-1); dorsal surface of the frontal adjacent to sutures with the postfrontal
3311 possesses a longitudinal and deep depression (51-1); dorsal surface of postfrontal depressed with deep
3312 pits (59-1); supratemporal is present and broad (73-0); opisthotic with fossa immediately lateral to the
3313 foramen magnum (132-1); multiple zahnreihen in maxilla and dentary (164-1).

3314 **Unnamed clade (*Howesia browni* + *Eohyosaurus wolvaardti*)**

3315 Unambiguous synapomorphies. Maxilla-jugal with anguli oris crest (27-1); supratemporal fossa medial to
3316 the supratemporal fenestra on the parietal well-exposed in dorsal view and mainly dorsally or
3317 dorsolaterally facing (82-0).

3318 **Unnamed clade (Allokotosauria + *Teyujagua paradoxa* + Archosauriformes)**

3319 Unambiguous synapomorphies. Posterior margin of quadrate in lateral view sigmoidal, with a concave
3320 dorsal portion and convex ventral portion (90-2); basioccipital with a transversely narrow embayment or
3321 ridge between basal tubera (125-1); scapulacoracoid not fused (226-1); interclavicle not webbed between

3322 lateral and posterior processes (237-1); postacetabular process of the ilium mainly posteriorly oriented
3323 (268-1); distal end of fibula angled anterodorsally in lateral view (288-0).

3324 **Allokotosauria Nesbitt, Flynn, Pritchard, Parrish, Ranivoharimanana & Wyss 2015**

3325 Unambiguous synapomorphies. Medial process of squamosal long, forming entirely or almost entirely the
3326 posterior border of the supratemporal fenestra (70-1); supratemporal absent (73-2); dorsal end of
3327 quadrate hooked posteriorly in lateral view (91-1); vomerine dentition relatively large, similar to those of
3328 the marginal dentition (97-1); palatine dentition relatively large, similar to those of the marginal dentition
3329 (101-1); dentition on the anterior ramus of the pterygoid relatively large, similar to those of the marginal
3330 dentition (105-1); pterygoid, lateral/distal end of the posterior margin of the lateral ramus curved
3331 posteriorly (109-1); tooth bearing portion of the dentary ventrally curved or deflected at its anterior end
3332 (145-2); articular, retroarticular process anteroposteriorly short, being poorly developed posteriorly to
3333 the glenoid fossa (162-1); distal condyles of the femur uneven with the lateral condyle projecting distally
3334 distinctly beyond the medial condyle (282-0); ventral tubercle of the pedal unguals well-developed and
3335 extended ventral to the articular portion of the ungual (307-1).

3336 **Unnamed clade (*Trilophosaurus buettneri* + *Azendohsaurus madagaskarensis*)**

3337 Unambiguous synapomorphies. Posterior end of the horizontal process of the maxilla distinctly ventrally
3338 deflected from the main axis of the alveolar margin (24-1); postfrontal-frontal suture distinctly
3339 posteromedially inclined (57-1); opisthotic and exoccipital fused (127-1); paroccipital processes of the
3340 opisthotics extend laterally or slightly posterolaterally (130-0); posteriormost dentary teeth on the
3341 posterior half of lower jaw (168-1); multiple maxillary and dentary tooth crowns distinctly mesiodistally
3342 expanded above the root (170-1); postaxial cervicals with epipophyses (190-1); second sacral rib is a single
3343 unit, i.e. not bifurcated (216-0); ulna with olecranon process (249-1); ulna with lateral tuber on the
3344 proximal portion (250-1); proximal articular surface of the femur well-ossified, being flat or convex (279-
3345 0); attachment of the caudifemoralis musculature on the posterior surface of the femur crest-like and
3346 with intertrochanteric fossa, and not convergent with proximal end (280-1).

3347 **Unnamed clade (*Teyujagua paradoxa* + *Archosauriformes*)**

3348 Unambiguous synapomorphies. Jugal bulges ventrolaterally at the point where its three processes meet
3349 (39-1); extension of the ventral process of the postorbital ends much higher than the ventral border of
3350 the orbit (61-0); medial extent of the supratemporal fossa of the parietal restricted to the lateral edge of
3351 the parietal (83-0); posttemporal fenestra absent or developed as a foramen or very narrow slit (136-2);

3352 lower jaw with an external mandibular fenestra (152-1); serrations on the distal margin of the
3353 maxillary/dentary crowns usually apically restricted and low or absent on the mesial margin (172-1).

3354 **Archosauriformes Gauthier, Kluge & Rowe 1988**

3355 Unambiguous synapomorphies. Snout at the level of the anterior border of the orbit dorsoventrally taller
3356 than transversely broad (3-1), antorbital fenestra present (22-1); external nares not confluent (29-0);
3357 postparietal sheet-like, not much narrower than the supraoccipital (84-0); shape of the tooth bearing
3358 portion of the dentary dorsally curved for all or most of its anteroposterior length (145-1); dentary with
3359 posterocentral process (149-1); diapophysis and parapophysis of anterior to middle cervical postaxial
3360 vertebrae situated on different processes and well-separated (188-1).

3361 **Proterosuchidae Huene 1908**

3362 Unambiguous synapomorphies. Premaxilla strongly downturned, prenasal process obscured by the
3363 postnasal process in lateral view (5-2); postorbital, posterior process extends close to or beyond the level
3364 of the posterior margin of the supratemporal fenestrae (60-1); pterygoid with teeth on the lateral ramus
3365 (106-1); orientation of the parabasisphenoid horizontal (120-0); basioccipital-parabasisphenoid with a
3366 loose, overlapping suture (121-0); angular forming about half of the dorsoventral height of the mandible
3367 at its greatest width (159-1).

3368 **Unnamed clade (*Erythrosuchus africanus* + *Euparkeria capensis*)**

3369 Unambiguous synapomorphies. simple continuous contact between premaxilla and maxilla (15-0);
3370 anterior process of the jugal is dorsoventrally expanded anteriorly (38-1); supratemporal absent (73-2);
3371 anterior process of the quadratojugal is distinctly present and the lower temporal bar is complete, but the
3372 process terminates well posterior to the base of the posterior process of the jugal (88-2); quadrate,
3373 posterior margin in lateral view continuously concave (90-1); paroccipital processes of the opisthotics
3374 extend laterally or slightly posterolaterally (130-0); surangular with a laterally or ventrolaterally projecting
3375 shelf with a lateral edge (155-2); serrations on the distal margin of the maxillary/dentary crowns and on
3376 both margins (172-2); dichoccephalous proximal end of middle dorsal ribs (214-0); second sacral rib is a
3377 single unit, i.e. not bifurcated (216-0); coracoid, posterior border unexpanded posteriorly (232-0); shape
3378 of the preacetabular process of the ilium approximately straight-sided with a distinct angle between the
3379 anterior and dorsal margins (265-1); dorsalmost margin of acetabulum is unsculptured (271-0); pubic
3380 symphysis restricted anteriorly and obscured by the pubic shaft in lateral view (275-1); pedal centrale
3381 absent as a separate ossification (291-1); both distal tarsal 1 and 2 are absent (292-2); perforating foramen

3382 between astragalus and calcaneum absent (295-1); no concave gap on the proximal surface of metatarsal
3383 V (301-0).

3384 Discussion

3385 The resolution of the tree topology is distinctly higher in the pruned analyses for both the analyses
3386 (Figs. 33-34). Our findings indicate that the taxa previously considered as “protorosaurs” (*Czatkowiella*
3387 *harae*, *Protorosaurus speneri*, *Jesairosaurus lehmani*, Tanystropheidae, Dinocephalosauridae, and
3388 *Prolacerta broomi*) do not form a monophyletic grouping (Figs. 31-34), corroborating the findings of
3389 various previous analyses (e.g. Dilkes 1998; Ezcurra 2016; Pritchard et al. 2015; Rieppel et al. 2003). We
3390 recovered *Protorosaurus speneri* as the sister taxon to all other Archosauromorpha in analyses 3 and 4,
3391 and as the sister taxon of all Archosauromorpha except for *Czatkowiella harae* in analysis 1. This result is
3392 also consistent with recent analyses (e.g. Ezcurra 2016; Pritchard et al. 2015), and we therefore suggest
3393 abandoning the term “protorosaur” for taxa that are less closely related to *Protorosaurus speneri* than to
3394 tanystropheids, *Prolacerta broomi*, rhynchosaurs, allokotosaurs, or archosauriforms, given the current
3395 framework of early archosauromorph relationships.

3396 The phylogenetic position of *Jesairosaurus lehmani*

3397 *Jesairosaurus lehmani* was originally considered as a “protorosaur” that is closely related to
3398 Tanystropheidae (Jalil 1997). More recently, Ezcurra (2016) recovered *Jesairosaurus lehmani* as the sister
3399 taxon to Tanystropheidae. The position of *Jesairosaurus lehmani* is not stable in our analyses. In analysis
3400 4 it is recovered as the sister taxon of Tanystropheidae, *Fuyuansaurus acutirostris*, and
3401 Dinocephalosauridae (Fig. 34). This position is reasonably well-supported by a Bremer support of 3.
3402 However, in analysis 1B and analysis 3, *Jesairosaurus lehmani* is also recovered as the sister taxon to
3403 Dinocephalosauridae, but it is equally closely related to both Tanystropheidae and Crocopoda (Fig. 31b,
3404 33). In analysis 1A and analysis 2A and 2B it is part of the large polytomy that includes most non-
3405 archosauriform archosauromorphs (Figs. 31a, 32). With the currently available morphological information
3406 for *Jesairosaurus lehmani*, its position as a non-crocopod archosauromorph is well-supported, but its exact
3407 relationships within this group remains contentious.

3408 Dinocephalosauridae

3409 *Dinocephalosaurius orientalis* has been included in three previous phylogenetic analyses. In the
3410 analysis of Rieppel et al. (2008), it formed a polytomy with drepanosaurs, tanystropheids, and
3411 *Jesairosaurus lehmani*. In the analysis of Liu et al. (2017), which is derived from the same character

matrices employed by Rieppel et al. (2008), *Dinocephalosaurus orientalis* was recovered within Tanystropheidae as the sister taxon to all other included tanystropheids. Finally, *Dinocephalosaurus orientalis* was also included in the phylogenetic analysis of De Oliveira et al. (2020), in which it was recovered in a clade with *Jesairosaurus lehmani* that represented the sister clade to all other archosauromorphs. However, the overall resolution of this analysis was poor and both *Dinocephalosaurus orientalis* and *Jesairosaurus lehmani* were pruned for the final analysis presented in De Oliveira et al. (2020). In analysis 1B and analyses 3 and 4 *Dinocephalosaurus orientalis* is found in a clade with *Pectodens zhenyuensis*, a taxon which has previously not been considered in a quantitative phylogenetic analysis (Figs. 31b, 33-34). For analysis 1B this clade has a Bremer support of 1, whereas for analyses 3 and 4 these supports are 4 and 2, respectively. In analysis 1A and analysis 2A-B this clade is not recovered, and both *Dinocephalosaurus orientalis* and *Pectodens zhenyuensis* are part of the large polytomy that includes most non-archosauriform archosauromorphs (Fig. 31a, 32). The presence of more *Dinocephalosaurus*-like taxa has also been alluded to through the description of IVPP V22788, an embryonic specimen that is very similar to *Dinocephalosaurus orientalis* but differs in several aspects, most notably a lower number of cervical vertebrae (Li et al. 2017b). Due to the very early ontogenetic stage of this specimen, it has not been referred to a separate taxon and it has also not been included here, since very early ontogenetic features would have likely introduced bias into the analyses. Nevertheless, the clade formed by *Dinocephalosaurus orientalis* and *Pectodens zhenyuensis* that is found in analysis 1B and our pruned analyses, combined with the existence of at least one more *Dinocephalosaurus*-like taxon, merits the erection of a new higher-level taxon to describe this clade. Dinocephalosauridae is therefore erected. It can be distinguished from other archosauromorph clades through the combination of the following characters: absence of a posterior process of the jugal, ventrally displaced glenoid fossa of the mandible, an elongated free-ending anterior process of the cervical ribs, and a straight metatarsal V. In analysis 4 Dinocephalosauridae forms a monophyletic clade together with Tanystropheidae (Fig. 34), whereas in analyses 1B and 3 it forms a distinct lineage within non-archosauriform archosauromorphs (Figs. 31, 33).

The monophyly of Tanystropheidae

A monophyletic Tanystropheidae is recovered in analyses 1B, 3, and 4 (Figs. 31B, 33-34), which agrees with most previous analyses (e.g. Benton & Allen 1997; Dilkes 1998; Ezcurra 2016; Jalil 1997; Pritchard et al. 2015). In analyses 1A and 2A-B a monophyletic Tanystropheidae is not recovered (Figs. 31A, 32). Analyses 1 and 2 include all relevant “protorosaur” OTUs, regardless of completeness, and therefore also include taxa that are solely known from a few isolated remains (*Tanystropheus*

“conspicuus”, *Augustaburiania vatagini*) or a single, partial postcranial specimen (*Sclerostropheus fossai*, *Ellessaurus gondwanoccidens*, *Raibliania calligaris*). Therefore, it is unsurprising that these analyses are poorly resolved in this part of the tree and that the resolution is dramatically increased after pruning these and other OTUs for which less than 25% of characters could be scored. Nevertheless, analysis 1B, which is comparatively well-resolved and includes all tanystropheids except for “*Tanystropheus antiquus*”, corroborates the assignment of the poorly known taxa *Raibliania calligaris*, *Sclerostropheus fossai*, and *Augustaburiania vatagini* to Tanystropheidae, as had previously been suggested but not tested cladistically (Fig. 31b). Furthermore, *Ellessaurus gondwanoccidens* is also recovered within Tanystropheidae, corroborating the result of De Oliveira et al. (2020). However, whereas *Ellessaurus gondwanoccidens* was recovered as the sister taxon to all other tanystropheids in De Oliveira et al. (2020), it is found in a large polytomy in analysis 1B that is deeply nested within Tanystropheidae.

It is important to note that the cranial morphology of the two best-known tanystropheid species, *Tanystropheus hydroides* and *Macrocnemus bassanii*, was recently revised, revealing a large cranial disparity between the two (Miedema et al. 2020; Spiekman et al. 2020). The analyses presented here are the first to incorporate this new information, yet still confirm the monophyly of the Tanystropheidae. Analyses 1A, 1B, and 2B indicate that **AMNH FARB 7206** is closely related to *Tanytrachelos ahynis* (Figs. 31, 32b), but do not support its referral to this taxon as has previously been proposed (Pritchard et al. 2015), since *Langobardisaurus pandolfii* represents the closest related OTU to *Tanytrachelos ahynis*. A detailed study of **AMNH FARB 7206** and other specimens from the Lockatong Formation are required to assess whether this material can be assigned to a separate taxon.

Fuyuansaurus acutirostris is recovered within Tanystropheidae or among tanystropheid taxa (Figs. 31-34). However, its position within the group is unstable. In analysis 4 it is recovered as the sister taxon to all other Tanystropheidae, whereas in analyses 1B and 3 it is found deeply nested within Tanystropheidae. *Fuyuansaurus acutirostris* had previously not been included in any phylogenetic analysis, and its phylogenetic placement was deemed uncertain in its initial description, since it shared several characters with known tanystropheid taxa (e.g. the presence of 12 to 13 cervical vertebrae, elongate cervical vertebrae with low neural spines, cervical ribs with an anterior process), but also deviated from them in several traits such as the absence of a thyroid fenestra and elongation of the snout (Fraser et al. 2013). These considerations are also reflected in analysis 4, in which *Fuyuansaurus acutirostris* is found within Tanystropheidae, but not deeply nested within the clade (Fig. 34).

Ozimek volans is another taxon that has been tentatively referred to Tanystropheidae. It differs clearly from other tanystropheids in its extremely gracile and elongate appendicular elements and the morphology of its pectoral girdle (Dzik & Sulej 2016). *Ozimek volans* is considered to be most closely related to *Sharovipteryx mirabilis*, although this has not been investigated quantitatively so far. *Sharovipteryx mirabilis* was not included here, since it is generally not considered within Archosauromorpha and is only known from poorly preserved remains. *Sharovipteryx mirabilis* has been interpreted as a gliding reptile (Gans et al. 1987), and due to the highly derived, gracile morphology of *Ozimek volans*, a similar lifestyle was also tentatively proposed for this taxon (Dzik & Sulej 2016). The phylogenetic placement of *Ozimek volans* was recently tested and it was found well-nested within Tanystropheidae as the sister taxon to a *Langobardisaurus pandolfii* - *Tanytrachelos ahynis* clade (Pritchard & Sues 2019). The presence of a possible gliding reptile would represent a remarkable ecomorphological divergence within the tanystropheid clade. Our results corroborate the placement of *Ozimek volans* within Tanystropheidae. Both analyses 3 and 4 recover *Ozimek volans* as the sister taxon to *Amotosaurus rotfeldensis*, whereas analyses 1A and 2 find it in the large polytomy that also includes all other tanystropheids. In analysis 1B, *Ozimek volans* is part of a large polytomy that includes all tanystropheids except *Macrocnemus* spp., **AMNH FARB 7206**, *Langobardisaurus pandolfii*, and *Tanytrachelos ahynis* (Figs. 31-34). *Ozimek volans* was scored here based on its original description (Dzik & Sulej 2016), which largely employs reconstruction drawings for clarification of morphological details. A personal observation of all the referred specimens, possibly in combination with additional aid of μ CT methodologies, would have to confirm the presence of tanystropheid synapomorphies, such as the configuration of the skull and the cervical vertebrae and accompanying ribs, within this taxon.

The *Macrocnemus* taxa form a generic clade in analyses 1, 3, and 4 that is either the sister group to all other Tanystropheidae (Figs. 31B, 33) or to all other Tanystropheidae excluding *Fuyansaurus acutirostris* (Fig. 34). This can likely be attributed to the many plesiomorphic cranial characters this genus exhibits in comparison to *Tanystropheus* spp. (Jaquier et al. 2017; Miedema et al. 2020). The *Tanystropheus* taxa are recovered within a clade that also includes *Raiblikania calligaris* in analysis 2B, highlighting the close affinity of the former to the *Tanystropheus* genus (Fig. 32b). *Tanystropheus longobardicus* and *Tanystropheus hydroides* are also recovered in a generic clade that is deeply nested within Tanystropheidae in the pruned analyses (Figs. 33-34). Although the topology of Tanystropheidae is fully resolved in analysis 4, it is poorly supported (Fig. 34). The Bremer support for all nodes within Tanystropheidae is 1, except for the generic nodes of *Macrocnemus* and *Tanystropheus*, which both have a Bremer support of 4. This is also reflected in the topologies of the other analyses, in which many nodes

within Tanystropheidae are collapsed. The lack of resolution within tanystropheids, even when excluding the least informative OTUs, is attributable to the poorly known cranial morphology of most tanystropheid taxa except for *Macrocnemus* spp. and *Tanystropheus* spp. Complete skulls are known for both *Tanytrachelos ahynis* and *Langobardisaurus pandolfii*, but their cranial morphology is exceedingly hard to infer due to the poor preservation of available specimens, which is related to diagenetic factors (Olsen 1979; Renesto & Dalla Vecchia 2000). Additional specimens or studies employing high-resolution tomographic technologies will hopefully contribute to our future understanding of the considerable cranial disparity present within Tanystropheidae, and aid in resolving intra-tanystropheid relationships.

The monophyly of Crocopoda

Crocopoda is a recently erected clade that includes all archosauromorph taxa that are more closely related to *Trilophosaurus buettneri*, *Azendohsaurus madagaskarensis*, *Rhynchosaurus articeps*, and *Proterosuchus fergusi* than to *Protorosaurus speneri* and *Tanystropheus longobardicus* (Ezcurra 2016, but see Pritchard & Sues 2019, Simões et al. 2018, and Spiekman et al. 2020, which found Crocopoda to be polyphyletic). The monophyly of this clade is recovered here in analyses 2, 3, and 4 (Figs. 31-34) and is well-supported (Bremer support of 7 in analysis 4). All analyses recovered a monophyletic Allokotosauria and Rhynchosauria, which is in correspondence with other recent analyses (Ezcurra 2016, Nesbitt et al. 2015 and subsequent modifications of these matrices). In these analyses *Prolacerta broomi* was more closely related to Archosauriformes than both allokotosaurs and rhynchosaurs. In analyses 2, 3, and 4 *Prolacerta broomi* is recovered within Crocopoda as the sister taxon to all other members of this clade, and it is found outside Crocopoda in analysis 1 (Figs. 31-34). *Prolacerta broomi* is found to be more distantly related to Archosauriformes than both rhynchosaurs and allokotosaurs are through the combination of the following traits, which are absent in either all or most other crocopods included in the analysis: a thin postnarial process of the premaxilla (also present in *Teyujagua paradoxa*), a concave alveolar margin of the maxilla in lateral view, absence of an anguli-ori crest (also absent in *Trilophosaurus buettneri* and Archosauriformes), absence of an elevated orbital rim (also absent in *Trilophosaurus buettneri* and *Euparkeria capensis*), a U-shaped frontoparietal suture (also present in *Euparkeria capensis*), dorsoventrally low posterolateral processes of the parietal in occipital view, a posterodorsally incompletely ossified parabasisphenoid, a horizontally oriented parabasisphenoid (also present in *Trilophosaurus buettneri* and *Proterosuchus* spp.), a loose attachment between the parabasisphenoid and basioccipital (also present in *Proterosuchus* spp.), the absence of pneumatic foramina between the parabasisphenoid and basioccipital (also absent in *Trilophosaurus buettneri* and *Euparkeria capensis*), and

no paroccipital contribution of the prootic. This has important macroevolutionary implications, since *Prolacerta broomi* was previously considered to be very closely related to Archosauriformes and has been treated as such in discussions on character trait evolution (e.g. Ezcurra & Butler 2015a; Pinheiro et al. 2016; Pritchard & Sues 2019).

Teyujagua paradoxa is consistently recovered as the sister taxon to Archosauriformes (Figs. 31-34). However, in analysis 4 Allokotosauria is recovered as the sister clade to *Teyujagua* and Archosauriformes (Bremer support of 2), whereas analysis 3 finds Rhynchosauria to be the sister clade to this node (Bremer support of 1) and analyses 1 and 2 resulted in a polytomy between Allokotosauria, Rhynchosauria, and the clade encompassing *Teyujagua paradoxa* and Archosauriformes. Therefore, our results are inconclusive regarding the relative position of Allokotosauria and Rhynchosauria among non-archosauriform Crocopoda.

Conclusion

Our results corroborate the polyphyly of “Protorosauria” as established by previous studies (e.g. Dilkes 1998; Ezcurra 2016; Pritchard et al. 2015). Consequently, the usage of a historical “protosaur” clade that includes tanystropheids, dinocephalosaurids, and *Prolacerta broomi* should be abandoned. The Chinese taxa *Pectodens zhenyuensis* and *Dinocephalosaurus orientalis* form a newly erected clade, Dinocephalosauridae. *Fuyuansaurus acutirostris* is recovered within Tanystropheidae despite the presence of several plesiomorphic characters. *Jesairosaurus lehmani* is a non-crocopodan archosauromorph that is closely related to tanystropheids and dinocephalosaurids. The interrelationships within Tanystropheidae are poorly resolved, which can be attributed to the poorly known cranial morphology of most tanystropheid taxa. *Prolacerta broomi* is recovered as the sister taxon to all other Crocopoda and is thus more distantly related to Archosauriformes than previously considered.

Institutional abbreviations

AMNH – American Museum of Natural History, New York, New York, USA

AUP – University of Aberdeen, Palaeontology collection, Aberdeen, Scotland

BP – Evolutionary Studies Institute, University of Witwatersrand, Johannesburg, South Africa

BSPG - Bayerische Staatssammlung für Paläontologie und Geologie, Munich, Germany

FMNH - Field Museum of Natural History, Chicago, Illinois, USA

- 3564 GMPKU - Geological Museum of Peking University, Beijing, China
- 3565 IGWuG - Institut für Geologische Wissenschaften und Geiseltalmuseum, Martin-Luther-Universität Halle-
3566 Wittenberg, Halle, Germany
- 3567 IVPP - Institute of Vertebrate Paleontology and Paleoanthropology, Beijing, China
- 3568 KUVP - Kansas University Museum of Natural History, Lawrence, Kansas, USA
- 3569 LPV – Chengdu Center of the China Geological Survey, Chengdu, Sichuan, China
- 3570 MCSN - Museo Cantonale di Scienze Naturali di Lugano, Lugano, Switzerland
- 3571 MCSNB - Museo Civico di Scienze Naturali "E. Caffi" Bergamo, Bergamo, Italy
- 3572 MFSN - Museo Friulano di Scienze Naturali, Udine, Italy
- 3573 MGUWr - Geological Museum, Institute of Geological Sciences, University of Wrocław, Wrocław, Poland
- 3574 MSNM - Museo di Storia Naturale, Milan, Italy
- 3575 NMS – National Museums Scotland, Edinburgh, UK
- 3576 NHMW – Naturhistorisches Museum Wien, Vienna, Austria
- 3577 NMK – Naturkundemuseum im Ottoneum, Kassel, Germany
- 3578 OMNH – Sam Noble Oklahoma Museum of Natural History, Norman, Oklahoma, USA
- 3579 P – Palaeontological Collection of the Department of Geology and Palaeontology, University of Innsbruck,
3580 Innsbruck, Austria
- 3581 PIMUZ - Paläontologisches Institut und Museum der Universität Zürich, Zurich, Switzerland
- 3582 PIN - Paleontological Institute of the Russian Academy of Sciences, Moscow, Russia
- 3583 RC – Rubidge Collection, Wellwood, Graaff-Reinet, South Africa
- 3584 RCSHC –Royal College of Surgeons Hunterian Collection, London, England
- 3585 SAM-PK - Iziko South African Museum, Cape Town, South Africa
- 3586 SMNS – Staatliches Museum für Naturkunde, Stuttgart, Germany
- 3587 SMNK - Staatliches Museum für Naturkunde Karlsruhe, Germany

- 3588 TMM – Texas Memorial Museum, Austin, Texas, USA
- 3589 TWCMS - Sunderland Museum and Winter Gardens, Tyne & Wear Archives & Museums, Sunderland,
3590 England
- 3591 UA – University of Antananarivo, Antananarivo, Madagascar
- 3592 UCMP – University of California Museum of Paleontology, Berkeley, California, USA
- 3593 UFSM – Universidade Federal de Santa Maria, Santa Maria, Brazil
- 3594 UMMP – University of Michigan Museum of Paleontology, Ann Arbor, Michigan, USA
- 3595 UMZC – University Museum of Zoology, Cambridge, England
- 3596 UNIPAMPA – Universidade Federal do Pampa, São Gabriel, Brazil
- 3597 UWBM – Burke Museum of Natural History and Culture, University of Washington, Seattle, Washington,
3598 USA
- 3599 VMNH – Virginia Museum of Natural History, Martinsville, Virginia, USA
- 3600 WMsN - LWL-Museum für Naturkunde, Westfälisches Landesmuseum mit Planetarium, Münster,
3601 Germany
- 3602 YPM - Yale Peabody Museum, New Haven, Connecticut, USA
- 3603 ZAR – Zarzaitine Collection, Muséum National d'Histoire Naturelle, Paris, France
- 3604 ZMNH - Zhejiang Museum of Natural History, Hangzhou, China
- 3605 ZPAL - Institute of Paleobiology, Polish Academy of Sciences, Warsaw, Poland

3606 Acknowledgements

3607 We kindly thank Mark Norell and Carl Mehling (AMNH), Kevin Padian and Pat Holroyd (UCMP), Christian
3608 Sidor and Meredith Rivin (UWBM), Claire Browning and Roger Smith (SAM-PK), Anna Paganoni (MCSNB),
3609 Bernhard Zipfel, Sifelani Jirah, and Jonah Choiniere (BP), Rudolf Stockar (MCSN), Cristiano Dal Sasso and
3610 Stefania Nosotti (MSNM), Cristina Lombardo (MPUM), Nour-Eddine Jalil (ZAR), Christian Klug and Beat
3611 Scheffold (PIMUZ), Alexander Hastings and Christina Byrd (VMNH), Rainer Schoch (SMNS), Eberhard
3612 “Dino” Frey (SMNK), Lothar Schöllmann (WMsN), Cornelia Kurz (NMK), Giuseppe Muscio, Luca Simonetto,
3613 and Fabia Dalla Vecchia (MFSN), Li Chun (IVPP), Da-Yong Jiang (GMPKU), and Olivier Rieppel and William

Simpson (FMNH), for access to specimens under their care. Thodoris Argyriou, Gabriel Aguirre Fernandez, Dylan Bastiaans, Feiko Miedema, and Olivier Rieppel are thanked for discussions. Martín Ezcurra and Sterling Nesbitt kindly provided photographs of several specimens of *Azendohsaurus madagaskarensis*, *Pamelaria dolichotrachela*, and *Proterosuchus alexanderi*.

References

- Abdala F, Hancox PJ, and Neveling J. 2005. Cynodonts from the uppermost Burgersdorp Formation, South Africa, and their bearing on the biostratigraphy and correlation of the Triassic *Cynognathus* Assemblage Zone. *Journal of Vertebrate Paleontology* 25:192-199. 10.1671/0272-4634(2005)025[0192:CFTUBF]2.0.CO;2
- Arthaber Gv. 1922. Über Entwicklung, Ausbildung und Absterben der Flugsaurier. *Paläontologische Zeitschrift* 4:1-47.
- Bartholomai A. 1979. New lizard-like reptiles from the Early Triassic of Queensland. *Alcheringa* 3:225-234.
- Bassani F. 1886. Sui fossili e sull'eta degli schisti bituminosi triasici di Besano in Lombardia. *Atti Società Italiana di scienze naturali* 29:15-72.
- Bennett SC. 1996. The phylogenetic position of the Pterosauria within the Archosauromorpha. *Zoological Journal of the Linnean Society* 118:261-308.
- Benton MJ. 1983. The Triassic reptile *Hyperodapedon* from Elgin: functional morphology and relationships. *Philosophical Transactions of the Royal Society of London B, Biological Sciences* 302:605-718.
- Benton MJ. 1984. The relationships and early evolution of the Diapsida. In: *Ferguson MWJ, ed The structure, evolution, and development of reptiles London: Symposia of the Zoological Society of London* 52:575-596.
- Benton MJ. 1985. Classification and phylogeny of the diapsid reptiles. *Zoological Journal of the Linnean Society* 84:97-164.
- Benton MJ. 2005. *Vertebrate Palaeontology*. Wiley-Blackwell 3rd Edition:472 pages.
- Benton MJ, and Allen JL. 1997. *Boreopricea* from the Lower Triassic of Russia, and the relationships of the prolacertiform reptiles. *Palaeontology* 40:931-953.
- Benton MJ, and Walker AD. 1996. *Rhombopholis*, a prolacertiform reptile from the Middle Triassic of England. *Palaeontology* 39:763-782.
- Bickelmann C, Müller J, and Reisz RR. 2009. The enigmatic diapsid *Acerosodontosaurus piveteaui* (Reptilia: Neodiapsida) from the Upper Permian of Madagascar and the paraphyly of “younginiform” reptiles. *Canadian Journal of Earth Sciences* 46:651-661. 10.1139/E09-038
- Bizzarini F, and Muscio G. 1995. Un nuovo rettile (Reptilia, Prolacertiformes) dal Norico di Preone (Udine, Italia Nordorientale). Nota preliminare. *Gortania - Atti del Museo Friulano di Storia Naturale* 16:67-76.
- Borsuk-Białynicka M, and Evans SE. 2003. A basal archosauriform from the Early Triassic of Poland. *Acta Palaeontologica Polonica* 48.
- Borsuk-Białynicka M, and Evans SE. 2009a. Cranial and mandibular osteology of the Early Triassic archosauriform *Osmolskina czatkowicensis* from Poland. *Palaeontologia Polonica* 65:235–281.
- Borsuk-Białynicka M, and Evans SE. 2009b. A long-necked archosauromorph from the Early Triassic of Poland. *Palaeontologia Polonica* 65:203-234.
- Borsuk-Białynicka M, and Lubka M. 2009. Procolophonids from the Early Triassic of Poland. *Palaeontologia Polonica* 65:107-144.

- 3657 Borsuk-Białynicka M, and Sennikov AG. 2009. Archosauriform postcranial remains from the Early Triassic
3658 karst deposits of southern Poland. *Palaontol Pol* 65:283-328.
- 3659 Botha-Brink J, and Smith RMH. 2011. Osteohistology of the Triassic Archosauromorphs *Prolacerta*,
3660 *Proterosuchus*, *Euparkeria*, and *Erythrosuchus* from the Karoo Basin of South Africa. *Journal of*
3661 *Vertebrate Paleontology* 31:1238-1254.
- 3662 Brazeau MD. 2011. Problematic character coding methods in morphology and their effects. *Biological*
3663 *Journal of the Linnean Society* 104:489-498.
- 3664 Broili F, and Fischer E. 1918. *Trachelosaurus fischeri* nov. gen. nov. sp. Ein neuer Saurier aus dem
3665 Buntsandstein von Bernburg. *Jahrbuch der Königlich Preussischen Geologischen Landesanstalt zu*
3666 *Berlin* 37:359-414.
- 3667 Broom R. 1905a. Preliminary notice of some new fossil reptiles collected by Mr. Alfred Brown at Aliwal
3668 North, South Africa. *Rec Albany Mus* 1:269-275.
- 3669 Broom R. 1905b. Notice of some new fossil reptiles from the Karroo beds of South Africa. *Records of the*
3670 *Albany Museum* 1:331-337.
- 3671 Broom R. 1913a. Note on *Mesosuchus browni*, Watson, and on a new South African Triassic
3672 pseudosuchian (*Euparkeria capensis*). *Records of the Albany Museum* 2:394-396.
- 3673 Broom R. 1913b. On the South-African Pseudosuchian *Euparkeria* and Allied Genera. Proceedings of the
3674 Zoological Society of London: Wiley Online Library. p 619-633.
- 3675 Broom R. 1914. A new Thecodont Reptile. *Proceedings of the Zoological Society of London*:1072-1077.
- 3676 Broom R. 1922. An imperfect skeleton of *Youngina Capensis*, Broom, in the collection of the Transvaal
3677 Museum. *Annals of the Transvaal Museum* 8:273-276.
- 3678 Broom R. 1925. On the origin of lizards. Proceedings of the Zoological Society of London: Wiley Online
3679 Library. p 1-16.
- 3680 Broom R. 1937. A further contribution to our knowledge of the fossil reptiles of the Karroo. *Journal of*
3681 *Zoology* 107:299-318.
- 3682 Broom R, and Robinson JT. 1948. Some New Fossil Reptiles from the Karroo Beds of South Africa. *Journal*
3683 *of Zoology* 118:392-407.
- 3684 Butler RJ, Ezcurra MD, Liu J, Sookias RB, and Sullivan C. 2019. The anatomy and phylogenetic position of
3685 the erythrosuchid archosauriform *Guchengosuchus shiguaiensis* from the earliest Middle Triassic
3686 of China. *PeerJ* 7:e6435. 10.7717/peerj.6435
- 3687 Butler RJ, Ezcurra MD, Montefeltro FC, Samathi A, and Sobral G. 2015. A new species of basal rhynchosaur
3688 (Diapsida: Archosauromorpha) from the early Middle Triassic of South Africa, and the early
3689 evolution of Rhynchosauria. *Zoological Journal of the Linnean Society* 174:571-588.
- 3690 Caldwell MW. 1995. Developmental constraints and limb evolution in Permian and extant
3691 lepidosauromorph diapsids. *Journal of Vertebrate Paleontology* 14:459-471.
3692 10.1080/02724634.1995.10011572
- 3693 Calzavara M, Muscio G, and Wild R. 1980. *Megalancosaurus preonensis* n.g., n.sp., a new reptile from the
3694 Norian of Friuli, Italy. *Gortania - Atti del Museo Friulano di Storia Naturale* 2:59-64.
- 3695 Camp CL. 1945. *Prolacerta* and the protorosaurian reptiles. Part I and Part II. *American Journal of Science*
3696 243:17-32, 84-101.
- 3697 Carroll RL. 1981. Plesiosaur ancestors from the Upper Permian of Madagascar. *Philosophical Transactions*
3698 *of the Royal Society of London B, Biological Sciences* 293:315-383. 10.1098/rstb.1981.0079
- 3699 Case EC. 1928. A cotylosaur from the Upper Triassic of western Texas. *Journal of the Washington Academy*
3700 *of Sciences* 18:177-178.
- 3701 Casey MM, Fraser NC, and Kowalewski M. 2007. Quantative Taphnomy of a Triassic Reptile *Tanytrachelos*
3702 *ahynis* from the Cow Branch Formation, Dan River Basin, Solite Quarry, Virginia. *PALAIOS* 22:598-
3703 611.

- 3704 Castiello M, Renesto S, and Bennett SC. 2016. The role of the forelimb in prey capture in the Late Triassic
3705 reptile *Megalancosaurus* (Diapsida, Drepanosauromorpha). *Historical Biology* 28:1090-1100.
- 3706 Chatterjee S. 1980. *Malerisaurus*, A New Eosuchian Reptile from the Late Triassic of India. *Philosophical*
3707 *Transactions of the Royal Society of London B: Biological Sciences* 291:163-200.
- 3708 Chatterjee S. 1986. *Malerisaurus langstoni*, a new diapsid reptile from the Triassic of Texas. *Journal of*
3709 *Vertebrate Paleontology* 6:297-312.
- 3710 Cohen K, Finney S, Gibbard P, and Fan J-X. 2013. The ICS international chronostratigraphic chart. *Episodes*
3711 36:199-204.
- 3712 Colbert EH. 1945. The Dinosaur Book: The Ruling Reptiles and their Relatives. *Man and Nature Publications*
3713 *Handbook*.
- 3714 Colbert EH. 1965. The Age of Reptiles. *Norton, New York*:262 p.
- 3715 Colbert EH. 1987. The Triassic Reptile *Prolacerta* in Antartica. *American Museum Novitates*:1-19.
- 3716 Colbert EH, and Olsen PE. 2001. A new and unusual aquatic reptile from the Lockatong Formation of New
3717 Jersey (Late Triassic, Newark Supergroup). *American Museum Novitates* 2001:1-24.
3718 10.1206/0003-0082(2001)334<0001:ANAUAR>2.0.CO;2
- 3719 Conrad J. 2008. Phylogeny and systematics of Squamata (Reptilia) based on morphology. *Bulletin of the*
3720 *American Museum of Natural History* 310.
- 3721 Cope ED. 1900. The Crocodilians, lizards and snakes of North America. *Washington: Government Printing*
3722 *Office*.
- 3723 Cowen R. 1981. Homonyms of *Podopteryx*. *Journal of Paleontology* 55:483.
- 3724 Cubo J, and Jalil N-E. 2019. Bone histology of *Azendohsaurus laaroussii*: Implications for the evolution of
3725 thermometabolism in Archosauromorpha. *Paleobiology* 45:317-330.
- 3726 Currie PJ. 1980. A new younginid (Reptilia: Eosuchia) from the Upper Permian of Madagascar. *Canadian*
3727 *Journal of Earth Sciences* 17:500-511. 10.1139/e80-046
- 3728 Currie PJ. 1981. The vertebrae of *Youngina* (Reptilia: Eosuchia). *Canadian Journal of Earth Sciences* 18:815-
3729 818.
- 3730 Dalla Vecchia FM. 2020. *Raibliania calligarisi* gen. n., sp. n., a new tanystropheid (Diapsida,
3731 Tanystropheidae) from the Upper Triassic (Carnian) of northeastern Italy. *Rivista Italiana di*
3732 *Paleontologia e Stratigrafia* 126:197-222. 10.13130/2039-4942/13041
- 3733 De Oliveira TM, Oliveira D, Schultz CL, Kerber L, and Pinheiro FL. 2018. Tanystropheid archosauromorphs
3734 in the Lower Triassic of Gondwana. *Acta Palaeontologica Polonica*. 10.4202/app.00489.2018
- 3735 De Oliveira TM, Pinheiro FL, Stock Da Rosa ÁA, Dias Da Silva S, and Kerber L. 2020. A new archosauromorph
3736 from South America provides insights on the early diversification of tanystropheids. *PLoS ONE*
3737 15:e0230890. 10.1371/journal.pone.0230890
- 3738 DeBraga M, and Reisz RR. 1995. A new diapsid reptile from the uppermost Carboniferous (Stephanian) of
3739 Kansas. *Palaeontology* 38:199-212.
- 3740 DeBraga M, and Rieppel O. 1997. Reptile phylogeny and the interrelationships of turtles. *Zoological*
3741 *Journal of the Linnean Society* 120:281-354.
- 3742 Demes B, and Krause DW. 2005. Suction feeding in a Triassic protorosaur? *Science* 308:1112-1113.
- 3743 Desojo JB, Ezcurra MD, and Schultz CL. 2011. An unusual new archosauriform from the Middle–Late
3744 Triassic of southern Brazil and the monophyly of Doswelliidae. *Zoological Journal of the Linnean*
3745 *Society* 161:839-871.
- 3746 Dias-da-Silva S, Pinheiro FL, Da-Rosa ÁAS, Martinelli AG, Schultz CL, Silva-Neves E, and Modesto SP. 2017.
3747 Biostratigraphic reappraisal of the Lower Triassic Sanga do Cabral Supersequence from South
3748 America, with a description of new material attributable to the parareptile genus *Procolophon*.
3749 *Journal of South American Earth Sciences* 79:281-296. 10.1016/j.jsames.2017.07.012
- 3750 Dilkes DW. 1995. The rhynchosaur *Howesia browni* from the Lower Triassic of South Africa. *Palaeontology*
3751 38:665-686.

- 3752 Dilkes DW. 1998. The Early Triassic rhynchosaur *Mesosuchus browni* and the interrelationships of basal
3753 archosauromorph reptiles. *Philosophical Transactions of the Royal Society of London B: Biological*
3754 *Sciences* 353:501-541. 10.1098/rstb.1998.0225
- 3755 Dilkes DW, and Arcucci AB. 2012. *Proterochampsia barrionuevoi* (Archosauriformes: Proterochampsia)
3756 from the Late Triassic (Carnian) of Argentina and a phylogenetic analysis of Proterochampsia.
3757 *Palaeontology* 55:853-885.
- 3758 Dilkes DW, and Sues H-D. 2009. Redescription and phylogenetic relationships of *Doswellia kaltenbachii*
3759 (Diapsida: Archosauriformes) from the Upper Triassic of Virginia. *Journal of Vertebrate*
3760 *Paleontology* 29:58-79.
- 3761 Dong W, Lin S, and Chen Y. 1997. Stratigraphy (Lithostratic) of Guizhou Province. *China University of*
3762 *Geosciences Press, Beijing*.
- 3763 Dutuit J. 1972. Découverte d'un dinosaure ornithischien dans le Trias supérieur de l'Atlas occidental
3764 marocain. *Comptes Rendus de l'Académie des Sciences* 275:2841-2844.
- 3765 Dzik J, and Sulej T. 2007. A review of the early Late Triassic Krasiejów biota from Silesia, Poland.
3766 *Palaeontologia Polonica*:3-27.
- 3767 Dzik J, and Sulej T. 2016. An early Late Triassic long-necked reptile with a bony pectoral shield and gracile
3768 appendages. *Acta Palaeontologica Polonica* 61:805-823.
- 3769 Edinger T. 1924. Rückenmark im Wirbelkörper! *Anatomischer Anzeiger* 57:515-519.
- 3770 El-Toubi MR. 1949. The post-cranial osteology of the lizard, *Uromastix aegyptia* (Forskål). *Journal of*
3771 *Morphology* 84:281-292.
- 3772 Ellenberger P. 1977. Quelques précisions sur l'anatomie et la place systématique très spéciale de
3773 *Cosesaurus Aviceps*. (Ladinien Su périeur de Montral, Catalogne). *Cuadernos de geología ibérica*=
3774 *Journal of iberian geology: an international publication of earth sciences*:169-188.
- 3775 Ellenberger P. 1978. L'origine des oiseaux. Historique et méthodes nouvelles. Les problèmes des
3776 Archaeornithes. La venue au jour de *Cosesaurus aviceps*. *Mémoires Travaux EPHE, Institut*
3777 *Montpellier* 4:91-117.
- 3778 Ellenberger P, and De Villalta JF. 1974. Sur la présence d'un ancêtre probable des oiseaux dans le
3779 Muschelkalk supérieur de Catalogne (Espagne). Note préliminaire. *Acta geológica hispánica*
3780 9:162-168.
- 3781 Evans SE. 1980. The skull of a new eosuchian reptile from the Lower Jurassic of South Wales. *Zoological*
3782 *Journal of the Linnean Society* 70:203-264. 10.1111/j.1096-3642.1980.tb00852.x
- 3783 Evans SE. 1981. The postcranial skeleton of the Lower Jurassic eosuchian *Gephyrosaurus bridensis*.
3784 *Zoological Journal of the Linnean Society* 73:81-116. 10.1111/j.1096-3642.1981.tb01580.x
- 3785 Evans SE. 1986. The braincase of *Prolacerta broomi* (Reptilia, Triassic). *Neues Jahrbuch für Geologie und*
3786 *Paläontologie Abhandlungen* 173:181-200.
- 3787 Evans SE. 1987. The braincase of *Youngina capensis* (Reptilia: Diapsida; Permian). *Neues Jahrbuch für*
3788 *Geologie und Paläontologie Monatshefte* 1987:193-203.
- 3789 Evans SE. 1988. The early history and relationships of the Diapsida. In *The Phylogeny and Classification of*
3790 *the Tetrapods, Volume 1: Amphibians, Reptiles, Birds, by Benton, M J, Clarendon Press, Oxford*
3791 *Systematics Association Special Volume No. 35A*:221-260.
- 3792 Evans SE. 2009. An early kuehneosaurid reptile from the Early Triassic of Poland. *Palaeontologia Polonica*
3793 65:145-178.
- 3794 Evans SE, and Borsuk-Białynicka M. 2009. A small lepidosauromorph reptile from the Early Triassic of
3795 Poland. *Palaeontologia Polonica* 65:179-202.
- 3796 Evans SE, and Jones MEH. 2010. The origin, early history and diversification of lepidosauromorph reptiles.
3797 *New aspects of Mesozoic biodiversity*: Springer, 27-44.

- 3798 Evans SE, and Kermack K. 1994. Assemblages of small tetrapods from the Early Jurassic of Britain. In: Fraser
3799 NC, and Sues H-D, eds. *In the shadow of the dinosaurs: Early Mesozoic tetrapods*: Cambridge
3800 University Press, 271-283.
- 3801 Evans SE, and King MS. 1993. A new specimen of *Protorosaurus* (Reptilia: Diapsida) from the Marl Slate
3802 (late Permian) of Britain. *Proceedings of the Yorkshire Geological Society* 49:229-234.
- 3803 Evans SE, and Van Den Heever JA. 1987. A new reptile (Reptilia: Diapsida) from the Upper Permian
3804 *Daptocephalus* zone of South Africa. *South African Journal of Science* 83:724-730.
- 3805 Ewer RF. 1965. The anatomy of the thecodont reptile *Euparkeria capensis* Broom. *Philosophical*
3806 *Transactions of the Royal Society B* 248:379-435.
- 3807 Ezcurra MD. 2016. The phylogenetic relationships of basal archosauromorphs, with an emphasis on the
3808 systematics of proterosuchian archosauriforms. *PeerJ* 4:e1778. 10.7717/peerj.1778
- 3809 Ezcurra MD, and Butler RJ. 2015a. Post-hatchling cranial ontogeny in the Early Triassic diapsid reptile
3810 *Proterosuchus fergusi*. *Journal of Anatomy* 226:387-402.
- 3811 Ezcurra MD, and Butler RJ. 2015b. Taxonomy of the proterosuchid archosauriforms (Diapsida:
3812 Archosauromorpha) from the earliest Triassic of South Africa, and implications for the early
3813 archosauriform radiation. *Journal of Anatomy* 58:141-170.
- 3814 Ezcurra MD, and Butler RJ. 2018. The rise of the ruling reptiles and ecosystem recovery from the Permo-
3815 Triassic mass extinction. *Proceedings of the Royal Society B: Biological Sciences* 285.
3816 10.1098/rspb.2018.0361
- 3817 Ezcurra MD, Desojo JB, and Rauhut OWM. 2015. Redescription and phylogenetic relationships of the
3818 proterochampsid *Rhadinosuchus gracilis* (Diapsida: Archosauriformes) from the early Late Triassic
3819 of southern Brazil. *Ameghiniana* 52:391-417.
- 3820 Ezcurra MD, Fiorelli LE, Martinelli AG, Rocher S, von Baczko MB, Ezpeleta M, Taborda JR, Hechenleitner
3821 EM, Trotteyn MJ, and Desojo JB. 2017. Deep faunistic turnovers preceded the rise of dinosaurs in
3822 southwestern Pangaea. *Nature ecology & evolution* 1:1477-1483. 10.1038/s41559-017-0305-5
- 3823 Ezcurra MD, Gower DJ, Sennikov AG, and Butler RJ. 2019. The osteology of the holotype of the early
3824 erythrosuchid *Garjainia prima* (Diapsida: Archosauromorpha) from the upper Lower Triassic of
3825 European Russia. *Zoological Journal of the Linnean Society* 185:717-783.
- 3826 Ezcurra MD, Lecuona A, and Martinelli A. 2010. A new basal archosauriform diapsid from the Lower
3827 Triassic of Argentina. *Journal of Vertebrate Paleontology* 30:1433-1450.
- 3828 Ezcurra MD, Montefeltro F, and Butler RJ. 2016. The early evolution of rhynchosaurs. *Frontiers in Ecology*
3829 *and Evolution* 3:142. 10.3389/fevo.2015.00142
- 3830 Ezcurra MD, Scheyer TM, and Butler RJ. 2014. The origin and early evolution of Sauria: reassessing the
3831 Permian saurian fossil record and the timing of the crocodile-lizard divergence. *PLoS ONE*
3832 9:e89165.
- 3833 Feduccia A. 1996. The origin and evolution of Birds. *Yale University Press New Haven and London*.
- 3834 Feduccia A, and Wild R. 1993. Birdlike Characters in the Triassic Archosaur *Megalanosaurus*.
3835 *Naturwissenschaften* 80:564-566.
- 3836 Feist-Burkhardt S, Götz AE, Szulc J, Borkhataria R, Geluk M, Haas J, Hornung J, Jordan P, Kempf O, and
3837 Michalík J. 2008. Triassic. *The geology of central Europe* 2:749-821.
- 3838 Fichter J. 1995. Katalog des publizierten Materials aus der palaontologischen Sammlung des
3839 Naturkundemuseums der Stadt Kassel. *Philippia* 7:129-157.
- 3840 Flynn JJ, Nesbitt SJ, Michael Parrish J, Ranivoharimanana L, and Wyss AR. 2010. A new species of
3841 *Azendohsaurus* (Diapsida: Archosauromorpha) from the Triassic Isalo Group of southwestern
3842 Madagascar: cranium and mandible. *Palaeontology* 53:669-688.
- 3843 Ford DP, and Benson RB. 2018. A redescription of *Orovenator mayorum* (Sauropsida, Diapsida) using
3844 high-resolution μ CT, and the consequences for early amniote phylogeny. *Papers in*
3845 *Palaeontology*.

- 3846 Ford DP, and Benson RB. 2020. The phylogeny of early amniotes and the affinities of Parareptilia and
3847 Varanopidae. *Nature ecology & evolution* 4:57-65. 10.1038/s41559-019-1047-3
- 3848 Formoso KK, Nesbitt SJ, Pritchard AC, Stocker MR, and Parker WG. 2019. A long-necked tanystropheid
3849 from the Middle Triassic Moenkopi Formation (Anisian) provides insights into the ecology and
3850 biogeography of tanystropheids. *Palaeontologia Electronica* 22:1-15. 10.26879/988
- 3851 Fraser N. 1982. A new rhynchocephalian from the British Upper Trias. *Palaeontology* 25:709-725.
- 3852 Fraser N, and Walkden G. 1984. The postcranial skeleton of the Upper Triassic spheodontid
3853 *Planocephalosaurus robinsonae*. *Palaeontology* 27:575-595.
- 3854 Fraser NC, and Furrer H. 2013. A new species of *Macrocnemus* from the Middle Triassic of the eastern
3855 Swiss Alps. *Swiss Journal of Geosciences* 106:199-206. 10.1007/s00015-013-0137-5
- 3856 Fraser NC, Grimaldi DA, Olsen PE, and Axsmith B. 1996. A Triassic Lagerstätte from eastern North America.
3857 *Nature* 380:615-619. 10.1038/380615a0
- 3858 Fraser NC, and Rieppel O. 2006. A New Protorosaur (Diapsida) from the Upper Buntsandstein of the Black
3859 Forest, Germany. *Journal of Vertebrate Paleontology* 26:866-871. 10.1671/0272-
3860 4634(2006)26[866:anpdf]2.0.co;2
- 3861 Fraser NC, Rieppel O, and Li C. 2013. A long-snouted protosaurus from the Middle Triassic of southern
3862 China. *Journal of Vertebrate Paleontology* 33:1120-1126. 10.1080/02724634.2013.764310
- 3863 Fröbisch J, Schoch RR, Müller J, Schindler T, and Schweiss D. 2011. A new basal sphenodontid synapsid
3864 from the Late Carboniferous of the Saar-Nahe Basin, Germany. *Acta Palaeontologica Polonica*
3865 56:113-120.
- 3866 Gans C, Darevski I, and Tatarinov LP. 1987. *Sharovipteryx*, a reptilian glider? *Palaeobiology* 13:415-426.
- 3867 Gardner NM, Holiday CM, and O'Keefe FR. 2010. The Braincase of *Youngina capensis* (Reptilia, Dipsida):
3868 New Insights from High-Resolution CT Scanning of the Holotype. *Palaeontologia Electronica* 13.
- 3869 Gauffre F-X. 1993. The prosauropod dinosaur *Azendohsaurus laaroussii* the upper Triassic of Morocco.
3870 *Palaeontology* 36:897-908.
- 3871 Gauthier JA. 1984. A Cladistic Analysis of the Higher Categories of the Diapsida. *PhD thesis, University of*
3872 *California, Berkeley*:564 p.
- 3873 Gauthier JA. 1994. The diversification of the amniotes. In *Spencer RS ed Major features of vertebrate*
3874 *evolution Knoxville: The University of Tennessee*:129-159.
- 3875 Gauthier JA, Estes R, and De Queiroz K. 1988a. A phylogenetic analysis of Lepidosauromorpha. In *The*
3876 *Phylogenetic Relationships of the Lizard Families, by Estes, R, ed Stanford University Press, Palo*
3877 *Alto, California*:15-98.
- 3878 Gauthier JA, Kluge AG, and Rowe T. 1988b. Amniote Phylogeny and the Importance of Fossils. *Cladistics*
3879 4:105-209.
- 3880 Goloboff PA, and Catalano SA. 2016. TNT version 1.5, including a full implementation of phylogenetic
3881 morphometrics. *Cladistics* 32:221-238. 10.1111/cla.12160
- 3882 Goodrich E. 1942. The hind foot of *Youngina* and fifth metatarsal in Reptilia. *Journal of Anatomy* 76:308.
- 3883 Gottmann-Quesada A, and Sander PM. 2009. A redescription of the early archosauromorph *Protorosaurus*
3884 *speneri* Meyer, 1832, and its phylogenetic relationships. *Palaeontographica Abteilung A*:123-220.
- 3885 Gow CE. 1975. The morphology and relationships of *Youngina capensis* Broom and *Prolacerta broomi*
3886 Parrington. *Palaeontologica Africana* 18:89-131.
- 3887 Gower D. 2003. Osteology of the early archosaurian reptile *Erythrosuchus africanus*, Broom. *Annals of the*
3888 *South African Museum* 110:1-88.
- 3889 Gower DJ. 1996. The tarsus of erythrosuchid archosaurs, and implications for early diapsid phylogeny.
3890 *Zoological Journal of the Linnean Society* 116:347-375.
- 3891 Gower DJ. 1997. The braincase of the early archosaurian reptile *Erythrosuchus africanus*. *Journal of*
3892 *Zoology* 242:557-576.

- 3893 Gower DJ, and Sennikov AG. 1996. Morphology and phylogenetic informativeness of early archosaur
3894 braincases. *Palaeontology* 39:883-906.
- 3895 Gower DJ, and Sennikov AG. 1997. *Sarmatosuchus* and the early history of the Archosauria. *Journal of*
3896 *Vertebrate Paleontology* 17:60-73.
- 3897 Grand A, Corvez A, Duque Velez LM, and Laurin M. 2013. Phylogenetic inference using discrete characters:
3898 performance of ordered and unordered parsimony and of three-item statements. *Biological*
3899 *Journal of the Linnean Society* 110:914-930. 10.1111/bij.12159
- 3900 Gregory J. 1945. Osteology and relationships of *Trilophosaurus*. *University of Texas Publication* 4401:273-
3901 359.
- 3902 Groenewald GH, and Kitching JW. 1995. Biostratigraphy of the *Lystrosaurus* assemblage zone. In
3903 *Biostratigraphy of the Beaufort Group (Karoo Supergroup)*, by Rubidge BS, eds Pretoria: Council
3904 for Geosciences 1.
- 3905 Hancox P. 2000. The continental Triassic of South Africa. *Zentralblatt für Geologie und Paläontologie Teil*
3906 *I* 1998:1285-1324.
- 3907 Haubold HA, and Schaumberg G. 1985. Die Fossilien des Kupferschiefers: Pflanzen-und Tierwelt zu Beginn
3908 des Zechsteins; eine Erzlagerstätte und ihre Paläontologie. *Ziensen*.
- 3909 Haughton S. 1922. On the reptilian genera *Euparkeria* Broom, and *Mesosuchus* Watson. *Transactions of*
3910 *the Royal Society of South Africa* 10:81-88.
- 3911 Haughton S. 1924a. On a skull and partial skeleton of *Mesosuchus browni* Watson. *Transactions of the*
3912 *Royal Society of South Africa* 12:17-26.
- 3913 Heckert AB. 2004. *Late Triassic microvertebrates from the lower Chinle Group (Otischalkian-Adamanian:*
3914 *Carnian)*, southwestern USA: New Mexico Museum of Natural History and Science.
- 3915 Hone DW, and Benton MJ. 2007. An evaluation of the phylogenetic relationships of the pterosaurs among
3916 archosauromorph reptiles. *Journal of Systematic Palaeontology* 5:465-469.
- 3917 Hone DW, and Benton MJ. 2008. A new genus of rhynchosaur from the Middle Triassic of south-west
3918 England. *Palaeontology* 51:95-115.
- 3919 Hsiou AS, De França MAG, and Ferigolo J. 2015. New data on the *Clevosaurus* (Sphenodontia:
3920 Clevosauridae) from the Upper Triassic of southern Brazil. *PLoS ONE* 10:1-21.
3921 10.1371/journal.pone.0137523
- 3922 Hsiou AS, Nydam RL, Simões TR, Pretto FA, Onary S, Martinelli AG, Liparini A, de Vivar Martínez PRR, Soares
3923 MB, and Schultz CL. 2019. A New Clevosaurid from the Triassic (Carnian) of Brazil and the Rise of
3924 Sphenodontians in Gondwana. *Scientific Reports* 9:1-12. 10.1038/s41598-019-48297-9
- 3925 Huene FRv. 1902. Übersicht über die Reptilien der Trias. *Geologische und Paläontologische Abhandlungen*
3926 *(Neue Serie)* 6:1-84.
- 3927 Huene FRv. 1905. Über die Trias-Dinosaurier Europas. *Zeitschrift der Deutschen Geologischen Gesellschaft*
3928 57:345-349.
- 3929 Huene FRv. 1908. Die Dinosaurier der europäischen Triasformation mit Berücksichtigung der
3930 aussereuropäischen Vorkommnisse. *Geologische und Paläontologische Abhandlungen*
3931 *Supplement* 1:1-419.
- 3932 Huene FRv. 1911. Über *Erythrosuchus*, Vertreter der neuen Reptil-Ordnung Pelycosimia. *Geologische und*
3933 *Paläontologische Abhandlungen* 10:1-60.
- 3934 Huene FRv. 1931. Über *Tanystropheus* und verwandte Formen. *Neues Jahrbuch für Geologie und*
3935 *Paläontologie, BB* 67:65-86.
- 3936 Huene FRv. 1946. Die grossen Stämme der Tetrapoden in den geologischen Zeiten. *Biologisches*
3937 *Zentralblatt* 65:268-275.
- 3938 Huene FRv. 1954. Ein neuer Protorosauride. *NEues Jahrbuch für Geologie und Paläontologie, Monatshefte*
3939 5:228-230.

- 3940 Hutchinson M, Skinner A, and Lee M. 2012. *Tikiguania* and the antiquity of squamate reptiles (lizards and
3941 snakes). *Biology Letters* 8:665-669.
- 3942 Huxley TH. 1871. *A manual of the anatomy of vertebrated animals*. London: J. & A. Churchill.
- 3943 Irmis RB, Mundil R, Martz JW, and Parker WG. 2011. High-resolution U–Pb ages from the Upper Triassic
3944 Chinle Formation (New Mexico, USA) support a diachronous rise of dinosaurs. *Earth and Planetary
3945 Science Letters* 309:258-267.
- 3946 Ivakhnenko MF, and Kurochkin EN. 2008. *Fossil Reptiles and Birds Part 1*. Moscow: GEOS.
- 3947 Jalil N-E. 1990. Sur deux crânes de petits Sauria (Amniota, Diapsida) du Trias moyen d'Algérie. *Comptes
3948 rendus de l'Académie des sciences Série 2, Mécanique, Physique, Chimie, Sciences de l'univers,
3949 Sciences de la Terre* 311:731-736.
- 3950 Jalil N-E. 1997. A new prolacertiform diapsid from the Triassic of North Africa and the interrelationships
3951 of the Prolacertiformes. *Journal of Vertebrate Paleontology* 17:506-525.
3952 10.1080/02724634.1997.10010998
- 3953 Jalil N-E. 1999. Continental Permian and Triassic vertebrate localities from Algeria and Morocco and their
3954 stratigraphical correlations. *Journal of African Earth Sciences* 29:219-226.
- 3955 Jalil N, and Knoll F. 2002. Is *Azendohsaurus laaroussii* (Carnian, Morocco) a dinosaur? *Journal of Vertebrate
3956 Paleontology* 22:70A.
- 3957 Jaquier VP, Fraser NC, Furrer H, and Scheyer TM. 2017. Osteology of a New Specimen of *Macrocnemus*
3958 aff. *M. fuyuanensis* (Archosauromorpha, Protorosauria) from the Middle Triassic of Europe:
3959 Potential Implications for Species Recognition and Paleogeography of Tanystropheid
3960 Protorosaurs. *Frontiers in Earth Science* 5. 10.3389/feart.2017.00091
- 3961 Jaquier VP, and Scheyer TM. 2017. Bone Histology of the Middle Triassic Long-Necked Reptiles
3962 *Tanystropheus* and *Macrocnemus* (Archosauromorpha, Protorosauria). *Journal of Vertebrate
3963 Paleontology*. 10.1080/02724634.2017.1296456
- 3964 Jiang D-Y, Rieppel O, Fraser NC, Motani R, Hao W-C, Tintori A, Sun Y-L, and Sun Z-Y. 2011. New information
3965 on the protorosaurian reptile *Macrocnemus fuyuanensis* Li et al., 2007, from the Middle/Upper
3966 Triassic of Yunnan, China. *Journal of Vertebrate Paleontology* 31:1230-1237.
3967 10.1080/02724634.2011.610853
- 3968 Jiang D, Motani R, Hao W, Rieppel O, Sun Y, Tintori A, Sun Z, and Schmitz L. 2009. Biodiversity and
3969 sequence of the Middle Triassic Panxian marine reptile fauna, Guizhou Province, China. *Acta
3970 Geologica Sinica-English Edition* 83:451-459. 10.1111/j.1755-6724.2009.00047.x
- 3971 Kearney M, and Rieppel O. 2006. Rejecting “the given” in systematics. *Cladistics* 22:369-377.
- 3972 Kuhn-Schnyder E. 1947. Der Schädel von *Tanystropheus*. *Eclogae Geologicae Helvetiae* 40:390.
- 3973 Kuhn-Schnyder E. 1954. Über die Herkunft der Eidechsen. *Endeavour* 13:215-221.
- 3974 Kuhn-Schnyder E. 1959. Hand und Fuss von *Tanystropheus longobardicus* (Bassani). *Eclogae Geologicae
3975 Helvetiae* 52:921-941.
- 3976 Kuhn-Schnyder E. 1962. Ein weinterer Schädel von *Macrocnemus bassanii* Nopsca aus der anisichen Stufe
3977 der Trias des Monte San Giorgio (Kt. Tessin, Schweiz). *Paläontologische Zeitschrift* 36:110-133.
- 3978 Kuhn-Schnyder E. 1963. Wege der Reptiliensystematik. *Paläontologische Zeitschrift* 37:61-87.
- 3979 Kuhn-Schnyder E. 1967. Das Problem der Euryapsida. *Éditions du Centre national de la recherche
3980 scientifique* 163:335-348.
- 3981 Kuhn-Schnyder E. 1974. Die Triasfauna der Tessiner Kalkalpen. *Vierteljahresschrift der naturforschenden
3982 Gesellschaft in Zürich, Neujahrsblatt* 118:1-119.
- 3983 Kuhn O. 1971. *Die Saurier der Deutschen Trias*. Altötting: Geiselberger.
- 3984 LaBarbera MC, and Rieppel O. 2005. Suction feeding in a Triassic protorosaur? Response. *Science*
3985 308:1113.
- 3986 Lane H. 1945. New mid-Pennsylvanian reptiles from Kansas. *Transactions of the Kansas Academy of
3987 Science* 47:381-390.

- 3988 Langer MC, and Schultz CL. 2000. A new species of the Late Triassic rhynchosaur *Hyperodapedon* from the
3989 Santa Maria Formation of south Brazil. *Palaeontology* 43:633-652.
- 3990 Legler B, and Schneider JW. 2008. Marine ingressions into the Middle/Late Permian saline lake of the
3991 Southern Permian Basin (Rotliegend, Northern Germany) possibly linked to sea-level highstands
3992 in the Arctic rift system. *Palaeogeography, Palaeoclimatology, Palaeoecology* 267:102-114.
- 3993 Lehman J-P. 1971. Nouveaux vertébrés fossiles du Trias de la Série de Zarzaitine. *Annales de Paléontologie*
3994 (*Vertébrés*) 57:71-93.
- 3995 Lessner EJ, Parker WG, Marsh AD, Nesbitt SJ, Irmis RB, and Mueller BD. 2018. New insights into Late
3996 Triassic dinosauromorph-bearing assemblages from Texas using apomorphy-based
3997 identifications. *PaleoBios* 35.
- 3998 Li C. 2003. First Record of Protorosaurid Reptile (Order Protorosauria) from the Middle Triassic of China.
3999 *Acta Geologica Sinica* 77:419-423. 10.1111/j.1755-6724.2003.tb00122.x
- 4000 Li C. 2007. A juvenile *Tanystropheus* sp. (Protorosauria, Tanystropheidae) from the Middle Triassic of
4001 Guizhou, China. *Vertebrata Palasiatica* 45:41.
- 4002 Li C, Fraser NC, Rieppel O, and Wu X-C. 2018. A Triassic stem turtle with an edentulous beak. *Nature*
4003 560:476-479. 10.1038/s41586-018-0419-1
- 4004 Li C, Fraser NC, Rieppel O, Zhao L-J, and Wang L-T. 2017a. A new diapsid from the Middle Triassic of
4005 southern China. *Journal of Paleontology*:1-7. 10.1017/jpa.2017.12
- 4006 Li C, Rieppel O, and Fraser NC. 2017b. Viviparity in a Triassic marine archosauromorph reptile. *Vertebrata*
4007 *Palasiatica* 55:210-217.
- 4008 Li C, Rieppel O, and LaBarbera MC. 2004. A Triassic aquatic protorosaur with an extremely long neck.
4009 *Science* 305:1931.
- 4010 Li C, Zhao L-J, and Wang L-T. 2007. A new species of *Macrocnemus* (Reptilia: Protorosauria) from the
4011 Middle Triassic of southwestern China and its palaeogeographical implication. *Science in China*
4012 *Series D: Earth Sciences* 50:1601-1605. 10.1007/s11430-007-0118-5
- 4013 Liu J, Organ CL, Benton MJ, Brandley MC, and Aitchison JC. 2017. Live birth in an archosauromorph reptile.
4014 *Nature communications* 8:14445. 10.1038/ncomms14445
- 4015 Liutkus-Pierce CM, Fraser NC, and Heckert AB. 2014. Stratigraphy, sedimentology, and paleontology of
4016 the Upper Triassic Solite Quarry, North Carolina and Virginia. Elevating Geoscience in the
4017 Southeastern United States: New Ideas about Old Terranes—Field Guides for the 2014 GSA
4018 Southeastern Section Meeting, Blacksburg, Virginia: Boulder, CO, Geological Society of America.
4019 p 255-269.
- 4020 Lucas SG. 2010. The Triassic timescale based on nonmarine tetrapod biostratigraphy and biochronology.
4021 *Geological Society, London, Special Publications* 334:447-500. 10.1144/SP334.15
- 4022 MacDougall MJ, Tabor NJ, Woodhead J, Daoust AR, and Reisz RR. 2017. The unique preservational
4023 environment of the Early Permian (Cisuralian) fossiliferous cave deposits of the Richards Spur
4024 locality, Oklahoma. *Palaeogeography, Palaeoclimatology, Palaeoecology* 475:1-11.
- 4025 Menning M, and Hendrich A. 2016. Deutsche Stratigraphische Kommission: Stratigraphische Tabelle von
4026 Deutschland 2016.
- 4027 Merck J. 1997. A phylogenetic analysis of the euryapsid reptiles. *PhD dissertation, University of Texas at*
4028 *Austin, Austin, Texas*:785 p.
- 4029 Meyer Hv. 1830. *Protorosaurus*. *Isis von Oken*:517-519.
- 4030 Meyer Hv. 1832. Palaeologica zur Geschichte der Erde und ihrer Geschöpfe. *S Schmerber*.
- 4031 Meyer Hv. 1855. Die Saurier des Muschelkalkes mit Rücksicht auf die Saurier aus buntem Sandstein und
4032 Keuper. In: Keller H, ed. *Zur Fauna der Vorwelt, zweite Abtheilung*. Frankfurt a.m.: Heinrich Keller.
- 4033 Meyer Hv. 1856. Zur Fauna der Vorwelt—Saurier aus dem Kupferschiefer der Zechstein-Formation.
4034 *Keller*:24 p.

- Miedema F, Spiekman SNF, Fernandez V, Reumer JWF, and Scheyer TM. 2020. Cranial morphology of the tanystropheid *Macrocnemus bassanii* unveiled using synchrotron microtomography. *Scientific reports* 10:12412. 10.1038/s41598-020-68912-4
- Modesto SP, and Sues H-D. 2004. The skull of the Early Triassic archosauromorph reptile *Prolacerta broomi* and its phylogenetic significance. *Zoological Journal of the Linnean Society* 140:335-351.
- Montefeltro FC, Langer MC, and Schultz CL. 2010. Cranial anatomy of a new genus of hyperodapedontine rhynchosaur (Diapsida, Archosauromorpha) from the Upper Triassic of southern Brazil. *Earth and Environmental Science Transactions of the Royal Society of Edinburgh* 101:27-52.
- Müller J. 2004. The relationships among diapsid reptiles and the influence of taxon selection. In *Recent advances in the origin and early radiation of vertebrates*, by Arratia G, Wilson MVH, and Cloutier R, eds Verlag Dr Friedrich Pfeil, München:379-408.
- Muscio G. 1996. Preliminary note on a specimen of Prolacertiformes (Reptilia) from the Norian (Late Triassic) of Preone (Udine, North-Eastern Italy). *Gortania - Atti del Museo Friulano di Storia Naturale* 18:33-40.
- Nesbitt SJ. 2011. The early evolution of archosaurs: relationships and the origin of major clades. *Bulletin of the American Museum of Natural History* 352:292 p. 10.1206/352.1
- Nesbitt SJ, Butler RJ, Ezcurra MD, Barrett PM, Stocker MR, Angielczyk KD, Smith RM, Sidor CA, Niedźwiedzki G, and Sennikov AG. 2017a. The earliest bird-line archosaurs and the assembly of the dinosaur body plan. *Nature* 544:484. 10.1038/nature22037
- Nesbitt SJ, Flynn JJ, Pritchard AC, Parrish JM, Ranivoharimanana L, and Wyss AR. 2015. Postcranial anatomy and relationships of *Azendohsaurus madagaskarensis*. *Bulletin of the American Museum of Natural History* 398:1-126. 10.1206/amnb-899-00-1-126.1
- Nesbitt SJ, Stocker MR, Ezcurra MD, Fraser NC, Heckert AB, Marsh A, Parker W, Mueller B, and Pritchard AC. 2017b. The 'strange reptiles' of the Triassic: the morphology, ecology, and taxonomic diversity of the clade Allokotosauria illuminated by the discovery of an early diverging member. *SVP Program and Abstracts* 2017:168.
- Nopsca FB. 1923. Neubeschreibung des Trias-Pterosauriers *Tribelesodon*. *Paläontologische Zeitschrift* 5:161-181.
- Nopsca FB. 1930. Notizen über *Macrocnemus Bassanii* nov. gen. et spec. *Centralblatt für Mineralogie, Geologie und Paläontologie B* 7:252-255.
- Nosotti S. 2007. *Tanystropheus longobardicus* (Reptilia, Protorosauria): Re-interpretations of the anatomy based on new specimens from the Middle Triassic of Besano (Lombardy, northern Italy). *Memorie della Società Italiana di Scienze Naturali e del Museo Civico di Storia Naturale di Milano* 35:1-88.
- Ochev VG. 1979. New Lower Triassic archosaurs from the eastern part of the European USSR. *Palaeontological Journal* 1:104-109.
- Olsen PE. 1979. A new aquatic eosuchian from the Newark Supergroup (Late Triassic-Early Jurassic) of North Carolina and Virginia. *Postilla* 176:1-14.
- Olson EC, and Broom R. 1937. New genera and species of tetrapods from the Karroo beds of South Africa. *Journal of Paleontology*:613-619.
- Ortlam D. 1966. Fossile Böden als Leithorizonte für die Gliederung des Höheren Buntsandsteins im nördlichen Schwarzwald und südlichen Odenwald. *Geologisches Jahrbuch* 84:485-590.
- Osborn HF. 1903. The reptilian subclasses Diapsida and Synapsida and the early history of the Diaptosauria. *Memoirs of the American Museum of Natural History* 1:449-519.
- Otschev VG. 1986. Concerning the Middle Triassic reptiles from the southern Cis-Ural region. *Ezhegodnik Vsesoyuznogo Paleontologicheskogo Obshchestva* 29:171-179.
- Owen R. 1842. Description of parts of the skeleton and teeth of five species of the genus *Labyrinthodon* (*Lab. leptognathus*, *Lab. pachygnathus*, and *Lab. ventricosus*, from the Coton-end and Cubbington Quarries of the Lower Warwick Sandstone; *Lab. Jaegeri*, from Guy's Cliff, Warwick; and *Lab.*

- 4083 *scutulatus*, from Leamington); with remarks on the probable identity of the *Cheirotherium* with
- 4084 this genus of extinct batrachians. *Transactions of the Geological Society, London* 2:515-543.
- 4085 Padian K. 1997. Pterosauiromorpha. In *Encyclopedia of dinosaurs*, by Currie, PJ, and Padian, K, eds San
- 4086 Diego, Academic Press:617-618.
- 4087 Padian K, and Chiappe LM. 1998. The origin and early evolution of birds. *Biological Reviews* 73:1-42.
- 4088 Parker WG, and Martz JW. 2010. The Late Triassic (Norian) Adamanian–Revueltian tetrapod faunal
- 4089 transition in the Chinle Formation of Petrified Forest National Park, Arizona. *Earth and*
- 4090 *Environmental Science Transactions of the Royal Society of Edinburgh* 101:231-260.
- 4091 10.1017/S1755691011020020
- 4092 Parks P. 1969. Cranial anatomy and mastication of the Triassic reptile *Trilophosaurus* MSc. University of
- 4093 Texas at Austin.
- 4094 Parrington FR. 1935. On *Prolacerta broomi*, gen. et sp. n. and the origin of lizards. *Annals and Magazine*
- 4095 *of Natural History Series* 10 16:197-205.
- 4096 Parrington FR. 1956. A Problematic Reptile from the Upper Permian. *The Annals and magazine of natural*
- 4097 *history; zoology, botany, and geology* 12:333-336.
- 4098 Parrish JM. 1992. Phylogeny of the Erythrosuchidae (Reptilia: Archosauriformes). *Journal of Vertebrate*
- 4099 *Paleontology* 12:93-110.
- 4100 Peabody FE. 1952. *Petrolacosaurus kansensis* Lane, a Pennsylvanian reptile from Kansas. *University of*
- 4101 *Kansas Paleontological Contributions - Vertebrata*:1-41.
- 4102 Peacock BR, Smith RM, and Sidor CA. 2019. A novel archosauromorph from Antarctica and an updated
- 4103 review of a high-latitude vertebrate assemblage in the wake of the end-Permian mass extinction.
- 4104 *Journal of Vertebrate Paleontology* 38. 10.1080/02724634.2018.1536664
- 4105 Peters D. 2000. A reexamination of four Prolacertiformes with implications for pterosaur phylogenesis.
- 4106 *Rivista Italiana di Paleontologia e Stratigrafia* 106:293-336.
- 4107 Peters D. 2005. Suction feeding in a Triassic protosauromorph? *Science* 308:1112.
- 4108 Peyer B. 1930. *Tanystropheus longobardicus* Bass. sp. (Vorläufige Mitteilung). *Cbl Miner usw*:336-337.
- 4109 Peyer B. 1931. Die Triasfauna der Tessiner Kalkalpen II. *Tanystropheus longobardicus* Bass. sp.
- 4110 *Abhandlungen der Schweizerischen Paläontologischen Gesellschaft* 50:9-110.
- 4111 Peyer B. 1937. Die Triasfauna der Tessiner Kalkalpen XII. *Macrocnemus bassanii* Nopsca. *Abhandlungen*
- 4112 *der Schweizerischen Paläontologischen Gesellschaft* 54:1-87.
- 4113 Pinheiro FL, França MA, Lacerda MB, Butler RJ, and Schultz CL. 2016. An exceptional fossil skull from South
- 4114 America and the origins of the archosauriform radiation. *Scientific Reports* 6:22817.
- 4115 Pinheiro FL, Simão-Oliveira DD, and Butler RJ. 2019. Osteology of the archosauromorph *Teyujagua*
- 4116 *paradoxa* and the early evolution of the archosauriform skull. *Zoological Journal of the Linnean*
- 4117 *Society* XX:1-40. 10.1093/zoolinnean/zlz093
- 4118 Pinna G. 1980. *Drepanosaurus unguicaudatus*, nuovo genere e nuova specie di Lepidosauo del trias alpino
- 4119 (Reptilia). *Atti della Società italiana di scienze naturali e del Museo civico di storia naturale di*
- 4120 *Milano* 121:181-192.
- 4121 Pinna G. 1984. Osteologia di *Drepanosaurus unguicaudatus*, Lepidosauo triassico del Sottordine
- 4122 *Lacertilia*. *Atti della Società Italiana Scienze Naturali* 124:7-28.
- 4123 Pinna G. 1986. On *Drepanosaurus unguicaudatus*, an Upper Triassic Lepidosaurian from the Italian Alps.
- 4124 *Journal of Paleontology* 60:1127-1132.
- 4125 Pinna G. 1993. The Norian Reptiles from Northern Italy. *Paleontologia Lombarda Nuova Serie* 2:115-124.
- 4126 Premru E. 1991. Beschreibung eines neuen Fundes von *Macrocnemus bassanii* Nopsca (Reptilia,
- 4127 Squamata, Prolacertiformes) aus der Grenzbitumenzone (Anis/Ladin) des Monte San Giorgio
- 4128 (Besano, I). *Diplomarbeit an der Philosophischen Fakultät II der Universität Zürich*.

- 4129 Pritchard AC, Gauthier JA, Hanson M, Bever GS, and Bhullar B-AS. 2018. A tiny Triassic saurian from
4130 Connecticut and the early evolution of the diapsid feeding apparatus. *Nature communications*
4131 9:1213.
- 4132 Pritchard AC, and Nesbitt SJ. 2017. A bird-like skull in a Triassic diapsid reptile increases heterogeneity of
4133 the morphological and phylogenetic radiation of Diapsida. *Royal Society Open Science* 4.
- 4134 Pritchard AC, and Sues H-D. 2019. Postcranial remains of *Teraterpeton hrynewichorum* (Reptilia:
4135 Archosauromorpha) and the mosaic evolution of the saurian postcranial skeleton. *Journal of*
4136 *Systematic Palaeontology* 17:1745-1765. 10.1080/14772019.2018.1551249
- 4137 Pritchard AC, Turner AH, Irmis RB, Nesbitt SJ, and Smith ND. 2016. Extreme Modification of the Tetrapod
4138 Forelimb in a Triassic Diapsid Reptile. *Current Biology* 26:1-8.
- 4139 Pritchard AC, Turner AH, Nesbitt SJ, Irmis RB, and Smith ND. 2015. Late Triassic tanystropheids (Reptilia,
4140 Archosauromorpha) from Northern New Mexico (Petrified Forest Member, Chinle Formation) and
4141 the biogeography, functional morphology, and evolution of Tanystropheidae. *Journal of*
4142 *Vertebrate Paleontology*:e911186. 10.1080/02724634.2014.911186
- 4143 Rauhut OWM, Heyng AM, López-Arbarello A, and Hecker A. 2012. A New Rhynchocephalian from the Late
4144 Jurassic of Germany with a Dentition That Is Unique amongst Tetrapods. *PLoS ONE* 7.
- 4145 Reisz R, Modesto S, and Scott D. 2000. *Acanthotoposaurus bremneri* and the origin of the Triassic
4146 archosauromorph reptile fauna of South Africa. *South African Journal of Science* 96:443-445.
- 4147 Reisz RR. 1977. *Petrolacosaurus*, the Oldest Known Diapsid Reptile. *Science* 196:1091-1093.
- 4148 Reisz RR. 1981. A diapsid reptile from the Pennsylvanian of Kansas. *Special Publication of the Natural*
4149 *History Museum, University of Kansas* 7.
- 4150 Reisz RR, Berman DS, and Scott DM. 1984. The Anatomy and Relationships of the Lower Permian Reptile
4151 *Araucoscelis*. *Journal of Vertebrate Paleontology* 4:57-67.
- 4152 Reisz RR, Heaton MJ, and Pynn BR. 1982. Vertebrate fauna of late Pennsylvanian rock lake shale near
4153 Garnett, Kansas: Pelycosauria. *Journal of Paleontology*:741-750.
- 4154 Reisz RR, Laurin M, and Marjanović D. 2010. *Apsisaurus witteri* from the Lower Permian of Texas: yet
4155 another small Varanopsid Synapsid, not a Diapsid. *Journal of Vertebrate Paleontology* 30:1628-
4156 1631.
- 4157 Reisz RR, Modesto SP, and Scott DM. 2011a. A new Early Permian reptile and its significance in early
4158 diapsid evolution. *Proc R Soc B* 278:3731-3737.
- 4159 Reisz RR, Modesto SP, and Scott DM. 2011b. A new Early Permian reptile and its significance in early
4160 diapsid evolution. *Proceedings of the Royal Society B* 278:3731-3737.
- 4161 Renesto S. 1994a. *Megalanosaurus*, a possibly arboreal archosauromorph (Reptilia) from the Upper
4162 Triassic of northern Italy. *Journal of Vertebrate Paleontology* 14:38-52.
- 4163 Renesto S. 1994b. A new prolacertiform reptile from the Late Triassic of Northern Italy. *Rivista Italiana di*
4164 *Paleontologia e Stratigrafia* 100:285-306.
- 4165 Renesto S. 1994c. A reinterpretation of the pectoral girdle and anterior limb of *Drepanosaurus*
4166 *unguicaudatus* (Reptilia, Diapsida). *Zoological Journal of the Linnean Society* 111:247-264.
- 4167 Renesto S. 2000. Bird-Like Head on a Chameleon Body: New Specimens of the Enigmatic Diapsid Reptile
4168 *Megalanosaurus* from the Late Triassic of Northern Italy. *Rivista Italiana di Paleontologia e*
4169 *Stratigrafia* 106:157-180.
- 4170 Renesto S. 2005. A new specimen of *Tanystropheus* (Reptilia Protorosauria) from the Middle Triassic of
4171 Switzerland and the ecology of the genus. *Rivista Italiana di Paleontologia e Stratigrafia* 111:377-
4172 394.
- 4173 Renesto S, and Avanzini M. 2002. Skin remains in a juvenile *Macrocnemus bassanii* NOPCSA (Reptilia,
4174 Prolacertiformes) from the Middle Triassic of northern Italy. *Neues Jahrbuch für Geologie und*
4175 *Paläontologie Abhandlungen*:31-48.

- 4176 Renesto S, and Binelli G. 2006. *Vallesaurus cenensis* Wild, 1991, a Drepanosaurid (Reptilia, Diapsida) from
4177 the Late Triassic of Northern Italy. *Rivista Italiana di Paleontologia e Stratigrafia* 112:77-94.
- 4178 Renesto S, and Dalla Vecchia FM. 2000. The unusual dentition and feeding habits of the prolacertiform
4179 reptile *Langobardisaurus* (Late Triassic, Northern Italy). *Journal of Vertebrate Paleontology*
4180 20:622-627. 10.1671/0272-4634(2000)020[0622:tudafh]2.0.co;2
- 4181 Renesto S, and Dalla Vecchia FM. 2005. The skull of the holotype of *Megalanosaurus preonensis*
4182 (Diapsida, Drepanosauridae) from the Upper Triassic of Northern Italy. *Rivista Italiana di*
4183 *Paleontologia e Stratigrafia* 111:247-257.
- 4184 Renesto S, and Dalla Vecchia FM. 2007. A revision of *Langobardisaurus rossii* Bizzarini and Muscio, 1995
4185 from the Late Triassic of Friuli (Italy). *Rivista Italiana di Paleontologia e Stratigrafia* 113:191-201.
- 4186 Renesto S, Dalla Vecchia FM, and Peters D. 2002. Morphological evidence for bipedalism in the Late
4187 Triassic prolacertiform reptile *Langobardisaurus*. *Palaeobiodiversity and Palaeoenvironments*
4188 82:94-106.
- 4189 Renesto S, and Paganoni A. 1995. A new *Drepanosaurus* (Reptilia, Neodiapsida) from the Upper Triassic
4190 of Northern Italy. *Neues Jahrbuch für Geologie und Paläontologie Abhandlungen* 197:87-99.
- 4191 Renesto S, Spielmann JA, Lucas SG, and Spagnoli GT. 2010. The taxonomy and paleobiology of the Late
4192 Triassic (Carnian-Norian: Adamanian-Apachean) drepanosaurs (Diapsida: Archosauromorpha:
4193 Drepanosauromorpha): Bulletin 46. *New Mexico Museum of Natural History and Science* 46.
- 4194 Rieppel O. 1989. The hind limb of *Macrocnemus bassani* (Nopsca) (Reptilia, Diapsida): Development and
4195 functional anatomy. *Journal of Vertebrate Paleontology* 9:373-387.
- 4196 Rieppel O. 1994. Osteology of *Simosaurus* and the interrelationships of stem-group Sauropterygia
4197 (Reptilia, Diapsida). *Fieldiana, Geology, New Series* 28:1-28.
- 4198 Rieppel O. 2001. A new species of *Tanystropheus* (Reptilia: Protorosauria) from the Middle Triassic of
4199 Makhtesh Ramon, Israel. *Neues Jahrbuch für Geologie und Paläontologie Abhandlungen* 221:271-
4200 287.
- 4201 Rieppel O. 2002. Feeding mechanics in Triassic stem-group sauropterygians: the anatomy of a successful
4202 invasion of Mesozoic seas. *Zoological Journal of the Linnean Society* 135:33-63.
- 4203 Rieppel O, Fraser NC, and Nosotti S. 2003. The monophyly of Protorosauria (Reptilia, Archosauromorpha):
4204 a preliminary analysis. *Atti della Società italiana di scienze naturali e del Museo civico di storia*
4205 *naturale di Milano* 144:359-382.
- 4206 Rieppel O, and Gronowski RW. 1981. The loss of the lower temporal arcade in diapsid reptiles. *Zoological*
4207 *Journal of the Linnean Society* 72:203-217.
- 4208 Rieppel O, Jiang D-Y, Fraser NC, Hao W-C, Motani R, Sun Y-L, and Sun Z-Y. 2010. *Tanystropheus* cf. *T.*
4209 *longobardicus* from the early Late Triassic of Guizhou Province, southwestern China. *Journal of*
4210 *Vertebrate Paleontology* 30:1082-1089. 10.1080/02724634.2010.483548
- 4211 Rieppel O, and Kearney M. 2007. The poverty of taxonomic characters. *Biology & Philosophy* 22:95-113.
- 4212 Rieppel O, Li C, and Fraser NC. 2008. The skeletal anatomy of the Triassic protosaur *Dinocephalosaurus*
4213 *orientalis*, from the Middle Triassic of Guizhou Province, southern China. *Journal of Vertebrate*
4214 *Paleontology* 28:95-110. 10.1671/0272-4634(2008)28[95:tsaott]2.0.co;2
- 4215 Rieppel O, Mazin J-M, and Tchernov E. 1999. Sauropterygia from the Middle Triassic of Makhtesh Ramon,
4216 Negev, Israel. *Fieldiana, Geology, New Series* 40:1-85.
- 4217 Rigo M, Galli M, and Jadoul F. 2009. Late Triassic biostratigraphic constraints in the Imagna Valley (western
4218 Bergamasc Alps, Italy). *Albertiana* 37:39-42.
- 4219 Romer AS. 1956. Osteology of the Reptiles. *Chicago: University of Chicago Press*:772 p.
- 4220 Romer AS. 1966. Vertebrate paleontology. *Chicago: University of Chicago Press* 3rd edition:468 p.
- 4221 Romer AS. 1968. Notes and Comments on Vertebrate Paleontology. *The University of Chicago Press*.
- 4222 Rubidge BS. 2005. Re-uniting lost continents—fossil reptiles from the ancient Karoo and their wanderlust.
4223 *South African Journal of Geology* 108:135-172.

- 4224 Rubidge BS, Erwin DH, Ramezani J, Bowring SA, and de Klerk WJ. 2013. High-precision temporal calibration
4225 of Late Permian vertebrate biostratigraphy: U-Pb zircon constraints from the Karoo Supergroup,
4226 South Africa. *Geology* 41:363-366.
- 4227 Saller F, Renesto S, and Dalla Vecchia FM. 2013. First record of *Langobardisaurus* (Diapsida, Protorosauria)
4228 from the Norian (Late Triassic) of Austria, and a revision of the genus. *Neues Jahrbuch für Geologie
4229 und Paläontologie Abhandlungen* 268:83-95.
- 4230 Sanz JL, and López-Martínez N. 1984. The prolacertid lepidosaurian *Cosesaurus aviceps* Ellenberger &
4231 Villalta, a claimed «protoavian» from the Middle Triassic of Spain. *Geobios* 17:747-755.
- 4232 Scheyer TM, Spiekman SNF, Butler RJ, Ezcurra MD, Sues H-D, and Jones MEH. 2020a. *Colobops*, a juvenile
4233 rhynchocephalian reptile (Lepidosauromorpha), not a diminutive archosauromorph with an
4234 unusually strong bite. *Royal Society Open Science* 7:1-14. 10.1098/rsos.192179
- 4235 Scheyer TM, Wang W, Li C, Miedema F, and Spiekman SNF. 2020b. Osteological re-description of
4236 *Macrocnemus fuyuanensis* (Archosauromorpha, Tanystropheidea) from the Middle Triassic of
4237 China. *Vertebrata Palasiatica* 58:169-187. 10.19615/j.cnki.1000-3118.200525
- 4238 Schmidt M. 1928. *Die Lebewelt unserer Trias*. Öhringen: Hohenlohe'sche Buchhandlung.
- 4239 Schmidt M. 1938. *Die Lebewelt unserer Trias (Nachtrag)*. Öhringen: Hohenlohe'sche Buchhandlung.
- 4240 Sen K. 2003. *Pamelaria dolichotrachela*, a new prolacertid reptile from the Middle Triassic of India. *Journal
4241 of Asian Earth Sciences* 21:663-681.
- 4242 Sengupta S, Ezcurra MD, and Bandyopadhyay S. 2017. A new horned and long-necked herbivorous stem-
4243 archosaur from the Middle Triassic of India. *Scientific Reports* 7:8366.
- 4244 Sennikov AG. 1997. An enigmatic reptile from the Upper Permian of the Volga River Basin. *Paleontological
4245 Journal* 31:94-101.
- 4246 Sennikov AG. 2005. A new specialized prolacertilian (Reptilia: Archosauromorpha) from the Lower Triassic
4247 of the Orenburg Region. *Paleontological Journal* 39:199-209.
- 4248 Sennikov AG. 2011. New tanystropheids (Reptilia: Archosauromorpha) from the Triassic of Europe.
4249 *Paleontological Journal* 45:90-104. 10.1134/s0031030111010151
- 4250 Senter P. 2004. Phylogeny of Drepanosauridae (Reptilia: Diapsida). *Journal of Systematic Palaeontology*
4251 2:257-268.
- 4252 Sharov AG. 1970. [Unusual reptile from the Lower Triassic of Fergana]. *Paleontologicheskii Zhurnal* 1:127-
4253 131.
- 4254 Sharov AG. 1971. [New flying reptiles from the Mesozoic of Kazakhstan and Kirgizstan.]. *Trudy
4255 Paleontologicheskogo Instituta AN SSSR* 130:104-113.
- 4256 Shishkin MA, and Sulej T. 2009. The Early Triassic temnospondyls of the Czatkowice 1 tetrapod
4257 assemblage. *Palaeontologia Polonica* 65:77.
- 4258 Simões TR, Caldwell MW, Palci A, and Nydam RL. 2016. Giant taxon-character matrices: quality of
4259 character constructions remains critical regardless of size. *Cladistics* 33:198-219.
- 4260 Simões TR, Caldwell MW, Tałanda M, Bernardi M, Palci A, Vernygora O, Bernardini F, Mancini L, and
4261 Nydam RL. 2018. The origin of squamates revealed by a Middle Triassic lizard from the Italian Alps.
4262 *Nature* 557:706.
- 4263 Skawiński T, Tałanda M, and Sachs S. 2015. *Megacnemus* – a forgotten reptile, presumably from the
4264 Triassic of Poland. *EAVP Poster*.
- 4265 Skawiński T, Ziegler M, Czepiński Ł, Szermański M, Tałanda M, Surmik D, and Niedźwiedzki G. 2017. A re-
4266 evaluation of the historical 'dinosaur' remains from the Middle-Upper Triassic of Poland. *Historical
4267 Biology* 29:442-472. 10.1080/08912963.2016.1188385
- 4268 Smith R, Rubidge B, and Van der Walt M. 2012. Therapsid biodiversity patterns and paleoenvironments of
4269 the Karoo Basin, South Africa. In: Chinsamy-Turan A, ed. *Forerunners of Mammals: Radiation,
4270 Histology, Biology Indiana University Press, Bloomington, Indiana*. Bloomington, Indiana: Indiana
4271 University Press, 30-62.

- 4272 Smith RMH, and Evans SE. 1996. New material of *Youngina*: evidence of juvenile aggregation in Permian
4273 diapsid reptiles. *Palaeontology* 39:289-303.
- 4274 Sobral G, and Müller J. 2019. The braincase of *Mesosuchus browni* (Reptilia, Archosauromorpha) with
4275 information on the inner ear and description of a pneumatic sinus. *PeerJ* 7:e6798.
- 4276 Sobral G, Sookias RB, Bhullar B-AS, Smith RMH, Butler RJ, and Müller J. 2016. New information on the
4277 braincase and inner ear of *Euparkeria capensis* Broom: implications for diapsid and archosaur
4278 evolution. *Royal Society Open Science* 3.
- 4279 Sookias RB. 2016. The relationships of the Euparkeriidae and the rise of Archosauria. *Royal Society Open*
4280 *Science* 3.
- 4281 Sookias RB, and Butler RJ. 2013. Euparkeriidae. *Geological Society, London, Special Publications*
4282 379:SP379. 376.
- 4283 Sookias RB, Sennikov AG, Gower DJ, and Butler RJ. 2014. The monophyly of Euparkeriidae (Reptilia:
4284 Archosauriformes) and the origins of Archosauria: a revision of *Dorosuchus neoetus* from the
4285 Mid-Triassic of Russia. *Palaeontology* 57:1177-1202.
- 4286 Spener CM. 1710. Disquisitio de crocodilo in lapide scissili expresso, aliisque Lithozois. *Misc Berol ad*
4287 *increment sci, ex scr Soc Regiae Sci exhibits* 1:92-110.
- 4288 Spiekman SNF. 2018. A new specimen of *Prolacerta broomi* from the lower Fremouw Formation (Early
4289 Triassic) of Antarctica, its biogeographical implications and a taxonomic revision. *Scientific Reports*
4290 8:17996. 10.1038/s41598-018-36499-6
- 4291 Spiekman SNF, Bleeker R, Dorst M, de Haan R, Winkelhorst H, and Voeten DFAE. 2019. Tanystropheids
4292 from the Winterswijkse Steengroeve – rare but recurring elements in the Vossenveld
4293 paleoassemblage. *Grondboor & Hamer (Staringia 16)* 73:208-215. 10.5167/uzh-182944
- 4294 Spiekman SNF, Neenan JM, Fraser NC, Fernandez V, Rieppel O, Nosotti S, and Scheyer TM. 2020. Aquatic
4295 habits and niche partitioning in the extraordinarily long-necked Triassic reptile *Tanystropheus*.
4296 *Current Biology* 30:1-7. 10.1016/j.cub.2020.07.025
- 4297 Spiekman SNF, Neenan JM, Fraser NC, Fernandez V, Rieppel O, Nosotti S, and Scheyer TM. submitted. The
4298 cranial morphology of *Tanystropheus hydroides* (Tanystropheidae, Archosauromorpha) as
4299 revealed by synchrotron microtomography. *PeerJ*
- 4300 Spiekman SNF, and Scheyer TM. 2019. A taxonomic revision of the genus *Tanystropheus*
4301 (Archosauromorpha, Tanystropheidae). *Palaeontologia Electronica* 22:1-46. 10.26879/1038
- 4302 Spielmann JA, Heckert AB, and Lucas SG. 2005. The Late Triassic archosauromorph *Trilophosaurus* as an
4303 arboreal climber. *Rivista Italiana di Paleontologia e Stratigrafia* 111:395-312.
- 4304 Spielmann JA, Lucas SG, Hunt AP, and Heckert AB. 2006. Reinterpretation of the holotype of *Malerisaurus*
4305 *langstoni*, a diapsid reptile from the Upper Triassic Chinle Group of West Texas. *New Mexico*
4306 *Museum Natl Hist Sci Bull* 37:543-547.
- 4307 Spielmann JA, Lucas SG, Rinehart LF, and Heckert AB. 2008. The Late Triassic archosauromorph
4308 *Trilophosaurus*. *New Mexico Museum Naturall History and Science Bulletin* 43:1-177.
- 4309 Stockar R. 2010. Facies, depositional environment, and palaeoecology of the Middle Triassic Cassina beds
4310 (Meride Limestone, Monte San Giorgio, Switzerland). *Swiss Journal of Geosciences* 103:101-119.
4311 10.1007/s00015-010-0008-2
- 4312 Stocker MR, Zhao L-J, Nesbitt SJ, Wu X-C, and Li C. 2017. A short-snouted, Middle Triassic phytosaur and
4313 its implications for the morphological evolution and biogeography of Phytosauria. *Scientific*
4314 *Reports* 7:46028.
- 4315 Sues H-D, and Olsen PE. 2015. Stratigraphic and temporal context and faunal diversity of Permian-Jurassic
4316 continental tetrapod assemblages from the Fundy rift basin, eastern Canada. *Atlantic Geology*
4317 51:139-205. 10.4138/atlgol.2015.006

- 4318 Sullivan C, Reisz RR, and May WJ. 2000. Large dissorophoid skeletal elements from the Lower Permian
4319 Richards Spur fissures, Oklahoma, and their paleoecological implications. *Journal of Vertebrate*
4320 *Paleontology* 20:456-461.
- 4321 Szulc J, Racki G, and Bodzioch A. 2017. Comment on "An early Late Triassic long-necked reptile with a bony
4322 pectoral shield and gracile appendages" by Jerzy Dzik and Tomasz Sulej. *Acta Palaeontologica*
4323 *Polonica* 62:287-288. 10.4202/app.00352.2017
- 4324 Tackett LS, and Tintori A. 2019. Low drilling frequency in Norian benthic assemblages from the southern
4325 Italian Alps and the role of specialized durophages during the Late Triassic. *Palaeogeography,*
4326 *Palaeoclimatology, Palaeoecology* 513:25-34. 10.1016/j.palaeo.2018.06.034
- 4327 Tatarinov LP. 1978. Triassic Prolacertilians of the USSR. *Paleontological Journal* 12:88-100.
- 4328 Tatarinov LP. 1989. [The systematic position and way of life of the problematic Upper Triassic reptile
4329 *Sharovipteryx mirabilis*]. *Paleontologicheskii Zhurnal* 2:110-112.
- 4330 Tatarinov LP. 1994. Terrestrial vertebrates from the Triassic of the USSR with comments on the
4331 morphology of some reptiles. In *Evolution, Ecology and Biogeography of the Triassic Reptiles, by*
4332 *Mazin, J-M and Pinna, G, eds Paleontologia Lombarda, New Series, 2:165-170.*
- 4333 Trotteyn MJ, and Ezcurra MD. 2014. Osteology of *Pseudochampsia ischigualastensis* gen. et comb. nov.
4334 (Archosauriformes: Proterochampsidae) from the early Late Triassic Ischigualasto Formation of
4335 northwestern Argentina. *PLoS ONE* 9.
- 4336 Tschanz K. 1986. Funktionelle Anatomie der Halswirbelsäule von *Tanystropheus longobardicus* (Bassani)
4337 aus der Trias (Anis/Ladin) des Monte San Giorgio (Tessin) auf der Basis vergleichend
4338 morphologischer Untersuchungen an der Halsmuskulatur rezenter Echsen. *PhD thesis Universität*
4339 *Zürich.*
- 4340 Tverdokhlebov VP, Tverdokhlebova GI, Surkov MV, and Benton MJ. 2003. Tetrapod localities from the
4341 Triassic of the SE of European Russia. *Earth-Science Reviews* 60:1-66.
- 4342 Unwin DM, Alifanov VR, and Benton MJ. 2000. Enigmatic small reptiles from the Middle-Late Triassic of
4343 Kirgizstan. In *The age of dinosaurs in Russia and Mongolia, by Benton M J, Kurochkin E N, Shishkin*
4344 *M A, Unwin D M, eds Cambridge: Cambridge University Press:140-159.*
- 4345 Vaughn PP. 1955. The Permian reptile *Araeoscelis* restudied. *Bulletin of the Museum of Comparative*
4346 *Zoology at Harvard College* 113:303-469.
- 4347 Walker AD. 1969. The reptile fauna of the 'Lower Keuper' Sandstone. *Geological Magazine* 106:470-476.
- 4348 Watson DMS. 1912. *Mesosuchus browni*, gen. et spec. nov. *Records of the Albany Museum* 2:298-299.
- 4349 Watson DMS. 1917. A Sketch Classification of the Pre-Jurassic Tetrapod Vertebrates. *Journal of Zoology*
4350 87:167-186.
- 4351 Watson DMS. 1957. On *Millerisaurus* and the Early History of the Sauropsid Reptiles B. *Philosophical*
4352 *Transactions of the Royal Society of London B: Biological Sciences* 240:325-400.
- 4353 Welman J. 1998. The taxonomy of the South African proterosaurs (Reptilia, Archosauromorpha). *Journal*
4354 *of Vertebrate Paleontology* 18:340-347.
- 4355 Werning S, and Irmis R. 2010. Reconstructing the ontogeny of the Triassic basal archosauromorph
4356 *Trilophosaurus* using bone histology and limb bone morphometrics. *Journal of Vertebrate*
4357 *Paleontology* 30.
- 4358 Whiteside DI, and Duffin CJ. 2017. Late Triassic terrestrial microvertebrates from Charles Moore's
4359 'Microlestes' quarry, Holwell, Somerset, UK. *Zoological Journal of the Linnean Society* 179:677-
4360 705. 10.1111/zoj.12458
- 4361 Whiteside DI, Duffin CJ, Gill PG, Marshall JEA, and Benton MJ. 2016. The Late Triassic and Early Jurassic
4362 fissure faunas from Bristol and South Wales: stratigraphy and setting. *Palaeontologia Polonica*
4363 67:257-287. 10.4202/pp.2016.67_257

- 4364 Whiteside DI, and Marshall JE. 2008. The age, fauna and palaeoenvironment of the Late Triassic fissure
4365 deposits of Tytherington, South Gloucestershire, UK. *Geological Magazine* 145:105-147.
4366 10.1017/S0016756807003925
- 4367 Wild R. 1973. Die Triasfauna der Tessiner Kalkalpen XXII. *Tanystropheus longobardicus* (Bassani) (Neue
4368 Ergebnisse). *Schweizerische Paläontologische Abhandlungen* 95:1-182.
- 4369 Wild R. 1980a. Neue Funde von *Tanystropheus* (Reptilia, Squamata). *Schweizerische Paläontologische*
4370 *Abhandlungen* 102.
- 4371 Wild R. 1980b. *Tanystropheus* (Reptilia : Squamata) and its importance for stratigraphy. *Mémoires de la*
4372 *Société Géologique de France*, n s 139:201-206.
- 4373 Wild R. 1987. An example of biological reasons for extinction: *Tanystropheus* (Reptilia, Squamata).
4374 *Mémoires de la Société Géologique de France*, n s 150:37-44.
- 4375 Wild R. 1991. *Aetosaurus* (Reptilia, Thecodontia) from the Upper Triassic (Norian) of Cene near Bergamo,
4376 Italy, with a revision of the genus. *Rivista Italiana di Paleontologia e Stratigrafia Museo Civico di*
4377 *Scienze Naturali "E Caffi" Bergamo* 14:1-24.
- 4378 Wild R, and Oosterink H. 1984. *Tanystropheus* (Reptilia: Squamata) aus dem Unteren Muschelkalk von
4379 Winterswijk, Holland. *Grondboor en Hamer* 5:142-148.
- 4380 Williston SW. 1925. Osteology of the Reptiles. *Society for the Study of Amphibians and Reptiles*.
- 4381 Witmer LM. 1997. Craniofacial air sinus systems. In: Currie PJ, and Padian K, eds. *Encyclopedia of*
4382 *dinosaurs*. New York: Academic Press, 151-159.
- 4383 Woodhead J, Reisz R, Fox D, Drysdale R, Hellstrom J, Maas R, Cheng H, and Edwards RL. 2010. Speleothem
4384 climate records from deep time? Exploring the potential with an example from the Permian.
4385 *Geology* 38:455-458.
- 4386 Young C-C. 1973. The Discovery of Prolacertilia in Jimusar, Sinkiang. *Vertebrata PalAsiatica* 11:46-49.

4387

Table 1 (on next page)

Percentage of scored characters of each OTU for the character matrix used in this study.

1 Table 1. Percentage of scored characters of each OTU for the character matrix used in this study.

OTU	% of characters scored
<i>Petrolacosaurus kansensis</i>	87,3
<i>Orovenator mayorum</i>	47,6
<i>Youngina capensis</i>	90,6
<i>Acerosodontosaurus piveteaui</i>	31,6
<i>Claudiosaurus germaini</i>	64,2
<i>Gephyrosaurus bridensis</i>	78,2
<i>Planocephalosaurus robinsonae</i>	75,6
<i>Czatkowiella harae</i>	50,8
<i>Protorosaurus speneri</i>	73,3
<i>Jesairosaurus lehmani</i>	54,7
<i>Macrocnemus bassanii</i>	93,2
<i>Macrocnemus obristi</i>	8,1
<i>Macrocnemus fuyuanensis</i>	71,3
<i>Tanystropheus hydroides</i>	91,9
GMPKU P1527 T. cf. <i>hydroides</i>	24,4
<i>Tanystropheus longobardicus</i>	79,8
<i>Tanystropheus conspicuus</i>	4,6
" <i>Tanystropheus antiquus</i> "	5,2
<i>Sclerostropheus fossai</i>	4,9
<i>Raibliaia calligaris</i>	9,4
<i>Augustaburiania vatagini</i>	8,8
<i>Langobardisaurus pandolfii</i>	49,5
<i>Amotosaurus rothfeldensis</i>	45,9
AMNH FARB 7206	6,2
<i>Tanytrachelos ahynis</i>	37,1
<i>Ozimek volans</i>	31,3
<i>Ellesaurus gondwanoccidens</i>	8,1
<i>Pectodens zhenyuensis</i>	45,6
<i>Fuyuanosaurus acutirostris</i>	25,7
<i>Dinocephalosaurus orientalis</i>	64,8
<i>Prolacerta broomi</i>	96,7
<i>Pamelaria dolichotrachela</i>	59,3
<i>Azendohsaurus madagaskarensis</i>	94,5
<i>Trilophosaurus buettneri</i>	89,3
<i>Mesosuchus browni</i>	89,3
<i>Howesia browni</i>	46,6
<i>Eohyosaurus wolvaardti</i>	25,7
<i>Teyujagua paradoxa</i>	47,9
<i>Proterosuchus fergusi</i>	56,0
<i>Proterosuchus alexanderi</i>	74,9
<i>Euparkeria capensis</i>	90,2
<i>Erythrosuchus africanus</i>	84,4

2

Figure 1

Selected phylogenetic hypotheses for “protorosaur” relationships.

(A) Ezcurra 2016. (B) Pritchard et al. 2015. (C) Rieppel et al. 2003, which represent a compilation of the matrices of Benton & Allen (1997), Jalil (1997), and Dilkes (1998).

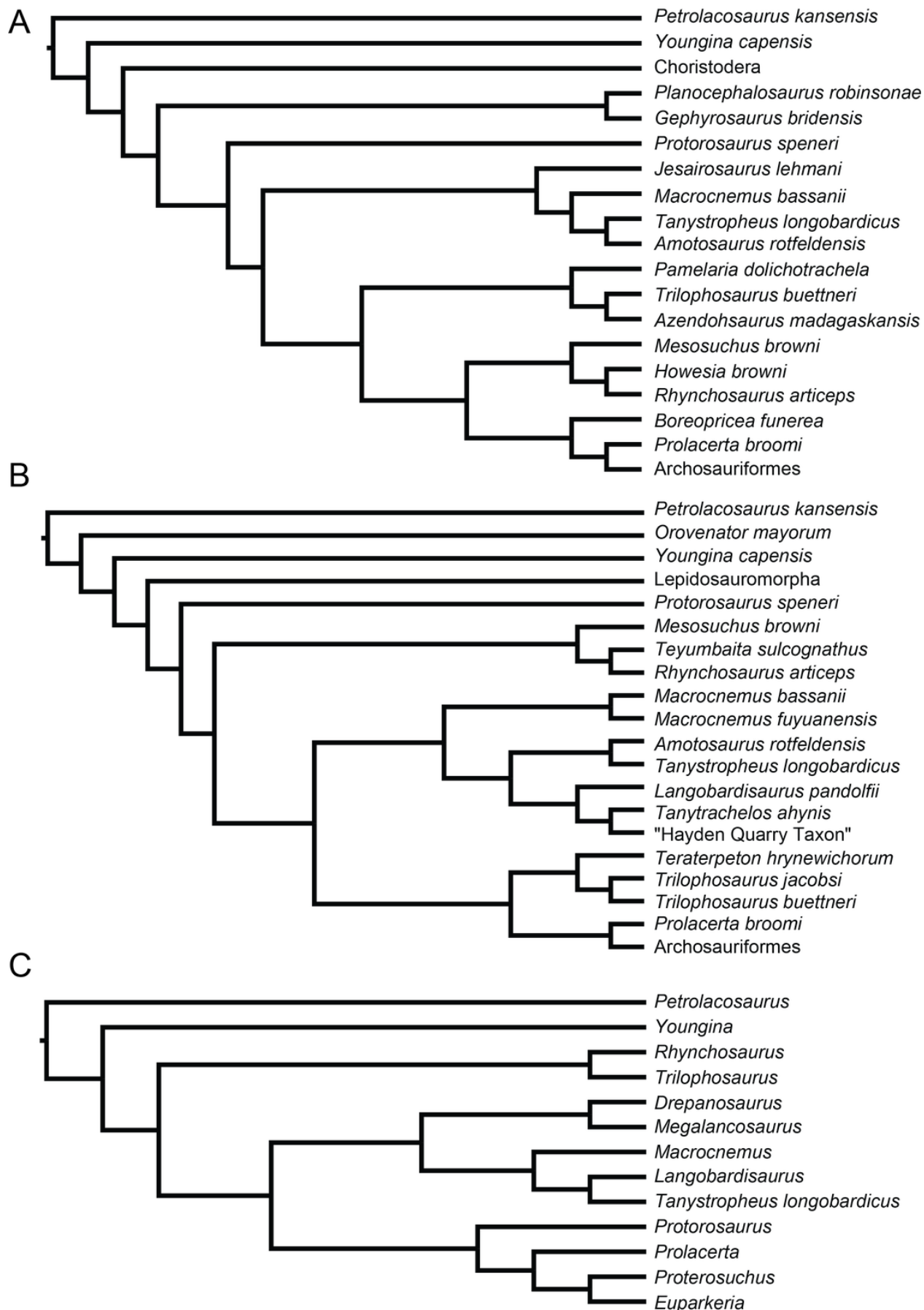


Figure 2

Illustration of character 17.

(A) State 0 in *Prolacerta broomi* (BP/1/5880, anterior snout in left lateral view). (B) State 1 in a digital reconstruction of *Tanystropheus hydroides* (PIMUZ T 2790, anterior snout in left lateral view). (C) State 3 in *Erythrosuchus africanus* (BP/1/4526, isolated right premaxilla in lateral view). (D) State 4 in a digital reconstruction of *Macrocnemus bassanii* (PIMUZ T 2477, anterior snout in right lateral and medial view).

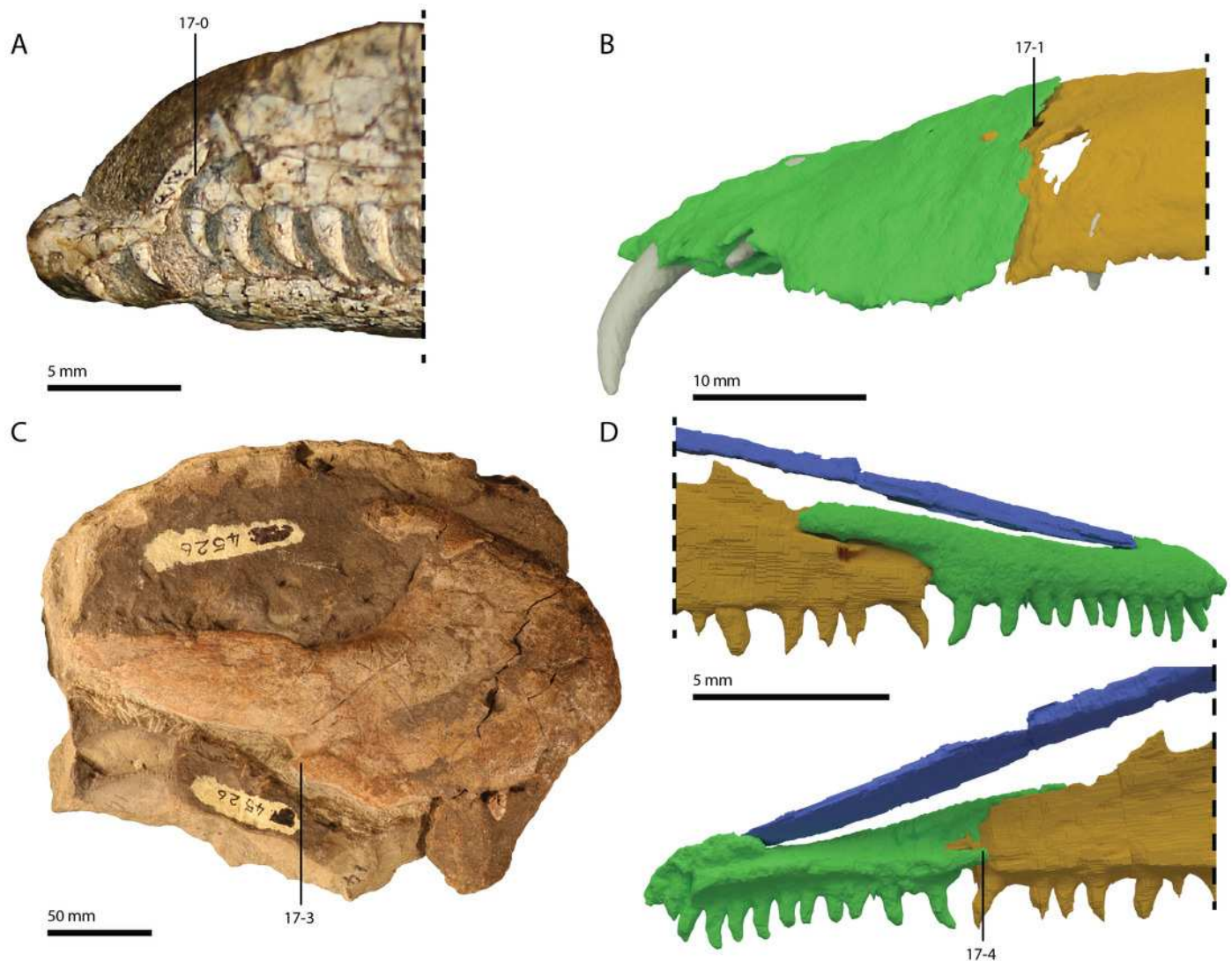


Figure 3

Illustration of character 20.

(A) State 0 in *Protorosaurus speneri* (NMK S 180, anterior part of the skull in right laterodorsal view). (B) State 1 in *Amotosaurus rotfeldensis* (SMNS 50830, right maxilla in medial view). (C) State 0 in *Youngina capensis* (AMNH FARB 5561, skull in right lateral view). (D) State 1 in *Macrocnemus fuyuanensis* (PIMUZ T 1559, disarticulated skull with right maxilla visible in lateral view).

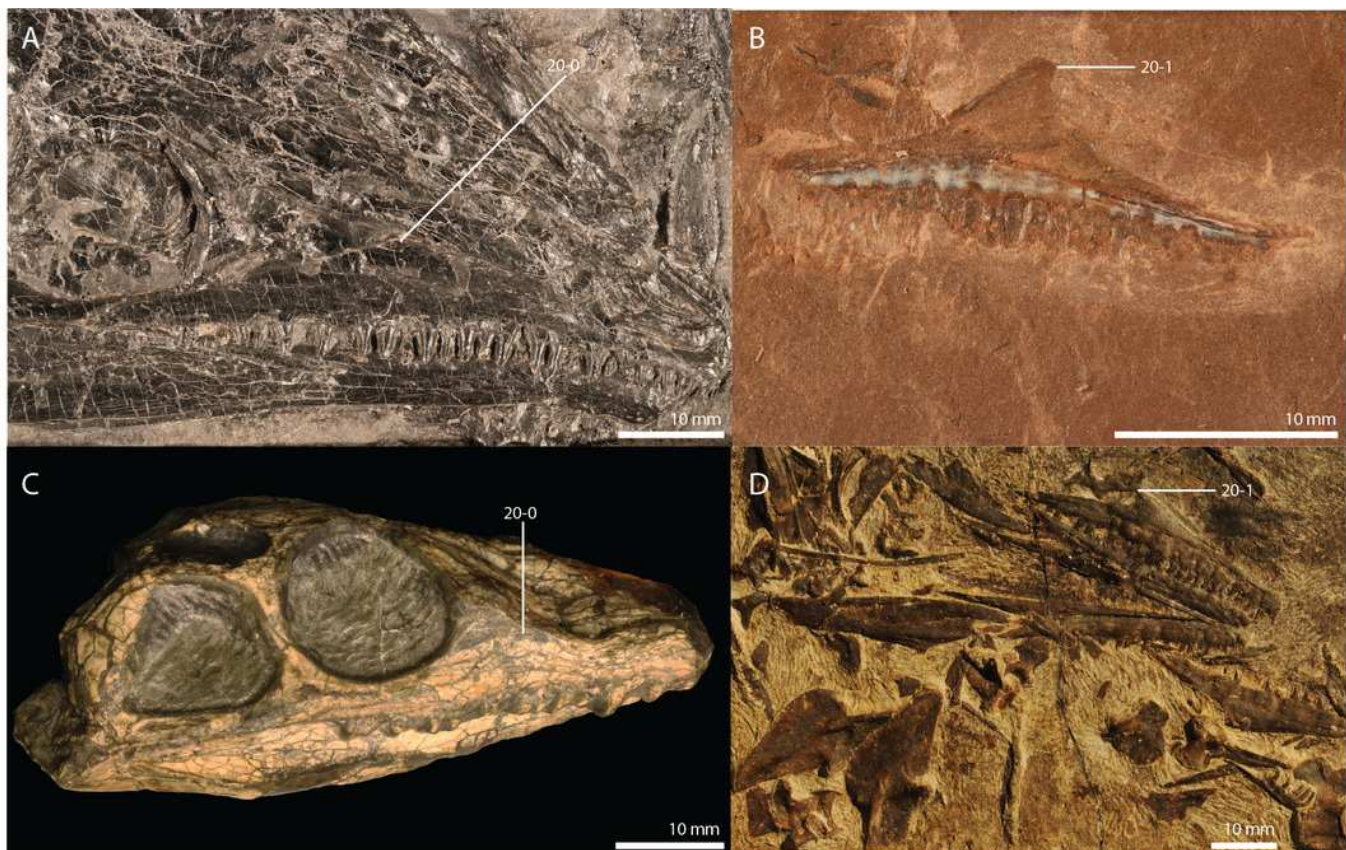


Figure 4

Illustration of character 23.

(A) State 0 in *Macrocnemus bassanii* (PIMUZ T 4822, skull in left lateral view). (B) State 1 in *Dinocephalosaurus orientalis* (IVPP V13767, anterior part of the skull in right laterodorsal view).

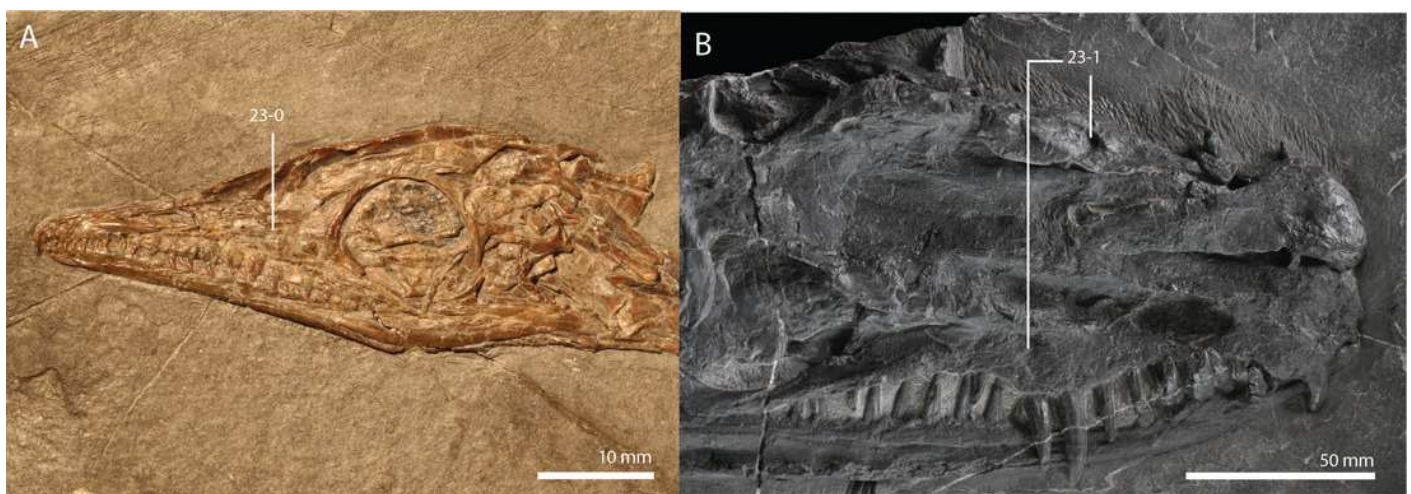


Figure 5

Illustration of character 25.

(A) State 0 in a digital reconstruction of *Tanystropheus hydroides* (PIMUZ T 2790, skull in right lateral view). (B) State 1 in a digital reconstruction of *Macrocnemus bassanii* (PIMUZ T 2477, skull in left lateral view). (C) State 2 in *Euparkeria capensis* (SAM-PK-5867, skull in right lateral view). (D) State 4 in *Dinocephalosaurus orientalis* (IVPP V13767, skull in right dorsolateral view).

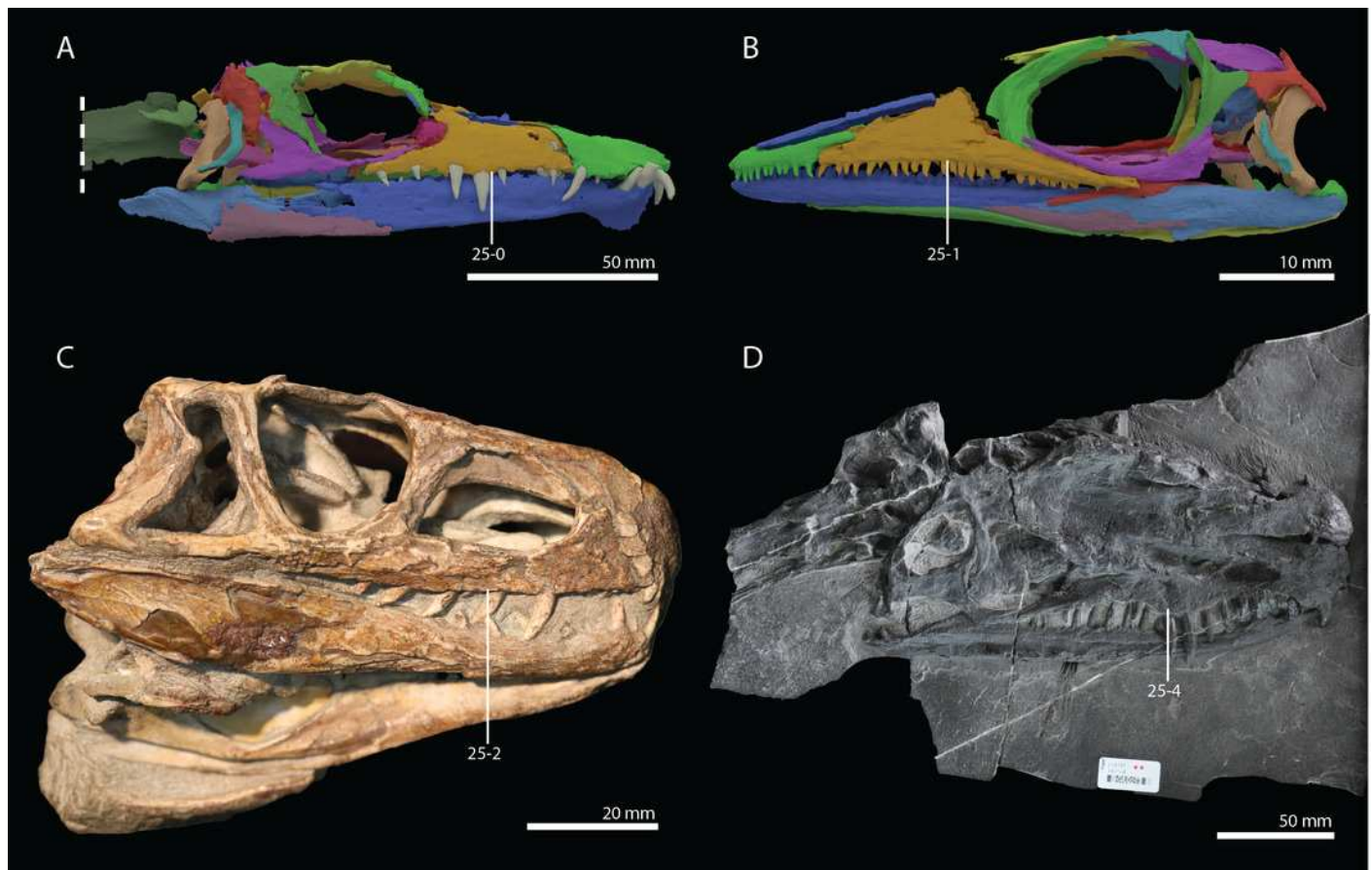


Figure 6

Illustration of character 31.

(A) State 0 in *Youngina capensis* (SAM-PK-K7578, skull in dorsal view). (B) State 1 in *Pectodens zhenyuensis* (IVPP V18578, skull in right lateral view).



Figure 7

Illustration of character 33.

(A) State 1 in *Dinocephalosaurus orientalis* (IVPP V13767, anterior part of the skull in right dorsolateral view). (B) State 1 in *Tanystropheus hydroides* (PIMUZ T 2819, anterior part of the skull in dorsal view). (C) State 0 in *Mesosuchus browni* (SAM-PK-6536, skull in dorsal view). (D) State 0 in *Euparkeria capensis* (SAM-PK-5867, skull in dorsal view).

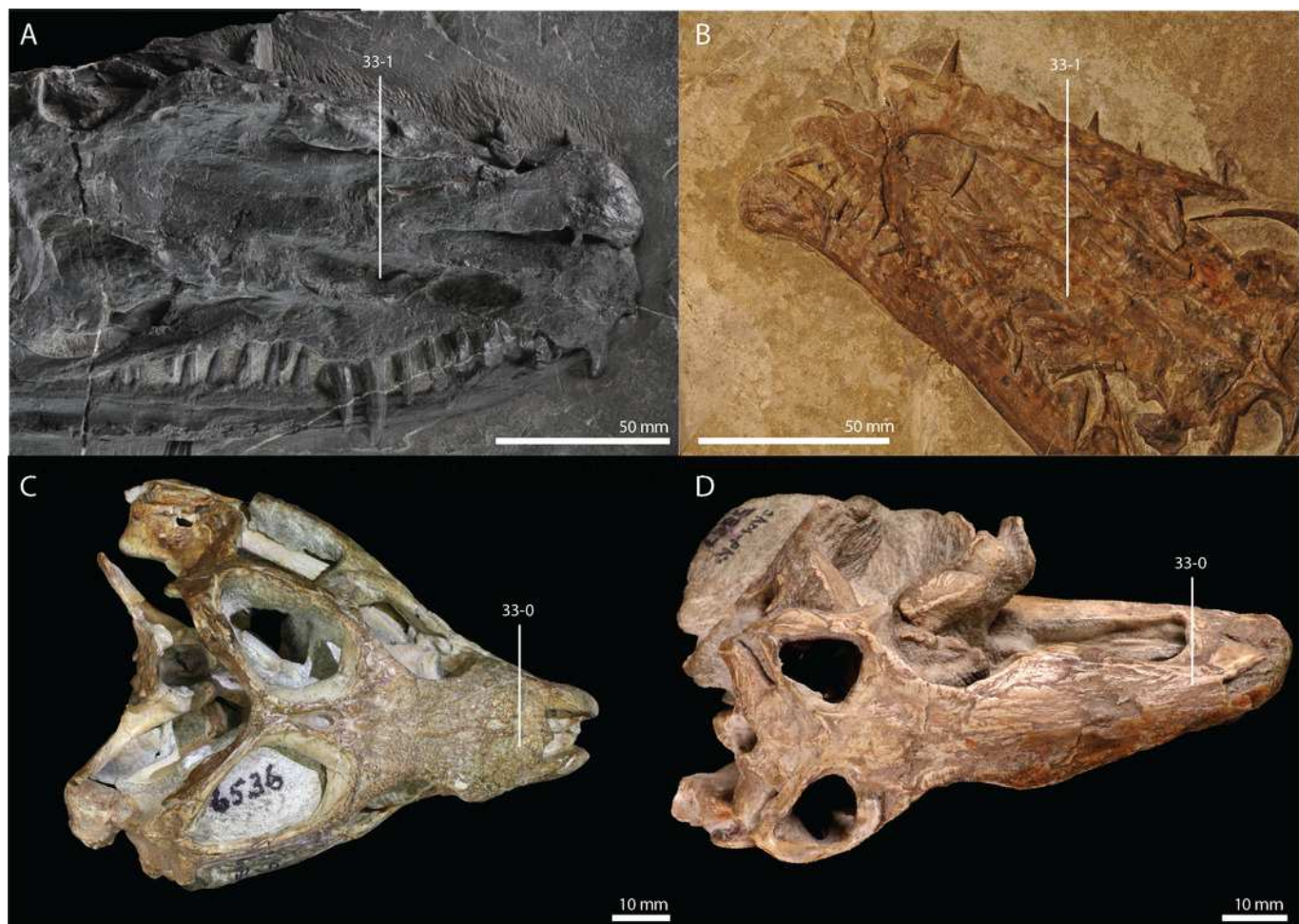


Figure 8

Illustration of characters 38 and 39.

(A) 38-1 and 39-0 in *Euparkeria capensis* (SAM-PK-5867, skull in left lateral view). (B) 38-1 and 39-1 in *Erythrosuchus africanus* (BP/1/5207, skull in right lateral view). (C) 38-0 and 39-1 in *Proterosuchus alexanderi* (NM QR 1484, skull in right lateral view). Image of *Proterosuchus alexanderi* courtesy of Martín Ezcurra.

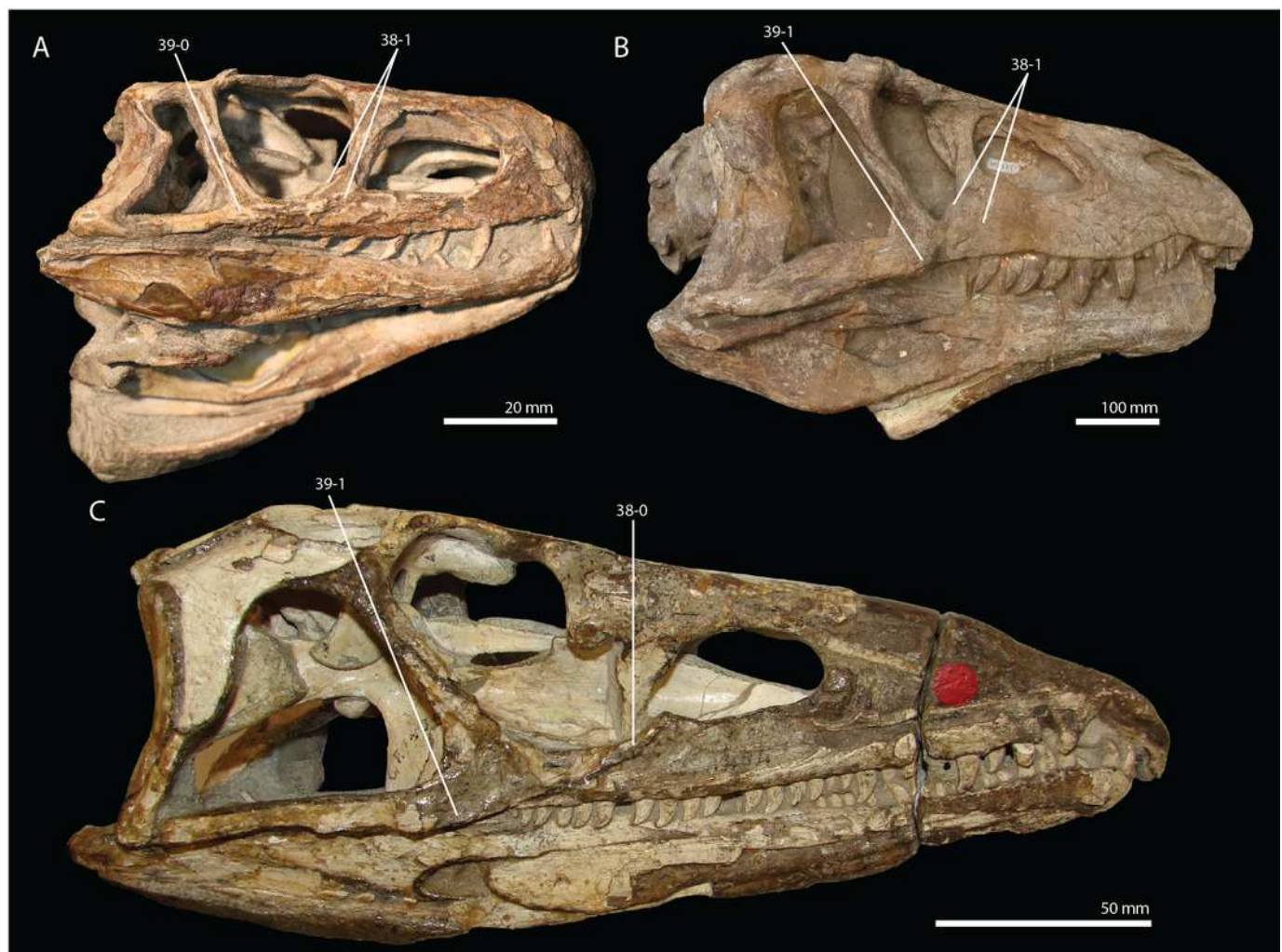


Figure 9

Figure 9. Illustration of character 42

(A) State 0 in *Tanystropheus longobardicus* (PIMUZ T 3901, skull in left lateral view). (B) State 1 in *Dinocephalosaurus orientalis* (IVPP V13767, skull in right laterodorsal view).

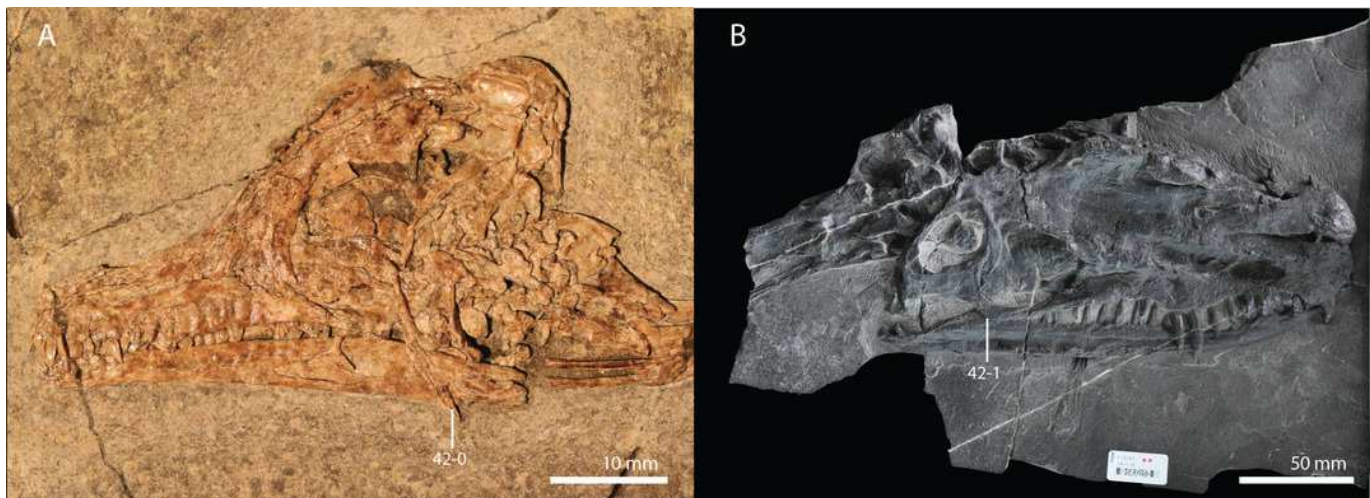


Figure 10

Illustration of character 55.

(A) State 1 in a digital reconstruction of *Tanystropheus hydroides* (PIMUZ T 2790, skull in dorsal view). (B) State 1 in *Tanystropheus longobardicus* (PIMUZ T 2484, frontal, parietal, and postfrontal in dorsal view). (C) State 0 in a digital reconstruction of *Macrocnemus bassanii* (PIMUZ T 2477, skull in dorsal view). (D) State 0 in *Prolacerta broomi* (BP/1/471, skull in dorsal view).

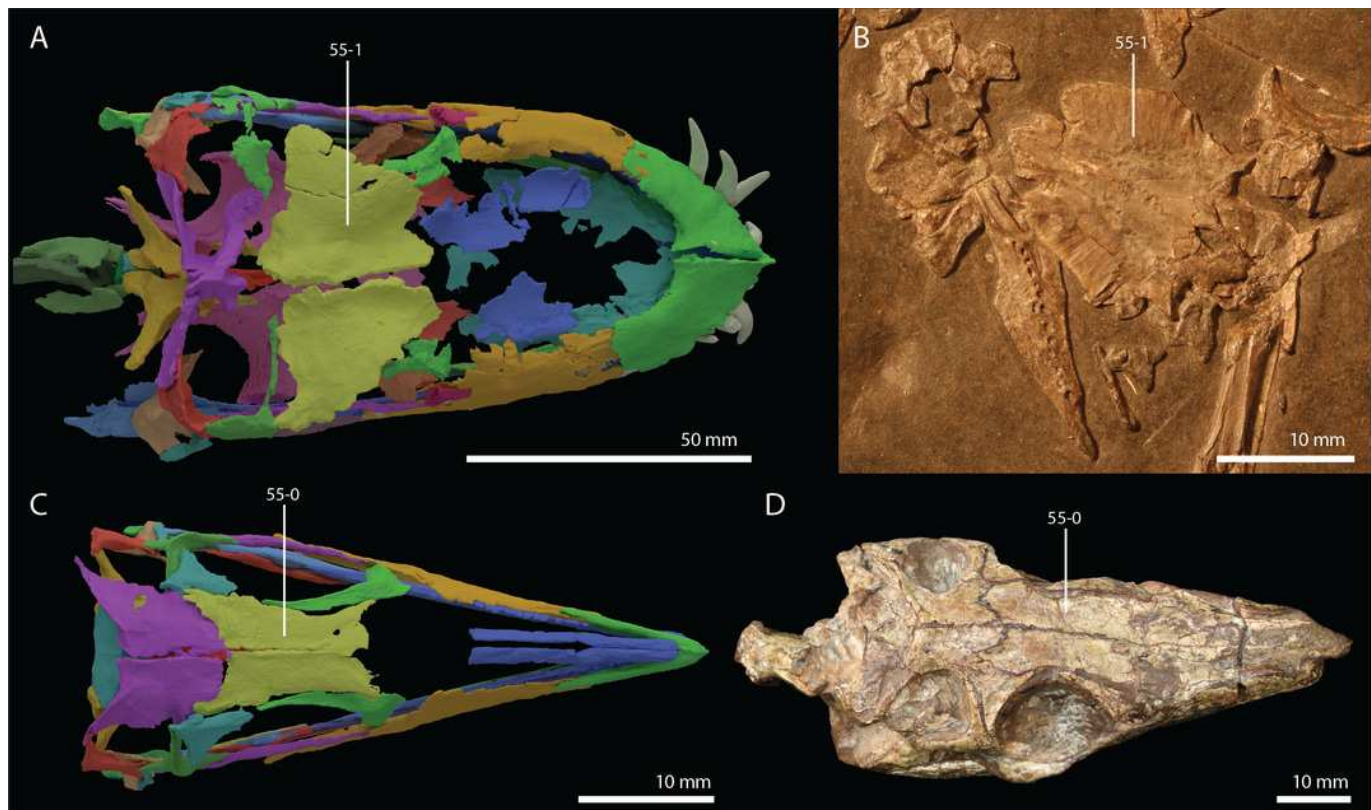


Figure 11

Illustration of character 57.

(A) State 0 in a digital reconstruction of *Macrocnemus bassanii* (PIMUZ T 2477, skull in dorsal view). (B) State 1 in *Tanystropheus longobardicus* (PIMUZ T 2484, frontal, parietal, and postfrontal in dorsal view). (C) State 2 in *Proterosuchus alexanderi* (NM QR 1484, skull in dorsal view). Image of *Proterosuchus alexanderi* courtesy of Martín Ezcurra.

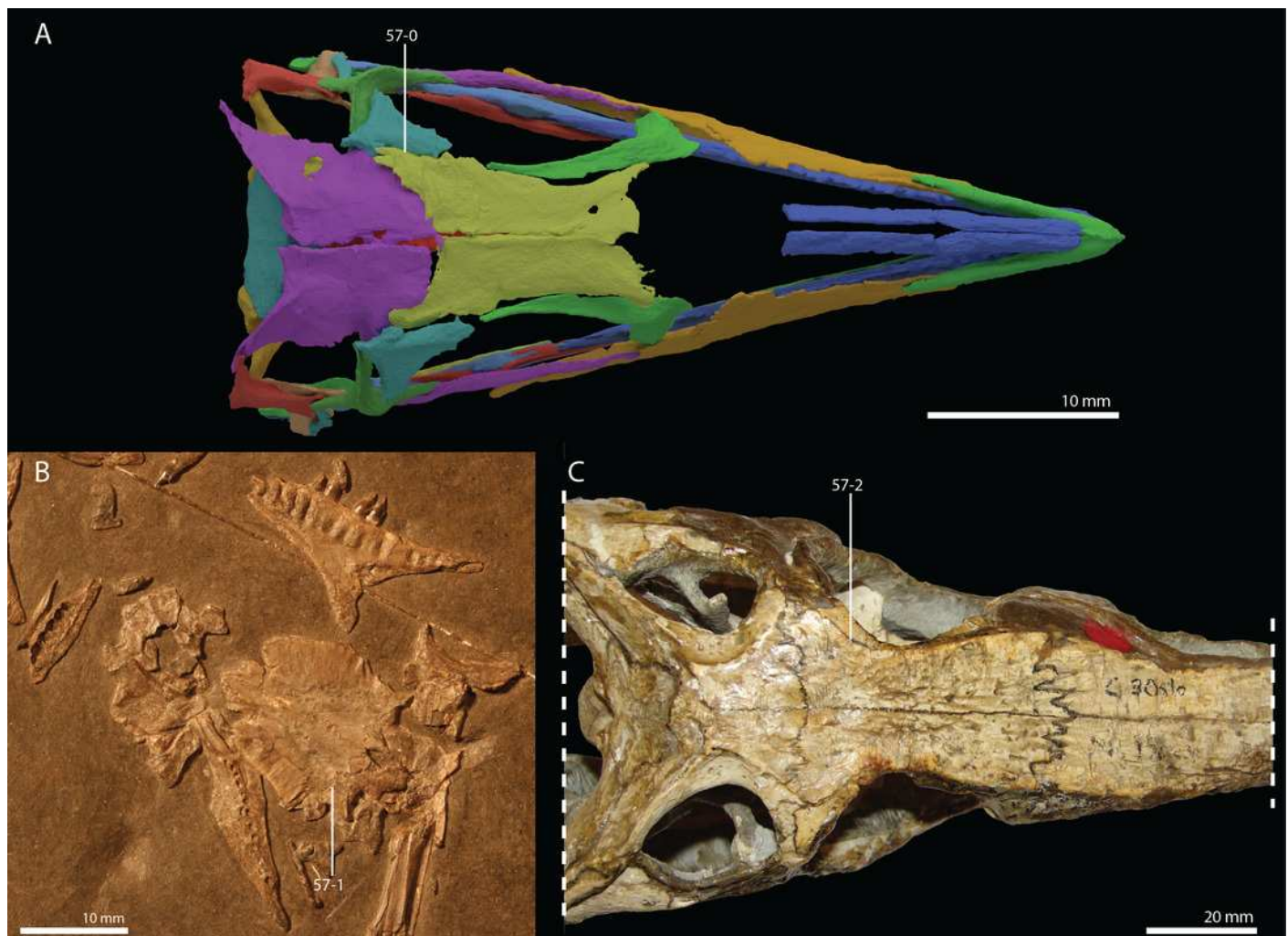


Figure 12

Illustration of characters 67 and 71.

(A) 67-0 in *Prolacerta broomi* (BP/1/5375, partial skull in left lateral view). (B) 67-1 in a digital reconstruction of *Tanystropheus hydroides* (PIMUZ T 2790, posterior part of the skull in right lateral view). (C-D) 67-0 and 71-0 in a digital reconstruction of *Macrocnemus bassanii* (PIMUZ T 2477, right squamosal in (C) lateral and (D) angled oblique anteromedial view). (E-F) 67-1 and 71-1 in a digital reconstruction of *Tanystropheus hydroides* (PIMUZ T 2790, right squamosal in (E) lateral and (F) anterior view).

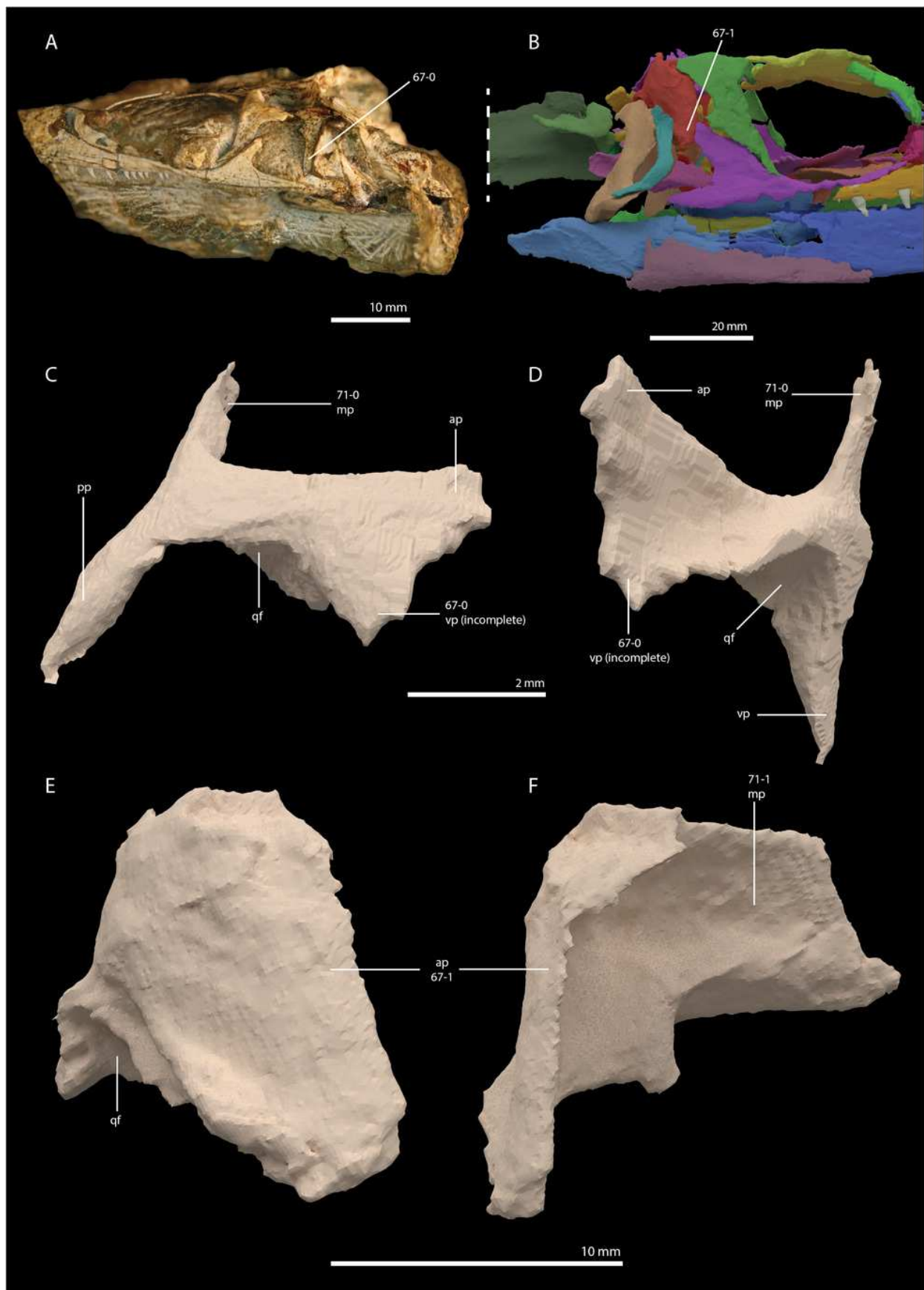


Figure 13

Illustration of characters 76, 79, 81, and 83

(A) 76-0, 79-1, 81-1, 83-0 in *Youngina capensis* (SAM-PK-K7578, posterior part of the skull in dorsal view). (B) 79-1, 81-0 in a digital reconstruction of *Macrocnemus bassanii* (PIMUZ T 2477, posterior part of the skull in dorsal view). (C) 76-0, 79-0, 81-1, 83-2 in *Tanystropheus hydroides* (PIMUZ T 2819, posterior part of the skull in dorsal view). (D) 76-1, 79-1, 81-1, 83-1 in *Dinocephalosaurus orientalis* (IVPP V13767, posterior part of the skull in right laterodorsal view).

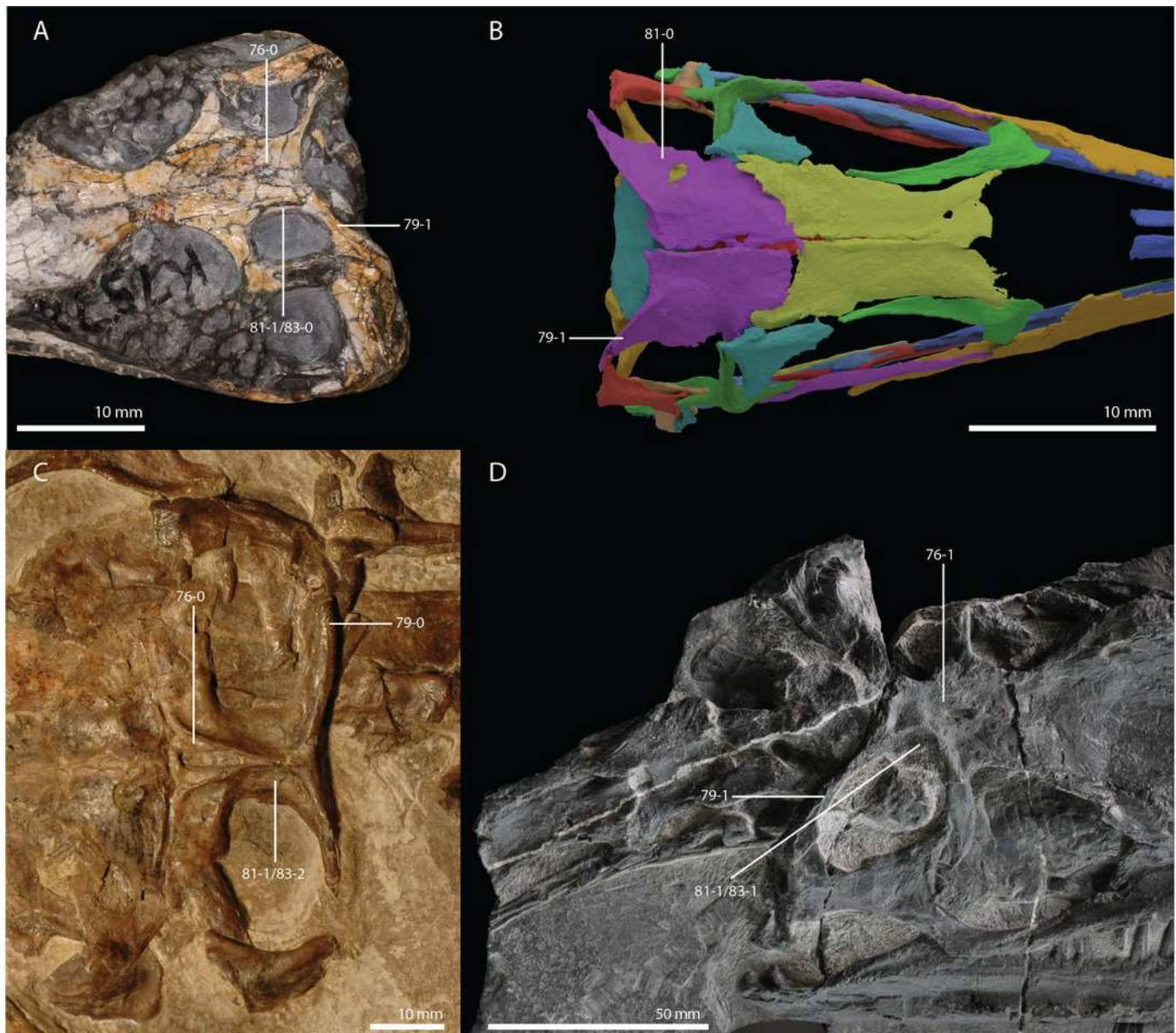


Figure 14

Illustration of characters 92, 93, and 94.

(A-B) 92-0, 93-1, 94-1 in a digital reconstruction of *Tanystropheus hydroides* (PIMUZ T 2790, right quadrate in (A) posterior and (B) medial view). (C) 94-0 in *Macrocnemus fuyuanensis* (PIMUZ T 1559, right quadrate in anterior view). (D) 92-0 and 93-0 in *Proterosuchus alexanderi* (NM QR 1484, left side of the skull in posterior/occipital view). Image of *Proterosuchus alexanderi* courtesy of Martín Ezcurra.

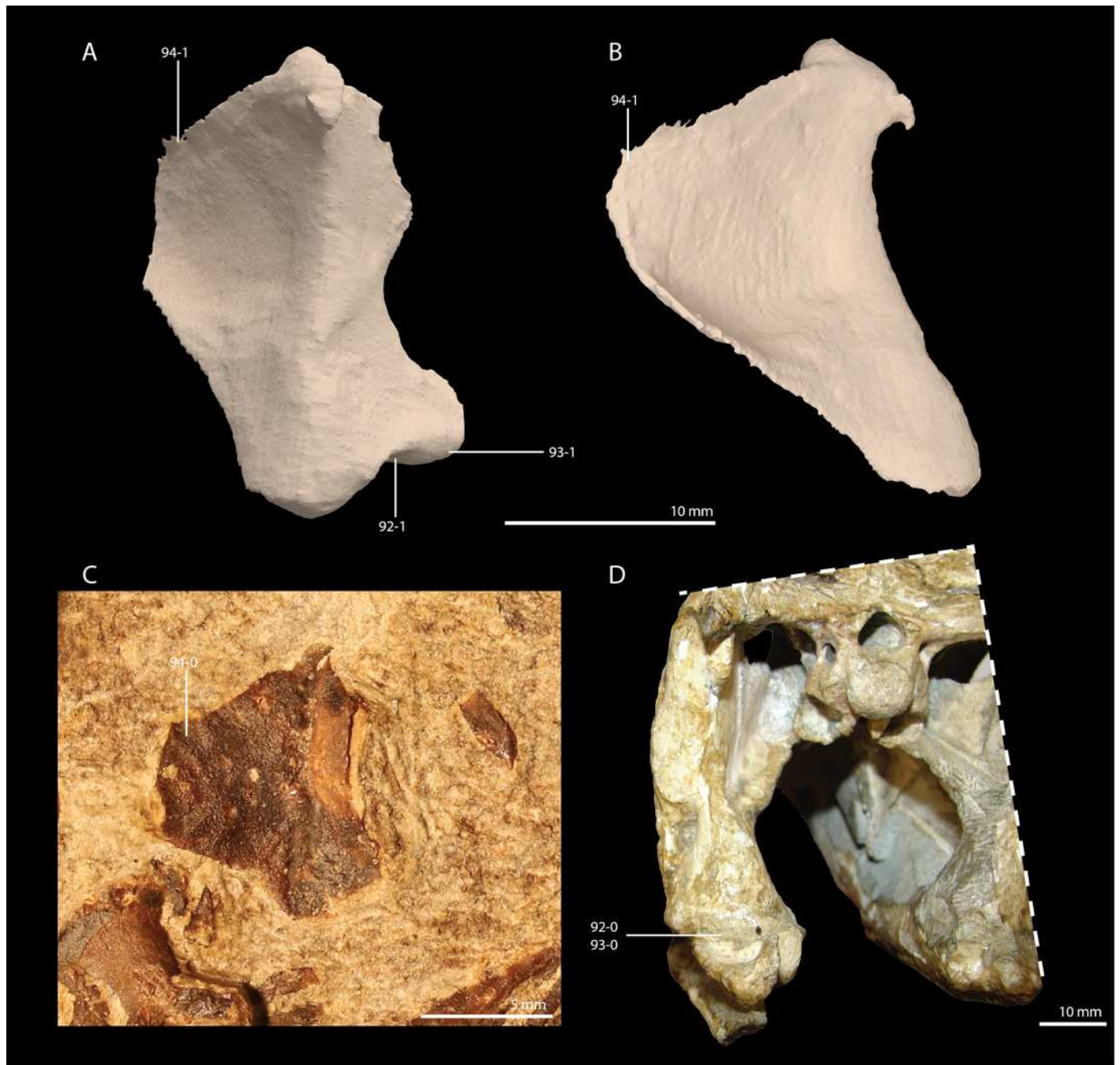


Figure 15

Illustration of characters 97, 101, 105, 108, 109, and 110.

(A) 105-0, 108-0, 109-0, and 110-1 in *Macrocnemus fuyuanensis* (palatal reconstruction, modified from Scheyer et al. 2020b). (B) 97-1, 101-1, 105-1, 108-0, 109-0, and 110-0 in *Azendohsaurus madagaskarensis* (palatal reconstruction, modified from Flynn et al. 2010). (C) 97-0, 101-1, 105-0, 108-0, and 109-1 in *Tanystropheus longobardicus* (palatal reconstruction, modified from Spiekman et al. 2020). (D) 97-1, 108-1, 109-1, and 110-0 in *Tanystropheus hydroides* (palatal reconstruction, modified from Spiekman et al. 2020).

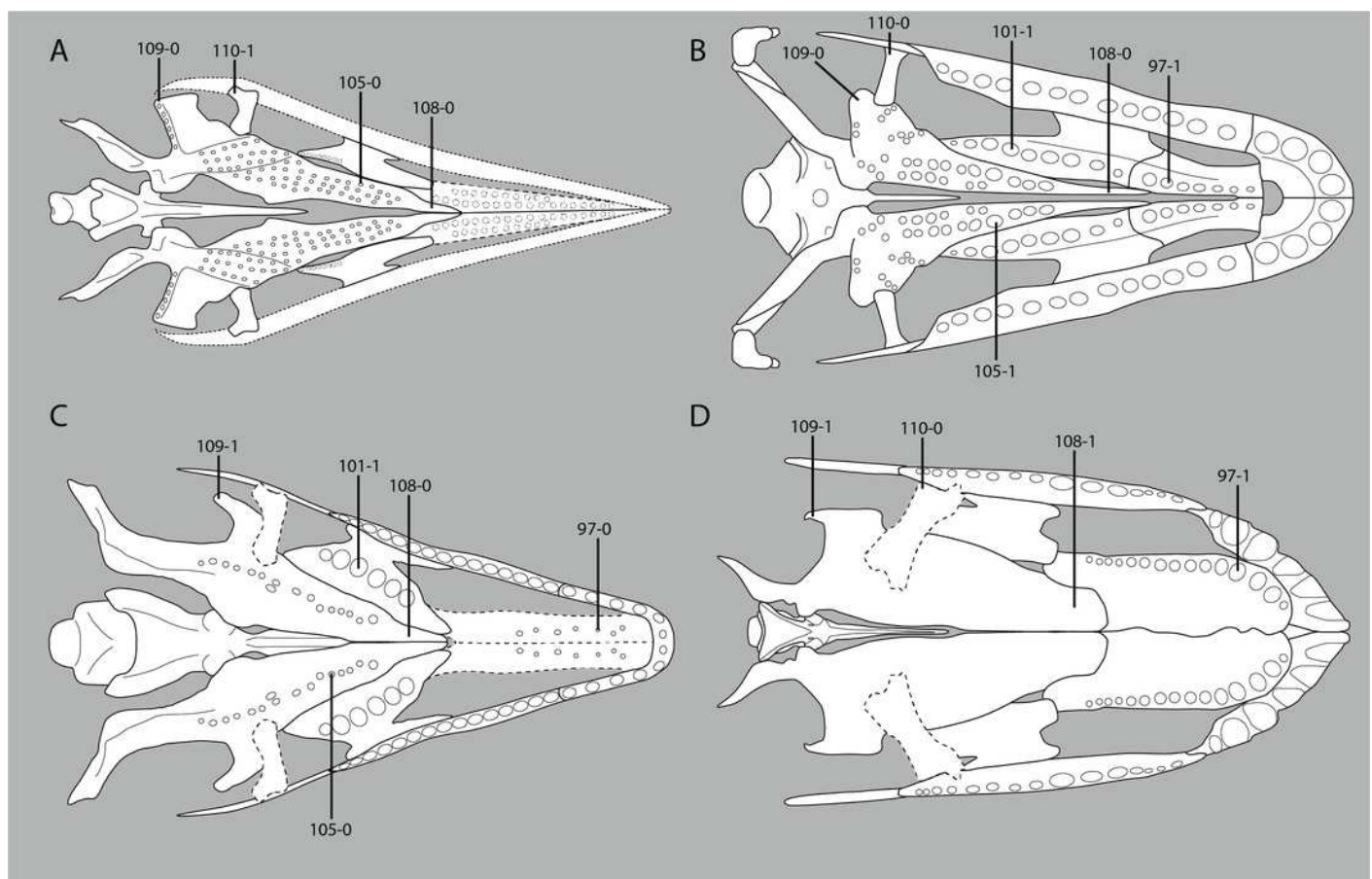


Figure 16

Illustration of characters 124 and 128.

(A) 124-0 and 128-1 in a digital reconstruction of *Macrocnemus bassanii* (PIMUZ T 2477, skull in posterior/occipital view). (B) 124-0 and 128-2 in *Erythrosuchus africanus* (BP/1/3893, partial braincase in posterior/occipital view). (C) 124-1 in a digital reconstruction of *Tanystropheus hydroides* (PIMUZ T 2790, skull in posterior view).

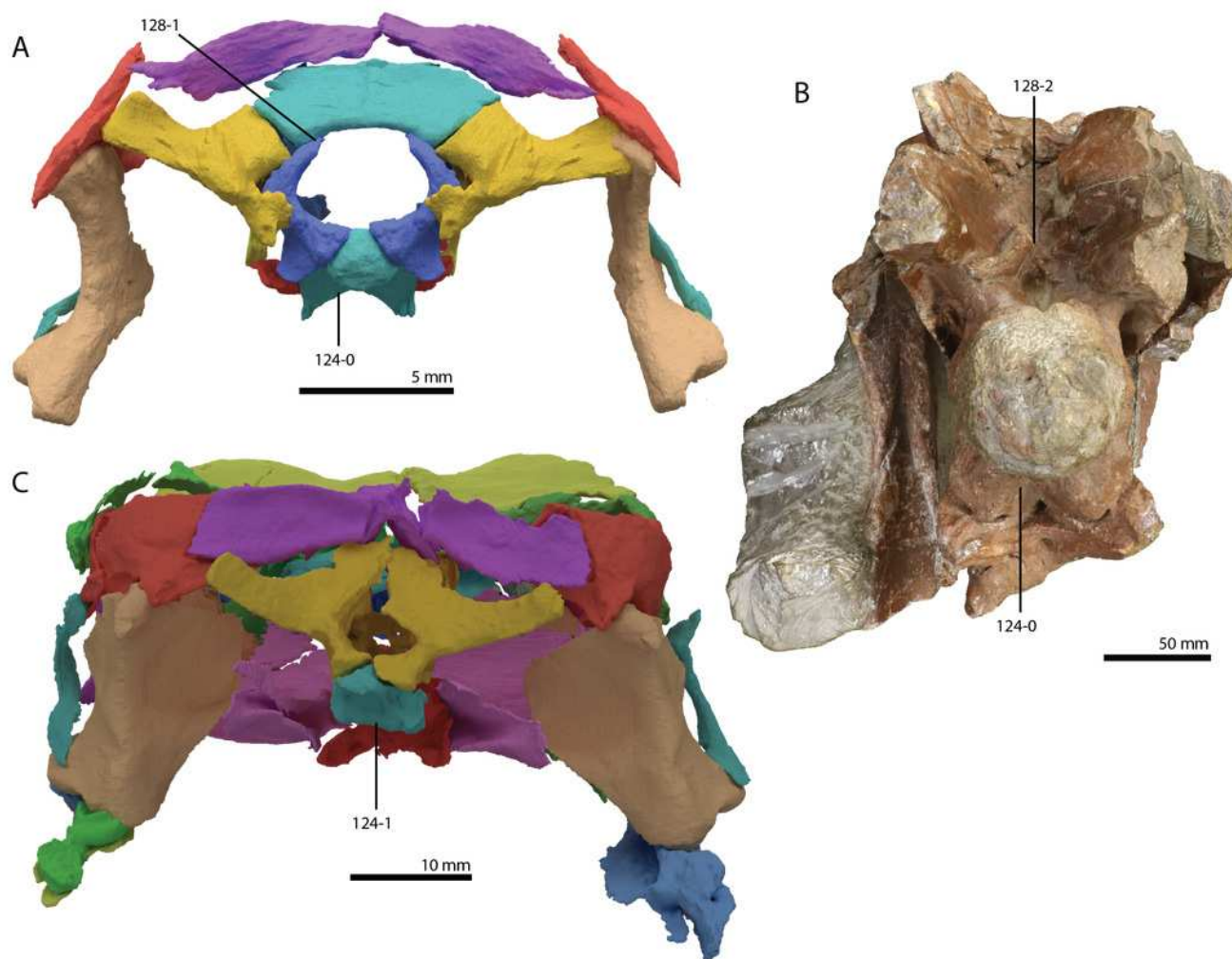


Figure 17

Illustration of characters 133, 137, 138, 139, and 140

(A) 133-1 in *Prolacerta broomi* (BP/1/2675, partial braincase in angled right lateroposteroventral view). (B) 133-3, 137-1, 138-1, 139-1, 140-2 in *Erythrosuchus africanus* (BP/1/3893, partial braincase in angled right lateroposterior view). (C) 133-2, 137-0, 138-1, 139-0, 140-0 in a digital reconstruction of *Macrocnemus bassanii* (PIMUZ T 2477, braincase right lateral view). (D) 133-2, 137-0, 138-1, 139-1, 140-1 in a digital reconstruction of *Tanystropheus hydroides* (PIMUZ T 2790, braincase right lateral view).

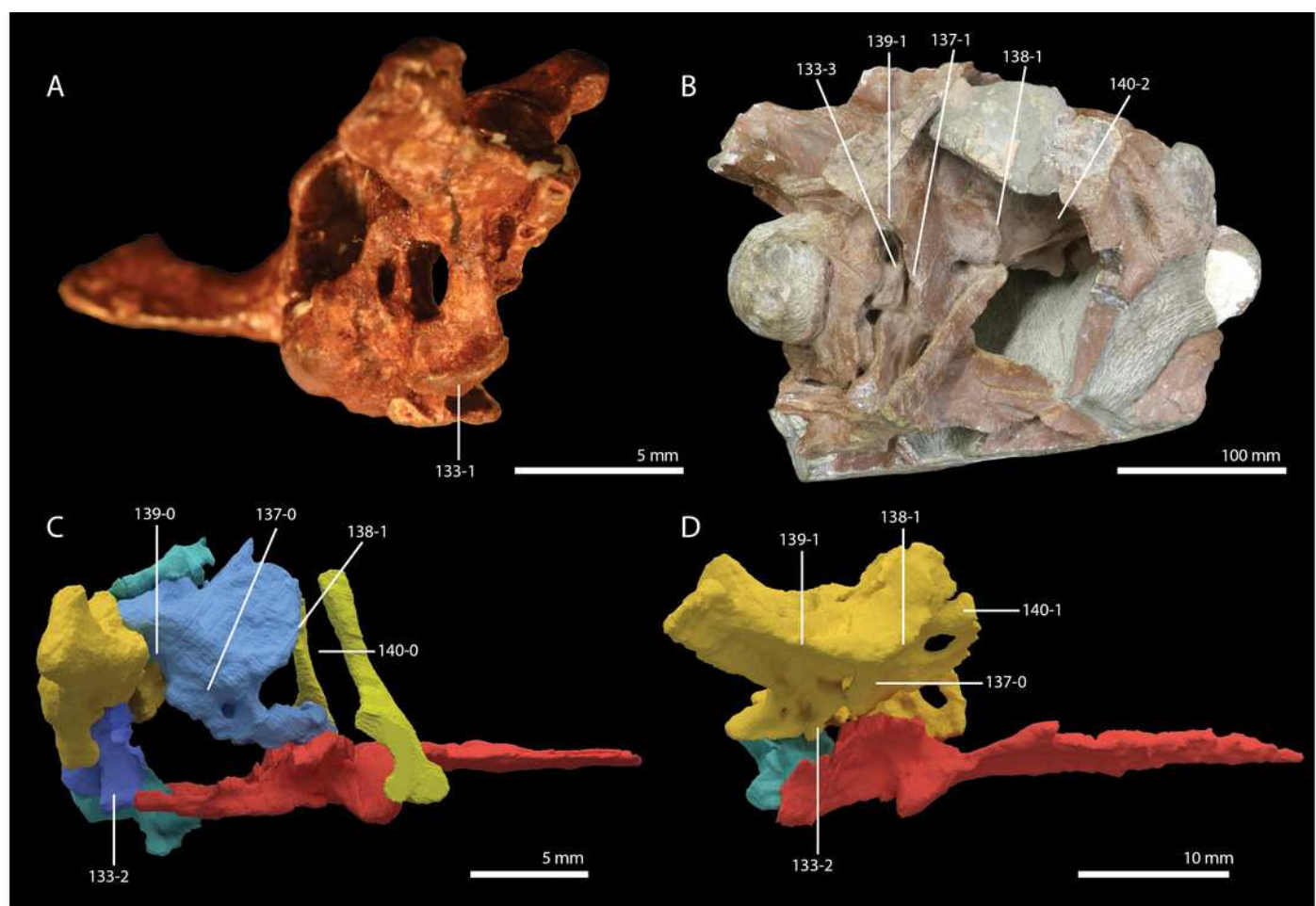


Figure 18

Illustration of characters 146, 158, 159, 161, and 165.

(A) 146-0, 158-0, 159-2, 161-0, and 165-0 in a digital reconstruction of *Macrocnemus bassanii* (PIMUZ T 2477, right lower jaw in lateral view). (B) 146-1, 158-1, 159-1, 161-1, and 165-1 in a digital reconstruction of *Tanystropheus hydroides* (PIMUZ T 2790, left lower jaw in lateral view).

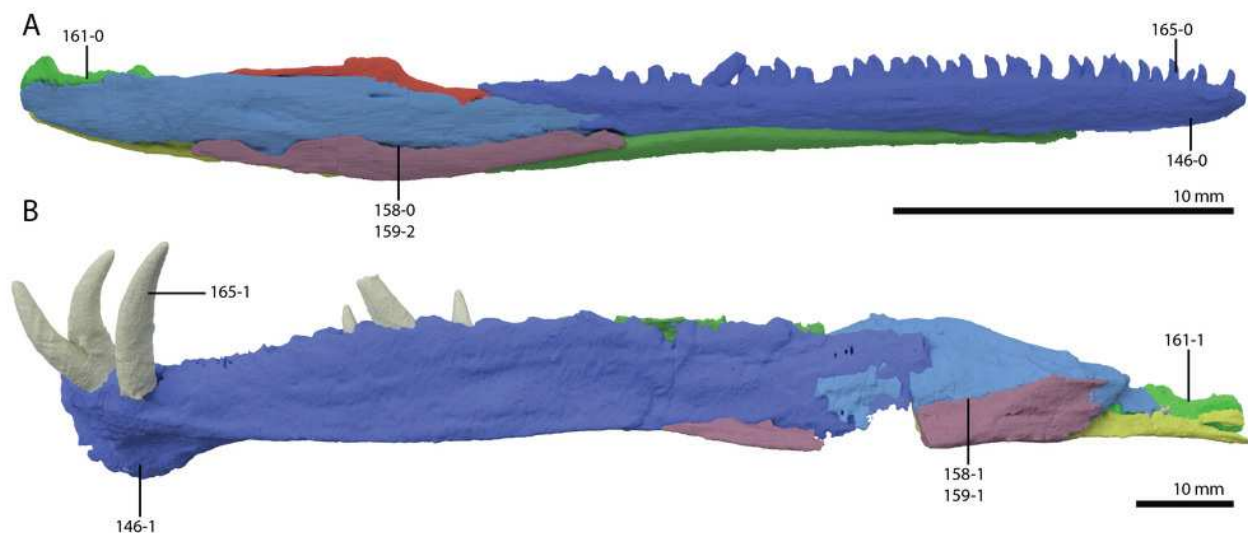


Figure 19

Illustration of character 178.

(A) State 4 in *Sclerostropheus fossai* (MCSNB 4035, mid-cervical vertebra in right lateral view). (B) State 3 in *Tanystropheus hydroides* (PIMUZ T 2819, mid-cervical vertebrae in left lateral view). (C) State 2 in *Fuyuansaurus acutirostris* (IVPP V17983, mid-cervical vertebrae in left lateral view). (D) State 0 in *Youngina capensis* (BP/1/3859, anterior cervical vertebrae right lateral view).

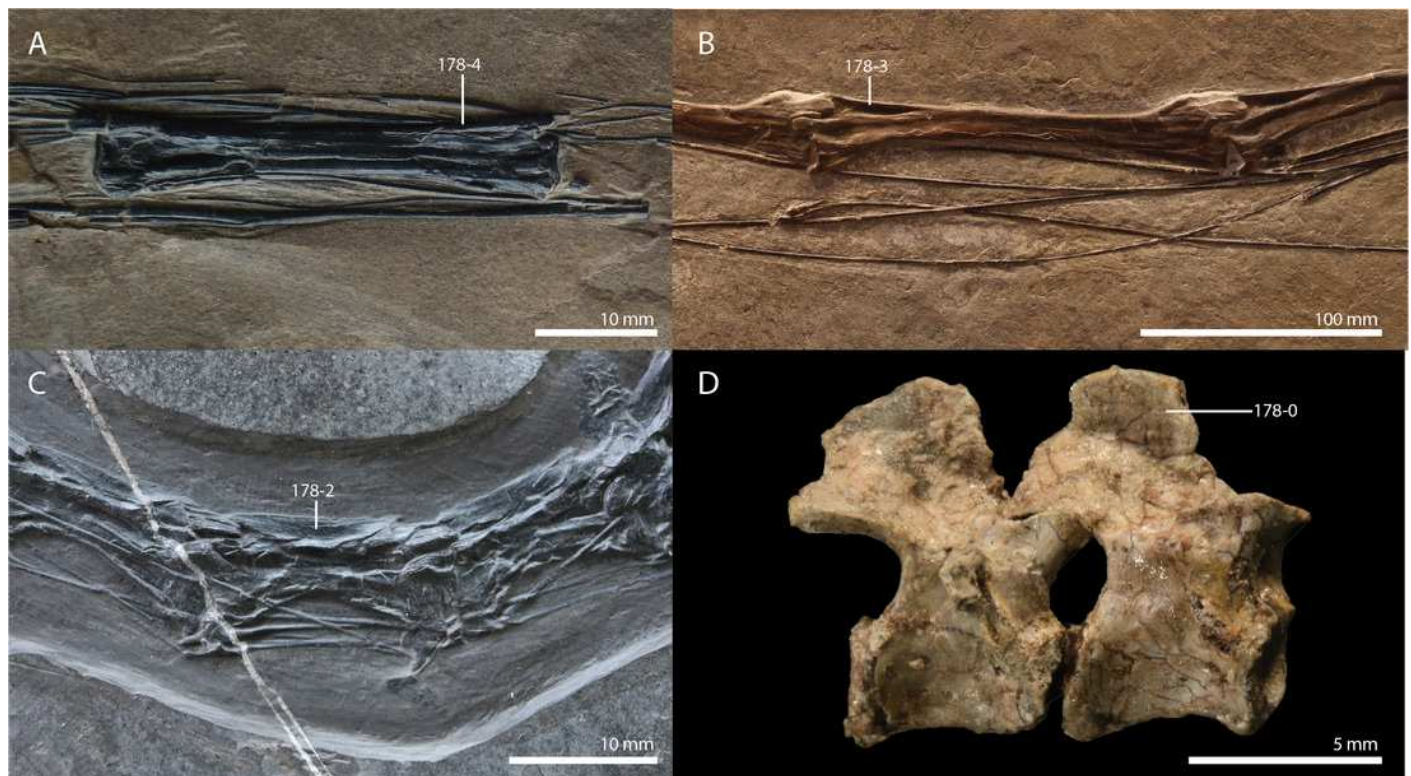


Figure 20

Illustration of characters 179 and 180.

(A) 179-1 and 180-2 in *Macrocnemus fuyuanensis* (IVPP V15001, anterior cervical vertebrae in right lateral view). (B) 179-0 and 180-0 in *Mesosuchus browni* (SAM-PK-5882, anterior cervical vertebrae in left lateral view).

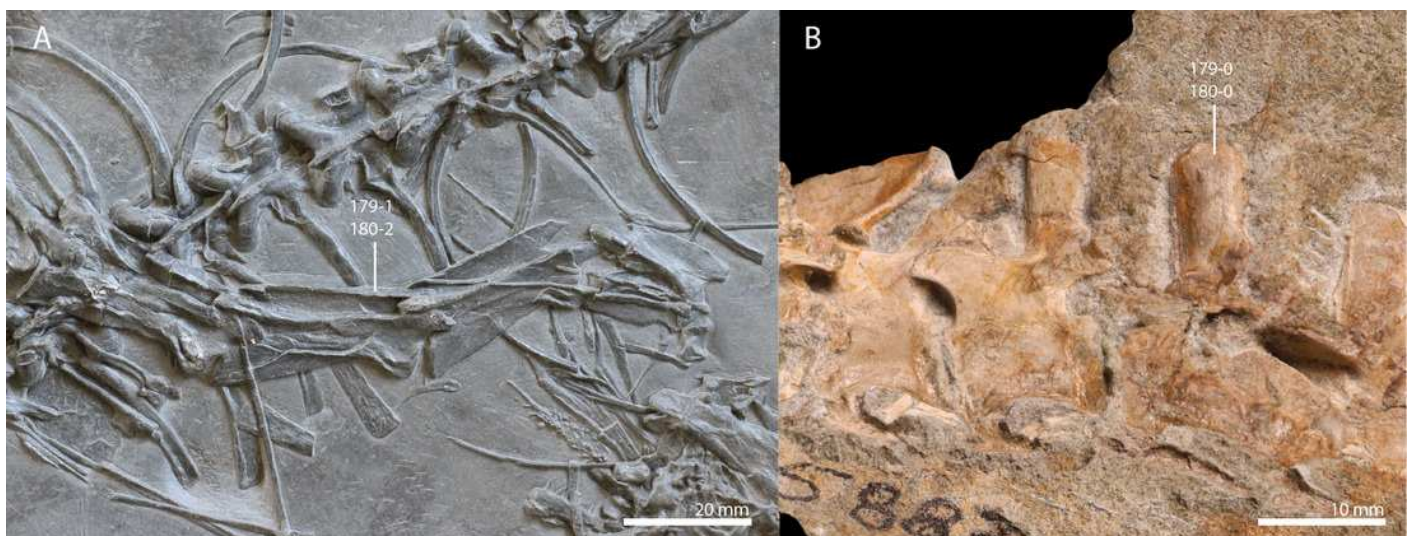


Figure 21

Illustration of character 184.

(A) State 1 in a digital reconstruction of *Tanystropheus hydroides* (PIMUZ T 2790, atlas-axis complex in right lateral view). (B) State 0 in a digital reconstruction of *Macrocnemus bassanii* (PIMUZ T 2477, atlas-axis complex in left lateral view).

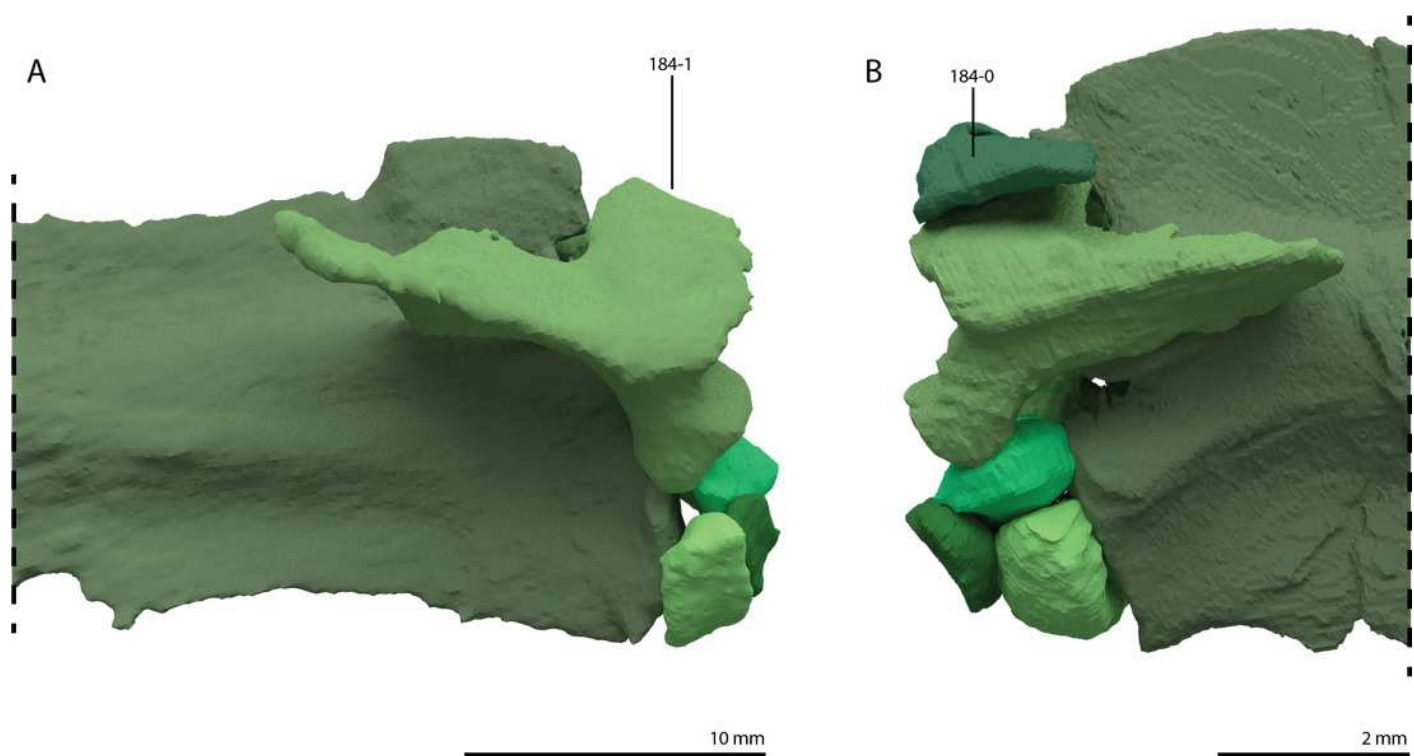


Figure 22

Illustration of character 191.

(A) State 0 in *Protorosaurus speneri* (WMSN P 47361, posterior cervical vertebrae in right lateral view). (B) State 1 in *Tanystropheus "conspicuus"* (U-MO BT 733, posterior part of mid-cervical vertebra in right lateral view).

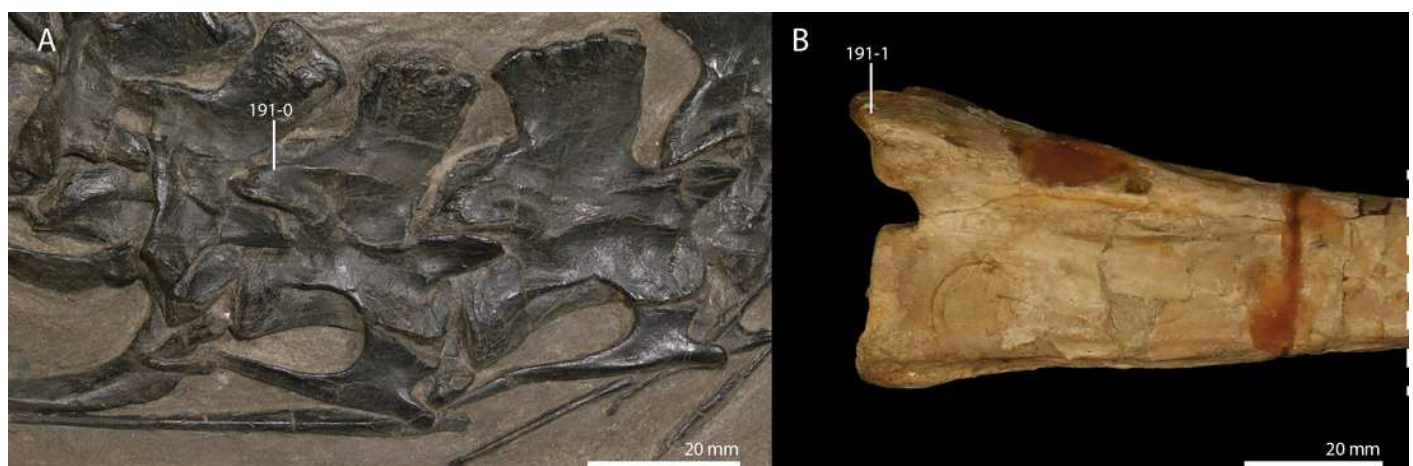


Figure 23

Illustration of character 192.

(A) State 0 in *Pamelaria dolichotrachela* (ISIR 316, anterior cervical vertebra in dorsal view).
 (B) State 1 in *Tanystropheus "conspicuus"* (U-MO BT 740, posterior part of mid-cervical vertebra in dorsal view). Image of *Pamelaria dolichotrachela* courtesy of Martín Ezcurra.



Figure 24

Illustration of character 196.

(A) State 0 in *Youngina capensis* (BP/1/3859, anterior cervical vertebra in ventral view). (B) State 1 in *Tanystropheus "conspicuus"* (U-MO BT 733, partial cervical vertebra in ventral view).

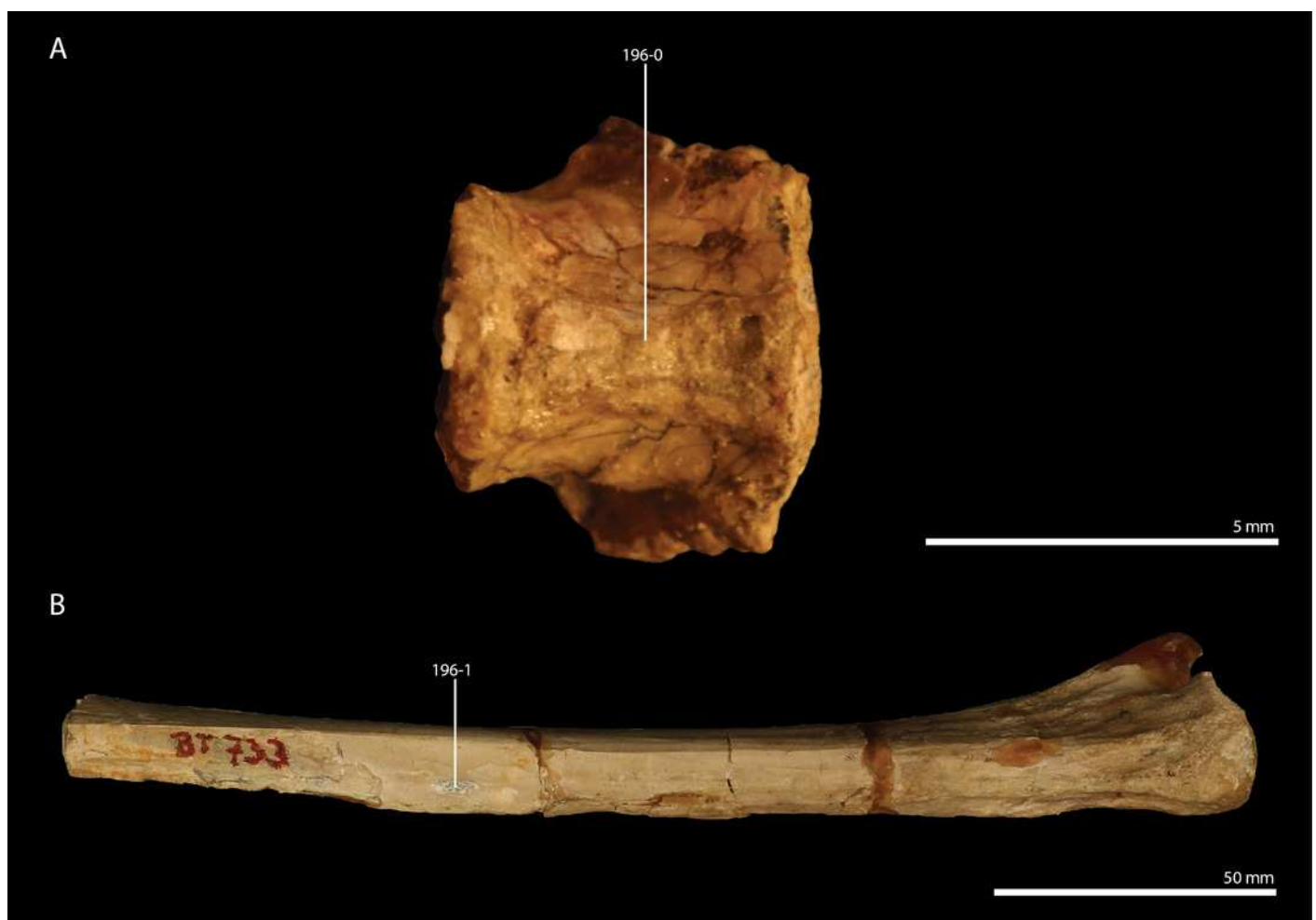


Figure 25

Illustration of characters 199 and 200.

(A) 199-2 and 200-1 in *Tanystropheus longobardicus* (PIMUZ T 3901, skull and partial cervical column in left lateral view). (B) 199-1 and 200-2 in *Tanytrachelos ahynis* (VMNH 120346a, partial skeleton including cervical column, cervical column in left lateral view). (C) 199-2 and 200-2 in *Pectodens zhenyuensis* (IVPP V18578, skull and cervical column in right lateral view).



Figure 26

Illustration of characters 202 and 203.

(A) 202-1 and 203-2 in *Tanystropheus longobardicus* (PIMUZ T 1277, disarticulated anterior dorsal vertebrae, indicated vertebra in angled left dorsolateral view). (B) 202-0 and 203-1 in *Mesosuchus browni* (SAM-PK-6046, dorsal vertebral column in left lateral view). (C) 202-0 and 203-0 in *Euparkeria capensis* (SAM-PK-6047A, dorsal vertebral column in right lateral view).

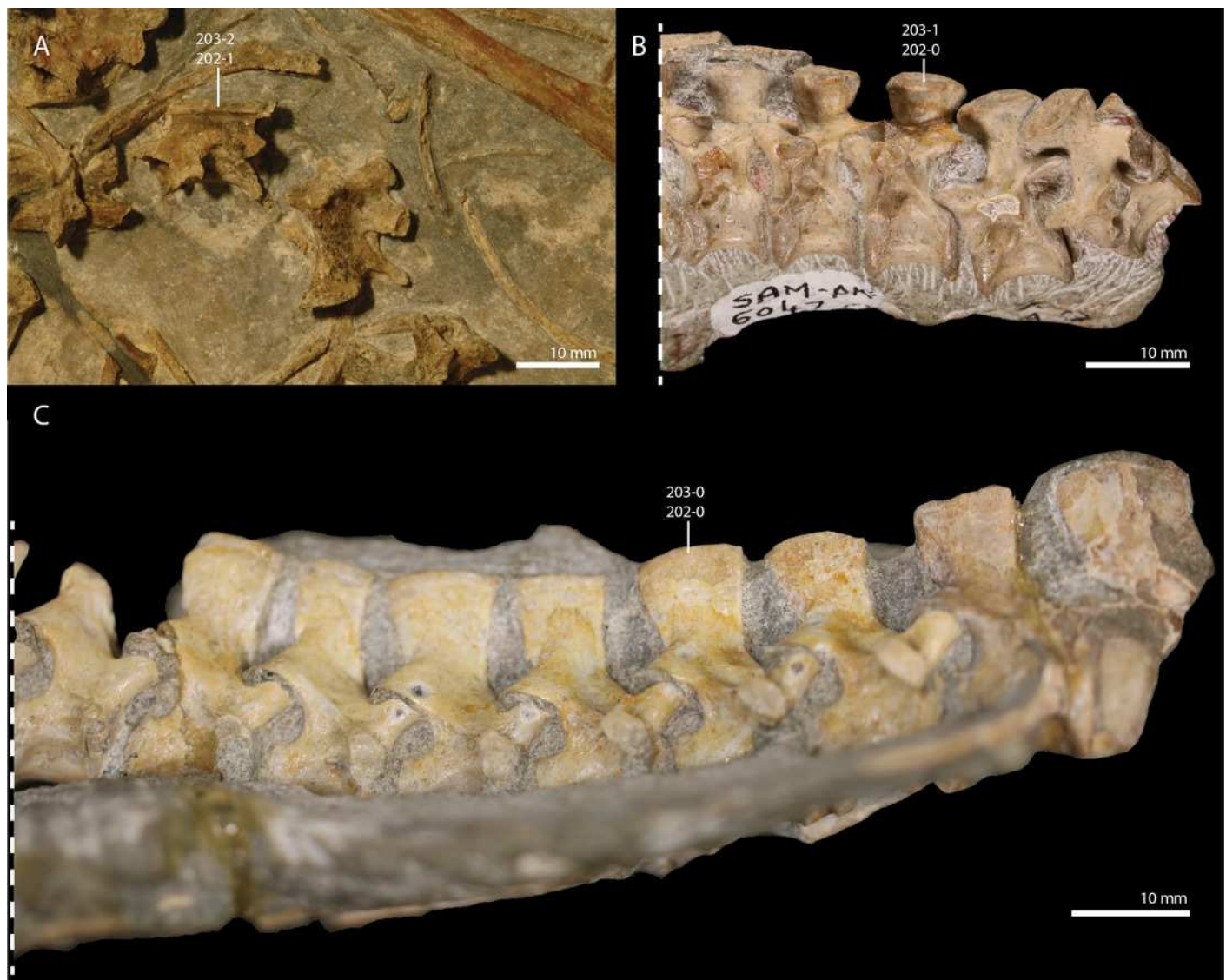


Figure 27

Illustration of character 224

(A) State 0 in *Protorosaurus speneri* (WMSN P 47361, largely complete skeleton in right lateral view, scale bar in cm). (B) State 1 in *Pectodens zhenyuensis* (IVPP V18578, largely complete skeleton, largely in ventral view).

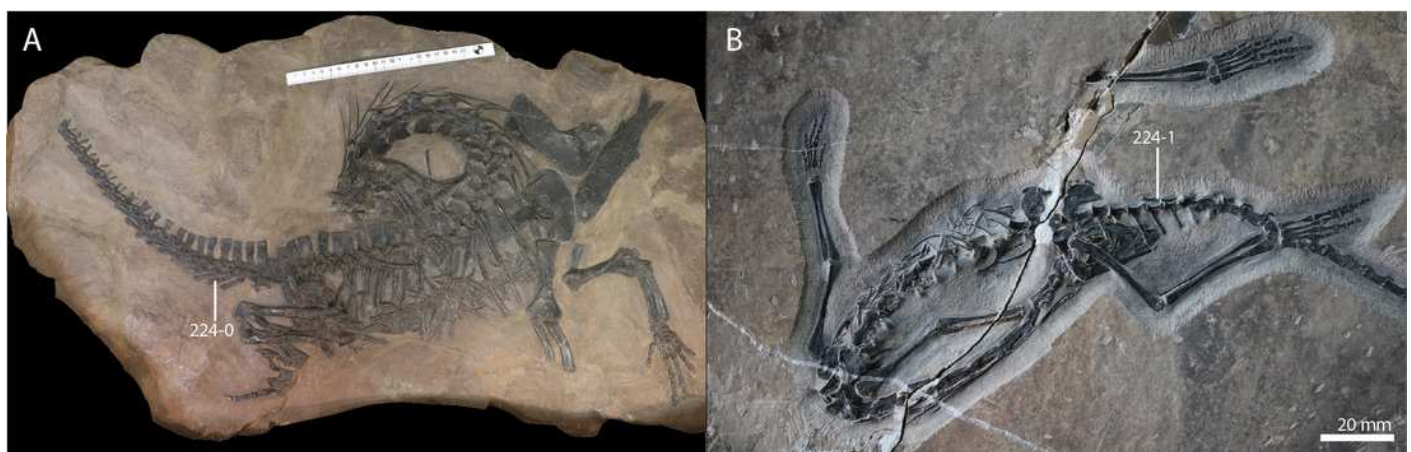


Figure 28

Illustration of character 225 state 1 in *Tanytrachelos ahynis* (VMNH 120013, largely complete skeleton exhibiting heterotopic bones).



Figure 29

Illustration of characters 227 and 228.

(A) 227-2 and 228-1 in *Tanystropheus longobardicus* (PIMUZ T 1277, left scapulocoracoid in medial view). (B) 227-0 and 228-0 in *Protorosaurus speneri* (WMSN P 47361, right scapulocoracoid in lateral view). (C) 227-1 and 228-0 in *Euparkeria capensis* (SAM-PK-5867, partial articulated skeleton including pectoral girdle in angled right lateroventral view).



Figure 30

Illustration of characters 266 and 278.

(A) 266-0 and 278-1 in *Macrocnemus fuyuanensis* (IVPP V15001, right half of the pelvic girdle in medial view). (B) 266-1 in *Tanystropheus longobardicus* (PIMUZ T 1277, right ilium in medial view). (C) 278-0 *Tanystropheus hydroides* (PIMUZ T 2817, ischia in lateral view).

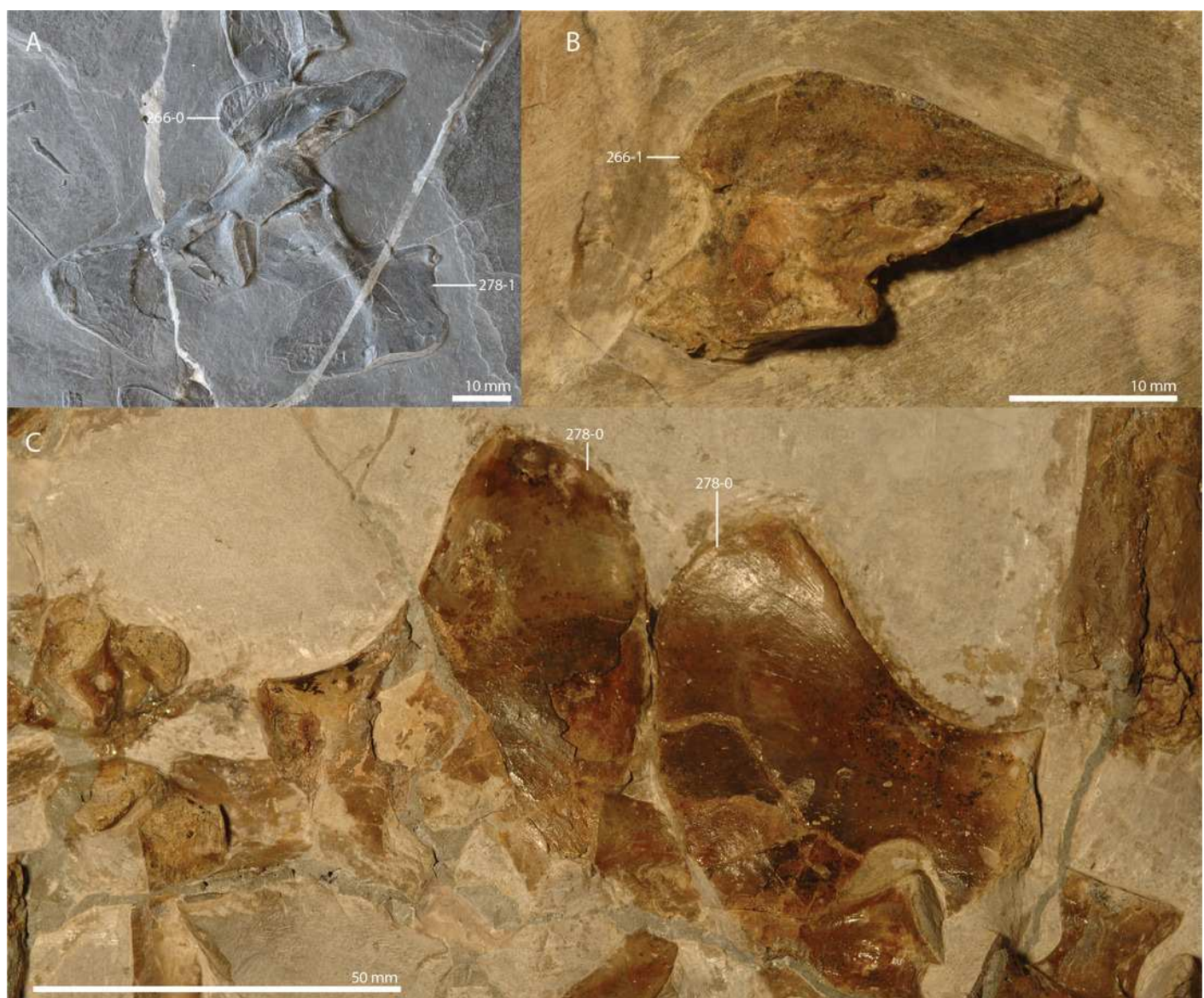


Figure 31

Strict consensus trees of analysis 1 (specified characters ordered; all taxa included in iteration A and all taxa except for "*Tanystropheus antiquus*" included in iteration B).

(A) Strict consensus tree of 1132 MPTs with 1177 steps of analysis 1 including "*Tanystropheus antiquus*". (B) Strict consensus tree of 587 MPTs with 1173 steps of analysis 1 excluding "*Tanystropheus antiquus*". Bremer values above 1 and Bootstrap frequencies above 50% are provided above and below each node, respectively.

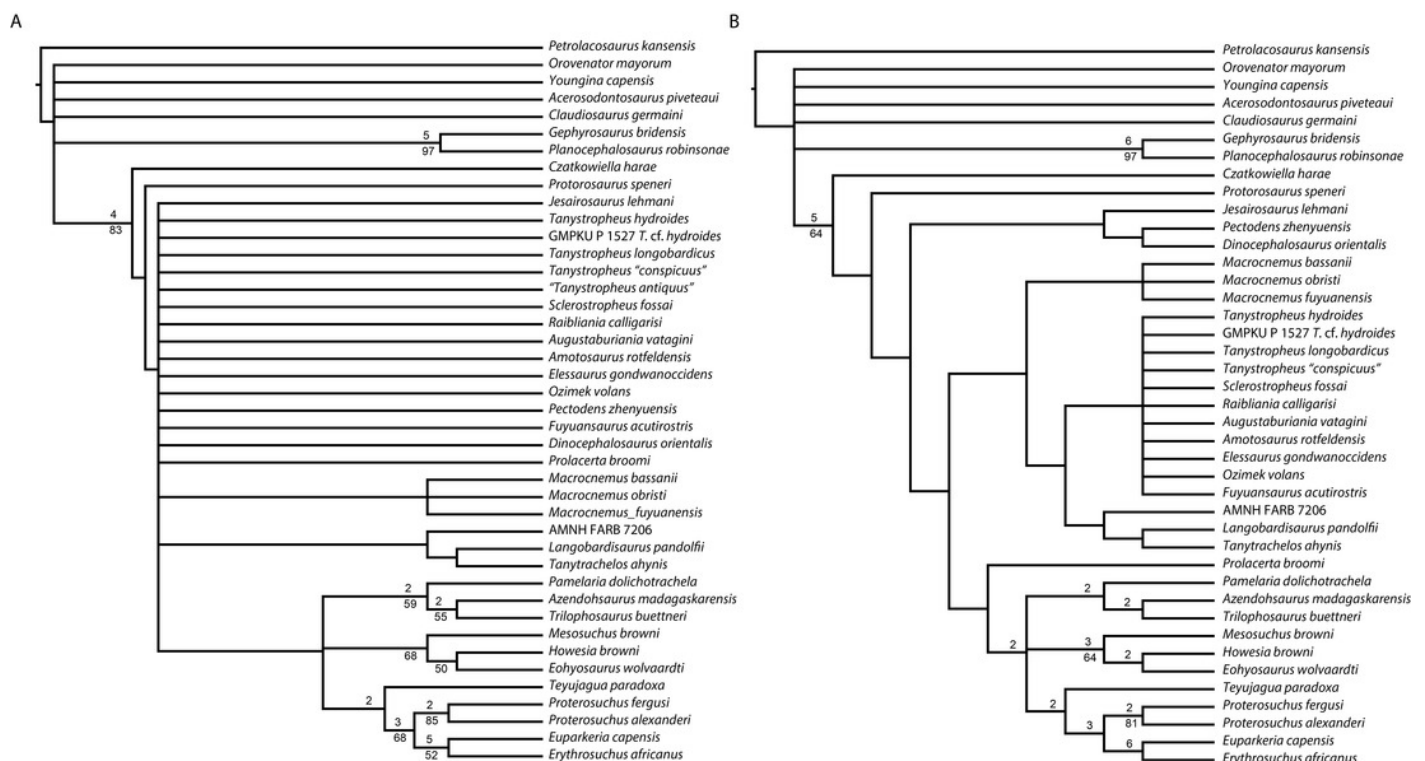


Figure 32

Strict consensus trees of analysis 2 (all characters unordered and ratio characters have been excluded; all taxa included in iteration A and all taxa except for "*Tanystropheus antiquus*" included in iteration B).

(A) Strict consensus tree out of 1646 MPTs with 974 steps of analysis 2 including "*Tanystropheus antiquus*". (B) Strict consensus tree of 1996 MPTs with 971 steps of analysis 2 excluding "*Tanystropheus antiquus*". Bremer values above 1 and Bootstrap frequencies above 50% are provided above and below each node, respectively.

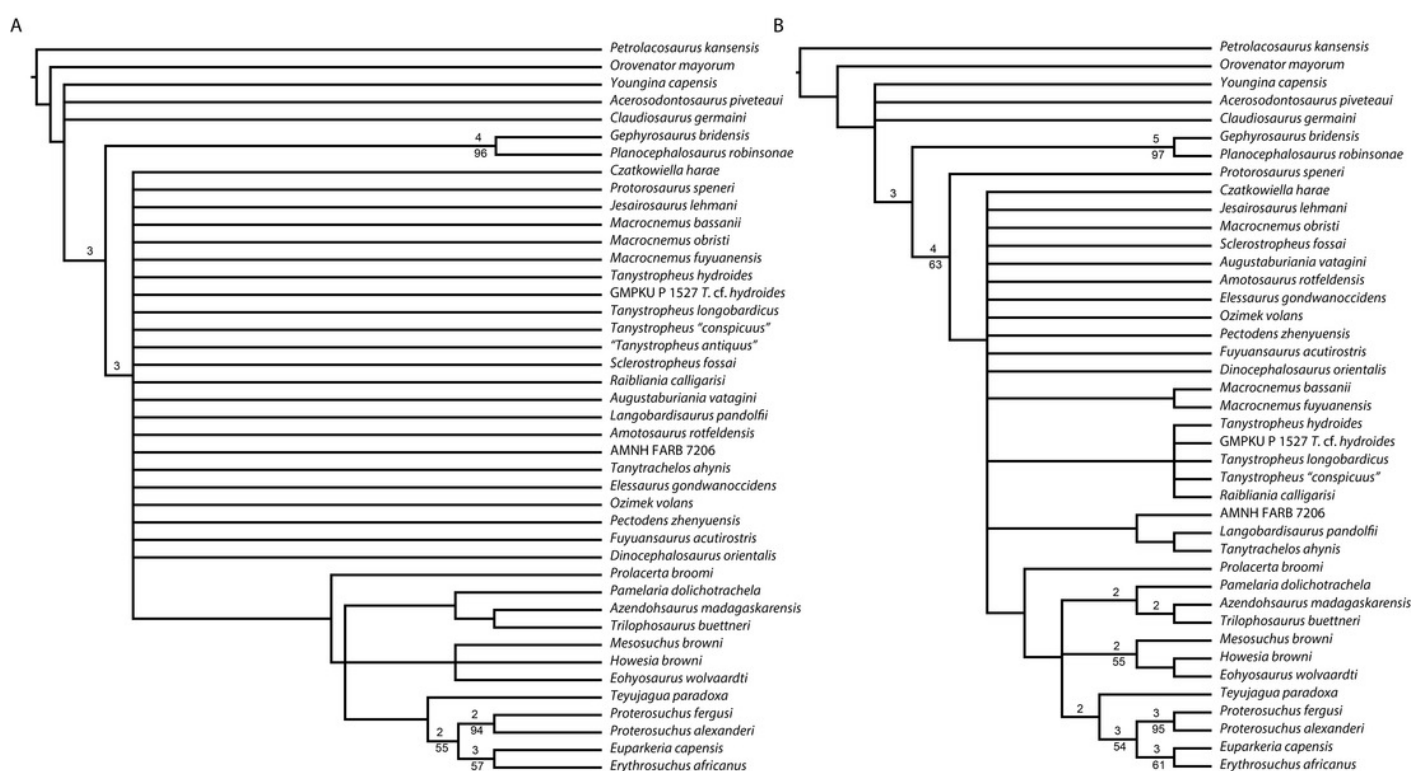


Figure 33

Strict consensus tree out of 11 MPTs with 1096 steps of analysis 3 (specified characters ordered; specified taxa pruned).

Bremer values above 1 and Bootstrap frequencies above 50% are provided above and below each node, respectively.

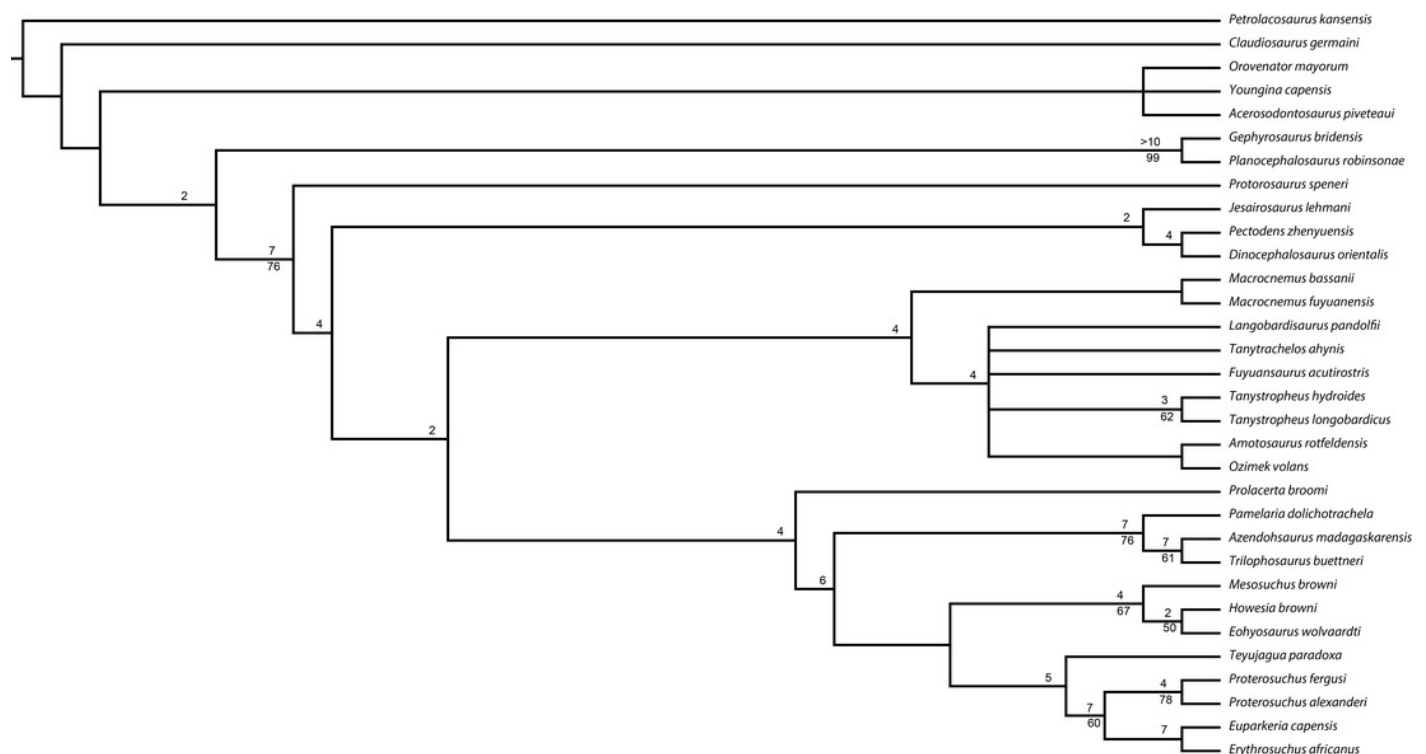


Figure 34

Strict consensus tree out of a single MPT with 934 steps of analysis 4 (all characters unordered and ratio characters have been excluded; specified taxa pruned).

Bremer values above 1 and Bootstrap frequencies above 50% are provided above and below each node, respectively.

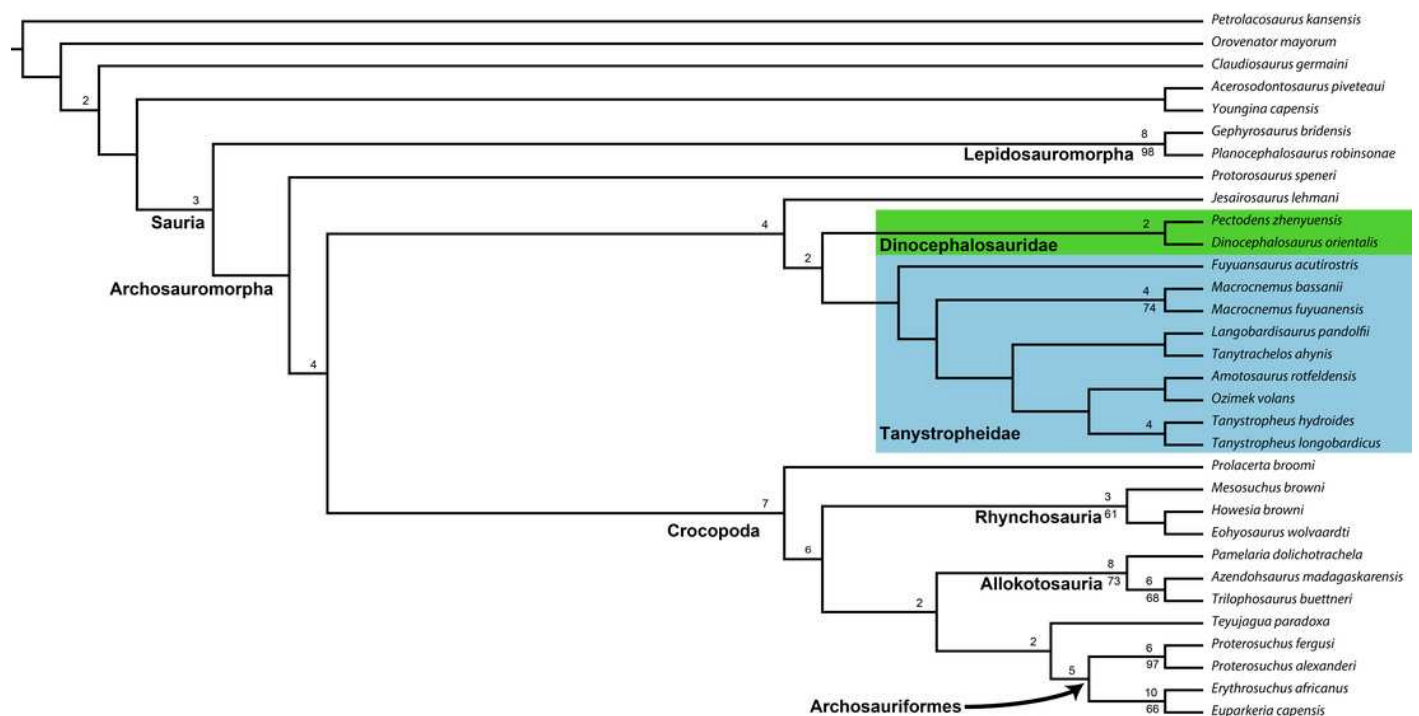


Figure 35

Time-calibrated phylogenetic tree based on the relationships recovered in analysis 4.

The black boxes indicate the possible temporal range of each OTU based on the available stratigraphic information (e.g. the age of Member II of the Guanling Formation, from which the only known specimen of *Pectodens zhenyuensis* is known, cannot be further restricted than being of Anisian age, and therefore the possible temporal range of *Pectodens zhenyuensis* covers the complete Anisian). The non-saurian diapsid taxa *Petrolacosaurus kansensis* and *Orovenator mayorum* from the Carboniferous and Early Permian, respectively, are not indicated to since they are considerably older than the other taxa of this study. Their phylogenetic position is indicated in Figure 34. The timescale based on the International Chronostratigraphic Chart of the International Commission on Stratigraphy (accessed May 2020).

